

THE ROLE OF PESTICIDE-INDUCED ALDEHYDE DEHYDROGENASE
INHIBITION IN THE PATHOGENESIS OF PARKINSON'S DISEASE

Thesis by

Arthur G. Fitzmaurice

In Partial Fulfillment of the Requirements

for the Degree of

Doctor of Philosophy

California Institute of Technology

Pasadena, California

2012

(Defended November 28, 2011)

© 2012

Arthur G. Fitzmaurice III

All Rights Reserved

ACKNOWLEDGEMENTS

This work was funded in part by the National Defense Science & Engineering Graduate (NDSEG) Fellowship, the National Institute of Environmental Health Sciences (NIEHS Grants P01ES016732, R01ES010544, 5R21ES16446-2, U54ES012078), the National Institute of Neurological Disorders and Stroke (NINDS Grant NS038367), the Veterans Administration Healthcare System (SW PADRECC), the Michael J. Fox Foundation, and the Levine Foundation.

This work was conducted under the supervision and guidance of Jeff M. Bronstein, M.D., Ph.D. Laboratory support came from Aswani Kotagiri, Ph.D., Sharon Li, Ph.D., Shubhangi Prabhudesai, Ph.D., Mark Stahl, M.D., Ph.D., Sheldon Wang, Ph.D., Aaron Lulla, Frances Cho, Julia Co, Brendan Cohn-Sheehy, and Molly Newborn. Epidemiologic analyses were conducted in collaboration with Beate Ritz, PhD. and Shannon L. Rhodes, Ph.D. Primary culture experiments were conducted in collaboration with Nigel Maidment, Ph.D. and Hoa Lam.

I am grateful for the service of the dissertation committee comprised of Jeff M. Bronstein, M.D., Ph.D. (Advisor), Michael R. Hoffmann, Ph.D. (Chair, Dean Emeritus of Graduate Studies), Paul H. Patterson, Ph.D., and Jared R. Leadbetter, Ph.D. Special thanks to the mentorship of Janet R. Hering, Ph.D. (Advisor) during the early years at Caltech.

On a personal note, I am indebted to my mentor Jeff Bronstein for taking a chance on me when I had little knowledge of neuroscience but a lot of passion

and compassion for contributing to research that may one day save lives. During my first week in the lab, Jeff articulated that our primary goal is not to get the best publications by trampling on other labs, withholding results, and so forth; rather, he said the publications would come if we worked hard, and he invited me to join him in the hospital to meet suffering patients and families if I ever needed to be reminded why we conduct our research. This affirmed me in making this decision halfway through my graduate career to transition to a new working environment and research focus that were more conducive to my development professionally and personally. Thank you, Jeff, for who you are for me and for the Parkinson's community.

Finally, I am graced by those I regard as family who have supported me in all ways. Graduate school has been a marathon (ten, actually). I am honored by your presence on this journey with me. May we continue to support each other in becoming the people we are meant to be.

A.M.D.G.

ABSTRACT

Parkinson's disease (PD) is a neurodegenerative disorder particularly characterized by the loss of dopaminergic neurons in the substantia nigra pars compacta. Its etiology is unknown but likely includes both genetic and environmental factors. Since pesticide use has been associated with PD occurrence, we conducted a screen to identify pesticides that impair the ubiquitin-proteasome system (UPS), a degradative process implicated in PD pathogenesis. Benomyl was identified as a UPS inhibitor in this screen and became the focus of this dissertation.

In an epidemiologic study, we used state-mandated Pesticide Use Reports to estimate chronic exposures and observed 65-92% increased PD risk in a population exposed to the fungicide benomyl. In experimental models, we found that benomyl induced selective dopaminergic neuronal loss *in vitro* with primary mesencephalic cultures and selective aminergic neuronal loss in a novel *in vivo* zebrafish system. Benomyl is readily metabolized to S-methyl N-butylthiocarbamate and its sulfoxide, a potent aldehyde dehydrogenase (ALDH) inhibitor. These thiocarbamates inhibited ALDH activity in primary neurons at submicromolar concentrations leading to accumulation of the dopamine metabolite 3,4-dihydroxyphenylacetaldehyde, the proposed neurotoxicant. This model for PD etiology via ALDH inhibition may help explain the selective vulnerability of dopaminergic neurons in PD.

To follow up on this finding, we developed a novel *ex vivo* neuronal assay to screen other pesticides for ALDH inhibitory activity. All dithiocarbamates tested

(e.g., mancozeb, maneb, ziram), two dicarboximides (captan, folpet), and two imidazoles (benomyl, triflumizole) inhibited ALDH activity, potentially via metabolic byproducts (e.g., carbon disulfide, thiophosgene). Exposures to ALDH-inhibiting pesticides (i.e., positive hits) applied in our study area were associated with dose-dependent twofold to fourfold increases in PD risk. Genetic variation in the *ALDH2* gene potentiated this risk considerably (up to sixfold) for people working where these pesticides were sprayed liberally.

This is the first report of a pesticide that damages dopaminergic neurons by inhibiting ALDH activity. The identification of multiple ALDH-inhibiting pesticides associated with increased PD risk supports the potential of ALDH as a novel therapeutic target and a subject for consideration by regulators and policymakers.

TABLE OF CONTENTS

ACKNOWLEDGEMENTS	III
ABSTRACT	V
TABLE OF CONTENTS	VII
LIST OF FIGURES	IX
LIST OF TABLES	XI
CHAPTER I	1
OVERVIEW	1
1. PARKINSON'S DISEASE ETIOLOGY	1
2. POTENTIAL MECHANISMS OF TOXICITY	1
3. EPIDEMIOLOGY	4
4. IMPLICATIONS	4
CHAPTER II	6
PESTICIDES AND PARKINSON'S DISEASE	6
1. INTRODUCTION	6
2. PATHOPHYSIOLOGY OF PARKINSON'S DISEASE	8
3. EPIDEMIOLOGY OF PARKINSON'S DISEASE	14
4. FROM ASSOCIATION TO CAUSALITY: DO PESTICIDES CAUSE PD AND IF SO, HOW?	19
5. SUMMARY	25
CHAPTER III	28
ALDEHYDE DEHYDROGENASE AS A POTENTIAL TARGET FOR TOXICANT-INDUCED PARKINSON'S DISEASE	28
1. INTRODUCTION	28
2. METHODS	30
3. RESULTS	38
4. DISCUSSION	45

CHAPTER IV	61
ALDEHYDE DEHYDROGENASE DYSFUNCTION INCREASES PARKINSON'S DISEASE RISK VIA GENE-ENVIRONMENT INTERACTIONS	61
1. INTRODUCTION	61
2. METHODS	63
3. RESULTS	69
4. DISCUSSION	73
5. CONCLUSION	76
CHAPTER V	89
IMPLICATIONS	89
1. IMPLICATIONS FOR PESTICIDE REGULATION	89
2. IMPLICATIONS FOR PARKINSON'S DISEASE ETIOLOGY	91
REFERENCES	95
APPENDICES	116
A. ZIRAM CAUSES DOPAMINERGIC CELL DAMAGE BY INHIBITING E1 LIGASE OF THE PROTEASOME	117
B. GEOCHEMICAL AND HYDROLOGIC CONTROLS ON THE MOBILIZATION OF ARSENIC DERIVED FROM HERBICIDE APPLICATION	126
C. GEOCHEMICAL PROCESSES CONTROLLING ARSENIC MOBILITY IN GROUNDWATER: A CASE STUDY OF ARSENIC MOBILIZATION AND NATURAL ATTENUATION	138
D. MECHANISMS OF ROTENONE-INDUCED PROTEASOME INHIBITION	152
E. PESTICIDES AND PARKINSON'S DISEASE	160

LIST OF FIGURES

- Figure II-1.** Proposed pathophysiology of Parkinson's disease
- Figure III-1.** Aldehyde dehydrogenase inhibition as a potential mechanism of benomyl-induced Parkinson's disease
- Figure III-2.** Dopaminergic neuronal damage in primary mesencephalic cultures exposed to benomyl or its metabolites
- Figure III-3.** Aminergic neuronal damage in *Danio rerio* larvae exposed to benomyl
- Figure III-4.** Inhibitory actions of benomyl and its metabolites
- Figure III-5.** Neuroprotection via reducing DOPAL accumulation with MAO inhibitor
- Figure IV-1.** *Ex vivo* neuronal ALDH inhibition by imidazole, dicarbonyl, and dithiocarbamate pesticides
- Figure IV-2.** *In vitro* mitochondrial ALDH inhibition by pesticides
- Figure IV-3.** Risk of PD (odds ratios and 95% confidence intervals) by quartiles of pesticide exposure
- Figure IV-4.** Gene-environment interaction analysis of aggregate exposure score and *ALDH2* clade
- Figure IV-S1.** Cladogram for determining Clade 1 (left) or Clade 2 (right) from single nucleotide polymorphisms in *ALDH2* gene

Figure V-1. Schematic of potential mechanisms by which pesticides may contribute to the pathogenesis of Parkinson's disease

LIST OF TABLES

- Table III-1.** Associations between PD and estimated ambient occupational or residential benomyl exposures
- Table III-S1.** Demographics of the Parkinson's Environment & Genes (PEG) Study
- Table III-S2.** Associations between PD risk and estimated ambient occupational or residential benomyl exposures, by quartiles in exposed controls
- Table III-S3.** Associations between PD risk and estimated ambient occupational or residential benomyl exposures, stratified by sex
- Table IV-1.** IC_{50} values of ALDH-inhibiting pesticides applied in PEG study area
- Table IV-2.** Associations between aggregate pesticide exposure and PD risk
- Table IV-3.** Associations between genetic variation in the *ALDH2* gene and PD risk
- Table IV-S1.** Demographics of PEG study subjects
- Table IV-S2.** Risk of PD by quartiles of pesticide exposure, estimated with occupational addresses
- Table IV-S3.** Risk of PD by quartiles of pesticide exposure, estimated with residential addresses
- Table V-1.** Agricultural application data for five pesticides found to have ALDH inhibitory capability

CHAPTER I

Overview

1. Parkinson's disease etiology

Parkinson's disease (PD) is the second most prevalent neurodegenerative disorder, affecting millions of people worldwide ¹. Motor symptoms include akinesia (inability to initiate movement), bradykinesia (slowness of movement), resting tremor, and balance problems, while non-motor symptoms include cognitive impairments, mood disturbances, sleep dysfunction, gastrointestinal problems, and dysautonomia. PD is a progressive disorder, and despite several effective therapies that treat many of the symptoms, there are no treatments that alter disease progression. Elucidating the etiology of PD is likely necessary to develop effective disease-modifying therapies. Exposure to pesticides has been associated with PD occurrence, so these compounds can serve as model toxicants to investigate neurotoxic mechanisms that may be relevant. A thorough review of the research associating pesticides and Parkinson's disease is provided in this dissertation (Chapter II).

2. Potential mechanisms of toxicity

Two characteristics of PD are the death of dopaminergic neurons and the formation of Lewy bodies comprised of synuclein and other protein aggregates. These offer two targets for the discovery of therapies against PD. One way healthy cells degrade protein aggregates is through the ubiquitin-proteasome system (UPS). UPS

dysfunction is an area of active study in PD research. McNaught and Jenner reported reduced UPS activity in brains of PD patients², and some investigators have used UPS inhibitors to recreate some features of PD *in vivo*, although these models remain controversial³⁻⁸. We found that the fungicide ziram damaged dopaminergic cells and elevated α -synuclein levels *in vitro* by inhibiting E1 ligase of the UPS (Appendix A,⁹). In contrast, here we report that benomyl damaged dopaminergic cells but did not increase α -synuclein levels *in vitro*, suggesting a different neurotoxic mechanism.

Although other areas of the central and peripheral nervous systems are affected¹⁰, why dopaminergic neurons in the substantia nigra are particularly vulnerable presents another area of active research, focusing on the neurotransmitter dopamine, its metabolism, and its receptors and transporters (e.g., D1, D2, VMAT2, DAT1). Dopamine and its metabolites have been reported to modify α -synuclein, supporting UPS dysfunction as a potential mechanism of toxicity within dopaminergic neurons¹¹⁻¹³. Burke et al. reported that administration of the dopamine metabolite 3,4-dihydroxyphenylacetaldehyde (DOPAL) was on the order of 400 times more toxic than dopamine itself *in vivo*¹⁴. Since DOPAL is a substrate for detoxification by aldehyde dehydrogenase (ALDH), ALDH inhibition is another potential toxic mechanism particularly relevant to dopaminergic neurons.

2.1 ALDH inhibition

The *ALDH* gene superfamily includes about 19 putatively functional genes that are ubiquitous throughout the body and important for the detoxification of various aldehydes including acetaldehyde in the liver and retinal in the eyes¹⁵. ALDH2 is the

predominant ALDH found in neuronal mitochondria; smaller levels of ALDH1A1 are present in the cytosol. Two substrates relevant to this study include the dopamine metabolite DOPAL and the lipid peroxidation product 4-hydroxy-2-nonenal (4-HNE). DOPAL has been described briefly. Increased 4-HNE was found in *post mortem* PD brains as adducts¹⁶ and as a component of Lewy bodies¹⁷. Furthermore, 4-HNE was reported to prevent α -synuclein fibrillation and form α -synuclein oligomers, which are toxic to dopaminergic neurons¹⁸.

In this dissertation, we use benomyl as a model compound, because it can inhibit both ALDH activity and the UPS^{19,20}. In this investigation with benomyl (Chapter III), we report that benomyl's ability to inhibit the UPS is conferred by its carbendazim moiety (via microtubule inhibition), and its ALDH inhibitory capability is conferred by butyl isocyanate and other downstream metabolites including S-methyl N-butylthiocarbamate (MBT). We report IC₅₀s that reveal that ALDH inhibition occurs at lower concentrations than UPS dysfunction. We also find that carbendazim is not toxic to dopaminergic neurons *in vitro*, whereas MBT recapitulates benomyl's neurotoxicity at low concentration. Although UPS inhibition may also be important at higher concentrations, ALDH inhibition damages dopaminergic neurons even at low exposures. We report that co-treatment with a MAO inhibitor attenuated this toxicity, suggesting a role for DOPAL accumulation as a toxic mechanism.

These findings motivated further investigations using three classes of pesticides (Chapter IV). We developed a novel assay to study ALDH inhibition in a neuronal system; we report that all tested dithiocarbamates and a subset of dicarboximides and

imidazoles inhibit ALDH activity. It had not been evident using other methods that so many pesticides inhibit ALDH activity.

3. Epidemiology

The UCLA Parkinson's Environment and Genes (PEG) epidemiologic study enables us to investigate whether some of these ALDH-inhibiting pesticides are associated with increased PD risk (Chapters III, IV). Here we report that high exposures to benomyl, captan, mancozeb, maneb, or ziram are associated with twofold to fourfold increases in PD risk. (According to state-mandated Pesticide Use Reports, the population had not been exposed to the other pesticides found to inhibit ALDH activity.) We also report a significant dose-dependent risk associated with aggregate exposure to more than one ALDH-inhibiting pesticide. Genetic variation in the *ALDH2* gene potentiates this risk considerably (up to sixfold) for people working where these pesticides were sprayed liberally.

4. Implications

This is the first report to associate ALDH inhibition, dopaminergic neuronal damage, and increased risk of PD with exposure to an environmental toxicant. Identification of multiple ALDH-inhibiting pesticides that are associated with increased PD risk suggests that modulating ALDH is a potential therapeutic target. This work has implications for the regulation of specific pesticides as well as for the elucidation of PD

etiology and potential treatments. Some of these are discussed at the end of this dissertation (Chapter V).

CHAPTER II

Pesticides and Parkinson's disease

1. Introduction

1.1 Clinical and pathological aspects of Parkinson's disease

Parkinson's disease (PD) is the second most prevalent neurodegenerative disorder, affecting millions of people worldwide ¹. While some cases of familial PD have been reported, the etiology of most cases is still unknown. Significant progress in understanding the pathophysiology of PD has been made from genetic and epidemiologic studies that have implicated defects in a few key biological processes as potential final common pathological pathways.

PD is a progressive motor disorder characterized by death of dopaminergic neurons in the region of the brain called the substantia nigra pars compacta, although other areas of the central and peripheral nervous system are involved ¹⁰. The loss of dopaminergic neurons in PD leads to motor symptoms that include akinesia (inability to initiate movement), bradykinesia (slowness of movement), resting tremor, and balance problems. Non-motor symptoms can include cognitive impairments, mood disturbances, sleep dysfunction, gastrointestinal problems, and dysautonomia. PD is a progressive disorder and despite several effective therapies that treat many of the symptoms, there are no treatments that alter disease progression. Uncovering the causes of PD is likely necessary to find effective disease-modifying therapies.

The pathological hallmark of PD is the presence of Lewy bodies, which are cytosolic inclusions with several molecular components although α -synuclein (α -syn) is the predominant protein²¹. Lewy bodies also contain ubiquitin, a polypeptide that targets proteins to the ubiquitin proteasome system (UPS) for degradation.

1.2 Genes versus environment

Despite the elucidation of approximately eighteen genes in familial PD and the identification of multiple risk factor genes using genome-wide association studies on thousands of patients, only a small fraction of PD risk has been accounted for²². Thus, environmental factors almost certainly play a major role in the pathogenesis of PD.

One of the first important clues that the environment may contribute to the pathogenesis of PD came in 1982 from the observation that a street drug contained a contaminant called 1-methyl-4-phenyl-1,2,3,6-tetrahydropyridine (MPTP) which caused almost overnight a clinical syndrome resembling PD. It was subsequently found that MPTP killed dopaminergic neurons by being converted enzymatically to 1-methyl 4-phenylpyridinium (MPP⁺), specifically entering dopamine neurons via the dopamine transporter, and inhibiting complex I in the mitochondrial respiratory chain. Notably, the chemical structure of the MPTP metabolite MPP⁺ is similar to paraquat, a commonly-used pesticide. These and other observations led to a series of epidemiologic studies probing pesticides as potential contributors to the etiology of PD.

Although genetics has not found the cause of 95% of PD cases, the identification of specific genes and their functions have provided important clues into pathological processes that appear to be involved in non-genetic forms of PD. For example,

mutations in the α -syn gene led to the finding that α -syn is the major component of Lewy bodies. Mutations in other genes have identified dysfunction of protein degradation (the UPS and autophagy) as possibly being involved in the pathogenesis of PD. Since other PD genes are involved in mitochondrial function and MPTP inhibits oxidative respiration, mitochondrial dysfunction also has been implicated in the pathogenesis of PD. We believe that environmental toxins may increase the risk of PD by causing dysfunction in these cellular processes. Here, we will review the evidence that pesticides are associated with the development of PD and the mechanisms by which they might act.

2. Pathophysiology of Parkinson's disease

2.1 Lewy bodies and α -synuclein homeostasis

Lewy bodies are the pathological hallmark of PD and the major component of these intracytosolic inclusions is α -syn²¹. α -syn exists in multiple forms including soluble monomers, oligomers and fibrils. The multimeric forms appear to be the toxic species and their formation is dependent on several factors including amino acid substitutions due to mutations in its gene, α -syn concentration, and the presence of dopamine and dopamine adducts^{11,23-25}. Exogenous factors such as pesticides have also been reported to increase α -syn aggregation. Given that α -syn aggregation appears central to the pathogenesis of PD and pesticides appear to promote this process via a variety of mechanisms, we will briefly discuss α -syn homeostasis.

2.1.1 α -synuclein

α -syn is a predominantly neuronal protein that was first implicated in the development of Alzheimer's disease. The identification of three mutations—A53T, A30P, and G188A—in its gene in a few families with dominantly-inherited PD led to the finding that fibrillar α -syn is the major component of Lewy bodies not only in these patients but also in sporadic PD ^{21,26-29}. Overexpression of normal α -syn by gene multiplication causes fairly typical PD ³⁰, and people who have an α -syn promoter that confers a higher level of expression are at higher risk of developing PD ^{31,32}. Thus, increased levels of normal α -syn increases one's risk of getting PD and if it is high enough, it causes it. Importantly with respect to this review, certain pesticides can cause α -syn levels to increase providing a theoretical mechanism to contribute to PD (see below for individual pesticides). Furthermore, pesticides can directly increase the rate of α -syn fibril formation adding another method they can contribute to the pathogenesis of PD ³³.

2.1.2 Ubiquitin-proteasome system dysfunction in Parkinson's disease

α -syn concentrations are determined by the relative amount of its expression and degradation, and the higher the concentration, the more likely it is to form aggregates. Both the UPS and autophagy have been shown to degrade α -syn. The soluble form appears to be degraded by the UPS, while the lysosomal pathway appears to degrade aggregated forms of the protein ³⁴⁻³⁷. The UPS is a highly-regulated, ATP-dependent, degradative multi-subunit pathway that helps clear the cell of damaged, misfolded, or

otherwise unneeded proteins. Proteins are targeted to the UPS by ubiquitin-activating enzymes (E1), ubiquitin-conjugating enzymes (E2), and ubiquitin-protein ligases (E3). Once polyubiquitinated, proteins are recognized by the 19S regulatory complex of the 26S proteasome and translocated to the 20S complex for degradation. Finally, ubiquitin is recycled via thiol proteases called deubiquitinating enzymes, which fall into the ubiquitin carboxyl-terminal hydrolase (UCH) or ubiquitin-specific processing protease (UBP) families³⁸.

Three known genetic causes of PD involve aspects of UPS function. Parkin gene mutations cause autosomal recessive PD and is an E3 ubiquitin ligase necessary for targeting proteins for degradation. UCH-L1 gene mutations cause autosomal dominant (AD) PD, and UCH-L1 is necessary for the recycling of ubiquitin. Finally, α -syn is a substrate for the UPS, and mutations and duplication of its gene cause AD PD. There is also evidence that UPS dysfunction is involved in sporadic PD. Reduced UPS activity has been found in brains of PD patients², and some investigators have found that administration of UPS inhibitors to rodents can recreate some of the features of PD although these models remain controversial³⁹⁻⁴⁴. Finally, we have found that several commonly-used pesticides inhibit the UPS and are associated with an increased risk of developing PD^{9,45}.

2.1.3 Autophagy and Parkinson's disease

Autophagy is a cellular process that involves protein and organelle degradation. Dysfunction of autophagy has long been known to be involved in disease but only recently has been implicated in the pathogenesis of PD. Gaucher's disease is an

autosomal recessive lysosomal storage disease caused by mutations in its gene that leads to dysfunction of autophagy and are associated with a marked increased risk of developing typical PD with Lewy bodies⁴⁶⁻⁴⁸. Another autosomal recessive Parkinsonian disorder (PARK9) is caused by a mutation in another lysosomal gene, ATP13A2⁴⁹. PINK1 has also been shown to be a modifier of autophagy, and mutations in its gene cause PD with Lewy bodies (PARK6)^{50,51}. Additional evidence for a role of autophagy in PD comes from studies of sporadic PD brains where increased numbers of autophasomes have been described⁵².

α -syn clearance is likely carried out by both the UPS and autophagy. Large aggregates of α -syn proteins are likely degraded by macroautophagy, but soluble α -syn can undergo degradation via an alternate lysosomal pathway, chaperone-mediated autophagy (CMA)⁵³. α -syn has also been found to damage lysosomal macroautophagy, and oligomers are resistant to CMA, adding further support for a possible role of protein degradation dysfunction in the pathogenesis of PD⁵⁴.

2.2 Mitochondrial dysfunction and oxidative stress

The role of mitochondrial dysfunction in the pathophysiology of PD was first suggested by the discovery that MPTP, a neurotoxin selective for nigral dopaminergic neurons, acts through inhibition of complex I of the electron transport chain. MPTP is converted by monoamine oxidase (MAO-B) to its toxic metabolite MPP⁺, it is rapidly concentrated by dopaminergic neurons into the mitochondria and produces cell death⁵⁵⁻⁵⁸. This discovery led to the findings that complex I activity is reduced not only in brains of PD patients but also in peripheral mitochondria^{59,60}. Furthermore, mutations in some

genes that code for mitochondrial associated proteins can cause PD (e.g., DJ1 and PINK1), and chronic systemic administration of complex I inhibitor (rotenone) in rodents reproduces many of the clinical and pathological aspects of PD ⁶¹.

The downstream targets of mitochondrial dysfunction remain unclear. ATP depletion is not necessary in the rotenone rodent model for its toxicity, but the generation of reactive oxygen species (ROS) appears to be essential. ROS are known to oxidize DNA, lipids, and proteins to cause cellular damage. Interestingly, ROS from complex I inhibition leads to UPS inhibition ⁶². Furthermore, the formation of ROS from complex I inhibition likely contributes to the Lewy-like bodies observed in the rotenone model ⁶³.

2.2.1 Aldehyde dehydrogenase (ALDH) inhibition

Another form of mitochondrial dysfunction implicated in PD involves the inhibition of aldehyde dehydrogenase 2 (ALDH2), a mitochondrial ALDH. This enzyme is responsible for the detoxification of aldehydes that could otherwise modify proteins. For example, the lipid peroxidation product 4-hydroxy-2-nonenal (4-HNE) is detoxified by ALDH2, and increased 4-HNE has been reported in *post mortem* PD brains as adducts ¹⁶ and as a component of Lewy bodies ¹⁷. Furthermore, 4-HNE has been shown to prevent α -syn fibrillation and form α -syn oligomers that are toxic to primary mesencephalic cultures ¹⁸. Another ALDH2 substrate, the dopamine metabolite 3,4-dihydroxyphenylacetaldehyde (DOPAL), has also been reported to induce α -syn aggregation and be toxic to dopaminergic neurons ¹¹. ALDH involvement in the pathogenesis of PD is not yet well-established, but preliminary *in vitro* and

epidemiologic studies have implicated this enzyme as a possible mediator of some pesticides' toxicity (see benomyl below).

2.3 Altered dopamine homeostasis

Conventional wisdom in the pathophysiology of PD is that dopaminergic neurons are selectively vulnerable, although more recent evidence suggests that neuronal loss is more widespread. One hypothesis for this possible vulnerability is via the metabolism of dopamine itself ⁶⁴.

Dopamine and its metabolites are toxic, and dopamine adducts have been shown to stabilize α -syn oligomers. DOPAL, a substrate for ALDH2, is particularly toxic. Interestingly, DOPAL is formed by the enzyme MAO-B, and blocking this enzyme with specific drugs appears to alter the progression of PD ⁶⁵. Thus, alterations in levels of dopamine or its metabolites might contribute to neuronal loss. Increased levels of VMAT2, a vesicular transporter that lowers cytosolic dopamine levels, lowers the risk of developing PD ⁶⁶. Further support for altered dopamine homeostasis in PD comes from a recent report that polymorphisms in the dopamine transporter (DAT) gene in combination with pesticide exposure also increase the risk of PD ⁶⁷.

Taken together, dysfunction of several cellular processes appears to contribute to the pathogenesis of PD. Aggregation of α -syn (oligomerization and possibly fibril formation) is the leading candidate for the final common pathway for neurons to die in PD. There is evidence that pesticides cause dysfunction in many of these processes, providing potential mechanisms for their toxicity (Figure II-1).

3. Epidemiology of Parkinson's disease

3.1 Environment and Parkinson's disease

Over the past two decades, several epidemiologic studies have identified a number of environmental factors that are associated with an altered risk of developing PD. Smoking tobacco is almost universally found to be associated with a lower risk of developing the disease⁶⁸. Caffeine and alcohol consumption have also been associated with reduced PD risk⁶⁹. Since all of these addictive behaviors are associated with reduced incidence, it has been proposed that they may be surrogate markers for a common behavioral phenotype of pre-clinical PD patients rather than these exposures all being protective. The use of nonsteroidal anti-inflammatory drugs has also been found to reduce the risk of PD, suggesting inflammation may be somehow involved in its pathogenesis⁷⁰.

A number of studies have found strong associations between an increased risk of PD and rural living, well-water consumption, farming occupations, and pesticide exposure. These reports have been reviewed extensively by others, so we will not review all the studies here⁷¹⁻⁷⁶. The association with pesticide exposure has been the most provocative association with developing PD to date, although almost all of these reports were based on self-reporting pesticide exposure (i.e., potential recall bias) and the diagnosis of PD was not confirmed⁷⁷. Despite these weaknesses, a meta-analysis of case-control studies obtained a combined odds ratio (OR) for PD risk of 1.94 (95% CI: 1.49-2.53)⁷⁸. Subsequent studies reported ORs up to 7.0⁷².

Recently, the issue of potential recall bias was mitigated by determining pesticide exposure in a prospective manner. Petrovitch *et al.* reported an increased risk of

developing PD in Japanese-American men who worked on a plantation and were exposed to pesticides⁷⁹. Similarly, Ascherio *et al.* found a 70% increased risk of developing PD in those who reported significant pesticide exposure⁸⁰. These reports add support for a true association between pesticides and PD but still are limited in that they did not identify individual toxicants and dose-response relationships could not be determined.

3.2 Specific pesticides as risk factors

There are a few ongoing studies that address both the issue of recall bias and identify specific pesticides that confer an altered risk of developing PD. The Agricultural Health Study (AHS) is a prospective study, including 84,740 private pesticide applicators (mostly farmers) and their spouses, recruited in 1993-1997 in Iowa and North Carolina. Pesticide exposure was self-reported but felt to be reliable. The diagnosis of PD was also self-reported but later confirmed by direct examination. The first report from this study found an association between PD with increasing lifetime days of use of any pesticide, but no specific pesticide could be definitively implicated due to lack of statistical power⁸¹. Recently, the investigators reported that PD was associated with rotenone (OR 2.5, CI 1.3-4.7) and paraquat use (OR 2.5, CI 1.4-4.7)⁸². The strengths of this study are that it is prospective, the diagnosis was confirmed by examination, and specific toxicants were identified. Its primary weakness is that it includes only 110 cases, limiting the power to test a number of pesticides individually and in combinations, as well as the ability to test gene-environment interactions. One additional limitation was that quantitation, types, and length of pesticide exposures were

self-reported. Despite these shortcomings, this study adds strong epidemiologic evidence that pesticides are associated with an increased risk of developing PD, especially for rotenone and paraquat.

Ritz and colleagues at UCLA have taken another approach to identifying specific pesticides that are associated with an altered risk of PD. We took advantage of the California Pesticide Use Reporting database and Geographic Information System land-use maps to estimate historical exposure. All commercial pesticide applications have been recorded by compound, quantity, and specific location since 1974. Thus, individual subject exposures can be approximated using the subject's residential and occupational addresses for the past 37 years. In this Parkinson's Environment Gene (PEG) study, neurologists specializing in movement disorders went into the field to confirm the diagnosis in over 350 incident PD cases in the Central Valley in California where pesticides are applied liberally and the risk of PD appears to be increased^{83,84}. A similar number of age- and sex-matched control subjects were also recruited from the same communities. In addition to several lifestyle and medical assessments, DNA and serum samples were also obtained.

Individual pesticides were investigated in the PEG study based on previous reports implicating the agents as possibly involved in the pathogenesis of PD based on previous epidemiologic and/or laboratory studies. Maneb and paraquat were investigated because administration of pesticides to rodents produces a nice model of PD (see below). Estimates for maneb and paraquat exposures incurred between 1974 and 1999 were generated based on subjects' residences. Exposure to both pesticides within 500 m of their homes increased PD risk by 75% (CI 1.13-2.73). Subjects aged \leq

60 yo were at much higher risk of developing PD when exposed to either maneb or paraquat alone (OR 2.27, CI 0.91-5.70) or to both pesticides in combination (OR 4.17, CI 1.15-15.16)⁸⁵. PEG investigators have found similar associations with organophosphate pesticides—diazinon (OR 1.73, CI 1.23-2.45) and chlorpyrifos (OR 1.50, CI 1.04-2.18)⁸⁶—and ziram (OR 3.01, CI 1.69-5.38). In subjects \leq 60 yo, exposure to both ziram and paraquat had a sixfold increase in PD risk (CI 1.94-18.33)⁸⁷. It is important to note that all estimates of exposures were not dependent on subject recall for total exposure or duration of exposure. Recent exposure to pesticides (1990 to 1999) was not generally associated with an increased risk of PD, consistent with the theory that PD pathology likely starts several years before it manifests itself clinically.

The population is exposed to pesticides in a variety of ways, not just inhalation from spraying and crop dusters. Gatto *et al.* looked at five pesticides that were likely to be detected in well water⁸⁸. Although local well water was not analyzed, these pesticides were identified based on their solubility, half-lives, and adsorptive properties. These included organophosphates (diazinon, dimethoate, chlorpyrifos), a carbamate (methomyl), and a sulfite ester (propargite). Excluding those who did not consume well water, potential inhalation and ingestion of each pesticide was associated with 23-57% increased risk of PD. Consuming well water potentiated this effect to a 41-75% increased risk. Up to a twofold increase was observed for those who consumed water with the highest potential contamination of at least one of these pesticides. Finally, those with PD were found to have consumed well water an average of 4.3 years longer than controls. Because PEG has enrolled over 350 cases, we have statistical power to test gene-environment interactions. Not surprisingly, the risk of developing PD in

pesticide-exposed subjects is clearly altered based on the subject's genetic background (see below).

3.3 Gene-environment interactions

Gene-environment interaction analyses for pesticides and PD have been rare due to small sample size and difficulty obtaining exposure data⁸⁹⁻⁹². Elbaz *et al.* found that pesticides had a modest effect in subjects who were not CYP2D6 poor metabolizers, had an increased effect in poor metabolizers (approximately twofold), but poor metabolizers were not at increased PD risk in the absence of pesticide exposure⁹⁰. Hancock *et al.* found a gene-environment association in PD for pesticides and nitric oxide synthase 1 polymorphisms⁹¹. Kelada *et al.* described a very modest risk of developing PD with specific *DAT* alleles but a 5.7-fold increase (CI 1.73-18.53) in developing PD in subjects with occupational exposure to pesticides. These studies added proof of concept that the effect of environmental exposures on the risk of developing PD is at least partially dependent on one's genetic background⁹². Unfortunately, exposure assessments were very limited in all of these studies, and individual toxins could not be determined.

Gene-environment analysis in Ritz's PEG study has only recently begun but has already revealed intriguing results. We replicated the *DAT* polymorphism's interaction with pesticide exposure described by Kelada *et al.* for at least maneb and paraquat⁶⁷. Unexposed subjects with more susceptibility alleles had a 30% increased risk of developing PD, whereas exposed subjects had an almost fivefold increased risk (OR 4.53, CI 1.70-12.1). Importantly, there was a gene dose effect as well. In a similar

manner, variations in *PON1*, the gene that encodes Paraoxonase 1 that metabolizes chlorpyrifos and diazinon, potentiated the increased PD risks associated with these organophosphates⁸⁶. For example, diazinon was associated with a 73% increased risk of PD (CI 1.23-2.45), but the risk increased to 267% (CI 1.09-6.55) in individuals that carry 2 *PON1* risk alleles. Variations in the dinucleotide repeat sequence (REP1) within the α -syn promoter appear to alter the risk to paraquat exposure⁹³. Finally, we have preliminary evidence that variations in *ALDH2* gene potentiate the increased risks associated with dithiocarbamates and other pesticides that inhibit ALDH activity⁹⁴.

Clearly, the number of potential gene-environment interactions is enormous, but we have clear proof of concept that these interactions need to be considered to truly understand environmental risks in PD. It will take very large sample sizes and good exposure analysis to obtain a better understanding of the many potential interactions that confer the bulk of PD risk factors. Alternatively, a candidate gene approach coupled with a better understanding of the pharmacokinetics and toxicity of specific pesticides may allow us to test gene-environment interactions using smaller sample sizes.

4. From association to causality: Do pesticides cause PD and if so, how?

Epidemiologic studies have clearly established the association between pesticide exposure and the development of PD. The possibility that this association represents causality has been strengthened by recent studies that have addressed the problem of recall bias and have demonstrated a dose-effect relationship. Now that some individual pesticides have been implicated, mechanistic studies could be pursued. These studies

are reviewed within the context of our current understanding of the pathophysiology of PD.

4.1 Rotenone

Rotenone is produced naturally in roots of certain plant species such as the jicama vine. It is a widely-used domestic garden pesticide, and because it is degraded by the sun in a matter of days, users tend to spray rotenone frequently. Rotenone is also a well-characterized, high-affinity, specific inhibitor of complex I of the mitochondrial respiratory electron transport chain. Low complex I activity had been reported to be associated with PD both in brain and peripheral mitochondria, but it was not known whether this is causal or a surrogate marker for something else. To further investigate this, Greenamyre and colleagues chronically administered the complex I inhibitor, rotenone, systemically into rodents. Some of these rats developed selective dopaminergic neuronal death as well as many of the motor features of PD. Importantly, neurons developed intracytoplasmic inclusions that were found to contain α -syn⁶¹. α -Syn pathology in the gastrointestinal tract has also been described in the rotenone model similar to that seen in PD⁹⁵. Even small amounts of rotenone delivered intragastrically reproduces many of the same features described in rats given rotenone subcutaneously, but in this model the various stages of PD are reproduced in a progressive manner⁹⁶.

The mechanisms of rotenone toxicity are not completely clear but likely are more dependent on oxidative stress than energy failure⁹⁷. The downstream targets of

rotenone-induced oxidative damage are likely vast, but the UPS appears to be one of them^{45,62,63}.

Until recently, there had not been convincing epidemiologic reports linking rotenone exposure to PD. Dhillon *et al.* reported more than a tenfold increase in risk, although this study was limited because exposures were self-reported⁹⁸. The Agricultural Health Study did find a 2.5-fold increase risk with prospective questionnaires, adding further support for rotenone as a PD risk factor⁸². Furthermore, many organic farmers in the 1970s used rotenone as a natural pesticide, and a number of them have developed PD at a young age, although scientific confirmation of these anecdotal reports are lacking. Other pesticides that are complex I inhibitors are used even less frequently than rotenone, so little is known about associations with PD, although one would predict a similar effect.

4.2 Paraquat

One of the first pesticides investigated for its potential link to PD was paraquat due to its structural similarity to MPTP, the drug that caused acute parkinsonism in drug addicts. MPTP kills dopaminergic neurons by being metabolized to MPP⁺ by MAO-B, entering dopamine cells via the dopamine transporter, and then inhibiting complex I in the mitochondrial respiratory chain. Paraquat is ubiquitously used as an herbicide to control weed growth, and exposure to paraquat is associated with an increased risk of PD⁹⁹⁻¹⁰¹.

Additional support for paraquat increasing the risk of PD comes from animal studies. Mice infused with paraquat for three consecutive weeks exhibit dopamine cell

loss and cytosolic α -syn aggregates¹⁰²⁻¹⁰⁴. The mechanism by which paraquat causes dopamine cell death is not clear. Since it is structurally very similar to MPTP, it was presumed that paraquat acted in a similar manner. Surprisingly, unlike MPP+, paraquat is not a substrate for the dopamine transporter and does not inhibit complex I except at very high concentrations¹⁰⁵. Paraquat toxicity does appear to be dependent on increasing oxidative stress, and its action as a redox-cycler appears likely involved in its toxicity¹⁰⁶.

4.3 Dithiocarbamates (maneb and ziram)

Dithiocarbamates (DTCs) are a class of some of the most commonly-used organic fungicides. They are classified into two groups based on whether there is a carbonyl (group 1) or hydrogen on the nitrogen carbamate. Most DTCs are complexed with metals including zinc (e.g., ziram and zaneb), iron (e.g., ferbam) and manganese (e.g., maneb). DTCs first became relevant to PD researchers in 1985 when Corsini *et al.* found that diethyldithiocarbamate pretreatment enhanced MPTP toxicity in mice¹⁰⁷. They proposed that diethyldithiocarbamate would potentiate MPTP toxicity by inhibiting superoxide dismutase since they believed at that time that MPTP acted primarily as a redox cyler. Thiruchelvam *et al.* later reported that maneb potentiated the toxicity of paraquat preferentially in the nigrostriatal dopaminergic system^{108,109}. Furthermore, maneb and paraquat exposure was found to exacerbate α -synucleinopathy in A53T transgenic mice¹¹⁰.

The animal models using maneb and paraquat were intriguing, but it was only recently that an association between maneb and paraquat exposure and PD was

reported⁸⁵. Similar to the animal studies, residential exposure to maneb and paraquat together is associated with a 114% increased risk of newly-diagnosed PD. Furthermore, the risk of PD was increased to 317% for cases \leq 60 yo. Neither pesticide alone was associated with PD, but there were few subjects with maneb-only exposure so the true effect for maneb alone could not be assessed. When both occupational and residential exposures were taken into account, subjects exposed to maneb and paraquat alone had a 126% and 50% increased risk of developing PD, respectively, but for exposure to maneb and paraquat together, the risk increased to 8.75% (CI: 2.3-33.2) in the younger group⁸⁷. These epidemiologic data taken together with the animal data are quite compelling that these pesticides truly increase the risk of PD.

As mentioned above, DTCs are a large group of fungicides with similar structures. We identified another DTC, ziram, in an unbiased screen to identify pesticides that inhibit the proteasome⁴⁵. Maneb and some other DTCs were also found to inhibit the UPS but at higher concentrations⁹. Ziram selectively killed dopaminergic neurons in primary cultures and increased α -syn levels in the remaining neurons. Systemic administration of ziram alone into mice caused progressive motor dysfunction and dopaminergic neuronal damage⁹. Furthermore, subjects exposed to ziram alone had a 201% (CI: 1.69-5.38) increase of risk of developing PD and a 598% (CI: 1.95-18.3) increase of risk when exposed with paraquat in subjects \leq 60 yo⁸⁷. These data add further support for the role of DTCs as causal risk factors for PD.

It is still not completely clear how DTCs act biologically. We have found that they do not increase oxidative stress and therefore are unlikely acting through the mitochondrial respiratory chain⁴⁵. DTCs clearly inhibit the UPS, and their potencies

depend on whether they contain a tertiary or a secondary amine group. Ziram was studied extensively given its high potency to inhibit the UPS, and we found that it acts by interfering with the ubiquitin E1 ligase with an IC_{50} of 161 nM⁹. Zhou *et al.* reported that maneb also inhibited the UPS but at higher concentrations (IC_{50} of approximately 6 μ M) and increased protein carbonyls suggesting increased oxidative stress¹¹¹. We also found that maneb inhibits the UPS at much higher concentrations than ziram, but we did not find evidence of oxidative stress. Differences may very well be due to differences in the techniques used, since we used an *in vivo* 26S UPS assay and DCF fluorescence to detect ROS and Zhou *et al.* used an *in vitro* 20S UPS assay and protein carbonyl immunohistochemistry for detection of oxidative stress. Recently, we found that both maneb and ziram inhibit ALDH2 with IC_{50} s of 220 nM adding another potential mechanism of toxicity, especially to dopaminergic neurons⁹⁴. Since ziram does not contain manganese, it is very unlikely that it is the manganese in maneb that confers its toxicity as some have suggested.

4.4 Benomyl

Another important fungicide implicated in PD pathogenesis is the benzimidazole compound benomyl. It was developed as a microtubule inhibitor and is sprayed on fruits, nuts, and leaves to prevent fungal growth. Preliminary findings from the PEG study revealed benomyl exposure increased PD risk by 138% (CI: 1.33-4.27)⁹⁴.

Benomyl metabolizes spontaneously into another fungicide (carbendazim) and enzymatically into several thiocarbamate compounds. We have shown that benomyl and carbendazim are UPS inhibitors, although they are not as potent as ziram^{45,112}.

Furthermore, benomyl has also been reported to inhibit mitochondrial aldehyde dehydrogenase (ALDH) ¹⁹. Although these studies focused on hepatic ALDH, we recently reported that benomyl exposure reduced ALDH2 activity *ex vivo* in rat neuronal suspensions ¹¹². We have also found that exposure to benomyl or one of its ALDH2-inhibiting metabolites (S-methyl-N-butylthiocarbamate, or MBT) causes dopaminergic neuronal death *in vitro*, while the UPS-inhibiting metabolite (carbendazim) did not. These findings, combined with the observation that DTCs also inhibit ALDH2, suggest that ALDH2 inhibition may be an important mechanism in pesticide toxicity with respect to PD.

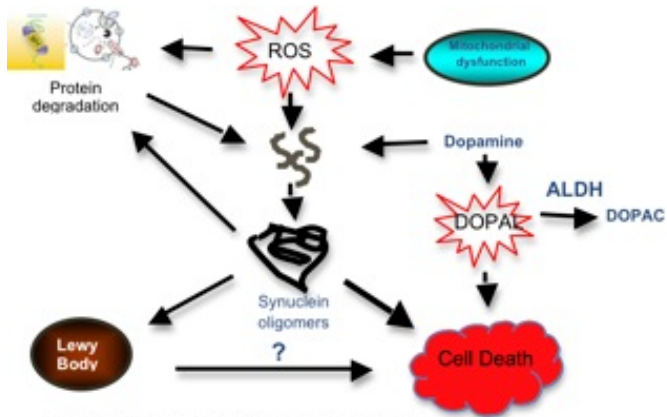
The toxicity of ALDH2 inhibition is likely due to the accumulation of toxic aldehydes. We would predict that ALDH2 inhibition would lead to increased levels of DOPAL and 4-HNE adducts, and preliminary studies in primary cultures support this hypothesis. Furthermore, the loss of dopaminergic neurons due to benomyl was attenuated by co-treatment with the MAO-B inhibitor pargyline which decreases DOPAL formation ¹¹². Since accumulations of DOPAL and 4-HNE have been reported to induce α -syn aggregation ¹¹, these findings support ALDH2 inhibition as an important mediator of pesticide toxicity in PD.

5. Summary

The causes of PD are not completely understood, but both genetic and epidemiologic studies suggest that dysfunction of one or more biological processes leads to α -syn aggregation and neuronal death. Epidemiologic studies have clearly shown PD to be associated with pesticide exposure, and specific pesticides conferring

at least some of this increased risk have recently been identified. The fact that administration of pesticides to animals recapitulates many of the behavioral and pathological features of PD provides evidence that the associations found in epidemiologic studies are causal. Elucidating the mechanisms of pesticide toxicity in mammals not only strengthens the hypothesis that exposure to these toxicants can increase the risk of developing PD, but also furthers our understanding of the pathophysiology of the disease in general. It is clear that the list of pesticides discussed in this chapter is not complete and that pesticides are not the only environmental toxicant that alters the risk of PD, but the preponderance of evidence taken together supports an important role for pesticides in the pathogenesis of PD. A better understanding of these issues will take us one step closer to a cure.

Figure II-1. Proposed pathophysiology of Parkinson's disease



CHAPTER III

Aldehyde dehydrogenase as a potential target for toxicant-induced Parkinson's disease

1. Introduction

Parkinson's disease (PD) is the second most prevalent neurodegenerative disorder, affecting millions of people worldwide. Symptoms result from the progressive degeneration of neurons, most notably the dopaminergic neurons in the substantia nigra pars compacta. More than half these neurons are lost by the time symptoms manifest themselves,¹¹³ so it is crucial to elucidate mechanisms of toxicity to dopaminergic neurons so that therapies can be developed to slow or reverse disease progression. Yet, the etiology of most PD cases remains elusive. Despite the identification of several genes that cause familial PD and polymorphisms that alter risk, only a small fraction of total risk can be accounted for genetically.¹¹⁴ Thus, environmental factors almost certainly play an important role in the pathogenesis of PD.

Over the past few decades, epidemiologic studies have consistently reported associations between PD occurrence and rural living, well-water consumption, farming occupations, and pesticide exposure.^{79-82,90,91,98,115-117} Most of these studies have been limited by the potential for recall bias and the inability to identify specific toxicants as risk factors. Despite these shortcomings, pesticide exposure has consistently been associated with increased risk of developing PD. We recently developed a novel method for investigating potential epidemiologic associations that does not rely on subject recall but rather estimates exposures to specific agents using geocoding of

occupational and residential addresses and state-mandated commercial pesticide application records.^{118,119} Relying on this method, we found that exposures to a number of specific pesticides markedly increased the risk of developing PD.^{67,85-88,93}

The term “pesticides” refers to a diversity of compounds (including fungicides, herbicides, etc.) that differ greatly in their structures and mechanisms through which they kill their intended pests. Studies investigating pesticide toxicity in vertebrates commonly use acute exposures and rarely consider the effects of chronic low-level exposures more relevant to human disease. One proposed mechanism for pesticide neurotoxicity is the inhibition of protein degradation via the ubiquitin-proteasome system (UPS). We recently found that several pesticides inhibited the UPS in a cell-based screen,²⁰ and some of these (e.g., ziram, maneb) were associated with an increased risk of PD in an epidemiologic study.^{85,87} The fungicide benomyl was selected for the present study not only because it was identified in our screen as a UPS inhibitor,²⁰ but also because it has other activities that might be relevant to the pathogenesis of PD. For example, the fungicidal action of benomyl is thought to result from microtubule assembly impairment,¹²⁰ a mechanism that has been implicated in PD.¹²¹ Microtubule inhibitors have been shown to inhibit the UPS⁶² and cause selective dopaminergic cell death and aggregation of α -synuclein, the predominant component of an intracytosolic Lewy body, the pathologic hallmark of PD.¹²¹ Furthermore, benomyl has been reported to inhibit aldehyde dehydrogenase (ALDH) activity in liver and brain mitochondria,^{19,122} although this has not been demonstrated in brain tissue. The mitochondrial-associated ALDH2 is of particular interest since it is involved in the metabolism of toxic aldehydes in brain tissue, including the dopamine (DA) metabolite 3,4-

dihydroxyphenylacetaldehyde (DOPAL). This brain-specific function of ALDH2 offers potential relevance of its inhibition to the preferential loss of dopaminergic neurons observed in PD.

The present work is the first of its kind to integrate human patients, environmental exposure data, and cellular and *in vivo* models in the study of PD. We report that benomyl exposure was associated with increased PD risk in a human population and was selectively toxic to dopaminergic cells *in vitro* and *in vivo*. By conducting experiments with benomyl and several of its metabolites, we determined that benomyl's neurotoxicity was primarily conferred by its ALDH inhibitory activity. This investigation suggests that chronic benomyl exposure is a risk factor for PD by inhibiting ALDH and resulting in the accumulation of toxic aldehydes in dopaminergic neurons. These findings identify ALDH dysfunction as a plausible pathway in PD pathogenesis and a novel therapeutic target for developing disease-modifying therapies.

2. Methods

2.1 Epidemiologic study

2.1.1 Human subjects

This study was conducted as part of the UCLA Parkinson's Environment & Genes (PEG) Study. Subject recruitment methods and case definition criteria have been described in detail.⁸⁷ Briefly, PD cases were recruited through neurologists, large medical groups, and public service announcements between January 2001 and December 2010. Eligibility criteria for cases (recruited between January 2001 and

January 2008) included (1) first PD diagnosis by a physician within three years of recruitment, (2) adequate health to be examined, (3) residence in one of the counties of interest, and (4) residence in California for at least 5 years prior to recruitment. Eligible cases were examined by UCLA movement disorder specialists at least once and confirmed as having clinically “probable” PD according to published criteria.¹²³ Of 1167 PD patients initially invited, 604 did not meet eligibility criteria primarily due to having a first physician diagnosis of PD more than three years prior to baseline. Of the remaining 563 eligible patients, 473 were examined by our movement disorder specialists; 113 did not meet published criteria for idiopathic PD. The remaining 360 idiopathic PD patients are included in these analyses.

Population-based controls were recruited between January 2001 and January 2010, initially from Medicare lists (2001) and predominantly from residential tax assessor records from the same three counties. Two sampling strategies were implemented to increase enrollment success and achieve representativeness of the control population: random selection of residential parcels enrolled via mail and phone, and clustered random selection of five households enrolled via in-person visits. Eligibility criteria for controls included (2)-(4) above and being at least 35 years of age. Of 1996 eligible population controls, 1043 declined participation, were too ill to participate, or moved away prior to enrollment. 754 population controls had complete data for inclusion in these analyses.

Cases and controls completed a telephone interview for the collection of demographic (age, sex, race/ethnicity, education), risk factor (family history of PD, smoking behavior), and detailed residential and occupational history data. Written

informed consent was obtained from all enrolled subjects, and all procedures were approved by the UCLA Human Subjects Committee.

2.1.2 Ambient pesticide exposure estimates

Pesticide exposure assessments were performed using Pesticide Use Reports (PURs, collected by the California Department of Pesticide Regulation since 1974) and a geographic-information-system-based (GIS) computer model that has been described in detail.^{67,87,118,119} PURs provide information on the location and date of application, active ingredients, poundage applied, application method, crop type, and acreage of the field. Our model combines data from PURs, land-use maps (to determine locations of pesticide application more precisely), and geocoded lifetime occupational and residential addresses of subjects to derive the pounds of pesticide applied over 26 years (1974-1999). Occupational and residential exposures were considered separately, and a subject's ambient exposure was assumed to be proportional to the amount applied to crop acreage within a 500-meter radius surrounding the subject's occupational or residential address. Exposure was categorized by the median exposure in exposed controls resulting in a three-level variable (unexposed, exposure below the median, exposure equal to or above the median). For quartile analyses, exposure was categorized by quartiles of exposure in exposed controls resulting in a five-level variable (unexposed, four quartiles).

2.2 *In vivo* studies

All procedures using zebrafish and rats were approved by the UCLA Animal Research Committee. Zebrafish expressing GFP tagged to vesicular monoamine transporter protein (*ETvmat2:GFP*) were used to identify aminergic neurons in whole larvae.¹²⁴ Peripheral sensory neurons (trigeminal and Rohon-Beard) were visualized using the previously-described *Tg(sensory:GFP)* transgenic line.¹²⁵ Whole larvae were bathed in 1 μ M benomyl or vehicle (0.01% DMSO) from 5 h until 5 d postfertilization, anesthetized using 0.02% tricaine methanesulfonate, fixed in 4% paraformaldehyde overnight, and mounted in 1.2% agarose for confocal imaging at 20x magnification. For aminergic neurons, ~100 optical sections were gathered for each larva, spaced 1.34 μ M apart, using a Zeiss LSM 5 Pascal inverted microscope. For peripheral sensory neurons, ~60 optical sections were spaced 3 μ M apart, using a Zeiss LSM 510 inverted microscope. Cells were counted blindly in three-dimensional projections, and fluorescence in composite images was measured blindly using ImageJ (NIH).

Spontaneous zebrafish movement was monitored with ZebraLab (Viewpoint Life Sciences, Inc., Lyon, France). Total distance was measured by tracking individual larvae for 30 min. Larvae were considered immobile at 0-2 mm/s.

2.3 Primary neuronal cultures

2.3.1 Preparation and treatment

Primary neuronal cultures were prepared using a protocol adapted from Rayport *et al* and previously described.^{9,126} Briefly, cortical glial feeder cells were established on

polyornithine/laminin-coated coverslips, which formed the base of 10-mm-diameter wells cut into 35-mm culture dishes (MatTek Corporation, Ashland, MA), until they reached confluency (~5 d) and 5-fluorodeoxyuridine was added to prevent additional glial proliferation. Mesencephalic cells containing the substantia nigra pars compacta (excluding the ventral tegmental area) were dissected from coronal sections from brains of postnatal day 1 or 2 rat pups. The cells were dissociated in papain and plated onto the glial cells at densities of 4×10^5 per coverslip. Cultures were grown for 6-8 d and then treated by exchanging 1 mL of the media in each plate with 1 mL of fresh media amended with test compound(s) and DMSO (final concentration 0.01%).

2.3.2 Immunocytochemistry (TH, NeuN, α -synuclein)

After 48-h treatment, cultures were fixed in paraformaldehyde (4%) for 30 min, washed with PBS, blocked with normal donkey serum (5%) and Triton (0.5%) in PBS for 1-2 h, incubated with antibodies against tyrosine hydroxylase (TH, 1:1500, anti-rabbit, Calbiochem) and neuronal nuclei (NeuN, 1:200, anti-mouse, Millipore) overnight at 4°C, washed with 3x and 1x PBS, incubated with Alexa Fluor 488 (1:200, Invitrogen) and 555 (1:1500, Invitrogen) secondary antibodies at room temperature (RT) for 2 h, and washed with 0.1% Tween-20 in PBS and then with PBS before coverslipping. All TH-immunoreactive neurons were counted, and NeuN-immunoreactive neuron counts were estimated for each coverslip from neurons quantified in five representative fields of view using a 20x objective. Quantification was determined by blinded raters.

In some experiments, cultures were incubated with antibodies against TH and α -synuclein (1:500, anti-mouse, BD Biosciences) but not NeuN. Relative levels of α -

synuclein in TH-positive cells were determined as previously described.⁹ Briefly, exposure time was held constant as digital images were obtained using a 40x objective with filters for TH- and α -synuclein-immunoreactivity. Images were stacked into a single sequence, a polygonal region of interest was manually drawn around the TH⁺ neuron, and mean and total intensity of the α -synuclein-immunoreactive image were determined inside the region of interest using the GNU Image Manipulation Program (GIMP 2.6). Analyses of coverslips treated with TH, Alexa Fluor 488, and Alexa Fluor 555 antibodies (but not α -synuclein) revealed that bleed-through and cross-reactivity were negligible.

2.3.3 Determination of cellular contents of dopamine and its metabolites

Some cultures were extracted in perchloric acid (100 mM) and EDTA (0.1%) and stored at -80°C until analysis. Samples were separated on a C18 reverse phase column (TSKgel Super ODS 2 μ m particle size, 10 x 2.1 mm, maintained at 33°C, Tosoh Bioscience, Grove City, OH) using a mobile phase (2.5% methanol, 100 mg/L sodium-1-octane sulfonate, 42 mM citric acid, 38 mM sodium acetate, 50 mg/L EDTA) pumped at 0.2 mL/min (LC-10AD pump, Shimadzu, Columbia, MD). Monoamines and metabolites were oxidized on a glassy carbon electrode against a Ag/AgCl reference (Antec Leyden, Palm Bay, FL) with an applied potential of 0.75V. Data were collected using EzChrom software (Agilent, Santa Clara, CA).

2.4 ALDH activity assays

2.4.1 Primary neuronal suspensions

Mesencephalic neurons (postnatal day 2) were dissected and dissociated as described above (Section 4.3.1). Instead of plating, neurons were resuspended in buffer from the Aldefluor® kit (STEMCELL Technologies, Vancouver, Canada). Aldefluor® was added (1 $\mu\text{L}/\text{mL}$) to the neuronal suspension, and 300- μL aliquots were immediately transferred to culture tubes containing 3 μL of test compounds, resulting in final concentrations of 100 nM-20 μM . Culture tubes were incubated at 37°C for 30 min, gently shaking at the beginning and after 15 and 30 min. Using flow cytometry (Beckman XL-MCL FACs), cells were gated by forward- and side-scatter, and intracellular green fluorescence was measured on channel FL1. ALDH inhibition was determined by comparing fluorescence in the presence or absence of test compounds.

2.4.2 Enriched mitochondria preparations

Rat mitochondria were isolated mechanically from liver at 0.25 g/mL in homogenization buffer containing 5 mM Tris (pH 7.2), 0.25 M sucrose, and 0.5 mM EDTA.^{127,128} Homogenate was diluted to 0.02 g/mL and centrifuged (480 g, 4°C, 10 min). Supernatant was recovered and centrifuged (4200 g, 4°C, 7 min). Pellets from both centrifugations were combined, centrifuge-washed twice with 25 mL of buffer (4200 g, 4°C, 7 min), resuspended in 20 mL of buffer, aliquoted, and stored at -80°C.

Mitochondria preparation (10 μL) was exposed to test compound for 5 min in 170 μL of 50 mM pyrophosphate buffer (pH 9.0), 50 mM NAD^+ , 0.1 mM pyrazole, 0.5% w/v sodium deoxycholate, and 2 mM rotenone (added in 2.7 μL methanol) and transferred to a 96-well plate. Absorbance at 340 nm was monitored for 10 min at 5-s intervals after 1 mM acetaldehyde (20 μL) was added (SpectraMax® 340PC³⁸⁴ Absorbance Microplate

Reader with SoftMax® Pro data acquisition software, Molecular Devices). ALDH activity was determined from the slope as the increase in absorbance over time from 1-3 min.

2.5 26S proteasome activity assay

26S UPS activity was determined by FACs as previously described.²⁰ Briefly, neuroblastoma SK-N-MC cells transfected with an EGFP-degron fusion protein and passaged multiple times were grown at an initial density of 10^5 per mL (1 mL/well) in 24-well plates in DMEM/F12 media amended with 10% fetal bovine serum and 1% Pen-Strep. After cells reached confluency (3 d), media was replaced with fresh media amended with test compounds (2 mL/well). After 48 h, FACs was used to gate trypsinized cells by forward- and side-scatter and measure intracellular green fluorescence on channel FL1 (Beckman XL-MCL). The level of fluorescence corresponded to the level of EGFP-degron fusion protein that was not selectively degraded by the proteasome.¹²⁹ Thus, high fluorescence represents low UPS activity.

2.6 Statistical analyses

Demographic characteristics were compared for deviation from expected by chi-square test (categorical variables) or for difference in mean by t-test (age). Logistic regression analyses were performed on the epidemiologic data using SAS 9.1 (SAS Institute Inc., Cary, North Carolina). Odds ratios and 95% confidence intervals were estimated after adjusting for age (continuous variable), sex (male/female), county of residence (Fresno/Kern/Tulare), education (less than twelve years of schooling/twelve

years or completion of GED/more than twelve years), and smoking status (current/former/never). Sensitivity analyses were performed to assess the effects of adjustments for race (Caucasian/non-Caucasian) and family history of PD (first-degree family history present/absent). Additional sensitivity analyses were performed excluding twenty-three controls who had lived at an address for more than two years prior to 1999 in a cluster already represented during those years, and excluding forty-four cases and ninety-five controls who were missing one or more occupational addresses from 1974-1999. For trend tests, quartile categories were assigned scores of 0, 1, 2, 3, or 4 and entered into the logistic regression equation as a linear term. The Wald statistic was used as a test for linear trend of the odds ratio.

In biochemical assays, IC_{50} values were determined using sigmoidal curve fits of percent inhibition at varying concentrations (GraphPad PRISM 5). For all other analyses, statistical significance was determined using a paired t-test. Standard error values are given in the text and in figure error bars.

3. Results

3.1 Benomyl exposure is associated with increased incidence of PD

The Parkinson's Environment & Genes (PEG) Study is a population-based case-control epidemiologic study recruiting PD patients ("cases") and neurologically-normal subjects ("controls"), specifically designed to investigate the impact of ambient pesticide exposures on risk of PD. Three hundred sixty cases and seven hundred fifty-four controls were included in these analyses (Supplementary Table 1). Individuals were grouped for analyses in two different ways—unexposed vs. above vs. below median

exposure estimates, and unexposed vs. each of four quartiles—based on records of benomyl applied over twenty-six years (1974-1999) and estimated for areas within five hundred meters of their reported occupational or residential addresses.

Using occupational addresses, risk of PD increased 65% for individuals with an estimated ambient benomyl exposure at their workplace equal to or above the median as compared to those who were unexposed (OR=1.65, 95%CI: 1.17-2.32; Table 1). This risk increased to almost two-fold for those with estimated exposures in the highest quartile (OR=1.92, 95%CI: 1.25-2.96), demonstrating a dose-response trend across the quartiles ($p < 0.01$; Supplementary Table 2). We observed no association between benomyl exposure and PD based on residential addresses.

These findings did not change in sensitivity analyses adjusting for race/ethnicity or family history of PD, or when excluding subjects potentially over-representing particular residential clusters or missing one or more years of occupational data. This benomyl-PD association at occupational addresses was present for both males and females (OR_{males}=1.81, OR_{females}=1.42; Supplementary Table 3).

3.2 Benomyl causes selective dopaminergic cell damage *in vitro* and *in vivo*

Following up on this epidemiologic finding, we investigated benomyl's mechanisms of toxicity *in vitro* and *in vivo*. Since dopaminergic neurons are particularly vulnerable in PD, neurotoxicity was investigated in primary mesencephalic cultures using tyrosine hydroxylase immunoreactivity (TH⁺) as a marker for dopaminergic neurons and neuronal nuclei immunoreactivity (NeuN⁺) as a marker for total neurons. A representative field of view is shown at 20x magnification with filters distinguishing each

antibody (Figure III-2a-b). Benomyl was selectively toxic to dopaminergic neurons, resulting in a $24\pm 6\%$ decrease in TH⁺ cells at 100 nM and a $35\pm 4\%$ decrease at 1 μ M after 48-h exposures (Figure III-2b). There was no significant loss of total NeuN⁺ neurons at either concentration, demonstrating selective toxicity of benomyl. The total number of NeuN⁺ neurons (i.e., total neurons) did not significantly change despite the loss of TH⁺ neurons since TH⁺ cells only contributed on the order of 1% of total neurons counted.

In order to determine if dopaminergic neurons were selectively vulnerable in an *in vivo* model, we employed transgenic zebrafish (*Danio rerio*) lines that label specific neuronal populations. In the *ETvmat2:GFP* zebrafish line, neurons expressing vesicular monoamine transporter 2 (VMAT2) fluoresce green—these include dopaminergic, (nor)adrenergic, and serotonergic neurons.¹²⁴ *ETvmat2:GFP* embryos were exposed to 1 μ M benomyl from 5 hr postfertilization until 5 d postfertilization; whole-mounted embryos were scanned using confocal microscopy, and images were reconstituted to three-dimensional projections in order to count clusters of neurons corresponding to anterior (including olfactory bulb and telencephalon) and diencephalic VMAT2⁺ neurons (Figure III-3a-b). Neuronal counts decreased $24\pm 9\%$ in VMAT2⁺ anterior clusters ($P=0.041$, $n=19$; Figure III-3g) and $18\pm 9\%$ in VMAT2⁺ diencephalic clusters ($P=0.15$), constituting an overall $22\pm 8\%$ decrease in VMAT2⁺ neurons in these clusters ($P=0.043$). Fluorescence similarly decreased $25\pm 13\%$ (anterior, $P=0.16$; Figure III-3h), $38\pm 13\%$ (diencephalon, $P=0.061$), and $27\pm 12\%$ (overall, $P=0.089$). In order to determine if non-dopaminergic neurons were injured by benomyl, we employed the *Tg(sensory:GFP)* zebrafish line in which Rohon-Beard (Figure III-3c-d) and trigeminal (Figure III-3e-f)

sensory neurons fluoresce green. In contrast to the *ETvmat2:GFP* exposed embryos, there were no significant differences in GFP⁺ neuron counts or fluorescence in sensory neurons. Even the complex axons of these sensory neurons were unaffected by benomyl exposure, adding further support that benomyl is toxic to dopaminergic neurons in a selective manner (Figure III-3g-h).

Benomyl exposure under these conditions was not lethal to zebrafish larvae, but swimming behavior was altered. After two weeks of exposure, benomyl-treated zebrafish exhibited a $37\pm 5\%$ decrease in spontaneous swimming distance as compared to unexposed zebrafish, suggesting that benomyl's selective toxicity to dopaminergic neurons has functional significance *in vivo*.

3.3 Benomyl inhibits ALDH and UPS activities via different moieties

We previously found that benomyl can inhibit both the UPS and ALDH. Its decomposition is spontaneous but slow, creating a reservoir for slow release of carbendazim and butyl isocyanate (BIC) (Figure III-1). The ALDH inhibitory activity is caused by BIC and its downstream metabolites including *S*-methyl *N*-butylthiocarbamate (MBT) which is further converted by P450 enzymes to MBT sulfoxide (MBT-SO), a very potent ALDH inhibitor.¹⁹ The specific moiety responsible for benomyl's UPS inhibitory activity is less clear, although we do know that carbendazim is a well-established microtubule inhibitor¹³⁰⁻¹³² and microtubule inhibitors inhibit the UPS.⁶² We took advantage of these separate metabolic pathways to investigate potential mechanisms of action through which benomyl damages dopaminergic neurons.

In order to determine ALDH activity in primary neurons, we used a novel cell-based assay (Aldefluor®, STEMCELL Technologies, Vancouver, Canada) in which fluorescence increases with increasing ALDH activity. Exposure of *ex vivo* suspensions of 2-day-old nigral neurons to benomyl for 30 min resulted in concentration-dependent ALDH inhibition (Figure III-4a). ALDH activity was inhibited by $19 \pm 0.4\%$ ($p < 10^{-6}$, $n=3$) at the lowest concentration tested (100 nM), progressively increasing to $30 \pm 0.8\%$ inhibition at the highest concentration tested (10 μM ; $p < 10^{-27}$, $n=10$). MBT exposure (10 μM) inhibited ALDH activity by $12 \pm 1\%$ ($p < 10^{-4}$, $n=5$). In contrast, carbendazim was ineffective at concentrations investigated up to 20 μM (Figure III-4a).

The ALDH inhibitory IC_{50} s of benomyl and its metabolites were quantitated using an enriched mitochondria preparation from rat liver. Benomyl and BIC were essentially equipotent with IC_{50} s of 140 ± 20 nM and 120 ± 30 nM, respectively. MBT had a somewhat higher IC_{50} of 1.3 ± 0.2 μM (Figure III-4b). Carbendazim did not inhibit ALDH activity. These results are consistent with those observed by Staub *et al.* for hepatic mitochondria prepared from mice.¹⁹

To determine the moiety responsible for benomyl's UPS inhibitory activity, we used an SK-N-MC neuroblastoma cell line that constitutively expresses a GFP^u degen.^{20,129} In this assay, GFP accumulates and fluorescence increases when the UPS is not functioning properly. Benomyl inhibited the UPS with an IC_{50} of 5.7 ± 0.5 μM after 48 h of exposure (Figure III-4c). Carbendazim exposure had the same effect ($\text{IC}_{50} = 5.7 \pm 0.3$ μM), whereas MBT did not inhibit the UPS. Collectively, these experiments revealed that carbendazim is responsible for UPS dysfunction, presumably via microtubule inhibition, whereas BIC and its enzymatically-activated metabolites

(including MBT) inhibit ALDH activity. Since BIC is an unstable compound, MBT and carbendazim were used to distinguish between these mechanisms of action in further studies.

3.4 Benomyl neurotoxicity occurs via ALDH inhibition

To determine if benomyl's neurotoxicity is attributable to its ALDH or UPS inhibitory activity, cultures were exposed to MBT or carbendazim under the same conditions as described for benomyl treatment. MBT exposure (1 μ M) resulted in a $27\pm 6\%$ decrease in TH⁺ cells (Figure III-2b), comparable to benomyl exposure, and similarly had no effect on NeuN⁺ cells. In contrast, carbendazim exposure (1 μ M) alone had no significant effect on neuron counts, and there was no synergistic effect when cells were exposed simultaneously to MBT and carbendazim. Since MBT represents benomyl's ALDH inhibitory action, these results suggest that benomyl's neurotoxicity is due to ALDH inhibition at the concentrations tested.

Benomyl inhibited ALDH activity in primary neurons, and benomyl's ALDH-inhibiting metabolite recapitulated its toxicity to TH⁺ neurons in primary cultures, so we hypothesized that benomyl's selective toxicity to TH⁺ neurons was caused by the effects of ALDH inhibition on DA metabolism. A subset of primary cultures treated with benomyl was sacrificed at 3 h, and cells were extracted in perchloric acid and EDTA for measurement of DA content. It is well-established that DA is oxidized by monoamine oxidase (MAO) to form DOPAL, which is then further oxidized to 3,4-dihydroxyphenylacetic acid (DOPAC) by ALDH (Figure III-1). We were unable to measure [DOPAL] directly due to its instability and very low concentrations in cultures,

so we measured [DA] and [DOPAC] to determine if DA homeostasis shifted with benomyl treatment. [DOPAC] was $42 \pm 11\%$ less in benomyl-treated cultures ($p < 0.05$, $n = 16$), and [DA] remained relatively unchanged, so [DOPAC]/[DA] was $38 \pm 13\%$ less ($p < 0.05$), consistent with ALDH inhibition in these neurons.

To test the hypothesis that reducing the formation of toxic ALDH substrates (i.e., DOPAL) would attenuate benomyl's neurotoxic effect, we added the MAO inhibitor pargyline to primary cultures concurrently exposed to benomyl or MBT. TH⁺ neuronal loss was attenuated by $30 \pm 9\%$ ($n = 13-14$; Figure III-5) in cultures co-treated with pargyline (200 μM) and benomyl (1 μM). Pargyline completely prevented neurotoxicity in cultures treated with MBT (1 μM), a less potent ALDH inhibitor ($p < 0.05$, $n = 14-15$). Pargyline alone had no effect on TH⁺ neuronal counts at this concentration.

3.5 Benomyl neurotoxicity is independent of α -synuclein

Since the major pathologic hallmark of PD is the formation of Lewy bodies which are comprised primarily of α -synuclein aggregates, α -synuclein levels were measured using immunocytochemistry in surviving dopaminergic neurons after benomyl exposure. α -Synuclein levels did not change significantly in cells exposed to benomyl, MBT, carbendazim, or a combination of MBT and carbendazim (data not shown), suggesting that benomyl toxicity is independent of α -synuclein and dominated by alterations in DA homeostasis. This is in contrast to ziram toxicity which increases α -synuclein levels and causes dopaminergic cell injury by inhibiting E1 ligase activity in the UPS.⁹ Here, investigations with benomyl elucidate a novel mechanism (ALDH inhibition) by which a

pesticide may be associated with increased PD risk and dopaminergic cell damage independent of α -synuclein levels.

4. Discussion

We have been investigating the potential role environmental toxicants play in the etiology of PD with the dual goals of reducing risk through determining safer practices and gaining novel clues into the pathogenesis of the disease that may be generalizable to all PD patients. Epidemiologic associations between PD occurrence and general pesticide use have been confirmed in meta-analyses, but most previous studies relied on subject recall and did not have sufficient information or statistical power to determine associations with specific toxicants. The PEG Study overcomes these limitations with a novel GIS model that incorporates historical state-mandated commercial agricultural Pesticide Use Reports and land-use maps to determine the amounts of specific pesticides applied near subjects' occupational or residential addresses, providing estimates of subjects' relative ambient exposures in a heavy pesticide use region of California. We have used this method to report positive associations between PD onset and exposures to ziram, maneb, and paraquat.^{85,87}

Here we show that exposures to ambient benomyl at the workplace (based on benomyl application estimates over a 26-year period) were associated with 65% to almost two-fold increases in risk of developing PD, after accounting for known PD risk factors (e.g., age, sex). Analyses based on occupational addresses potentially incorporate the best estimates of subjects' ambient benomyl exposures since pesticide applications occur during the workday when subjects would have been at occupational

rather than residential addresses. Analyses of ambient exposures based on residential addresses showed no association with PD, likely because the population was randomly distributed at residential addresses during evenings or weekends when commercial pesticides were not applied. Notably, this model only estimates relative ambient exposures and does not take into account other routes of exposures such as occupational handling of pesticides and drinking well water, both associated with increased risk of PD, which could potentiate the estimated risk even further.^{88,133,134}

Our finding that ambient benomyl exposure was associated with increased PD risk offered an excellent opportunity to investigate the hypothesis that this association is causal and to determine the underlying mechanisms of toxicity. It is very difficult to establish causality from an epidemiologic association, particularly for a risk-increasing factor such as a toxicant. One approach to this end is to determine if exposure in experimental models can recapitulate some of the pathologic features of the disease. Since concentrations in the range of 1.3-50 μM are necessary for benomyl's intended use as a fungicide,¹³⁵⁻¹³⁷ we used a conservative concentration range of 0.1-1 μM to ensure relevance to actual exposures for humans. Here we report relatively selective dopaminergic neuronal damage in both an *in vitro* and a novel *in vivo* model. We found significant losses of TH⁺ neurons in primary cultures exposed to benomyl at low concentrations, while the survival of other neurons was unaffected. In order to further evaluate benomyl's selective toxicity, we developed a novel *in vivo* zebrafish model. Zebrafish are vertebrates with a well-developed dopaminergic system, and since the embryos are transparent, we can visualize specific neuronal types using fluorescent reporter genes. Two different transgenic lines were used: *ETvmat2:GFP* zebrafish¹²⁴ in

which the aminergic neurons are labeled with GFP, and *Tg(sensory:GFP)* zebrafish¹²⁵ that label trigeminal and Rohon-Beard sensory neurons. Aminergic neurons in zebrafish larvae were selectively damaged while sensory neurons were preserved after benomyl exposure, in a similar manner as observed in the mesencephalic cultures. In analyzing aminergic neurons, we focused on the most prominent clusters at 5 days postfertilization. The anterior clusters shown in Figure III-3a correspond to aminergic neurons in the olfactory bulb and telencephalon; the posterior clusters are diencephalic. Holzschuh *et al.* previously reported that these clusters also include (nor)adrenergic neurons, although they are predominantly dopaminergic.¹³⁸ There was significant loss in these clusters, whereas the non-aminergic trigeminal and Rohon-Beard neurons did not undergo any damage, suggesting selectivity for dopaminergic neurons.

Benomyl's action as a fungicide is thought to be due to its ability to impair microtubule assembly, interfering with mitosis and other processes.^{139,140} We found previously that microtubule inhibitors such as nocodazole and rotenone also inhibit the UPS.⁶² Here we report that the carbendazim moiety of benomyl, a known microtubule inhibitor, confers benomyl's UPS inhibitory activity. It is unlikely that microtubule or UPS dysfunction is responsible for benomyl's toxicity observed in these primary cultures or zebrafish, given the low concentrations used. The IC₅₀ for UPS inhibition by benomyl is 5.7 μ M, which is more than an order of magnitude higher than the concentrations needed to damage dopaminergic neurons in primary cultures. Furthermore, carbendazim had no effect on neuronal survival at 1 μ M, whereas MBT recapitulated benomyl's toxicity. Our data show that benomyl and MBT, but not carbendazim, inhibit ALDH activity in primary neurons. Since MBT is the toxic metabolite, ALDH inhibition

likely confers benomyl's neurotoxicity. Wey *et al.* recently reported TH⁺ neuronal loss in *Aldh1a1*^{-/-}*xAldh2*^{-/-} mice.¹⁴¹ Although environmental investigations like ours can be confounded by multiple simultaneous toxic mechanisms, their genetic approach targeting ALDH1 and ALDH2 yielded a result similar to what we observed *in vitro* and *in vivo*, supporting our hypothesis that benomyl exposure damages dopaminergic neurons via ALDH inhibition. The present work adds an epidemiologic PD association to demonstrate the relevance of this mechanism to PD pathogenesis.

Our observed alterations in DA metabolites after benomyl exposure add further support for ALDH inhibition as the cause of benomyl's neurotoxicity. Wey *et al.* also reported DOPAL accumulation concomitant with TH⁺ neuronal loss and behavioral deficits in mice lacking cytosolic and mitochondrial ALDHs.¹⁴¹ Burke *et al.* reported that DOPAL is 400-fold more toxic to dopaminergic neurons *in vivo* than its precursor (DA) or its ALDH product (DOPAC).^{14,142,143} Thus, ALDH inhibition leads to the accumulation of DOPAL and provides a mechanism for benomyl's selective toxicity to dopaminergic neurons. Consistent with this hypothesis, reducing DOPAL synthesis with an MAO inhibitor mitigated benomyl's toxicity.

In summary, pesticide exposure has been suggested to be a major risk factor for PD, and here we report an epidemiologic association between chronic benomyl exposure and increased PD risk. We found that dopaminergic neurons are selectively vulnerable to benomyl exposure both in neuronal cultures and in a novel *in vivo* zebrafish model. Benomyl and its metabolites are potent ALDH inhibitors, and several converging lines of evidence reveal ALDH inhibition as a mechanism of toxicity by which benomyl and other environmental toxicants may be associated with PD risk.

Augmenting ALDH activity may be a new therapeutic target for designing disease-modifying therapies for PD.

Figure III-1. Aldehyde dehydrogenase inhibition as a potential mechanism of benomyl-induced Parkinson's disease. Benomyl is efficiently metabolized to several potent ALDH inhibitors, so exposure leads to the accumulation of the toxic dopamine metabolite DOPAL. This offers a possible explanation for the selective toxicity to dopaminergic neurons observed in PD pathogenesis. ALDH is a potential therapeutic target to alter disease progression.

Abbreviations: BIC, butyl isocyanate; MBT, *S*-methyl *N*-butylthiocarbamate; MBT-SO, *S*-methyl *N*-butylthiocarbamate sulfoxide; DA, dopamine; DOPAL, 3,4-dihydroxyphenylacetaldehyde; DOPAC, 3,4-dihydroxyphenylacetic acid; GSH, glutathione; CYP, cytochrome P450; MAO, monoamine oxidase; ALDH, aldehyde dehydrogenase; Cys, cysteine residue

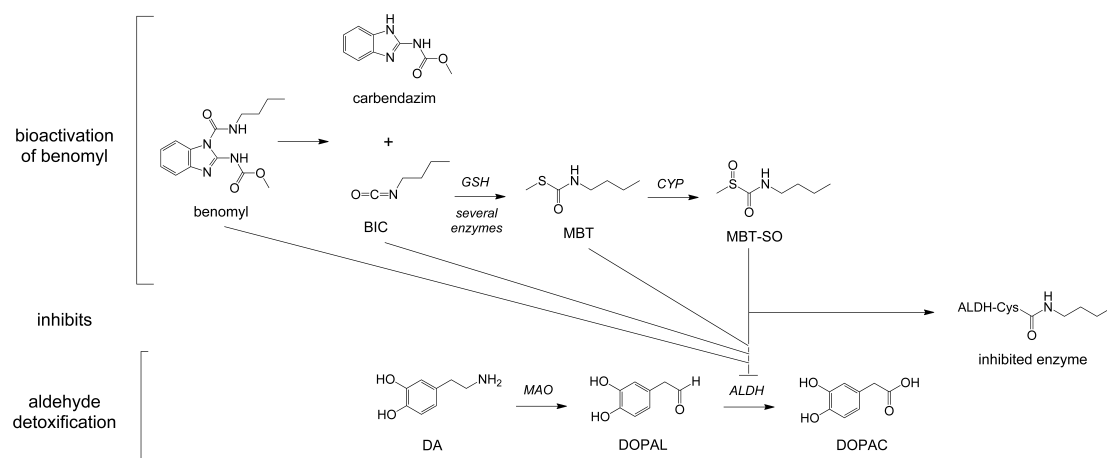


Figure III-2. Dopaminergic neuronal damage in primary mesencephalic cultures exposed to benomyl or its metabolites. Representative field of view (20x) shows immunoreactive (a) dopaminergic neurons (TH⁺) and (b) neuronal nuclei (NeuN⁺). (c) Exposure to 100 nM or 1 mM benomyl results in 24±6% ($P=0.0017$, $n=16$) and 35±4% ($P=5.5 \times 10^{-10}$, $n=47$) respective losses of TH⁺ neurons as compared to untreated cultures. MBT exposure recapitulates this effect ($P=5.5 \times 10^{-5}$, $n=28$), whereas carbendazim does not significantly damage dopaminergic neurons ($P=0.73$, $n=10$). Since MBT is either the proximal or penultimate benomyl metabolite that inhibits ALDH activity, there appears to be an association between neuronal damage and ALDH inhibition; proteasomal inhibition by the carbendazim moiety is not sufficient to kill cells under the same conditions. * $P<0.05$, ** $P<0.01$, *** $P<0.0001$

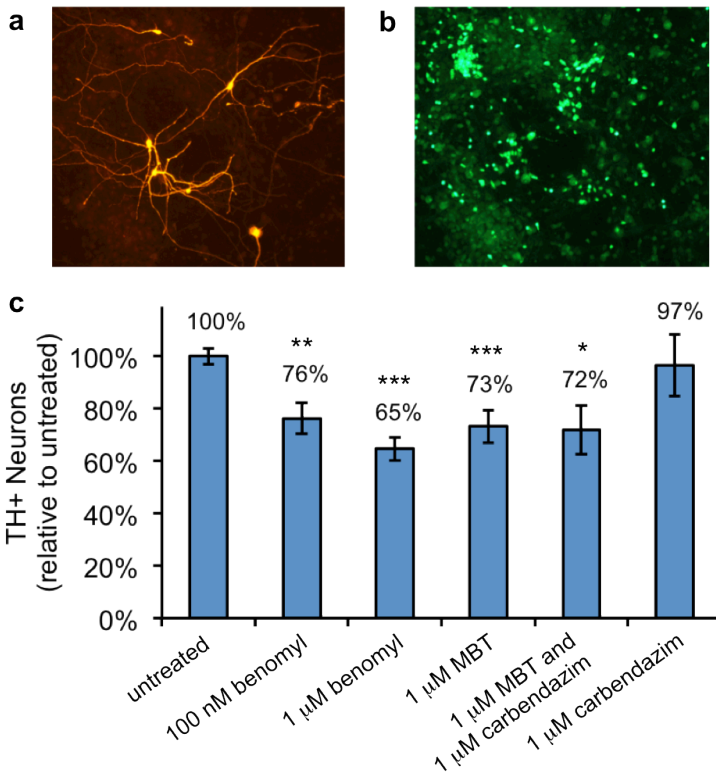


Figure III-3. Aminergic neuronal damage in *Danio rerio* larvae exposed to benomyl.

Representative confocal images of zebrafish larvae (a,c,e) unexposed or (b,d,f) bathed in 1 μ M benomyl from 5 hours postfertilization until 5 days postfertilization are shown.

(g) Neuronal counts (a-b) decreased in VMAT2⁺ anterior and diencephalic clusters of *ETvmat2:GFP* zebrafish exposed to benomyl (solid bars) but were unaffected in (c-d)

Rohon-Beard and (e-f) trigeminal neurons in *Tg(sensory:GFP)* zebrafish. (h)

Measurement of total fluorescence yielded the same results. * $P < 0.1$, ** $P < 0.05$

Abbreviations: LC, locus coeruleus; De, diencephalon; OB, olfactory bulb; Te,

telencephalon

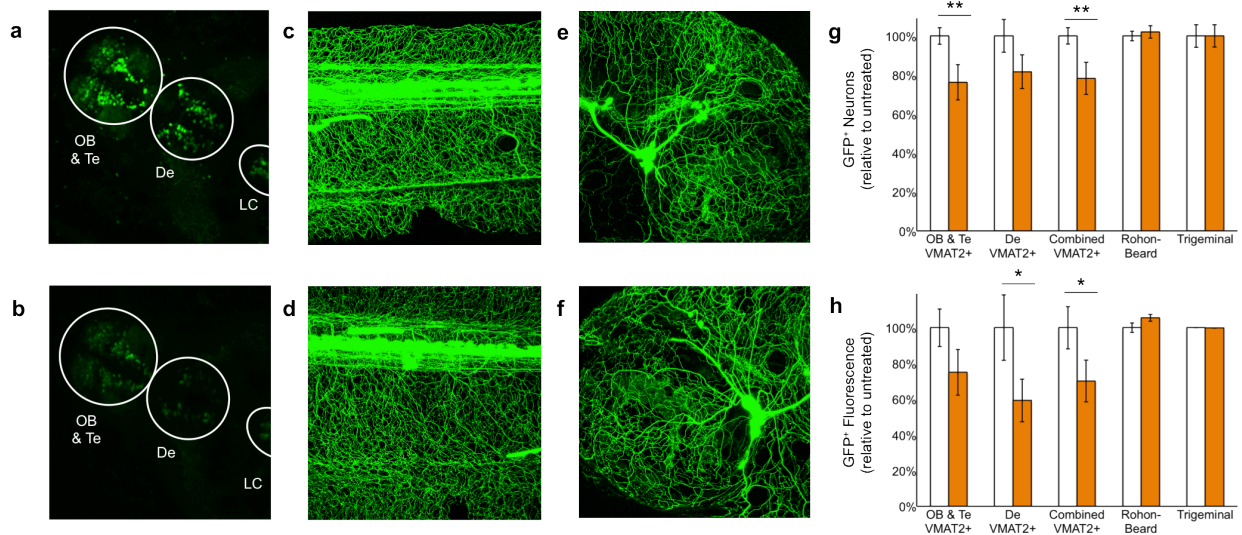
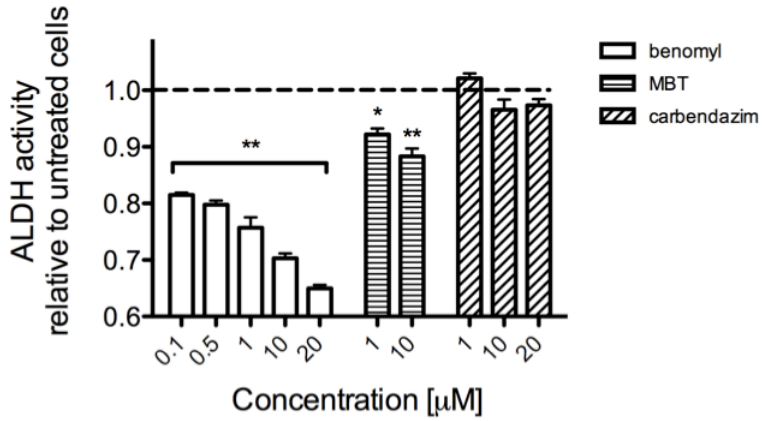
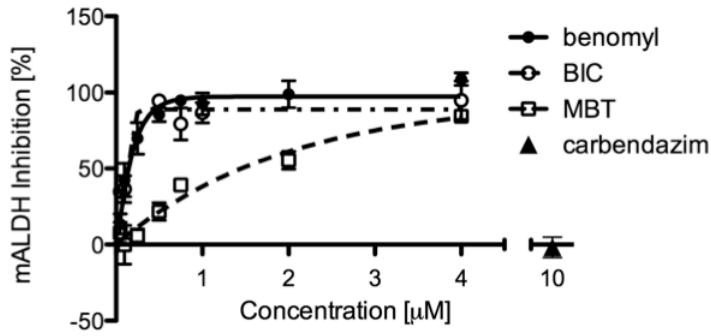
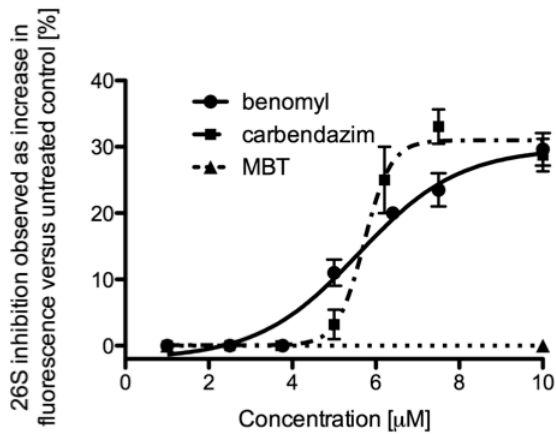


Figure III-4. Inhibitory actions of benomyl and its metabolites. (a) Exposure to benomyl or MBT inhibited ALDH activity *ex vivo* in mesencephalic neurons dissociated from 2-day-old rat pups (n=3-11). (b) Benomyl inhibited *in vitro* ALDH activity in rat hepatic mitochondria preparations with an IC_{50} of 140 ± 19 nM (n=2-4). BIC had essentially the same effect ($IC_{50} = 120 \pm 32$ nM; n=3-4); MBT was somewhat less potent with an IC_{50} of 1.3 ± 0.2 μ M (n=4-8). Carbendazim did not significantly inhibit ALDH activity at up to 20 μ M (n=4). (c) A reporter protein revealed that benomyl inhibited 26S UPS activity in SK-N-MC neuroblastoma cells with an IC_{50} of 5.7 ± 0.5 μ M (n=4-14). Carbendazim exposure had the same effect (IC_{50} of 5.7 ± 0.3 μ M, n=4-14), whereas MBT exposure up to 10 μ M had no effect (n=5). (d) Benomyl and its BIC/MBT metabolites inhibit ALDH activity at lower concentrations than benomyl and its carbendazim moiety inhibit the 26S UPS.

* $P < 0.01$, ** $P < 0.0001$

Abbreviations: SE, standard error; 26S UPS, ubiquitin-proteasome system

a**b****c****d**

IC_{50} [μM] (SE)	ALDH	26S UPS
benomyl	0.14 (0.02)	5.7 (0.5)
BIC	0.12 (0.03)	
MBT	1.3 (0.2)	>10 [#]
carbendazim	>10 [#]	5.7 (0.3)

[#]no inhibition up to 10 μM

Figure III-5. Neuroprotection via reducing DOPAL accumulation with MAO inhibitor. The neuronal loss resulting from 1 μM benomyl or MBT exposure was mitigated by co-treatment with the MAO inhibitor pargyline (200 μM , $n=13-28$). Because MAO-B inhibition reduces the metabolism of dopamine to DOPAL, this suggests that DOPAL is toxic to dopaminergic neurons, and that benomyl is toxic via DOPAL accumulation as a result of ALDH inhibition. * $P=0.0027$, ** $P=2.4 \times 10^{-4}$, *** $P=6.1 \times 10^{-5}$

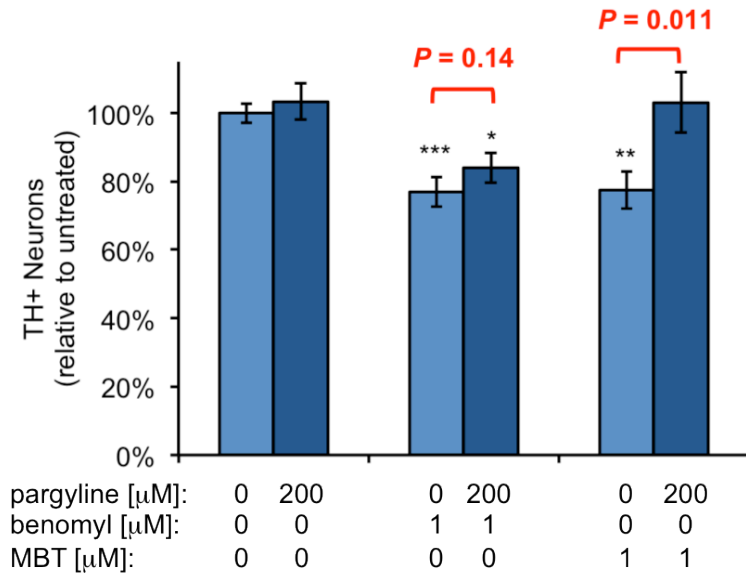


Table III-1. Associations between PD and estimated ambient occupational or residential benomyl exposures

Exposure^a	Cases (n=360)	Controls (n=754)	OR^b (95%CI)	P-value^c
Occupational, n(%)				
No	217 (60.3)	531 (70.4)	1.00	
Low	49 (13.6)	106 (14.1)	1.06 (0.71-1.59)	0.78
High	94 (26.1)	117 (15.5)	1.65 (1.17-2.32)	0.004
Residential, n(%)				
No	209 (58.1)	467 (61.9)	1.00	
Low	72 (20.0)	143 (19.0)	1.01 (0.70-1.45)	0.96
High	79 (21.9)	144 (19.1)	1.00 (0.70-1.43)	0.99

Abbreviations: OR = unconditional logistic odds ratio; CI = confidence interval

^a “Low” exposure defined as below the median value in exposed controls; “High” exposure defined as equal to or above the median value in exposed controls.

^b adjusted for age (continuous), sex (male/female), smoking status (current, former, never), county (Fresno, Kern, Tulare), and education (<12 yrs, =12 yrs, >12 yrs).

^c For multiple testing considerations, six tests were performed and a p-value of 0.008 was considered statistically significant.

Supplementary Table III-1. Demographics of the Parkinson's Environment & Genes (PEG) Study

Parameter	Cases (n=360)	Controls (n=754)	P-value^a
Gender, n (%)			
Female	154 (42.8)	402 (53.3)	
Male	206 (57.2)	352 (46.7)	0.001
Age ^b			
Mean (sd)	68.3 (10.2)	66.9 (11.2)	0.036
Range	34-88	35-99	
Race ^c , n (%)			
Caucasian, non-Hispanic	290 (80.6)	526 (69.8)	
Caucasian, Hispanic	47 (13.1)	144 (19.1)	
Native American	16 (4.4)	35 (4.6)	
African American	3 (0.8)	25 (3.3)	
Asian American	4 (1.1)	22 (2.9)	0.002
County, n (%)			
Fresno	163 (45.3)	310 (41.1)	
Kern	129 (35.8)	322 (42.7)	
Tulare	68 (18.9)	122 (16.2)	0.087
Smoking, n (%)			
Never	188 (52.2)	364 (48.3)	
Former	152 (42.2)	213 (28.3)	
Current	20 (5.6)	177 (23.5)	<0.001
Education, n (%)			
< 12 years	67 (18.6)	111 (14.7)	
= 12 years	96 (26.7)	156 (20.7)	
> 12 years	197 (54.7)	487 (64.6)	0.007
Family history of PD ^d , n (%)			
No	307 (85.3)	691 (91.6)	
Yes	53 (14.7)	63 (8.4)	0.001

^a P-value for chi-square test or t-test

^b age at diagnosis for cases; age at interview for controls

^c race information unrecorded for two controls

^d defined as first-degree relative with PD; data unrecorded and assumed negative for 27 controls

Supplementary Table III-2. Associations between PD risk and estimated ambient occupational or residential benomyl exposures, by quartiles in exposed controls

Exposure^a	Cases (n=360)	Controls (n=754)	OR^b (95%CI)	P-value^c
Occupational, n(%)				
No	217 (60.3)	531 (70.4)	1.00	
1 st Quartile	23 (6.4)	55 (7.3)	0.98 (0.57-1.68)	0.93
2 nd Quartile	26 (7.2)	51 (6.8)	1.14 (0.67-1.94)	0.62
3 rd Quartile	40 (11.1)	62 (8.2)	1.38 (0.87-2.18)	0.18
4 th Quartile	54 (15.0)	55 (7.3)	1.92 (1.25-2.96)	0.003
			<i>p-value for trend</i>	<i>0.0029</i>
Residential, n(%)				
No	209 (58.1)	467 (61.9)	1.00	
1 st Quartile	31 (8.6)	71 (9.4)	0.86 (0.53-1.39)	0.53
2 nd Quartile	41 (11.4)	72 (9.5)	1.17 (0.75-1.85)	0.49
3 rd Quartile	31 (8.6)	73 (9.7)	0.83 (0.51-1.34)	0.45
4 th Quartile	48 (13.3)	71 (9.4)	1.17 (0.75-1.81)	0.50
			<i>p-value for trend</i>	<i>0.72</i>

Abbreviations: OR = unconditional logistic odds ratio; CI = confidence interval

^a Exposure quartiles defined using distributions of exposed controls, separately for occupational or residential estimates

^b adjusted for age (continuous), sex (male/female), smoking status (current, former, never), county (Fresno, Kern, Tulare), and education (<12 yrs, =12 yrs, >12 yrs).

^c For multiple testing considerations, six tests were performed so a *P*-value of 0.008 was considered statistically significant.

Supplementary Table III-3. Associations between PD risk and estimated ambient occupational or residential benomyl exposures, stratified by sex

Exposure ^a	Males				Females			
	Cases (n=206)	Controls (n=352)	OR ^b (95%CI)	P-value ^c	Cases (n=154)	Controls (n=402)	OR ^b (95%CI)	P-value ^c
Occupational, n(%)								
No	112 (54.4)	235 (66.8)	1.00		105 (68.2)	296 (73.6)	1.00	
Low	30 (14.6)	54 (15.3)	1.16 (0.68-2.00)	0.59	19 (12.3)	52 (12.9)	0.91 (0.49-1.69)	0.76
High	64 (31.1)	63 (17.9)	1.81 (1.15-2.84)	0.010	30 (19.5)	54 (13.4)	1.42 (0.83-2.43)	0.20
Residential, n(%)								
No	114 (55.3)	216 (61.4)	1.00		95 (61.7)	251 (62.4)	1.00	
Low	44 (21.4)	61 (17.3)	1.24 (0.75-2.02)	0.40	28 (18.2)	82 (20.4)	0.80 (0.46-1.38)	0.42
High	48 (23.3)	75 (21.3)	1.06 (0.65-1.71)	0.82	31 (20.1)	69 (17.2)	0.92 (0.53-1.58)	0.76

Abbreviations: OR = unconditional logistic odds ratio; CI = confidence interval

^a “Low” exposure defined as below the median value in exposed controls; “High” exposure defined as equal to or above the median value in exposed controls.

^b adjusted for age (continuous), sex (male/female), smoking status (current, former, never), county (Fresno, Kern, Tulare), and education (<12 yrs, =12 yrs, >12 yrs).

- ^c For multiple testing considerations, six tests were performed and a p-value of 0.008 was considered statistically significant.

CHAPTER IV

Aldehyde dehydrogenase dysfunction increases Parkinson's disease risk via gene-environment interactions

1. Introduction

1.1 Pesticides and Parkinson's disease (PD)

Parkinson's disease (PD) is the second most prevalent neurodegenerative disorder, affecting millions of people worldwide ¹. PD is a progressive motor disorder characterized primarily by death of dopaminergic neurons in the substantia nigra pars compacta; other areas of the central and peripheral nervous systems have demonstrated cell death as well ¹⁰. A pathological hallmark of PD is the formation of intracytosolic Lewy bodies containing synuclein, ubiquitin, and other protein aggregates.

Although some familial cases have been reported, the etiology of most cases remains unknown. Rare Mendelian and high-risk genes account for only a small percentage of cases. Common but low-risk genetic variants have been detected by genome-wide association studies, but these only account for a small increase in risk. If an individual has all of the confirmed polymorphisms that have been associated with PD, the odds ratio would still be only 2.51, leaving the majority of the risk unaccounted for ¹¹⁴. A number of epidemiologic studies have

found associations between PD occurrence and rural living, well-water consumption, farming occupations, and pesticide exposure^{79-82,85,87,90,91,98,115-117}.

The mechanisms through which pesticides contribute to PD pathogenesis remain to be elucidated.

1.2 Aldehyde dehydrogenase (ALDH) inhibition

The UCLA Parkinson's Environment and Gene (PEG) Study, a case-control epidemiologic study, is unique in its ability to exploit state-mandated Pesticide Use Reports (PURs) rather than relying on subject recall to estimate lifetime occupational and residential pesticide exposures⁷⁷. Because this study is based in a heavily agricultural region, it has the statistical power to investigate specific pesticides. Previously, we reported results for specific pesticides^{85,87} and for gene-pesticide interactions in PD with maneb/paraquat^{67,88,144} and the organophosphates diazinon, chlorpyrifos, and parathion⁸⁶.

We recently showed that the fungicide benomyl damaged dopaminergic neurons by inhibiting ALDH activity, and was associated with increased PD risk (Chapter III). These findings motivated the present study in which we identify fourteen compounds that inhibit ALDH activity in neurons. More than 50% of the PEG study population had been exposed to one or more of these pesticides over 26 years; here we report increased PD risks associated with increased exposures to these pesticides. Furthermore, we report potentiation of increased risk when considering contributions of both aggregate pesticide exposure and

genetic variants in the *ALDH2* gene. This study provides strong evidence for the relevance of ALDH inhibition to PD pathogenesis.

2. Methods

2.1 Chemicals

All chemicals were obtained with the highest available purity. Pesticides were from Chem Service, Inc. or Sigma-Aldrich.

2.2 Measurement of ALDH activity in neuronal cell suspensions (*ex vivo*)

ALDH activity was measured in suspensions of neurons derived from the substantia nigra of newborn rats, in the presence or absence of test compounds, as previously described (Chapter III). Briefly, neuronal suspensions were derived from rat pups (postnatal day 2 to 9) anesthetized with ketamine. Mesencephalic blocks (1 mm³) containing the substantia nigra pars compacta were dissected from coronal sections. This tissue was dissociated in papain using a method adapted from Rayport et al.¹²⁶; neurons were resuspended in defined media and buffer; and ALDH inhibition was measured after 30-min exposure to test compounds and Aldefluor® (STEMCELL Technologies, Vancouver, Canada). The proprietary compound fluoresces upon ALDH activation, so intracellular fluorescence was measured with flow cytometry (FACs) on channel FL1 (Beckman XL-MCL). The higher the fluorescence, the higher the ALDH activity during incubation.

2.3 Measurement of ALDH activity in enriched rat hepatic mitochondria preparations (*in vitro*)

Rat hepatic mitochondria were isolated and mALDH activity was determined using a published method^{127,128}, as previously described (Chapter III). Briefly, mitochondria were isolated in sucrose. Absorbance was measured by spectrophotometry as NAD⁺ was converted to NADH after the addition of 1 mM acetaldehyde (SpectraMax® 340PC³⁸⁴ Absorbance Microplate Reader with SoftMax® Pro data acquisition software, Molecular Devices). *In vitro* mALDH activity was determined from the slope as the increase in absorbance over time from 1-3 min; inhibition was determined by comparing to the untreated control. IC₅₀ values were calculated using a sigmoidal curve fit of inhibition at varying concentrations (GraphPad PRISM 5).

2.4 Human subjects

This study was conducted as part of the UCLA Parkinson's Environment and Genes (PEG) Study, a population-based case-control study recruiting incident cases and neurologically-normal controls from three rural California counties (Fresno, Tulare, Kern). Written informed consent was obtained from all enrolled subjects, and all procedures were approved by the UCLA Human Subjects Committee. Subject recruitment methods and case definition criteria have been described in detail^{67,83}. Briefly, incident PD cases were recruited

between January 2001 and December 2007 through neurologists, large medical groups, and public service announcements. Cases were examined by UCLA movement disorder specialists at least once and confirmed as having clinically “probable” PD according to published criteria¹²³. Population-based controls were recruited from the same three counties, initially using Medicare lists and later, after implementation of the Health Insurance Portability and Accountability Act, from randomly-selected residential parcels identified from publicly-available tax-collector records providing addresses for all zoned living units in the three counties. More than 75% of control subjects were recruited using this latter method. There were no statistically-significant genotype or allele frequency differences between the Medicare-based and random parcel-based controls.

Eligibility criteria for cases included (1) having received a first PD diagnosis no longer than 3 years prior to recruitment, (2) being sufficiently healthy to be examined, (3) currently residing in one of the counties of interest, and (4) residing in California for at least 5 years prior to recruitment. Of the 563 eligible cases, 473 (84%) were examined on multiple occasions by a UCLA movement disorder specialist, 46 (8%) potential cases withdrew, 27 (5%) were too ill or died, and 17 (3%) moved out of the area prior to the exam. After examination, 113 (24%) patients were excluded due to diagnoses other than idiopathic PD; 360 cases were enrolled in the study. Eligibility criteria for controls included (1) not having PD; (2), (3), and (4) as above; and (5) being at least 35 years of age. Of the 688 eligible population controls, 285 (41%) declined participation, were too ill, or had moved out of the area before interview; 403

controls were enrolled in the study. Cases and controls completed a telephone interview for the collection of demographic (age, sex, race/ethnicity, education), risk factor (family history of PD, smoking behavior), and detailed occupational and residential history data.

2.5 Pesticide exposure assessment

Pesticide exposure assessments were performed using Pesticide Use Reports (PURs, collected by the California Department of Pesticide Regulation since 1974) and a geographic-information-system-based (GIS) computer model that has been described in detail^{67,118,119}. PURs provide information on the location and date of an application, the active ingredients, poundage applied, application method, crop type, and acreage of the field. Briefly, our model combines data from PURs, land-use maps (to determine locations of pesticide application more precisely), and geocoded lifetime residential and occupational addresses of subjects to estimate the pounds of pesticide applied over 26 years (1974-1999). A subject's ambient exposure was assumed to be proportional to the amount applied to crops within a 500-meter radius surrounding the subject's occupational or residential address (considered separately).

Pesticides were analyzed individually, and in terms of an Aggregate Exposure Score (AES) assessed for each individual to account for the number and amount of pesticides to which a subject was exposed. Exposure was categorized by quartiles of exposure in exposed controls, resulting in a five-level variable (unexposed plus four quartiles). The AES for an individual (i) was the

sum of the quartiles (0 for unexposed, or 1, 2, 3, 4) of exposure to each pesticide (j), for up to 10 pesticides specified in Section 3.2:

$$AES_i = \sum_j q_{i,j}$$

Thus, the AES for each subject had a minimum of 0 (subjects unexposed to the 10 pesticides of interest) and a potential maximum of 40 (subjects exposed to all 10 pesticides at the 4th quartile), although no subjects reached this maximum.

2.6 Genotype assessment

Relevant genetic contributions to PD risk were investigated using haplotypic cladistic analysis. Haplotype tagging single nucleotide polymorphisms (SNPs)¹⁴⁵⁻¹⁴⁷ for *aldehyde dehydrogenase 2 family (mitochondrial)* (NCBI geneID:217, *ALDH2*) were selected using Haploview v.4.2¹⁴⁸. Haplotypes are groups of associated polymorphic genetic markers (i.e., SNPs) that capture global gene structure in the form of chromosomal blocks that have remained unbroken by recombination events over the population history of the gene¹⁴⁷. The blocks can be identified by the high linkage disequilibrium between the SNPs^{146,147,149}. Within the haplotype block, one SNP may carry the same information as that one SNP plus many others; this one SNP is labeled a “tagSNP”¹⁴⁵. Using tagSNPs, it is possible to represent most of the variation in a region and minimize the number of SNPs for genotyping.

Most study participants provided blood or buccal samples for the extraction of DNA and consented to participation in genetic analyses. Of the 360 cases and 403 controls enrolled in the study, 350 cases and 336 controls were genotyped for five haplotype-tagging SNPs in *ALDH2* (rs737280, rs968529, rs16941667, rs16941669, rs9971942) as well as rs671 (*ALDH2*2*), a genetic variant in *ALDH2* associated with alcohol sensitivity in persons of East Asian ancestry¹⁵⁰. Genotyping was performed using the Applied Biosystems SNPLex array¹⁵¹; overall genotyping rate for included subjects was 95%. Haplotypes were derived using Phase 2.1¹⁵². Because of the multi-allelic nature of haplotypes, we used cladistic methods as implemented in the eHap v2.0 software¹⁵³ to cluster haplotypes based on shared recent ancestry.

2.7 Statistical analysis

All genetic markers were assessed for Hardy-Weinberg equilibrium in the controls using a chi-squared test. Genetic variants (5 SNPs and the haplotypic clade) were evaluated under an additive model. AES was evaluated as a continuous variable in logistic regression in all subjects combined. A single statistical interaction model was assessed by including the AES, the *ALDH2* clade (under an additive model), and their interaction term (score*clade) in a logistic regression model. For trend tests, quartile categories were assigned scores of 0, 1, 2, 3, or 4 and entered into the logistic regression equation as a linear term. The Wald statistic was used as a test for linear trend of the odds ratio. Odds ratios and 95% CIs were estimated after adjusting for age

(continuous variable), sex (male/female), and smoking status (ever/never). The p-values presented are uncorrected unless stated otherwise. We used SAS 9.1 (SAS Institute Inc., Cary, North Carolina) to perform logistic regression analyses.

3. Results

3.1 Identification of ALDH inhibitors using biochemical screen

We screened three classes of pesticides—dithiocarbamates, imidazoles, and dicarboximides—for their abilities to inhibit ALDH activity in a neuronal model. We used a concentration of 10 μ M since the EC_{50} values of pesticides against their targeted species are typically well above this concentration^{135-137,154-157}. All nine dithiocarbamates included in the screen inhibited ALDH (Figure IV-1c). Ziram was the most potent dithiocarbamate, eliciting $20 \pm 1.3\%$ less fluorescence as compared to untreated cells, reflecting lower ALDH activity. Ziram's sodium salt (sodium dimethyldithiocarbamate) and ultimate sulfur metabolite (carbon disulfide) elicited $8 \pm 1.4\%$ and $7 \pm 2.4\%$ less fluorescence, respectively, while its zinc metabolite (zinc chloride) did not affect ALDH activity. Among the imidazoles, benomyl elicited $30 \pm 0.8\%$ and triflumizole $13 \pm 2.4\%$ less fluorescence, while carbendazim and thiophanate-methyl did not inhibit ALDH. The dicarboximides captan and folpet respectively elicited $18 \pm 1.5\%$ and $17 \pm 1.9\%$ less fluorescence; vinclozolin had no effect.

We enriched hepatic mitochondria to determine IC_{50} s of five pesticides selected according to criteria described in 3.2 (Figure IV-2, Table IV-1). Benomyl

was the most potent with an IC_{50} of 140 ± 19 nM. Captan had an IC_{50} of 5.7 ± 0.6 μ M. Structurally-similar mancozeb and maneb had similar potencies (2.9 ± 0.9 and 4.6 ± 0.3 , respectively); however, ziram did not inhibit mALDH, suggesting the importance of pesticide metabolism to ALDH inhibition. We found ziram's sodium salt and zinc metabolite (zinc chloride) did not inhibit mALDH either (data not shown).

3.2 Targeting pesticides in the PEG study

The UCLA PEG study is a population-based case control study designed to investigate the individual and combined impact of genes and pesticides on risk of idiopathic PD. The study subjects contributing to these analyses are 338 cases (58% male, mean age 68.2) and 325 controls (50% male, mean age 67.3). PEG subjects are predominately Caucasian, almost equally divided between smokers and non-smokers, and have an expected prevalence of family history of PD (see Supplemental Table IV-S1).

We targeted pesticides based on the results of the ALDH screen. Benomyl, captan, mancozeb, maneb, and ziram each inhibited neuronal ALDH significantly; since 20-40% of the studied population (cases and/or controls) was exposed to each of these pesticides, there was sufficient statistical power to perform the analyses on each pesticide individually. Only 0.2-7% of the population (i.e., 1-46 individuals) was exposed to ferbam, folpet, thiram, triflumizole, or zineb; while the study did not have statistical power for individual analyses of these pesticides, they were included in determining Aggregate

Exposure Scores (see Section 2.5). The population was not exposed directly to carbon disulfide, metam sodium, or sodium dimethyldithiocarbamate, and disulfiram is not used as a pesticide, so these were excluded from epidemiologic analyses.

3.3 Increased PD risks associated with pesticide exposures

For each of the five pesticides analyzed independently (i.e., benomyl, captan, mancozeb, maneb, ziram), exposures were associated with increased PD risk (Figure IV-2, Supplemental Table IV-S2 & IV-S3). Exposures to the dithiocarbamates mancozeb, maneb, and ziram were associated with twofold to fourfold increases in risk of PD, comparing subjects at the fourth quartile level of exposure to those unexposed, and strong trends (i.e., dose-response) for increasing risk of PD with increasing quartile of exposure (p -values for trend <0.05 for one or both occupational or residential exposure). Benomyl and captan exposures at the 4th quartile were associated with 60-80% increased risks of PD, although we did not observe statistically-significant trends over all quartiles.

In addition to individual pesticides, we probed the data to determine whether PD risk increased with increasing exposures to multiple ALDH-inhibiting pesticides. We assessed each subject an AES, which weighted the number and amount (quartile) of pesticides to which each subject was exposed (see Section 2.5). Using occupational addresses, each additional quartile of pesticide exposure increased PD risk by 6%, after adjusting for age, sex, and smoking history (Table IV-2). That is, a typical individual exposed to the 4th quartile of all

ten ALDH-inhibiting pesticides would experience $(6\%)(4)(10)=240\%$ increased PD risk, or 2.4-fold increased risk, in addition to other risk factors. Using residential addresses, this increase in risk was 4%. These are greater increases in risk than commonly observed for age, the well-established risk factor for PD. In this population, age only had an odds ratio of 1.01 (Table IV-2)—that is, a 1% increase in risk per year of age.

3.4 ALDH2 genetic variation and gene-environment interaction

We observed little evidence of association between individual *ALDH2* SNPs and PD (Table IV-3). We were unable to assess rs671, the single known functional SNP in *ALDH2*, due to its rarity in our population (< 2% of subjects carried the minor allele). In haplotypic cladistic analysis (Table IV-3, Supplemental Figure IV-S1), we observed a suggestive 10-20% decrease in risk for the less prevalent *ALDH2* clade (“Clade 2”). These associations did not change when we limited our study sample to Caucasians only. In gene-environment interaction analyses (Figure IV-4), this suggestive protection conferred by Clade 2 was present only in subjects unexposed to pesticides or with an AES less than 4; for subjects with occupational AESs greater than 8, Clade 2 potentiated the risk conferred by pesticide exposure up to a sixfold increase in risk at highest AESs.

4. Discussion

4.1 Pesticides and ALDH inhibition

This is the first study to investigate the effects of several pesticides on ALDH activity in neurons. Previous studies have shown different capacities for dithiocarbamates to inhibit ALDH, but these were *in vitro* systems. For example, S-ethyl N,N-dipropylthiocarbamate (EPTC), metam, methyl isothiocyanate, dazomet, and related compounds inhibited ALDH activity in hepatic mitochondria, and EPTC in brain mitochondria, using an assay with excess acetaldehyde as the substrate ^{127,158,159}. Leiphon and Picklo reported that mancozeb and maneb—but not EPTC, ferbam, nabam, or zineb—inhibited brain mitochondrial ALDH after artificially inducing state 3-like respiration and using excess 4-hydroxy-2-nonenal (4-HNE) as the substrate ¹²². In the present study, each of the nine dithiocarbamates inhibited ALDH activity. In cases such as ferbam and zineb, intact cells appear able to metabolize the compounds to more potent metabolites, as would be expected *in vivo*. Similarly, we found ziram and sodium dimethyldithiocarbamate to be ineffective at inhibiting hepatic mALDH but potent inhibitors of neuronal ALDH *ex vivo*. Much of the inhibitory function of dithiocarbamates is likely attributable to the metabolite carbon disulfide, which we also found to inhibit ALDH *ex vivo*. One potential mechanism is through cross-linking ALDH, as carbon disulfide has been reported to cross-link proteins *in vitro* by bonding with amino groups to form dithiocarbamate residues which ultimately are converted to thiourea cross-linking structures ¹⁶⁰.

We previously reported that benomyl inhibits ALDH activity but not via its benzimidazole moiety, also known as carbendazim (Chapter III). Similarly, another carbendazim pre-cursor, thiophanate-methyl, did not inhibit ALDH. However, the imidazole triflumizole did inhibit ALDH activity. Because carbendazim and thiophanate-methyl do not alter ALDH activity, the imidazole ring likely does not confer ALDH inhibitory ability. Benomyl inhibits ALDH after metabolizing into thiocarbamate compounds¹⁹, which inhibit ALDH with similar mechanisms as described for dithiocarbamates. How triflumizole inhibits ALDH is a subject for further investigation.

Of the three dicarboximides investigated, the two that inhibited ALDH activity (captan and folpet) contained SCCl_3 . Again carbon disulfide offers a toxic mechanism. Furthermore, carbon tetrachloride was reported to inhibit mALDH by JNK-mediated phosphorylation^{161,162}. Moreover, the trichloromethane radical can stimulate lipid peroxidation^{163,164}, which yields the endproduct 4-HNE. 4-HNE has been reported to inhibit ALDH activity^{165,166} and is itself a substrate for detoxification by ALDH. This may be relevant to PD since increased 4-HNE was found in *post mortem* PD brains as adducts¹⁶ and as a component of Lewy bodies¹⁷. Furthermore, 4-HNE was shown to prevent α -synuclein fibrillation and form α -synuclein oligomers, which are toxic to primary mesencephalic cultures¹⁸. Taken together, these findings suggest several mechanisms through which pesticides can contribute to PD pathogenesis via ALDH inhibition.

4.2 Pesticides, *ALDH2*, and PD risk

We used the results of our ALDH screen to investigate a possible association between ALDH inhibition and PD risk. Each of the three dithiocarbamates applied in the PEG study area (mancozeb, maneb, ziram) was associated with a twofold to fourfold increase in PD risk in a dose-dependent manner. Two other pesticides applied in the PEG study area (benomyl, captan) inhibited ALDH activity and were suggestively associated with 60-80% increased PD risks when considered independently. More than 50% of our study population was exposed to at least one of these five ALDH-inhibiting pesticides, suggesting the broader relevance of this mechanism to other populations exposed to pesticides.

Taking into account aggregate exposures to these pesticides applied near occupational addresses, risk of PD increased 6% with each additional quartile of exposure that a subject encountered. Using residential estimates, this association was attenuated to 4%, possibly because occupational exposure may be a more accurate assessment of a subject's exposure since pesticides are applied during the workday. These are substantial findings, since these risks are greater than that for age, which is a major risk factor in PD but confers 1% increase in risk for each increasing year in age. This means that a typical individual exposed to the highest quartile of just one of these pesticides is subjected to 24% increased risk. This is the same increase in risk an 84-year-old experiences over a 60-year-old. Being exposed to two pesticides at high levels is like the risk of a 104-year-old versus a 60-year-old. Moreover, this risk is

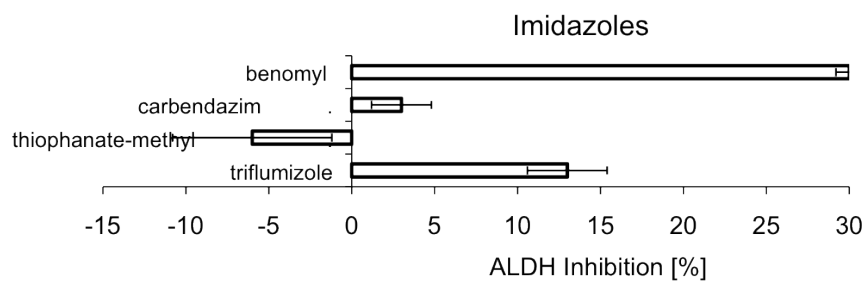
dramatically potentiated by genetic variation in the *ALDH2* gene, giving the highest-exposed individuals in this study a sixfold increase in risk. Again for comparison, all the known genetic risk factors only amount for a total 2.51-fold increase in risk, so the gene-environment consequence is substantial.

5. Conclusion

In summary, we found that various classes of pesticides inhibited neuronal ALDH activity and were associated with increased PD incidence in a dose-dependent manner. Genetic variation in *ALDH2* might confer some protection to unexposed populations but was associated with dramatically-increased PD risk for people working and living in areas where these pesticides had been sprayed. This report demonstrates the broad importance of ALDH as a potential therapeutic target in PD, and identifies pesticides that should be avoided to reduce risk of developing PD.

Figure IV-1. *Ex vivo* neuronal ALDH inhibition by (a) imidazole, (b) dicarboximide, and (c) dithiocarbamate pesticides

(a)



(b)



(c)

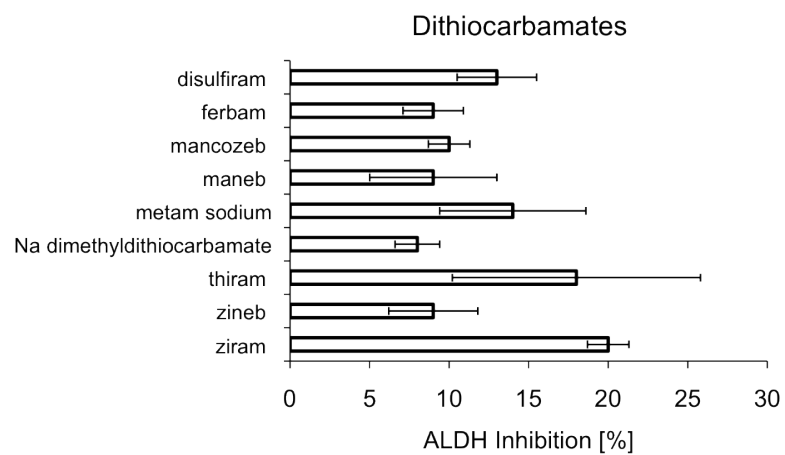


Figure IV-2. *In vitro* mitochondrial ALDH inhibition by pesticides. ALDH activity in rat hepatic mitochondria preparations was determined spectrophotometrically by measuring absorbance at 340 nm as NAD^+ was converted to NADH and acetaldehyde was converted to acetic acid in the presence of a potential inhibitor. Inhibition was determined relative to ALDH activity in preparations unexposed to pesticide.

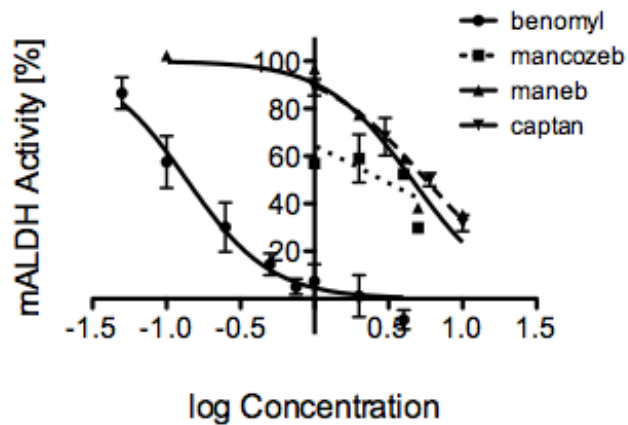
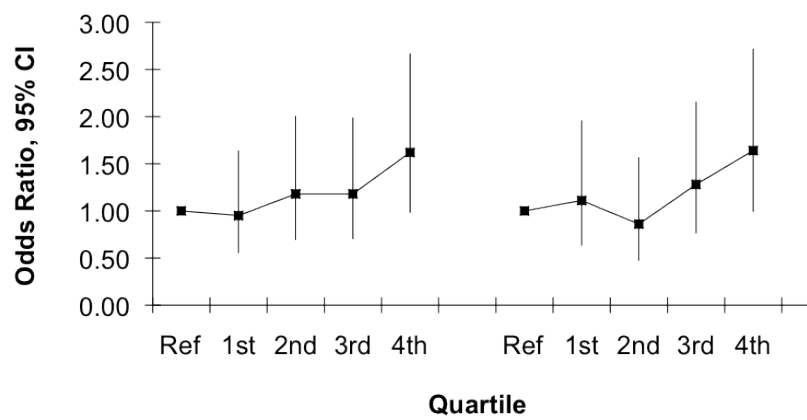


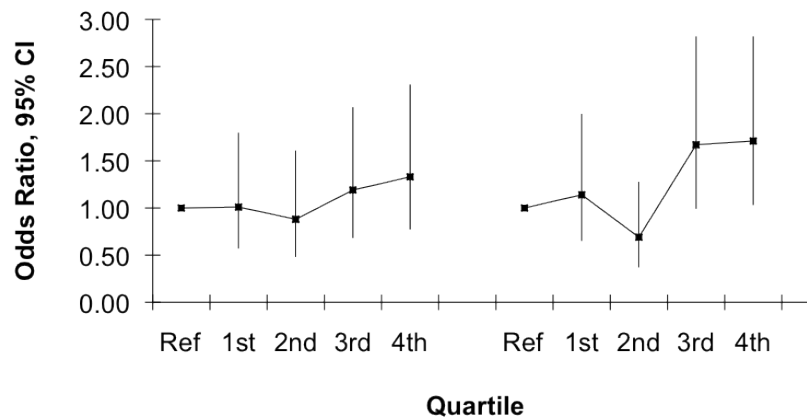
Figure IV-3. Risk of PD (odds ratios and 95% confidence intervals) by quartiles of pesticide exposure, using residential (left) or occupational estimates (right):

(a) benomyl, (b) captan, (c) mancozeb, (d) maneb, (e) ziram

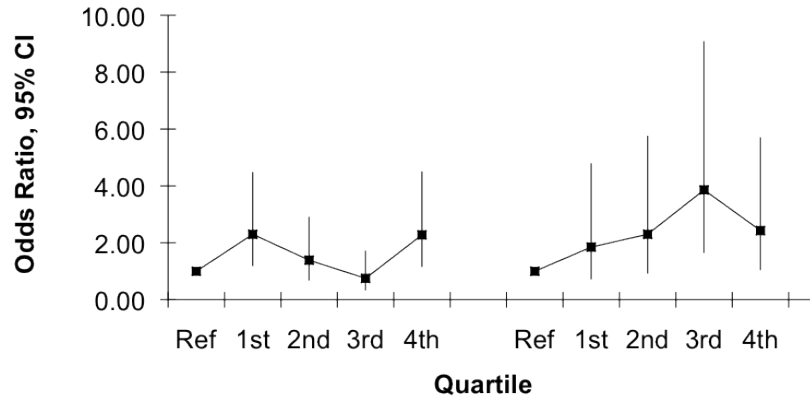
(a)



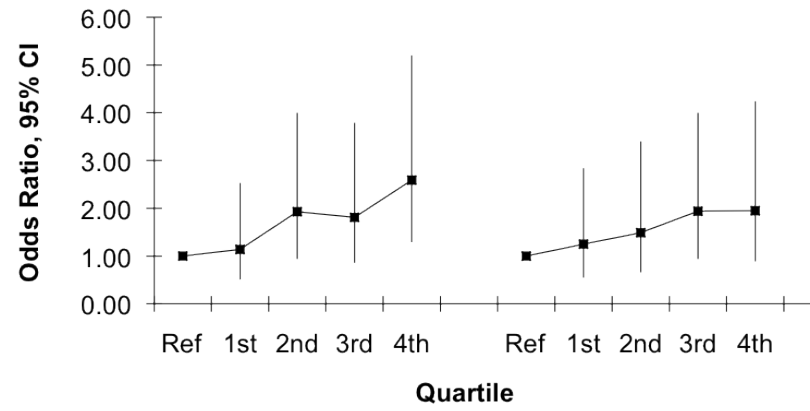
(b)



(c)



(d)



(e)

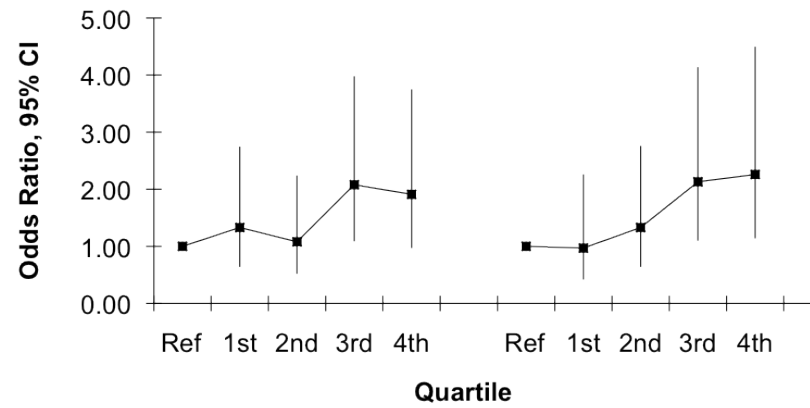


Figure IV-4. Gene-environment interaction analysis of aggregate exposure score and *ALDH2* clade

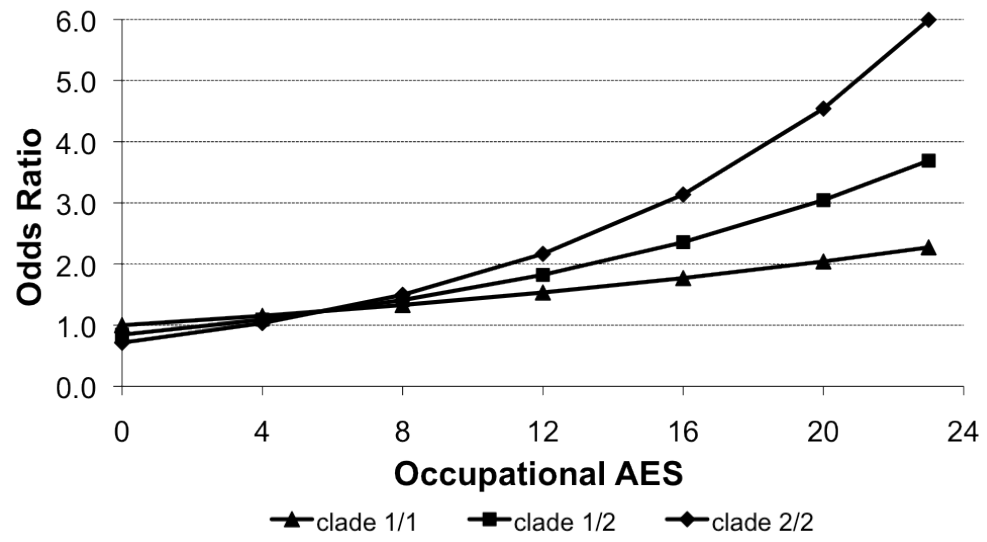


Table IV-1. IC₅₀ values of ALDH-inhibiting pesticides applied in PEG Study area

IC₅₀ [μM] (SE)	mALDH
benomyl	0.14 (0.02)
captan	5.7 (0.6)
mancozeb	2.9 (0.9)
maneb	4.6 (0.3)
ziram	ND*

*ND = not determined because no inhibition up to 10 μM, revealing importance of metabolites to ziram's function as an ALDH inhibitor

Table IV-2. Associations between aggregate pesticide exposure and PD risk

Aggregate Exposure Score ¹	Cases		Controls		OR ²	LCI	UCI	p-value
	n	%	n	%				
OCCUPATIONAL								
Age ³					1.01	1.00	1.02	
No exposure	168	48.0	189	56.3				
Any exposure	182	52.0	147	43.8	1.06	1.02	1.09	0.0004
Mean AES (stdev)	4.44	(6.11)	2.82	(4.46)				
Maximum AES	25		25					
RESIDENTIAL								
Age ³					1.01	0.99	1.02	
No exposure	115	44.3	166	49.4				
Any exposure	195	55.7	170	50.6	1.04	1.01	1.07	0.012
Mean AES (stdev)	4.28	(5.88)	3.12	(4.95)				
Maximum AES	24		24					

¹ Pesticides contributing to the Aggregate Exposure Score (AES) include benomyl, captan, ferbam, folpet, mancozeb, maneb, thiram, triflumizole, zineb, and ziram.

² Logistic regression odds ratios for each one point increase in Aggregate Exposure Score adjusted for age (continuous), sex (male/female), and smoking status (ever/never).

³ Logistic regression for age is provided for comparison.

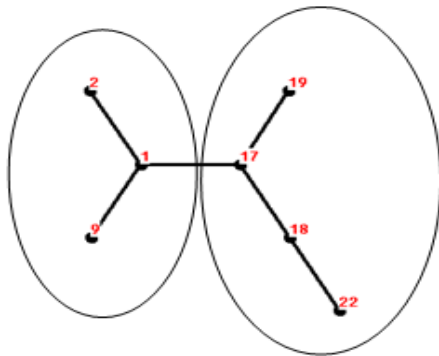
Table IV-3. Associations between genetic variation in the *ALDH2* gene and PD

risk

		All Subjects w/ Complete data							
		Cases (n=350)		Controls (n=336)		OR*	LCI	UCI	trend p-value
		n	%	n	%				
Clade	1/1	168	48.0	150	44.6				
	1/2	143	40.9	147	43.8	0.93	0.74	1.17	
	2/2	39	11.1	39	11.6	0.87	0.69	1.09	0.5404
ALDH2_rs737280	TT	162	47.1	147	44.6	1.00	reference		
	CT	143	41.5	144	43.6	0.95	0.75	1.19	
	CC	39	11.3	39	11.8	0.90	0.71	1.13	0.6322
	missing	6		6					
ALDH2_rs968529	CC	296	87.8	275	85.9	1.00	reference		
	CT	40	11.9	44	13.8	0.86	0.55	1.35	
	TT	1	0.3	1	0.3	0.74	0.47	1.17	0.5106
	missing	13		16					
ALDH2_rs671	GG	330	97.9	305	99.4	1.00	reference		
	AG	6	1.8	2	0.6	n.c.	n.c.	n.c.	
	AA	1	0.3	0	0.0	n.c.	n.c.	n.c.	0.1006
	missing	13		29					
ALDH2_rs16941667	CC	297	87.6	270	85.7	1.00	reference		
	CT	39	11.5	45	14.3	0.94	0.61	1.47	
	TT	3	0.9	0	0.0	0.89	0.57	1.38	0.7863
	missing	11		21					
ALDH2_rs16941669	TT	262	78.7	252	79.2	1.00	reference		
	GT	69	20.7	62	19.5	1.01	0.71	1.46	
	GG	2	0.6	4	1.3	1.03	0.72	1.48	0.9368
	missing	17		18					
ALDH2_rs9971942	CC	192	60.6	175	57.6	1.00	reference		
	CT	107	33.7	111	36.5	0.92	0.70	1.21	
	TT	18	5.7	18	5.9	0.85	0.65	1.11	0.5478
	missing	33		32					

* odds ratios adjusted for age (continuous), sex (male/female), and smoking status (ever/never)

Supplemental Figure IV-1. Cladogram for determining Clade 1 (left) or Clade 2 (right) from single nucleotide polymorphisms in *ALDH2* gene



		rs737280					
		rs968529					
		rs16941667					
		rs16941669					
		rs9971942					
1	F	C	C	C	F	C	0.585117
2	F	C	C	C	F	F	0.0135011
9	F	F	C	C	F	C	0.0649295
17	C	C	C	C	F	C	0.0193921
18	C	C	C	C	F	F	0.139254
19	C	C	C	C	G	C	0.100224
22	C	C	F	F	F	F	0.061542

Supplemental Table IV-1. Demographics of PEG study subjects

		Cases (n=338)		Controls (n=325)		p-value
		n	%	n	%	
Gender	Female	142	42.0	162	49.8	0.043
	Male	196	58.0	163	50.2	
Age	mean (sd)	68.2	(10.1)	67.3	(12.5)	0.363
	range	34 - 88		35 - 92		
Smoking	Never	177	52.4	146	44.9	0.081
	Former	142	42.0	150	46.2	
	Current	19	5.6	29	8.9	
Smoking	Never	177	52.4	146	44.9	0.055
	Ever	161	47.6	176	55.1	
Family History	No	287	84.9	292	89.8	0.056
	Yes	51	15.1	33	10.2	
Race	Caucasian	272	80.5	260	80.0	0.011
	Latino	43	12.7	26	8.0	
	Native American	16	4.7	16	4.9	
	African American	3	0.9	13	4.0	
	Asian American	4	1.2	10	3.1	
	Unspecified	0	0.0	0	0.0	

Supplemental Table IV-2. Risk of PD by quartiles of pesticide exposure, estimated with occupational addresses

		OCCUPATIONAL							
		Cases (n=350)		Controls (n=336)		OR	LCI	UCI	p-value
		n	%	n	%				
Benomyl	Unexposed	215	61.4	223	66.4	1.00	ref		
	1st Q	28	8.0	28	8.3	1.11	0.63	1.96	0.713
	2nd Q	22	6.3	26	7.7	0.86	0.47	1.57	0.615
	3rd Q	37	10.6	30	8.9	1.28	0.76	2.16	0.356
	4th Q	48	13.7	29	8.6	1.64	0.99	2.72	0.055
								<i>p for trend</i>	<i>0.073</i>
Captan	Unexposed	210	60.0	224	66.7	1.00	ref		
	1st Q	29	8.3	28	8.3	1.14	0.65	2.00	0.641
	2nd Q	19	5.4	28	8.3	0.69	0.37	1.28	0.234
	3rd Q	43	12.3	27	8.0	1.67	0.99	2.82	0.054
	4th Q	49	14.0	29	8.6	1.71	1.03	2.82	0.037
								<i>p for trend</i>	<i>0.023</i>
Mancozeb	Unexposed	279	79.7	307	91.4	1.00	ref		
	1st Q	12	3.4	7	2.1	1.85	0.71	4.80	0.208
	2nd Q	15	4.3	7	2.1	2.30	0.92	5.77	0.076
	3rd Q	26	7.4	7	2.1	3.86	1.64	9.09	0.002
	4th Q	18	5.1	8	2.4	2.43	1.04	5.71	0.041
								<i>p for trend</i>	<i>0.0001</i>
Maneb	Unexposed	278	79.4	293	87.2	1.00	ref		
	1st Q	13	3.7	11	3.3	1.25	0.55	2.84	0.602
	2nd Q	15	4.3	10	3.0	1.49	0.66	3.40	0.340
	3rd Q	23	6.6	12	3.6	1.94	0.94	4.00	0.073
	4th Q	21	6.0	10	3.0	1.95	0.89	4.24	0.094
								<i>p for trend</i>	<i>0.012</i>
Ziram	Unexposed	264	75.4	283	84.2	1.00	ref		
	1st Q	11	3.1	12	3.6	0.97	0.42	2.26	0.941
	2nd Q	17	4.9	14	4.2	1.33	0.64	2.76	0.450
	3rd Q	29	8.3	14	4.2	2.13	1.10	4.14	0.026
	4th Q	29	8.3	13	3.9	2.26	1.14	4.50	0.020
								<i>p for trend</i>	<i>0.0019</i>

Supplemental Table IV-3. Risk of PD by quartiles of pesticide exposure, estimated with residential addresses

		RESIDENTIAL							
		Cases (n=350)		Controls (n=336)		OR	LCI	UCI	p-value
		n	%	n	%				
Benomyl	Unexposed	204	58.3	214	63.7	1.00	ref		
	1st Q	28	8.0	31	9.2	0.95	0.55	1.64	0.844
	2nd Q	34	9.7	30	8.9	1.18	0.69	2.01	0.550
	3rd Q	36	10.3	31	9.2	1.18	0.70	1.99	0.536
	4th Q	48	13.7	30	8.9	1.62	0.98	2.67	0.058
								<i>p for trend</i>	<i>0.064</i>
Captan	Unexposed	234	66.9	234	69.6	1.00	ref		
	1st Q	27	7.7	26	7.7	1.01	0.57	1.80	0.961
	2nd Q	23	6.6	25	7.4	0.88	0.48	1.61	0.680
	3rd Q	31	8.9	26	7.7	1.19	0.68	2.07	0.540
	4th Q	35	10.0	25	7.4	1.33	0.77	2.31	0.308
								<i>p for trend</i>	<i>0.338</i>
Mancozeb	Unexposed	266	76.0	282	83.9	1.00	ref		
	1st Q	28	8.0	14	4.2	2.30	1.18	4.49	0.015
	2nd Q	18	5.1	13	3.9	1.39	0.67	2.92	0.379
	3rd Q	10	2.9	14	4.2	0.75	0.32	1.73	0.496
	4th Q	28	8.0	13	3.9	2.28	1.15	4.51	0.019
								<i>p for trend</i>	<i>0.031</i>
Maneb	Unexposed	264	75.4	288	85.7	1.00	ref		
	1st Q	14	4.0	12	3.6	1.14	0.51	2.53	0.752
	2nd Q	23	6.6	12	3.6	1.93	0.94	4.00	0.075
	3rd Q	20	5.7	12	3.6	1.81	0.86	3.79	0.119
	4th Q	29	8.3	12	3.6	2.59	1.29	5.20	0.007
								<i>p for trend</i>	<i>0.001</i>
Ziram	Unexposed	259	74.0	278	82.7	1.00	ref		
	1st Q	18	5.1	14	4.2	1.33	0.64	2.75	0.439
	2nd Q	16	4.6	15	4.5	1.08	0.52	2.24	0.836
	3rd Q	30	8.6	15	4.5	2.08	1.09	3.98	0.027
	4th Q	27	7.7	14	4.2	1.91	0.97	3.75	0.060
								<i>p for trend</i>	<i>0.007</i>

CHAPTER V

Implications

1. Implications for pesticide regulation

The findings presented in this dissertation have implications for pesticide regulation. Commercial pesticides undergo rigorous toxicological assessments before they can be used in agriculture. However, there are serious limitations to these risk characterizations. For example, the California Department of Pesticide Regulation (CA DPR) performs neurotoxicity assessments¹⁶⁷ that focus chiefly on acute effects, although chronic exposures appear to be relevant to PD pathogenesis. Also, they do not specifically look at relevant characteristics like protein aggregation or dopaminergic neuron survival. Although risk assessment procedures could potentially be improved, it would be infeasible to test for all possible sporadic disorders. Regardless, PD etiology remains ambiguous, so development of the most appropriate protocol would be contentious. However, sufficient evidence exists about the association between pesticide exposure and PD occurrence to warrant more stringent regulations.

In this dissertation, we identify multiple pesticides that are associated with PD occurrence in the UCLA Parkinson's Environment and Genes (PEG) epidemiologic study. We estimate relative ambient pesticide exposures based on occupational and residential addresses within 500 m of applications, because we expect inhalation to be the primary route of exposure. Fungicides like benomyl and the dithiocarbamates degrade in a matter of days, so they are not likely to be

toxic through consumption of food or drinking water. In fact, most pesticides are not detectable deep in soils or in drinking or surface waters. Moreover, because these compounds are labile, they need to be applied multiple times, effecting chronic exposures. This precludes acute toxicity and likely contributes to the chronic pathogenesis of PD. This estimation method likely underestimates the risk for people with occupations involving pesticides. The CA DPR identifies particular elevated exposures for employees who mix, load, and apply pesticides, as well as field workers and harvesters¹⁶⁷. They are subject to exposure through absorption in addition to inhalation. Because applications occur most often during the workday, we expect occupational addresses (rather than residential) to elicit more accurate estimates of the actual relative exposures.

According to the most recent Statewide Report available from the CA DPR, five of the pesticides found to inhibit ALDH activity in this study were included on the list of the top 100 pesticides applied (by poundage) in California in 2009 (Table V-1)¹⁶⁸. These were applied to such crops as almonds, grapes, tomatoes, and strawberries, which topped the list of crops by acreage treated with pesticides. Only maneb was also on the list of the top 100 pesticides by acreage in addition to poundage. Thus, metam sodium, ziram, captan, and mancozeb were applied liberally to smaller areas, so people working or residing near these fields were more likely to be exposed to higher concentrations. Over the course of the year, they were subjected to multiple applications of high concentrations. Acreage is recorded as the sum of the areas of the fields exposed for each application, so the high acreage associated with maneb

application could mean either a larger area with similar application profiles, or a similar area with more applications. The former would place more people at risk of exposure, while the latter would mean more days of potential exposure for the local inhabitants. Either way, these risks are substantial. Given their association with PD occurrence reported here, the liberal use of these pesticides should be reconsidered urgently.

2. Implications for Parkinson's disease etiology

Although this study focuses on only a few pesticides, these findings also have broader implications for the etiology of a spectrum of disorders that include Parkinson's disease (PD) and parkinsonisms. By using these pesticides as model compounds, we have identified a mechanism that may contribute to PD pathogenesis and result in dopaminergic cell loss and Lewy body formation.

Figure V-1 shows a simplified schematic of some of the potential mechanisms through which pesticide exposure may be neurotoxic. In this dissertation, investigation of ziram and its metabolites suggests that dithiocarbamates inhibit ALDH at least partially through the liberation of carbon disulfide (CS_2). CS_2 may also form from the dicarboximides captan and folpet, and the imidazole benomyl which is metabolized into thiocarbamate compounds (e.g., MBT). CS_2 was reported to cross-link proteins^{158,160}, which may irreversibly inhibit ALDH. Liberation of carbon tetrachloride (CCl_4) from chlorinated pesticides (e.g., captan, folpet) may inhibit ALDH directly^{161,162} or indirectly by inducing lipid peroxidation^{163,164}, which yields the endproduct 4-hydroxy-2-nonenal (4-HNE).

Since 4-HNE itself can inhibit ALDH activity^{165,166} and is a substrate for detoxification by ALDH, its accumulation can result in a toxic feedback loop with respect to ALDH inhibition.

Regardless of the mechanism, ALDH inhibition results in the accumulation of toxic aldehydes like 4-HNE and 3,4-dihydroxyphenylacetaldehyde (DOPAL), which may induce protein aggregation and inhibit the ubiquitin-proteasome system^{11,14,18,169}.

Thus, there are multiple potential mechanisms by which pesticides can inhibit ALDH activity and contribute to the pathogenesis of PD. Developing therapies to prevent ALDH inhibition or otherwise stimulate ALDH activity could potentially reduce PD progression.

Figure V-1. Schematic of potential mechanisms by which pesticides may contribute to the pathogenesis of Parkinson's disease

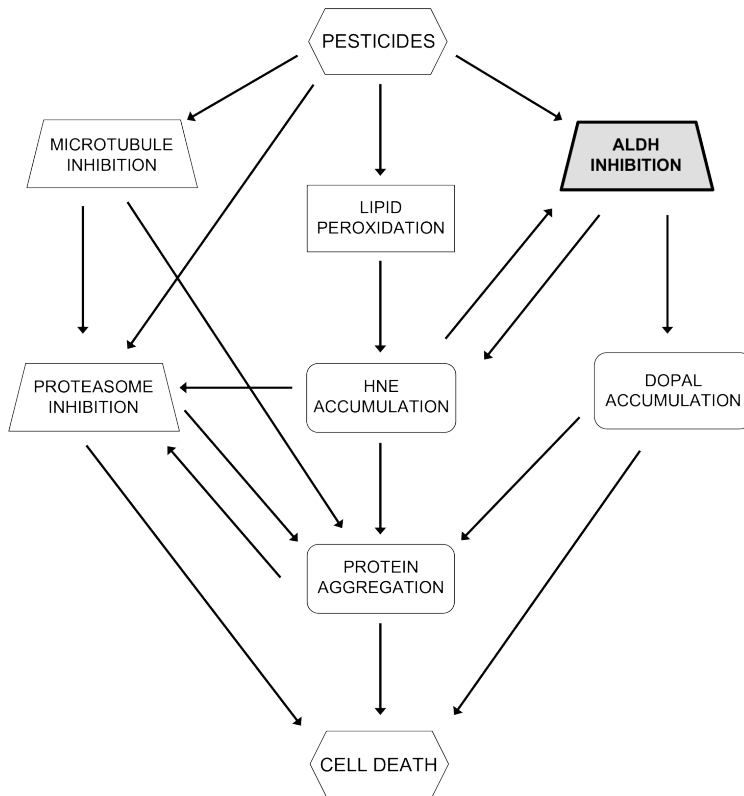


Table V-1. Agricultural application data for five pesticides found to have ALDH inhibitory capability

	Rank in Top 100		Poundage Applied	Number of Applications ¹
	by poundage	by acreage		
metam sodium	4		8,824,058	1,258
maneb	28	50	692,329	32,526
ziram	32		538,446	3,862
captan	46		325,464	5,233
mancozeb	52		277,572	7,162

¹ The number of applications includes only production agricultural applications and excludes post-harvest fumigation, structural pest control, landscape maintenance, and other applications.

REFERENCES

- 1 Dorsey, ER *et al.* Projected number of people with Parkinson disease in the most populous nations, 2005 through 2030. *Neurology*. **68**(5):384-386.
- 2 McNaught, KS, Jenner, P. Proteasomal function is impaired in substantia nigra in Parkinson's disease. *Neurosci. Lett.* **297**(3):191-194.
- 3 Bove, J *et al.* Proteasome inhibition and Parkinson's disease modeling. *Ann. Neurol.* **60**(2):260-264.
- 4 McNaught, KS, Olanow, CW. Proteasome inhibitor-induced model of Parkinson's disease. *Ann. Neurol.* **60**(2):243-247.
- 5 Schapira, AH *et al.* Proteasomal inhibition causes loss of nigral tyrosine hydroxylase neurons. *Ann. Neurol.* **60**(2):253-255.
- 6 Zeng, BY, Bukhatwa, S, Hikima, A, Rose, S, Jenner, P. Reproducible nigral cell loss after systemic proteasomal inhibitor administration to rats. *Ann. Neurol.* **60**(2):248-252.
- 7 Kordower, JH *et al.* Failure of proteasome inhibitor administration to provide a model of Parkinson's disease in rats and monkeys. *Ann. Neurol.* **60**(2):264-268.
- 8 Manning-Bog, AB *et al.* Lack of nigrostriatal pathology in a rat model of proteasome inhibition. *Ann. Neurol.* **60**(2):256-260.
- 9 Chou, AP *et al.* Ziram causes dopaminergic cell damage by inhibiting E1 ligase of the proteasome. *J. Biol. Chem.* **283**(50):34696-34703.
- 10 Braak, H *et al.* Staging of brain pathology related to sporadic Parkinson's disease. *Neurobiol. Aging.* **24**(2):197-211.

- 11 Burke, W *et al.* Aggregation of α -synuclein by DOPAL, the monoamine oxidase metabolite of dopamine. *Acta Neuropathol.* **115**(2):193-203.
- 12 Mazzulli, JR *et al.* Cytosolic catechols inhibit α -synuclein aggregation and facilitate the formation of intracellular soluble oligomeric intermediates. *J. Neurosci.* **26**(39):10068-10078.
- 13 Li, HT *et al.* Inhibition of α -synuclein fibrillization by dopamine analogs via reaction with the amino groups of α -synuclein. Implication for dopaminergic neurodegeneration. *FEBS J.* **272**(14):3661-3672.
- 14 Burke, WJ, Li, SW, Williams, EA, Nonneman, R, Zahm, DS. 3,4-dihydroxyphenylacetaldehyde is the toxic dopamine metabolite *in vivo*: Implications for Parkinson's disease pathogenesis. *Brain Res.* **989**(2):205-213.
- 15 Marchitti, SA, Deitrich, RA, Vasiliou, V. Neurotoxicity and metabolism of the catecholamine-derived 3,4-dihydroxyphenylacetaldehyde and 3,4-dihydroxyphenylglycolaldehyde: The role of aldehyde dehydrogenase. *Pharmacol. Rev.* **59**(2):125-150.
- 16 Yoritaka, A *et al.* Immunohistochemical detection of 4-hydroxynonenal protein adducts in Parkinson disease. *Proc. Natl. Acad. Sci. U. S. A.* **93**(7):2696-2701.
- 17 Castellani, RJ *et al.* Hydroxynonenal adducts indicate a role for lipid peroxidation in neocortical and brainstem Lewy bodies in humans. *Neurosci. Lett.* **319**(1):25-28.

- 18 Qin, Z *et al.* Effect of 4-hydroxy-2-nonenal modification on α -synuclein aggregation. *J. Biol. Chem.* **282**(8):5862-5870.
- 19 Staub, RE, Quistad, GB, Casida, JE. Mechanism for benomyl action as a mitochondrial aldehyde dehydrogenase inhibitor in mice. *Chem. Res. Toxicol.* **11**(5):535-543.
- 20 Wang, XF, Li, S, Chou, AP, Bronstein, JM. Inhibitory effects of pesticides on proteasome activity: Implication in Parkinson's disease. *Neurobiol. Dis.* **23**(1):198-205.
- 21 Spillantini, MG *et al.* α -Synuclein in Lewy bodies. *Nature.* **388**(6645):839-840.
- 22 Hardy, J. Genetic analysis of pathways to Parkinson disease. *Neuron.* **68**(2):201-206.
- 23 Burke, WJ *et al.* Aggregation of α -synuclein by DOPAL, the monoamine oxidase metabolite of dopamine. *Acta Neuropathol.* **115**(2):193-203.
- 24 Li, HT *et al.* Inhibition of α -synuclein fibrillization by dopamine analogs via reaction with the amino groups of α -synuclein. Implication for dopaminergic neurodegeneration. *FEBS J.* **272**(14):3661-3672.
- 25 Mazzulli, JR, Armakola, M, Dumoulin, M, Parastatidis, I, Ischiropoulos, H. Cellular oligomerization of α -synuclein is determined by the interaction of oxidized catechols with a C-terminal sequence. *J. Biol. Chem.* **282**(43):31621-31630.

- 26 Giasson, BI *et al.* A panel of epitope-specific antibodies detects protein domains distributed throughout human α -synuclein in Lewy bodies of Parkinson's disease. *J. Neurosci. Res.* **59**(4):528-533.
- 27 Kruger, R *et al.* Ala30pro mutation in the gene encoding α -synuclein in Parkinson's disease. *Nat. Genet.* **18**(2):106-108.
- 28 Nussbaum, RL, Polymeropoulos, MH. Genetics of Parkinson's disease. *Hum. Mol. Genet.* **6**(10):1687-1691.
- 29 Trojanowski, JQ, Goedert, M, Iwatsubo, T, Lee, VM. Fatal attractions: Abnormal protein aggregation and neuron death in Parkinson's disease and Lewy body dementia. *Cell Death Differ.* **5**(10):832-837.
- 30 Farrer, M *et al.* Comparison of kindreds with parkinsonism and α -synuclein genomic multiplications. *Ann. Neurol.* **55**(2):174-179.
- 31 Mueller, JC *et al.* Multiple regions of α -synuclein are associated with Parkinson's disease. *Ann. Neurol.* **57**(4):535-541.
- 32 Pals, P *et al.* α -Synuclein promoter confers susceptibility to Parkinson's disease. *Ann. Neurol.* **56**(4):591-595.
- 33 Uversky, VN, Li, J, Fink, AL. Pesticides directly accelerate the rate of α -synuclein fibril formation: A possible factor in Parkinson's disease. *FEBS Lett.* **500**(3):105-108.
- 34 Cuervo, AM, Stefanis, L, Fredenburg, R, Lansbury, PT, Sulzer, D. Impaired degradation of mutant α -synuclein by chaperone-mediated autophagy. *Science.* **305**(5688):1292-1295.

- 35 Liu, CW, Corboy, MJ, DeMartino, GN, Thomas, PJ. Endoproteolytic activity of the proteasome. *Science*. **299**(5605):408-411.
- 36 Mak, SK, McCormack, AL, Manning-Bog, AB, Cuervo, AM, Di Monte, DA. Lysosomal degradation of α -synuclein *in vivo*. *J. Biol. Chem.* **285**(18):13621-13629.
- 37 Zhang, NY, Tang, Z, Liu, CW. α -Synuclein protofibrils inhibit 26S proteasome-mediated protein degradation: Understanding the cytotoxicity of protein protofibrils in neurodegenerative disease pathogenesis. *J. Biol. Chem.* **283**(29):20288-20298.
- 38 Goldberg, AL. Protein degradation and protection against misfolded or damaged proteins. *Nature*. **426**(6968):895-899.
- 39 Bove, J *et al.* Proteasome inhibition and Parkinson's disease modeling. *Ann. Neurol.* **60**(2):260-264.
- 40 Kordower, JH *et al.* Failure of proteasome inhibitor administration to provide a model of Parkinson's disease in rats and monkeys. *Ann. Neurol.* **60**(2):264-268.
- 41 Manning-Bog, AB *et al.* Lack of nigrostriatal pathology in a rat model of proteasome inhibition. *Ann Neurol.* **60**(2):256-260.
- 42 McNaught, KS, Olanow, CW. Proteasome inhibitor-induced model of Parkinson's disease. *Ann Neurol.* **60**(2):243-247.
- 43 Schapira, AH *et al.* Proteasomal inhibition causes loss of nigral tyrosine hydroxylase neurons. *Ann. Neurol.* **60**(2):253-255.

- 44 Zeng, BY, Bukhatwa, S, Hikima, A, Rose, S, Jenner, P. Reproducible nigral cell loss after systemic proteasomal inhibitor administration to rats. *Ann. Neurol.* **60**(2):248-252.
- 45 Wang, X-F, Li, S, Chou, AP, Bronstein, JM. Inhibitory effects of pesticides on proteasome activity: Implication in Parkinson's disease. *Neurobiology of Disease.* **23**(1):198-205.
- 46 Aharon-Peretz, J, Rosenbaum, H, Gershoni-Baruch, R. Mutations in the glucocerebrosidase gene and Parkinson's disease in Ashkenazi Jews. *N. Engl. J. Med.* **351**(19):1972-1977.
- 47 Neumann, J *et al.* Glucocerebrosidase mutations in clinical and pathologically proven Parkinson's disease. *Brain.* **132**(Pt 7):1783-1794.
- 48 Sun, Y *et al.* Neuronopathic gaucher disease in the mouse: Viable combined selective saposin c deficiency and mutant glucocerebrosidase (V394L) mice with glucosylsphingosine and glucosylceramide accumulation and progressive neurological deficits. *Hum. Mol. Genet.* **19**(6):1088-1097.
- 49 Ramirez, A *et al.* Hereditary parkinsonism with dementia is caused by mutations in ATP13A2, encoding a lysosomal type 5 P-type ATPase. *Nat. Genet.* **38**(10):1184-1191.
- 50 Narendra, DP *et al.* PINK1 is selectively stabilized on impaired mitochondria to activate parkin. *PLoS Biol.* **8**(1):e1000298.
- 51 Samaranch, L *et al.* PINK1-linked parkinsonism is associated with Lewy body pathology. *Brain.* **133**(Pt 4):1128-1142.

- 52 Anglade, P *et al.* Apoptosis and autophagy in nigral neurons of patients with Parkinson's disease. *Histol. Histopathol.* **12**(1):25-31.
- 53 Massey, AC, Zhang, C, Cuervo, AM. Chaperone-mediated autophagy in aging and disease. *Curr. Top Dev. Biol.* **73**(205-235).
- 54 Martinez-Vicente, M *et al.* Dopamine-modified α -synuclein blocks chaperone-mediated autophagy. *J. Clin. Invest.* **118**(2):777-788.
- 55 Chiba, K, Trevor, AJ, Castagnoli, N, Jr. Active uptake of MPP⁺, a metabolite of MPTP, by brain synaptosomes. *Biochem. Biophys. Res. Commun.* **128**(3):1228-1232.
- 56 Gainetdinov, RR *et al.* Increased MPTP neurotoxicity in vesicular monoamine transporter 2 heterozygote knockout mice. *J. Neurochem.* **70**(5):1973-1978.
- 57 Javitch, JA, D'Amato, RJ, Strittmatter, SM, Snyder, SH. Parkinsonism-inducing neurotoxin, N-methyl-4-phenyl-1,2,3,6-tetrahydropyridine: Uptake of the metabolite N-methyl-4-phenylpyridine by dopamine neurons explains selective toxicity. *Proc. Natl. Acad. Sci. U. S. A.* **82**(7):2173-2177.
- 58 Langston, JW, Ballard, P, Tetrud, JW, Irwin, I. Chronic parkinsonism in humans due to a product of meperidine-analog synthesis. *Science.* **219**(4587):979-980.
- 59 Haas, RH *et al.* Low platelet mitochondrial complex I and complex II/III activity in early untreated Parkinson's disease. *Ann. Neurol.* **37**(6):714-722.

- 60 Schapira, AH *et al.* Mitochondrial complex I deficiency in Parkinson's disease. *J. Neurochem.* **54**(3):823-827.
- 61 Betarbet, R *et al.* Chronic systemic pesticide exposure reproduces features of Parkinson's disease. *Nat. Neurosci.* **3**(12):1301-1306.
- 62 Chou, AP, Li, S, Fitzmaurice, AG, Bronstein, JM. Mechanisms of rotenone-induced proteasome inhibition. *NeuroToxicology.* **31**(4):367-372.
- 63 Betarbet, R *et al.* Intersecting pathways to neurodegeneration in Parkinson's disease: Effects of the pesticide rotenone on DJ-1, α -synuclein, and the ubiquitin-proteasome system. *Neurobiol. Dis.* **22**(2):404-420.
- 64 Hastings, TG. The role of dopamine oxidation in mitochondrial dysfunction: Implications for Parkinson's disease. *J. Bioenerg. Biomembr.* **41**(6):469-472.
- 65 Olanow, CW *et al.* A double-blind, delayed-start trial of rasagiline in Parkinson's disease. *N Engl J Med.* **361**(13):1268-1278.
- 66 Glatt, CE, Wahner, AD, White, DJ, Ruiz-Linares, A, Ritz, B. Gain-of-function haplotypes in the vesicular monoamine transporter promoter are protective for Parkinson disease in women. *Hum. Mol. Genet.* **15**(2):299-305.
- 67 Ritz, BR *et al.* Dopamine transporter genetic variants and pesticides in Parkinson's disease. *Environ. Health Perspect.* **117**(6):964-969.
- 68 Ritz, B *et al.* Pooled analysis of tobacco use and risk of Parkinson disease. *Arch Neurol.* **64**(7):990-997.

- 69 Hellenbrand, W *et al.* Diet and Parkinson's disease. I: A possible role for the past intake of specific foods and food groups. Results from a self-administered food-frequency questionnaire in a case-control study. *Neurology*. **47**(3):636-643.
- 70 Wahner, AD, Bronstein, JM, Bordelon, YM, Ritz, B. Nonsteroidal anti-inflammatory drugs may protect against Parkinson disease. *Neurology*. **69**(19):1836-1842.
- 71 Alavanja, MC, Hoppin, JA, Kamel, F. Health effects of chronic pesticide exposure: Cancer and neurotoxicity. *Annu. Rev. Public Health*. **25**(155-197).
- 72 Brown, TP, Rumsby, PC, Capleton, AC, Rushton, L, Levy, LS. Pesticides and Parkinson's disease--is there a link? *Environ. Health Perspect*. **114**(2):156-164.
- 73 Di Monte, DA. The environment and Parkinson's disease: Is the nigrostriatal system preferentially targeted by neurotoxins? *Lancet Neurol*. **2**(9):531-538.
- 74 Kamel, F, Hoppin, JA. Association of pesticide exposure with neurologic dysfunction and disease. *Environ. Health Perspect*. **112**(9):950-958.
- 75 Le Couteur, DG, McLean, AJ, Taylor, MC, Woodham, BL, Board, PG. Pesticides and Parkinson's disease. *Biomedecine & Pharmacotherapy*. **53**(3):122-130.

- 76 Li, AA, Mink, PJ, McIntosh, LJ, Teta, MJ, Finley, B. Evaluation of epidemiologic and animal data associating pesticides with Parkinson's disease. *J. Occup. Environ. Med.* **47**(10):1059-1087.
- 77 Gartner, CE, Battistutta, D, Dunne, MP, Silburn, PA, Mellick, GD. Test-retest repeatability of self-reported environmental exposures in Parkinson's disease cases and healthy controls. *Parkinsonism & Related Disorders.* **11**(5):287-295.
- 78 Priyadarshi, A, Khuder, SA, Schaub, EA, Shrivastava, S. A meta-analysis of Parkinson's disease and exposure to pesticides. *NeuroToxicology.* **21**(4):435-440.
- 79 Petrovitch, H *et al.* Plantation work and risk of Parkinson disease in a population-based longitudinal study. *Arch. Neurol.* **59**(11):1787-1792.
- 80 Ascherio, A *et al.* Pesticide exposure and risk for Parkinson's disease. *Ann. Neurol.* **60**(2):197-203.
- 81 Kamel, F *et al.* Pesticide exposure and self-reported Parkinson's disease in the agricultural health study. *Am. J. Epidemiol.* **165**(4):364-374.
- 82 Tanner, CM *et al.* Rotenone, paraquat, and Parkinson's disease. *Environ. Health Perspect.* **119**(6):866-872.
- 83 Kang, GA *et al.* Clinical characteristics in early Parkinson's disease in a Central California population-based study. *Mov. Disord.* **20**(9):1133-1142.
- 84 Ritz, B, Yu, F. Parkinson's disease mortality and pesticide exposure in California 1984-1994. *Int. J. Epidemiol.* **29**(2):323-329.

- 85 Costello, S, Cockburn, M, Bronstein, J, Zhang, X, Ritz, B. Parkinson's disease and residential exposure to maneb and paraquat from agricultural applications in the central valley of california. *Am. J. Epidemiol.* **169**(8):919-926.
- 86 Manthripragada, AD, Costello, S, Cockburn, MG, Bronstein, JM, Ritz, B. Paraoxonase 1, agricultural organophosphate exposure, and Parkinson disease. *Epidemiology.* **21**(1):87-94.
- 87 Wang, A *et al.* Parkinson's disease risk from ambient exposure to pesticides. *Eur. J. Epidemiol.* **26**(7):547-555.
- 88 Gatto, NM, Cockburn, M, Bronstein, J, Manthripragada, AD, Ritz, B. Well-water consumption and Parkinson's disease in rural California. *Environ. Health Perspect.* **117**(12):1912-1918.
- 89 Deng, Y, Newman, B, Dunne, MP, Silburn, PA, Mellick, GD. Further evidence that interactions between CYP2D6 and pesticide exposure increase risk for Parkinson's disease. *Ann. Neurol.* **55**(6):897.
- 90 Elbaz, A *et al.* CYP2D6 polymorphism, pesticide exposure, and Parkinson's disease. *Ann. Neurol.* **55**(3):430-434.
- 91 Hancock, DB, Martin, ER, Vance, JM, Scott, WK. Nitric oxide synthase genes and their interactions with environmental factors in Parkinson's disease. *Neurogenetics.* **9**(4):249-262.
- 92 Kelada, SN *et al.* 5' and 3' region variability in the dopamine transporter gene (SLC6A3), pesticide exposure and Parkinson's disease risk: A hypothesis-generating study. *Hum. Mol. Genet.* **15**(20):3055-3062.

- 93 Gatto, NM *et al.* α -Synuclein gene may interact with environmental factors in increasing risk of Parkinson's disease. *Neuroepidemiology*. **35**(3):191-195.
- 94 Fitzmaurice, AG, Rhodes, SL, Cockburn, M, Ritz, B, Bronstein, JM. Biochemical and epidemiologic screens link pesticide exposure, aldehyde dehydrogenase inhibition, and Parkinson's disease. *Soc. Neurosci. Abstract* 752.3.
- 95 Drolet, RE, Cannon, JR, Montero, L, Greenamyre, JT. Chronic rotenone exposure reproduces Parkinson's disease gastrointestinal neuropathology. *Neurobiol. Dis.* **36**(1):96-102.
- 96 Pan-Montojo, F *et al.* Progression of Parkinson's disease pathology is reproduced by intragastric administration of rotenone in mice. *PLoS one*. **5**(1):e8762.
- 97 Sherer, TB *et al.* An *in vitro* model of Parkinson's disease: Linking mitochondrial impairment to altered α -synuclein metabolism and oxidative damage. *J. Neurosci.* **22**(16):7006-7015.
- 98 Dhillon, AS *et al.* Pesticide/environmental exposures and Parkinson's disease in East Texas. *J. Agromedicine*. **13**(1):37-48.
- 99 Hertzman, C, Wiens, M, Bowering, D, Snow, B, Calne, D. Parkinson's disease: A case-control study of occupational and environmental risk factors. *Am. J. Ind. Med.* **17**(3):349-355.
- 100 Liou, HH *et al.* Environmental risk factors and Parkinson's disease: A case-control study in Taiwan. *Neurology*. **48**(6):1583-1588.

- 101 Semchuk, KM, Love, EJ, Lee, RG. Parkinson's disease and exposure to agricultural work and pesticide chemicals. *Neurology*. **42**(7):1328-1335.
- 102 Brooks, AI, Chadwick, CA, Gelbard, HA, Cory-Slechta, DA, Federoff, HJ. Paraquat elicited neurobehavioral syndrome caused by dopaminergic neuron loss. *Brain Res*. **823**(1-2):1-10.
- 103 Manning-Bog, AB *et al*. The herbicide paraquat causes up-regulation and aggregation of α -synuclein in mice: Paraquat and α -synuclein. *J. Biol. Chem*. **277**(3):1641-1644.
- 104 McCormack, AL *et al*. Environmental risk factors and Parkinson's disease: Selective degeneration of nigral dopaminergic neurons caused by the herbicide paraquat. *Neurobiol. Dis*. **10**(2):119-127.
- 105 Richardson, JR, Quan, Y, Sherer, TB, Greenamyre, JT, Miller, GW. Paraquat neurotoxicity is distinct from that of MPTP and rotenone. *Toxicol. Sci*. **88**(1):193-201.
- 106 McCormack, AL *et al*. Role of oxidative stress in paraquat-induced dopaminergic cell degeneration. *J. Neurochem*. **93**(4):1030-1037.
- 107 Corsini, GU, Pintus, S, Chiueh, CC, Weiss, JF, Kopin, IJ. 1-methyl-4-phenyl-1,2,3,6-tetrahydropyridine (MPTP) neurotoxicity in mice is enhanced by pretreatment with diethyldithiocarbamate. *Eur. J. Pharmacol*. **119**(1-2):127-128.
- 108 Thiruchelvam, M, Brockel, BJ, Richfield, EK, Baggs, RB, Cory-Slechta, DA. Potentiated and preferential effects of combined paraquat and maneb

- on nigrostriatal dopamine systems: Environmental risk factors for Parkinson's disease? *Brain Res.* **873**(2):225-234.
- 109 Thiruchelvam, M *et al.* Age-related irreversible progressive nigrostriatal dopaminergic neurotoxicity in the paraquat and maneb model of the Parkinson's disease phenotype. *Eur. J. Neurosci.* **18**(3):589-600.
- 110 Norris, EH *et al.* Pesticide exposure exacerbates α -synucleinopathy in an A53T transgenic mouse model. *Am. J. Pathol.* **170**(2):658-666.
- 111 Zhou, Y, Shie, FS, Piccardo, P, Montine, TJ, Zhang, J. Proteasomal inhibition induced by manganese ethylene-bis-dithiocarbamate: Relevance to Parkinson's disease. *Neuroscience.* **128**(2):281-291.
- 112 Fitzmaurice, AG, Ackerman, LC, Lam, HA, Maidment, NT, Bronstein, JM. Aldehyde dehydrogenase inhibition by the fungicide benomyl leads to dopaminergic cell death: Relevance of dopamine metabolism to Parkinson's disease. *Soc Neurosci. Abstract* 655.24.
- 113 Fearnley, JM, Lees, AJ. Ageing and Parkinson's disease: Substantia nigra regional selectivity. *Brain.* **114**(2283-2301).
- 114 Nalls, MA *et al.* Imputation of sequence variants for identification of genetic risks for Parkinson's disease: A meta-analysis of genome-wide association studies. *Lancet.* **377**(9766):641-649.
- 115 Priyadarshi, A, Khuder, SA, Schaub, EA, Priyadarshi, SS. Environmental risk factors and Parkinson's disease: A metaanalysis. *Environ. Res.* **86**(2):122-127.

- 116 Firestone, JA *et al.* Pesticides and risk of Parkinson disease: A population-based case-control study. *Arch. Neurol.* **62**(1):91-95.
- 117 Moisan, F *et al.* The relation between type of farming and prevalence of Parkinson's disease among agricultural workers in five French districts. *Mov. Disord.* **26**(2):271-279.
- 118 Rull, RP, Ritz, B. Historical pesticide exposure in California using Pesticide Use Reports and land-use surveys: An assessment of misclassification error and bias. *Environ. Health Perspect.* **111**(13):1582-1589.
- 119 Goldberg, DW, Wilson, JP, Knoblock, CA, Ritz, B, Cockburn, MG. An effective and efficient approach for manually improving geocoded data. *Int. J. Health Geogr.* **7**(60):1-20.
- 120 Gupta, K *et al.* Antimitotic antifungal compound benomyl inhibits brain microtubule polymerization and dynamics and cancer cell proliferation at mitosis, by binding to a novel site in tubulin. *Biochemistry.* **43**(21):6645-6655.
- 121 Ren, Y, Liu, W, Jiang, H, Jiang, Q, Feng, J. Selective vulnerability of dopaminergic neurons to microtubule depolymerization. *J. Biol. Chem.* **280**(40):34105-34112.
- 122 Leiphon, LJ, Picklo, SMJ. Inhibition of aldehyde detoxification in CNS mitochondria by fungicides. *NeuroToxicology.* **28**(1):143-149.
- 123 Hughes, AJ, Ben-Shlomo, Y, Daniel, SE, Lees, AJ. What features improve the accuracy of clinical diagnosis in Parkinson's disease: A clinicopathologic study. 1992. *Neurology.* **57**(10 Suppl 3):S34-38.

- 124 Wen, L *et al.* Visualization of monoaminergic neurons and neurotoxicity of mptp in live transgenic zebrafish. *Dev. Biol.* **314**(1):84-92.
- 125 Sagasti, A, Guido, MR, Raible, DW, Schier, AF. Repulsive interactions shape the morphologies and functional arrangement of zebrafish peripheral sensory arbors. *Curr. Biol.* **15**(9):804-814.
- 126 Rayport, S *et al.* Identified postnatal mesolimbic dopamine neurons in culture: Morphology and electrophysiology. *J. Neurosci.* **12**(11):4264-4280.
- 127 Quistad, GB, Sparks, SE, Casida, JE. Aldehyde dehydrogenase of mice inhibited by thiocarbamate herbicides. *Life Sci.* **55**(20):1537-1544.
- 128 Tottmar, SO, Pettersson, H, Kiessling, KH. The subcellular distribution and properties of aldehyde dehydrogenases in rat liver. *Biochem. J.* **135**(4):577-586.
- 129 Bence, NF, Sampat, RM, Kopito, RR. Impairment of the ubiquitin-proteasome system by protein aggregation. *Science.* **292**(5521):1552-1555.
- 130 Howard, RJ, Aist, JR. Cytoplasmic microtubules and fungal morphogenesis: Ultrastructural effects of methyl benzimidazole-2-ylcarbamate determined by freeze-substitution of hyphal tip cells. *J. Cell Biol.* **87**(1):55-64.
- 131 Quinlan, RA, Pogson, CI, Gull, K. The influence of the microtubule inhibitor, methyl benzimidazol-2-yl-carbamate (MBC) on nuclear division

- and the cell cycle in *Saccharomyces cerevisiae*. *J. Cell Sci.* **46**(1):341-352.
- 132 Walker, GM. Cell cycle specificity of certain antimicrotubular drugs in *Schizosaccharomyces pombe*. *J. Gen. Microbiol.* **128**(1):61-71.
- 133 Goldman, SM *et al.* Solvent exposures and Parkinson disease risk in twins. *Ann. Neurol.*
- 134 Tanaka, K *et al.* Occupational risk factors for Parkinson's disease: A case-control study in Japan. *BMC Neurol.* **11**(83):1-6.
- 135 Boubaker, H, Saadi, B, Boudyach, EH, Benaoumar, AA. Resistance of *Verticillium theobromae* to benzimidazole fungicides in Morocco. *J. Appl. Sci.* **8**(21):3903-3909.
- 136 Potocnik, I *et al.* *In vitro* toxicity of selected fungicides from the groups of benzimidazoles and demethylation inhibitors to *Cladobotryum dendroides* and *Agaricus bisporus*. *J. Environ. Sci. Health B.* **44**(4):365-370.
- 137 Kataria, HR, Grover, RK. Effect of benomyl and thiophanate-methyl on metabolic activities of *Rhizoctonia solani kuhn*. *Ann. Microbiol.* **127A**(2):297-306.
- 138 Holzschuh, J, Ryu, S, Aberger, F, Driever, W. Dopamine transporter expression distinguishes dopaminergic neurons from other catecholaminergic neurons in the developing zebrafish embryo. *Mech. Dev.* **101**(1-2):237-243.

- 139 Morpurgo, G, Bellincampi, D, Gualandi, G, Baldinelli, L, Crescenzi, OS. Analysis of mitotic nondisjunction with *Aspergillus nidulans*. *Environ. Health Perspect.* **31**(1):81-95.
- 140 Oakley, BR, Morris, NR. Nuclear movement is β -tubulin-dependent in *Aspergillus nidulans*. *Cell.* **19**(1):255-262.
- 141 Wey, MC *et al.* Neurodegeneration and motor dysfunction in mice lacking cytosolic and mitochondrial aldehyde dehydrogenases: Implications for Parkinson's disease. *PLoS one.* **7**(2):e31522.
- 142 Burke, WJ *et al.* Neurotoxicity of mao metabolites of catecholamine neurotransmitters: Role in neurodegenerative diseases. *NeuroToxicology.* **25**(1-2):101-115.
- 143 Panneton, WM, Kumar, VB, Gan, Q, Burke, WJ, Galvin, JE. The neurotoxicity of dopal: Behavioral and stereological evidence for its role in Parkinson disease pathogenesis. *PLoS one.* **5**(12):e15251.
- 144 Gatto, NM *et al.* α -Synuclein gene may interact with environmental factors in increasing risk of Parkinson's disease. *Neuroepidemiology.* **35**(3):191-195.
- 145 Crawford, DC, Nickerson, DA. Definition and clinical importance of haplotypes. *Annu. Rev. Med.* **56**(303-320).
- 146 Daly, MJ, Rioux, JD, Schaffner, SF, Hudson, TJ, Lander, ES. High-resolution haplotype structure in the human genome. *Nat. Genet.* **29**(2):229-232.

- 147 Gabriel, SB *et al.* The structure of haplotype blocks in the human genome. *Science*. **296**(5576):2225-2229.
- 148 Barrett, JC, Fry, B, Maller, J, Daly, MJ. Haploview: Analysis and visualization of LD and haplotype maps. *Bioinformatics*. **21**(2):263-265.
- 149 Wall, JD, Pritchard, JK. Assessing the performance of the haplotype block model of linkage disequilibrium. *Am. J. Hum. Genet.* **73**(3):502-515.
- 150 Takeuchi, F *et al.* Confirmation of *aldh2* as a major locus of drinking behavior and of its variants regulating multiple metabolic phenotypes in a Japanese population. *Circ. J.* **75**(4):911-918.
- 151 Tobler, AR *et al.* The snplex genotyping system: A flexible and scalable platform for SNP genotyping. *J. Biomol. Tech.* **16**(4):398-406.
- 152 Stephens, M, Smith, NJ, Donnelly, P. A new statistical method for haplotype reconstruction from population data. *Am. J. Hum. Genet.* **68**(4):978-989.
- 153 Seltman, H, Roeder, K, Devlin, B. Evolutionary-based association analysis using haplotype data. *Genet. Epidemiol.* **25**(1):48-58.
- 154 LaMondia, JA, Douglas, SM. Sensitivity of *Botrytis cinerea* from Connecticut greenhouses to benzimidazole and dicarboximide fungicides. *Plant Dis.* **81**(729-732).
- 155 Hutchinson, CM, McGiffen, ME, Jr., Sims, JJ, Becker, JO. Fumigant combinations for *Cyperus esculentum* l control. *Pest. Manag. Sci.* **60**(4):369-374.

- 156 Deepak, SA *et al.* Developmental stage response of pearl millet downy mildew (*Sclerospora graminicola*) to fungicides. *Appl. Ecol. Environ. Res.* **4**(2):125-149.
- 157 Prom, LK. Laboratory, greenhouse, and field assessment of fourteen fungicides for activity against *Claviceps africana*, causal agent of sorghum ergot. *Plant Dis.* **87**(3):252-258.
- 158 Staub, RE, Sparks, SE, Quistad, GB, Casida, JE. S-methylation as a bioactivation mechanism for mono- and dithiocarbamate pesticides as aldehyde dehydrogenase inhibitors. *Chem. Res. Toxicol.* **8**(8):1063-1069.
- 159 Zimmerman, LJ, Valentine, HL, Valentine, WM. Characterization of S-(N,N-dialkylaminocarbonyl)cysteine adducts and enzyme inhibition produced by thiocarbamate herbicides in the rat. *Chem. Res. Toxicol.* **17**(2):258-267.
- 160 Valentine, WM, Amarnath, V, Amarnath, K, Rimmel, F, Graham, DG. Carbon disulfide mediated protein cross-linking by N,N-diethyldithiocarbamate. *Chem. Res. Toxicol.* **8**(1):96-102.
- 161 Hjelle, JJ, Grubbs, JH, Beer, DG, Petersen, DR. Inhibition of rat liver aldehyde dehydrogenase by carbon tetrachloride. *J. Pharmacol. Exp. Ther.* **219**(3):821-826.
- 162 Moon, KH, Lee, YM, Song, BJ. Inhibition of hepatic mitochondrial aldehyde dehydrogenase by carbon tetrachloride through JNK-mediated phosphorylation. *Free Radic. Biol. Med.* **48**(3):391-398.

- 163 Sipes, IG, Krishna, G, Gillette, JR. Bioactivation of carbon tetrachloride, chloroform and bromotrichloromethane: Role of cytochrome P-450. *Life Sci.* **20**(9):1541-1548.
- 164 Slater, TF, Sawyer, BC. The stimulatory effects of carbon tetrachloride and other halogenoalkanes on peroxidative reactions in rat liver fractions in vitro. General features of the systems used. *Biochem. J.* **123**(5):805-814.
- 165 Mitchell, DY, Petersen, DR. Inhibition of rat hepatic mitochondrial aldehyde dehydrogenase-mediated acetaldehyde oxidation by trans-4-hydroxy-2-nonenal. *Hepatology.* **13**(4):728-734.
- 166 Doorn, JA, Hurley, TD, Petersen, DR. Inhibition of human mitochondrial aldehyde dehydrogenase by 4-hydroxynon-2-enal and 4-oxonon-2-enal. *Chem. Res. Toxicol.* **19**(1):102-110.
- 167 Regulation, CEPADoP. Benomyl: Risk characterization document. (1999).
- 168 Regulation, CEPADoP. Summary of Pesticide Use Report data 2009. (2010).
- 169 Okada, K *et al.* 4-hydroxy-2-nonenal-mediated impairment of intracellular proteolysis during oxidative stress. Identification of proteasomes as target molecules. *J. Biol. Chem.* **274**(34):23787-23793.

APPENDICES

- A. Ziram causes dopaminergic cell damage by inhibiting E1 ligase of the proteasome**

- B. Geochemical and hydrologic controls on the mobilization of arsenic derived from herbicide application**

- C. Geochemical processes controlling arsenic mobility in groundwater: A case study of arsenic mobilization and natural attenuation**

- D. Mechanisms of rotenone-induced proteasome inhibition**

- E. Pesticides and Parkinson's disease**

APPENDIX A

**Ziram causes dopaminergic cell damage
by inhibiting E1 ligase of the proteasome**

Ziram Causes Dopaminergic Cell Damage by Inhibiting E1 Ligase of the Proteasome*

Received for publication, March 20, 2008, and in revised form, September 24, 2008. Published, JBC Papers in Press, September 25, 2008, DOI 10.1074/jbc.M802210200

Arthur P. Chou[‡], Nigel Maidment[§], Rebecka Klintonberg[¶], John E. Casida[¶], Sharon Li[‡], Arthur G. Fitzmaurice[‡], Pierre-Olivier Fernagut^{¶||}, Farzad Mortazavi^{¶||}, Marie-Francoise Chesselet^{¶||}, and Jeff M. Bronstein^{‡**1}

From the Departments of [‡]Neurology, [§]Psychiatry, and [¶]Neurobiology, University of California at Los Angeles David Geffen School of Medicine and the ^{**}Greater Los Angeles Veterans Administration Medical Center, Los Angeles, California 90095, and [¶]Environmental Chemistry and Toxicology Laboratory, Department of Environmental Science, Policy and Management, University of California, Berkeley, California 94720-3112

The etiology of Parkinson disease (PD) is unclear but may involve environmental toxins such as pesticides leading to dysfunction of the ubiquitin proteasome system (UPS). Here, we measured the relative toxicity of ziram (a UPS inhibitor) and analogs to dopaminergic neurons and examined the mechanism of cell death. UPS (26 S) activity was measured in cell lines after exposure to ziram and related compounds. Dimethyl- and diethyldithiocarbamates including ziram were potent UPS inhibitors. Primary ventral mesencephalic cultures were exposed to ziram, and cell toxicity was assessed by staining for tyrosine hydroxylase (TH) and NeuN antigen. Ziram caused a preferential damage to TH+ neurons and elevated α -synuclein levels but did not increase aggregate formation. Mechanistically, ziram altered UPS function through interfering with the targeting of substrates by inhibiting ubiquitin E1 ligase. Sodium dimethyldithiocarbamate administered to mice for 2 weeks resulted in persistent motor deficits and a mild reduction in striatal TH staining but no nigral cell loss. These results demonstrate that ziram causes selective dopaminergic cell damage *in vitro* by inhibiting an important degradative pathway implicated in the etiology of PD. Chronic exposure to widely used dithiocarbamate fungicides may contribute to the development of PD, and elucidation of its mechanism would identify a new potential therapeutic target.

Parkinson disease (PD)² is a common neurodegenerative disease characterized by relatively selective degeneration of dopa-

minergic (DA) neurons in the substantia nigra (nigrostriatal neurons). The etiology probably involves both environmental and genetic factors including pesticide exposure (1–3). Hundreds of pesticides are used alone or in combinations making it difficult to separate individual effects. Because no individual pesticide has been established by epidemiologic studies, we chose to perform an unbiased screen of potential toxicants for their ability to interfere with the ubiquitin-proteasome system (UPS), a biological pathway implicated in the etiology of PD. Impaired UPS activity has been reported in the brains of patients with PD, and mutations in two UPS genes, Parkin and UCHL-1, cause rare genetic forms of PD (4). Although these results are not universally reproduced (5–7), in some studies administration of UPS inhibitors to rodents recapitulates many of the clinical and pathological aspects of PD (8–10). We hypothesized that chronic pesticide exposure may increase the risk of developing PD by inhibiting the UPS. We screened several pesticides for their ability to inhibit the UPS and found a number of toxicants that can lower activity at relevant concentrations (11). We then focused on dithiocarbamate fungicides because they were found to be one of the most potent UPS inhibitors and are widely used in crop protection.

In the present study, zinc dimethyldithiocarbamate (ziram) was one of several dimethyl- and diethyldithiocarbamates found to inhibit the UPS at 0.15–1 μ M. Furthermore, ziram increased α -synuclein expression in DA cells, induced relatively selective DA cell damage *in vitro*, and inhibited the UPS by interfering with ubiquitin E1 ligase activity. *In vivo*, systemic administration of the more soluble sodium dimethyldithiocarbamate (NaDMDC) in mice resulted in motor deficits and damage to the nigrostriatal pathway. These findings help explain how chronic pesticide exposure could increase the risk of developing PD.

EXPERIMENTAL PROCEDURES

Chemicals—The test compounds (see Table 1) were from Chem Service (West Chester, PA), Sigma-Aldrich, or other commercial sources as the highest available purity, except for 7 and 8, which were synthesized by Karl Fisher in the Casida laboratory.

Measurement of 26 S Proteasome Activity and Cell Death in Cell Lines—26 and 20 S UPS activity and cell death were measured in human embryonic kidney (HEK) and neuroblastoma SK-N-MC cells by flow cytometry as previously described (12).

* This work was supported, in whole or in part, by National Institutes of Health Grant 5 U54 ESO12078. This work was also supported by Veterans Administration Grant SW PADRREC, the National Institutes of Health Medical Scientist Training Program (to A. P. C.), a postdoctoral fellowship from the Swedish Research Council (to R. K.), and funds from the Michael J. Fox Foundation (to F. M.). The costs of publication of this article were defrayed in part by the payment of page charges. This article must therefore be hereby marked "advertisement" in accordance with 18 U.S.C. Section 1734 solely to indicate this fact.

¹ To whom correspondence should be addressed: Dept. of Neurology, UCLA School of Medicine, Reed Neurological Research Center, 710 Westwood Plaza, Los Angeles, CA 90095. Fax: 310-206-9819; E-mail: jbronste@ucla.edu.

² The abbreviations used are: PD, Parkinson disease; E1, ubiquitin-activating enzyme; E2, ubiquitin-conjugating enzyme; E3, ubiquitin ligase; UPS, ubiquitin proteasome system; VMC, ventral mesencephalic cultures; TH, tyrosine hydroxylase; DA, dopaminergic; DMDC, dimethyldithiocarbamate; NaDMDC, sodium DMDC; HEK, human embryonic kidney; GFP, green fluorescent protein; SNc, substantia nigra pars compacta; ANOVA, analysis of variance.

Fluorescence of the green fluorescent protein degron fusion protein (GFP-U) was measured and expressed as a percentage of control.

Rat Primary Ventral Mesencephalic Cultures (VMC)—VMC were prepared by using a protocol adapted from Rayport *et al.* (13). Briefly, the cultures were prepared in two stages. In the first stage, cortical glial feeder cells were established on polyornithine/laminin-coated coverslips, which formed the base of a 10-mm-diameter well cut into 35-mm culture dishes, until they reached confluency in ~6 days. Fluorodeoxyuridine was then added to prevent additional glial proliferation. In the second stage, postnatal day 2 or 3 pups were anesthetized, and 1 mm³ mesencephalic blocks containing the ventral tegmental area were dissected from sagittal sections taken along the midline of the brain. The cells were dissociated and plated onto pre-established glial feeder cells at densities of 1×10^5 /coverslip. The mixed cultures were grown in chemically defined media containing fluorodeoxyuridine for 10 days before treatment and analysis.

Immunocytochemistry in VMCs and Cell Counts—At the conclusion of the experiment, the cultures were immediately washed and fixed in 4% paraformaldehyde for 30 min. The cultures were then incubated with anti-tyrosine hydroxylase (TH) antibodies (1:500; Calbiochem) and anti-NeuN antibodies (1:100; Chemicon) overnight at 4 °C. The cells were stained for 2 h with fluorescein isothiocyanate- and Cy3-conjugated secondary antibodies (Jackson ImmunoResearch). In some experiments, the cells were stained with anti-TH and anti- α -synuclein (1:500; Zymed Laboratories Inc.) antibodies. After staining and prior to counting, the coverslips were randomly assigned an identification number. TH- and NeuN-immunoreactive neuron counts were then determined manually by raters blinded to the experimental conditions. For TH, the entire coverslip was counted but for NeuN+ neurons, representative fields from each coverslip were counted and averaged because of their large number.

Determination of Dopamine Content in VMCs—VMCs were homogenized in 0.1 M perchloric acid containing 0.1% EDTA. Insoluble debris was removed by centrifugation, and the supernatant was filtered through a Millipore MC cartridge. The filtrate was analyzed for dopamine by high pressure liquid chromatography with electrochemical detection (Antec Leyden, Leiden, The Netherlands) using a mobile phase consisting of sodium acetate (75 mM), sodium dodecane sulfonate (0.75 mM), EDTA (10 mM), triethylamine (0.01%), acetonitrile (12%), methanol (12%), and tetrahydrofuran (1%), pH 5.5, pumped at a rate of 200 μ l/min (model LC-10AD; Shimadzu, Columbia, MD) through a 100 \times 2 mm column (3 μ m, Hypersil C18; Keystone Scientific, Bellefonte, PA). The data were collected and analyzed using ChromPerfect software (Justice Innovations, Mountain View, CA).

Quantitation of α -Synuclein Expression—TH-positive cells in each coverslip were identified under 10 \times , and digital images were obtained using a 40 \times objective for TH and α -synuclein immunoreactivity. Exposure times were held constant between coverslips. After acquisition, the images were randomly assigned an identification number, and the experimental conditions were blinded. All of the images were

stacked into a single sequence, a polygonal region of interest was manually drawn around the neuron, and the mean image intensity, total image intensity, and the area inside the region of interest were evaluated for each cell. Data analysis was performed with IPLab ver 3.x for Windows (Scanalytics Inc.) compensating for bleed-through between fluorescein isothiocyanate and Cy3 channels.

To determine whether ziram treatment leads to high molecular weight α -synuclein species, we performed Western blots on the detergent-soluble fractions of culture lysates. VMCs treated with either 1 μ M ziram or 5 μ M lactocystin were lysed in buffer containing 1% Triton X-100 and 0.1% SDS. The lysates were sonicated, and insoluble debris was removed by centrifugation. The protein concentrations were determined, and 10 μ g/lane were subjected to SDS-PAGE. The separated proteins were transferred to nitrocellulose membranes and incubated with an anti- α -synuclein antibody (BD Transduction Laboratories; 1:1000) followed by an anti-tubulin antibody for normalization.

Evaluation of E1 Ligase Activity—The effects of ziram on E1 ligase activity were investigated using Western blot analysis of treated cellular extracts to determine E1/E1-ubiquitin ratios and using purified enzyme preparations. Ziram-treated SK-N-MC cells were washed with phosphate-buffered saline and then lysed in a thiol stabilizing buffer using the method of Jha *et al.* (14). The samples were sonicated for 10 s, centrifuged for 15 min at 13,000 \times g, mixed with 2 parts thiol gel buffer (33 mM Tris-HCl, pH 6.8, 2.7 M urea, 2.5% sodium dodecyl sulfate, and 13% glycerol), and boiled for 2 min, and 10 μ g of protein/lane was loaded on a 12% SDS-PAGE gel (15). The proteins were electrophoretically transblotted onto nitrocellulose paper, and immunoblots were performed as previously described (16) using anti-E1 ligase antibody (BIOMOL, Plymouth Meeting, PA). Antigen-antibody interactions for immunoblots were visualized using horseradish peroxidase-conjugated secondary antibody and chemoluminescence substrate (Pierce).

For purified enzyme assays, human recombinant ubiquitin-activating E1 enzyme and biotinylated ubiquitin (both from BIOMOL) were incubated for 5 or 10 min in thiolester buffer as per the manufacturer's protocol. The reactions were stopped using thiol-stabilizing buffer, and the proteins were subjected to SDS-PAGE and transblotted onto nitrocellulose paper. E1-ubiquitin conjugates were determined using streptavidin-horseradish peroxidase and an enhanced chemiluminescence kit. Band densities were measured using a scanning densitometer.

Animal Studies—Male C57BL/6 mice were treated for 2 weeks by subcutaneous osmotic minipumps with NaDMDC 50 mg/kg/day) in phosphate-buffered saline or with phosphate-buffered saline only. The behavior of the mice was evaluated using the pole test as described by Fleming *et al.* (17) except that a cut-off time of 60 s was used. One week after the last behavioral testing, the mice were perfused with fixative, and their brains were sectioned for TH staining. Fiber density was measured with a computer-assisted image analysis system as previously described (18).

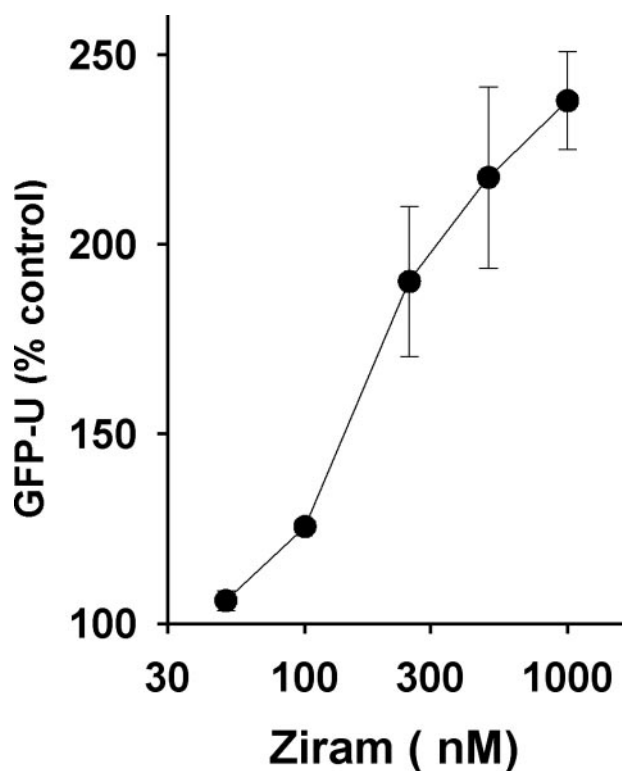


FIGURE 1. Ziram inhibits UPS in HEK cells with 24-h incubation prior to analysis by flow cytometry. The IC_{50} for ziram was 161 nM.

For stereological analysis in the substantia nigra pars compacta (SNc), the neurons were counted using the optical fractionator method with the Stereo Investigator software (Microbrightfield, Colchester, VT) coupled to a Leica DM-LB microscope with a Ludl XYZ motorized stage and z axis microcator (MT12; Heidenheim, Traunreut, Germany). The SNc was delineated at 5 \times objective using previously reported criteria (19, 20). After delineation at low magnification, every fourth section throughout the SNc was counted at 100 \times magnification.

Statistical Analysis—Statistical analysis was performed with GraphPad Prism software. Statistical significance was determined using one-way ANOVA with Dunnett's multiple comparison post-test and Bonferroni's multiple comparison post-test as appropriate. For histochemistry and behavior, statistical analysis was performed with GB-Stat software (Dynamic Microsystems, Inc., Silver Spring, MD, 2000) for Macintosh. A 2 \times 3 mixed design ANOVA was followed by post hoc analysis with Fisher's least significant difference. To maintain homogeneity of variance, an inverse transform was calculated (21) for each score in the pole test. The level of significance was set at $p < 0.05$.

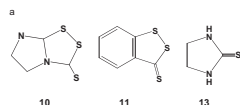
RESULTS

Ziram Inhibits 26 S Proteasome Activity in HEK Cells—We reported earlier that ziram inhibits 26 S UPS in SK-N-MC cells expressing a GFP-degron reporter system (11). To determine whether ziram causes a similar inhibition in a non-neuronal cell line, HEK cells were exposed, and GFP accumulation was measured using flow cytometry. We found that HEK cells were similarly sensitive to the 26 S inhibitory effects of ziram with an IC_{50} of 161 nM (Fig. 1).

TABLE 1

Structure-activity relationships for ziram-related compounds on 26 S UPS with 24-h treatment of SK-N-MC cells

Compound		Fluorescence as percent of control (mean \pm SD, n=4) ^b	
Name	Structure ^a	1 μ M	10 μ M
Dimethyldithiocarbamates			
1 Ziram	$[(CH_3)_2NC(S)S]_2Zn$	274 \pm 21**	466 \pm 42**
2 Sodium dimethyldithiocarbamate	$(CH_3)_2NC(S)SNa \cdot H_2O$	200 \pm 47*	337 \pm 67*
3 Dimethyldithiocarbamate	$(CH_3)_2NC(S)SH \cdot H_2O$	195 \pm 9**	363 \pm 40**
4 Thiram	$[(CH_3)_2NC(S)S]_2$	303 \pm 34**	408 \pm 22**
Diethyldithiocarbamates			
5 Diethyldithiocarbamate	$(C_2H_5)_2NC(S)SH$	167 \pm 24*	184 \pm 31*
6 Disulfiram	$[(C_2H_5)_2NC(S)S]_2$	258 \pm 25**	265 \pm 38**
Others			
7 Zinc chloride	ZnCl ₂	95 \pm 3	93 \pm 5
8 Carbon disulfide	CS ₂	108 \pm 8	101 \pm 6
9 Dimethylamine hydrochloride	$(CH_3)_2NH \cdot HCl$	91 \pm 4	96 \pm 2
10 Etem	heterocyclic ^c	98 \pm 5	190 \pm 10**
11 3H-1,2-Benzodithiole-3-thione	heterocyclic ^a	95 \pm 1	100 \pm 6
12 Enzone or GY-81	NaSC(S)SNa ^a	91 \pm 4	89 \pm 4
13 Ethylenethiourea	heterocyclic ^a	89 \pm 3	94 \pm 3
14 Sodium methylthiocarbamate	CH ₃ NHC(S)SNa	101 \pm 6	98 \pm 3
15 Methyl isothiocyanate	CH ₃ N=C=S	91 \pm 1	94 \pm 2



compound 10 is an oxidation product of maneb and other ethylenebis(dithiocarbamate) fungicides; 11 is an analog of 10 with phenyl instead of dihydroimidazole moiety; 12 decomposes readily to CS₂; 13 is a degradation product of ethylenebis(dithiocarbamate) fungicides

^bHigher number reflects UPS inhibition * $p < 0.05$; ** $p < 0.01$

Structure-Activity Relationships of Ziram-related Compounds for UPS Inhibition—Ziram and 14 related compounds were tested at 1 and 10 μ M for their ability to inhibit 26 S UPS activity in GFP-U-transfected SK-N-MC cells (Table 1). Ziram (1) and the other DMDC derivatives (sodium DMDC (2), free acid (3), and bis-disulfide (4)) were similarly very active. Two diethyldithiocarbamates (5 and 6) were also very potent. Thiram (4) and disulfiram (6) are cleaved into DMDC (3) and diethyldithiocarbamate (5), respectively. Ziram in aqueous solution dissociates to zinc ion (7) and forms dithio acid (3), which breaks down into carbon disulfide (8) and dimethylamine (9), all of which were inactive. The disulfide functionality of etem (10) (an ethylenebis(dithiocarbamate) fungicide oxidation product) can cleave to a dithiocarbamic acid possibly associated with its activity, whereas that of the phenyl analog (11) cannot give a dithiocarbamate. The carbon disulfide progenitor enzone (12) was also inactive. Environmental degradation converts ethylenebis(dithiocarbamate) fungicides to ethylenethiourea (13) and sodium methylthiocarbamate (14) to methyl isothiocyanate (15), all of which were inactive. Thus, the dialkyldithiocarbamate moiety is required to alter UPS activity. Furthermore, preincubation of ziram with the reducing agents GSH, dithiothreitol, or N-acetylcysteine completely abolished its inhibitory activity (data not shown).

Ziram Causes Dopaminergic Cell Damage in Primary VMC—Because proteasome inhibition has been implicated in the etiology of PD and ziram causes UPS dysfunction, dopaminergic cells might be selectively vulnerable to the toxicity of ziram. Primary VMC were exposed to ziram for 48 h, and then cellular toxicity was measured by counting TH immunopositive (TH+) cells and NeuN immunopositive (NeuN+) cells (a nonspecific neuronal marker). Ziram at 5 and 10 μ M was highly toxic to all cells, including the glial bed, causing the cell layers to lift off the coverslip after treatment or during immunostaining

Compound (μM)	% control (mean \pm SD)		
	TH+	NeuN+	TH+/NeuN+
Ziram			
control	100 \pm 7	100 \pm 4	1.00 \pm 0.05
0.1	111 \pm 22	108 \pm 15	0.93 \pm 0.11
0.25	76 \pm 7	81 \pm 5	1.00 \pm 0.07
0.5	60 \pm 10*	75 \pm 11	0.78 \pm 0.09*
1	59 \pm 10*	81 \pm 11	0.64 \pm 0.07**
Lactacystin			
control	100 \pm 7	100 \pm 4	1.00 \pm 0.05
1	89 \pm 7	84 \pm 4	1.18 \pm 0.10
2	84 \pm 11	81 \pm 6	1.12 \pm 0.14
5	79 \pm 15	71 \pm 6**	1.19 \pm 0.24
10	54 \pm 6**	50 \pm 7**	1.24 \pm 0.11

* $p < 0.05$ ** $p < 0.01$

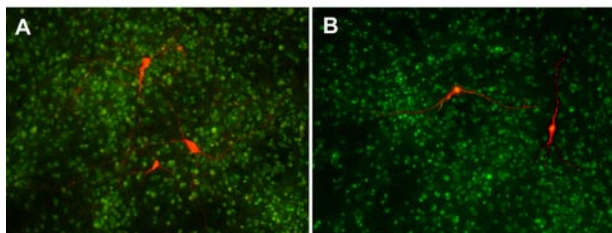


FIGURE 2. Ziram- and lactacystin-induced tyrosine hydroxylase cell damage in primary mesencephalic cultures. TH+ neurons were selectively vulnerable to ziram- but not lactacystin-induced damage. Shown below are representative photomicrographs of TH- (red) and NeuN-stained (green) mesencephalic cultures. A, control. B, ziram (1 μM).

(data not shown). At lower doses Ziram exposure had a significant overall effect on TH+ cell survival ($F_{4,110} = 4.52$, $p < 0.005$) reducing TH+ cell number at 0.5 and 1 μM ($p < 0.05$, Dunnett's post-hoc test versus control; Fig. 2). The small, non-significant decrease in total NeuN+ cells measured after ziram treatment therefore represents primarily the loss of the TH+ subset of the entire NeuN+ pool. The loss of TH+ cells is likely reflective of cell death and not simply the loss of expression because TH levels were increased in the surviving positive cells (data not shown).

The 20 S proteasome inhibitor lactacystin is reported to cause selective DA cell death in VMC, but this has not been a universal finding (28–32). In the present study lactacystin was toxic to NeuN+ neurons ($F_{4,110} = 13.12$, $p < 0.0001$) and to the TH+ subset of such neurons ($F_{4,110} = 4.26$, $p < 0.003$), but the TH+/NeuN+ ratios revealed that the effects of lactacystin were not specific to dopaminergic neurons ($F_{4,110} = 0.90$, $p > 0.05$; Fig. 2). Because ziram caused preferential loss of TH+ neurons and lactacystin did not, they appear to act via different mechanisms, despite the fact that they are both UPS inhibitors.

Ziram Toxicity Is Not Dopamine-dependent—One possible mechanism for the relative selective effect to TH+ neurons is that ziram interacts with dopamine metabolism to produce preferential toxicity. To test this hypothesis, ziram toxicity was measured in the presence of α -methyl L-tyrosine, an inhibitor of dopamine synthesis. Treatment of VMCs with α -methyl L-tyrosine (250 μM) for 48 h resulted in a decrease in dopamine content of $62 \pm 6\%$ compared with controls ($p \leq 0.05$) but did not significantly alter the number of TH+ cells. Reducing dopamine content with α -methyl L-tyrosine was ineffective in attenuating the toxicity of ziram to TH+ neurons (Fig. 3).

α -Synuclein Expression in VMCs—Several converging lines of evidence support a role for α -synuclein in the pathogenesis of

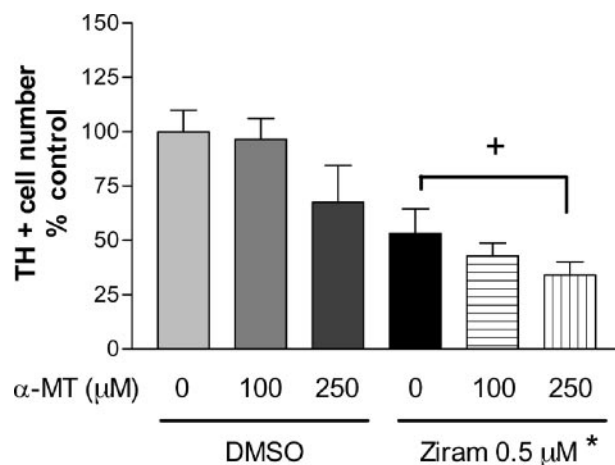


FIGURE 3. Inhibition of dopamine synthesis by α -methyl-L-tyrosine did not attenuate ziram-induced dopamine cell death ($n = 14$ –44 wells per condition). *, $p \leq 0.05$, ziram versus dimethyl sulfoxide (DMSO) control. +, not significant.

Treatment (μM)	Relative expression
Control	1.00 \pm 0.06
Ziram	
0.5	1.07 \pm 0.08
1.0	1.34 \pm 0.12*
Lactacystin 5	0.70 \pm 0.07*

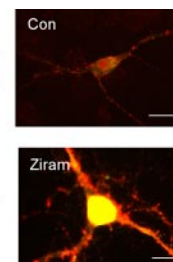


FIGURE 4. Ziram increases and lactacystin decreases α -synuclein levels in TH+ neurons. The cells were exposed for 48 h prior to analysis. The relative intensities were measured in a blinded manner in cells that were selected randomly ($n = 21$ –97 cells/condition). Representative α -synuclein-stained cells are shown on the right. Scale bars, 10 microns. **, $p \leq 0.01$. Con, control.

PD. Mutations in the α -synuclein gene or increased expression of wild-type α -synuclein cause PD in familial PD, and α -synuclein is a major component of Lewy bodies in sporadic PD (22). To determine whether ziram alters the levels of α -synuclein in VMCs, the neurons were stained for both TH and α -synuclein, and relative fluorescence was measured. TH+ neurons showed robust and punctate α -synuclein staining, suggesting that they are mature and terminally differentiated (23, 24). Ziram at 0.5 μM resulted in increased α -synuclein expression, whereas lactacystin at 5 μM decreased expression (Fig. 4). The sizes of the regions of interest were the same among all of the conditions varied in all of the experiments (data not shown).

An important pathological marker in PD is the formation of α -synuclein inclusions or aggregates. TH+ cells from ziram- and lactacystin-treated VMCs were determined to be either positive or negative for nuclear, perinuclear, or cytoplasmic α -synuclein inclusions by blinded raters. Aggregates were relatively common in both treated and untreated cells, but surprisingly no significant differences were found with ziram compared with controls. Interestingly, a decrease in nuclear and perinuclear aggregates was seen in the lactacystin-treated cultures (Table 2).

To determine whether ziram treatment results in increased formation of detergent-soluble α -synuclein oligomer formation, we subjected VMCs lysates to Western blot analysis. Both monomeric and oligomeric forms of α -synuclein were apparent

Ziram Causes Dopaminergic Cell Damage

TABLE 2

Ziram does not induce the formation of α -synuclein aggregates

$n = 21-97$ cells/condition.

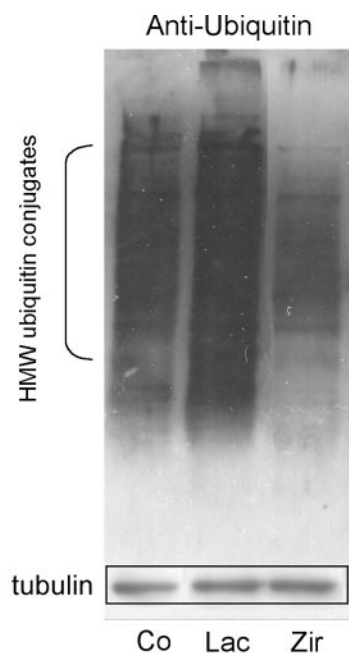
	Cells with inclusions		
	Nuclear	Perinuclear	Cytoplasmic
Control	32 \pm 5	22 \pm 4	4.3 \pm 2.1
Ziram		%	
0.5 μ M	38 \pm 6	24 \pm 5	6.6 \pm 2.9
1.0 μ M	19 \pm 9	14 \pm 8	4.8 \pm 4.8
Lactacystin (5 μ M)	19 \pm 4 ^a	8.6 \pm 3.1 ^b	7.4 \pm 2.9

^a $p = 0.04$.

^b $p = 0.01$.

in detergent-soluble fractions as previously described (25). Ziram treatment resulted in a nonsignificant trend for an increase in oligomeric forms of α -synuclein compared with controls (170 \pm 120% optical density units of controls, $n = 8$ for ziram and $n = 5$ for controls, $p = 0.18$). Oligomeric α -synuclein was unchanged in lactacystin-treated VMCs, and monomeric α -synuclein levels were similar in all three conditions (data not shown).

Ziram Inhibits E1 Ligase Activity—Ziram was found to inhibit the UPS using an assay that requires the substrate (*i.e.* degron) to be ubiquitinated via ubiquitin ligases and recognized by the 26 S proteasome before it can be degraded by 20 S proteases (12). Disruption of any of these steps would be detected in the screen. It has been suggested that another dithiocarbamate fungicide, maneb, inhibits the 20 S component of the UPS (26). To determine whether ziram acted in this manner, HEK cells were treated with ziram (1 and 10 μ M) for 24 h, but there was no change in 20 S chymotryptic activity (data not shown). The amount of α -subunit of the 20 S proteasome was also measured using Western blot analysis, and no differences were found (data not shown). Furthermore, our earlier study showed that ziram had no effect on 20 S UPS activity when added directly to cell lysate (11). Because 20 S proteolytic activity was not altered by ziram, Western blot analysis on lysates was performed from ziram-treated cells to determine whether ubiquitinated proteins accumulated. As expected, inhibition of the 20 S UPS by lactacystin and rotenone resulted in the accumulation of high molecular weight ubiquitin conjugates (Fig. 5). Conversely, ziram treatment resulted in a significant decrease in these proteins, suggesting that it inhibits the UPS by interfering with ubiquitin ligation. Polyubiquitin is added to proteins targeted for UPS degradation by a series of ligases (E1, E2, and E3 ligases). Dithiocarbamates can lead to GSH oxidation (27), and GSH depletion results in the loss of E1 ligase activity (14). Ziram does not appear to act by lowering GSH, because depleting cellular GSH using buthionine sulfoximine (1 mM) had no effect on UPS activity, and ziram did not alter the amount of reduced GSH in the cells at concentrations up to 50 μ M (data not shown). Ubiquitin is activated by E1 ligase in an ATP-dependent manner forming an E1-ubiquitin adduct before the ubiquitin is transferred to E2 ligase. Because activated ubiquitin binds covalently to a cysteine of E1, the thiol group of ziram might interfere with this reaction. Indeed, ziram markedly reduced E1 ligase activity as measured by a reduction of endogenous E1-ubiquitin conju-



Compound	Mean \pm SEM	% Control
Control	3.46 \pm 1.2	100
Lactacystin	21.41 \pm 7.0	618**
Ziram (1 μ M)	2.44 \pm 0.9	71*

FIGURE 5. Anti-ubiquitin Western blot analysis of lysates from cells following treatment with 5 μ M lactacystin, 0.1 μ M rotenone, or 1 μ M ziram. The relative densities were determined using the NIH Image program, normalized to tubulin immunoreactivity in the same blot, and expressed as percentages of untreated controls ($n = 4$). 20 S inhibition using lactacystin resulted in an increase in high molecular weight ubiquitin conjugates, whereas ziram treatment reduced them. **, $p \leq 0.01$; *, $p \leq 0.05$.

gates and the reduced formation of E1-ubiquitin conjugates in a purified preparation (Fig. 6).

Motor Deficits in NaDMDC-treated Mice—NaDMDC was used for *in vivo* experiments because of its greater solubility than the zinc DMDC salt, ziram, with a similar effect on proteasomal function (Table 1). The treatment of male C57BL/6 mice for 2 weeks with NaDMDC resulted in increased time to turn in the pole test, a deficit also seen in mice with dysfunction of the nigrostriatal pathway (Fig. 7). The effect persisted 8 weeks after cessation of drug treatment, indicating that it was not because of an acute drug effect. Striatal TH fiber density was nonsignificantly reduced across striatal regions at 2 weeks, with a significant reduction in the ventrolateral quadrant 9 weeks after drug treatment in the NaDMDC-treated animals (Table 3). Stereological TH immunoreactive neuron counts in the SNc of treated mice were not changed (Table 3). Thus, 2 weeks of treatment of mice with NaDMDC, an E1-activating enzyme inhibitor, resulted in a motor deficit with a minor loss of nigrostriatal dopaminergic fibers.

DISCUSSION

Pesticides, Ziram, and PD—The most consistent and strongest association between a group of environmental toxicants and the development of sporadic PD has been with chronic pesticide exposure, although no specific agents have been identified

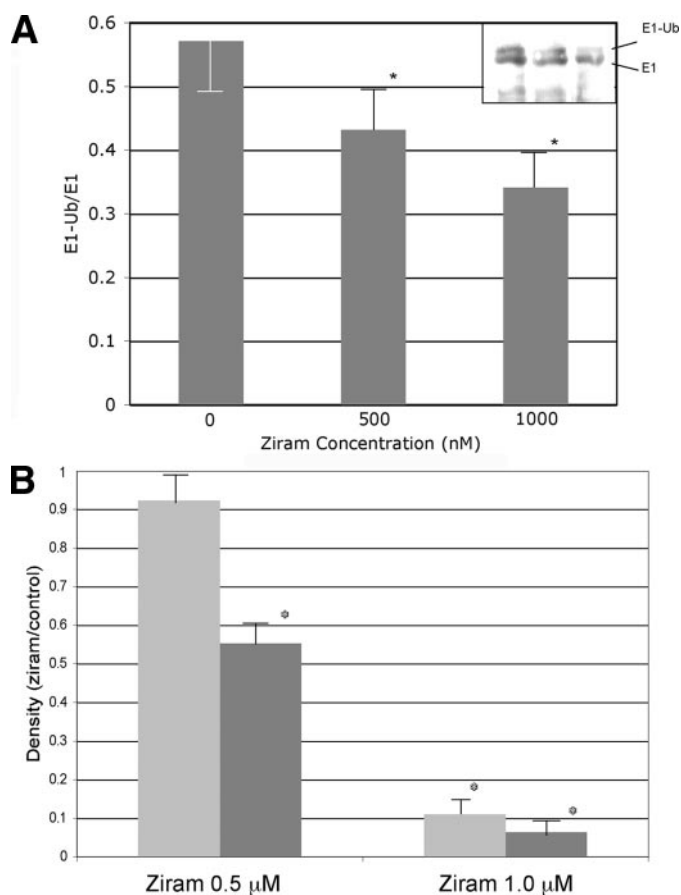


FIGURE 6. Effect of ziram on E1-ubiquitin conjugates and E1 ligase activity. A, endogenous E1-ubiquitin conjugates in lysates of ziram-treated HEK cells. Ziram resulted in a dose-dependent reduction in the E1-Ub/E1 ratio compared with untreated controls. The Western blot is shown in the inset. B, E1 ligase activity was inhibited by ziram in purified preparations after 5 and 10 min of incubation ($n = 4$, $p \leq 0.05$).

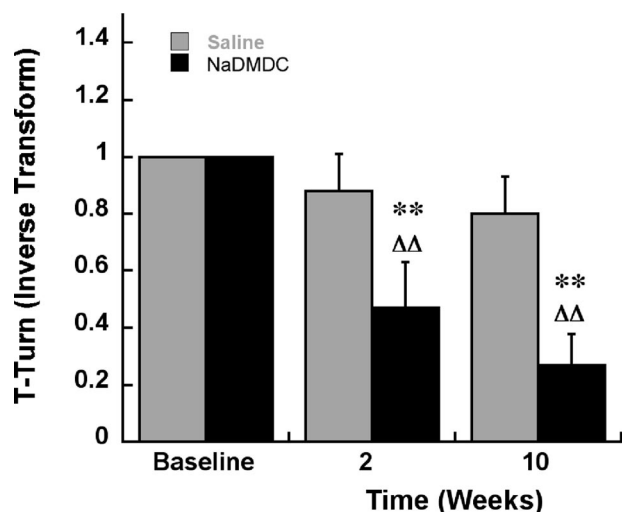


FIGURE 7. Motor deficits in mice determined by the pole test following 2 weeks of subcutaneous minipump treatment with NaDMDC at 50 mg/kg/day followed by an 8-week post-treatment period (10 weeks from the beginning of the experiment). Inverse Transform, reciprocal of the original data point. Baseline, 1 because untreated mice turn in less than 1 s. **, $p < 0.01$ compared with saline-treated mice at the same time point. $\Delta\Delta$ represents $p < 0.01$ compared with a base line within the same treatment group (2×3 Mixed design ANOVA, Fisher's LSD).

TABLE 3

Effect of subcutaneous treatment with NaDMDC on TH immunoreactivity (IR) fiber density in striatal subregions and stereological estimates of TH-IR neurons in the SNc

DL, dorsolateral; DM, dorsomedial; VL, ventrolateral; VM, ventromedial.

Region	Mean \pm S.E. ($n = 5$)			
	2W		2 + 9W	
	Control	Treated	Control	Treated
TH-IR fiber density				
DL striatum	1515 \pm 207	1456 \pm 221	1934 \pm 299	1951 \pm 269
DM striatum	1048 \pm 149	843 \pm 117	1435 \pm 199	1358 \pm 130
VL striatum	1439 \pm 142	1290 \pm 140	1833 \pm 254	1409 \pm 166 ^a
VM striatum	815 \pm 103	696 \pm 62	1073 \pm 174	946 \pm 152
TH-IR-positive neurons				
SNc	7980 \pm 491	7832 \pm 574	8251 \pm 214	7897 \pm 247

^a $p \leq 0.05$ compared with corresponding region in control mice at the same time point; ANOVA followed by Fisher PLSD.

(3). Preliminary data from our population-based study in central California that determined pesticide exposure using a state application registry has revealed some intriguing results. Subjects living within 500 meters of where ziram was applied were at an over 3-fold higher risk of developing PD compared with those with lower exposure.³ Chronic inhibition of the UPS has been implicated in the pathogenesis of PD, and some pesticides might increase the risk of developing PD by causing UPS dysfunction. The widely used pesticide ziram is one of the most potent inhibitors of 26 S UPS (11). This study further demonstrates that ziram kills TH+ cells in a relatively selective manner, increases α -synuclein levels, and inhibits E1 ligase activity, thus interfering with the targeting of proteins destined for UPS degradation. If these preliminary epidemiology findings are confirmed, and taken together with the results of this study, chronic ziram exposure would be a strong candidate as a PD-associated toxicant. The results presented here add a biologically plausible mechanism (at relevant concentrations) by which ziram may increase the risk of developing the disease.

Mechanism of Ziram Effect on the UPS—Uncovering how ziram causes UPS dysfunction and cell death might provide important clues to the selective vulnerability of DA neurons. Some of the results in primary cultures were surprising. Although ziram damaged (and probably killed) TH+ cells in a selective manner, this was not the case for the 20 S proteasome inhibitor lactacystin. Even though TH staining was used as a marker of DA cell survival, it is possible that the cells were still alive but simply lost their TH phenotype. However, this is unlikely because TH levels were actually increased in the remaining cells after ziram exposure (but not for lactacystin). Conflicting results on proteasome inhibitor-induced selective DA cell death may be due to differences in culturing techniques and conditions (28–32). Cultures in the current study contained DA neurons of the ventral tegmental region to increase the number of TH+ cells/well and power analysis. Because ventral tegmental region neurons are believed to be more resistant to stressors, the results likely underestimate the effects of ziram on SNc DA neurons. Indeed, pilot experiments using predominantly nigral cultures yielded similar results. The fact that different effects were found with ziram compared with

³ B. Ritz, J. M. Bronstein, and S. Costello, unpublished data.

Ziram Causes Dopaminergic Cell Damage

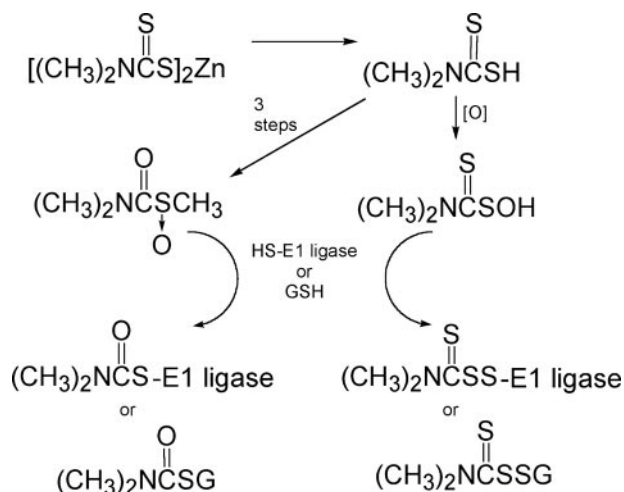


FIGURE 8. Alternative mechanisms for ziram oxidative activation and reaction with 26 S E1 ligase or GSH.

lactacystin suggests that they act through different mechanisms. As opposed to lactacystin, a 20 S protease inhibitor, we show that ziram acts upstream by interfering with ubiquitin ligation. Because ubiquitinylation is also important in many cellular processes in addition to the UPS, including modification of protein function, facilitation of cell surface receptor turnover, and control of gene transcription, it is possible that some of the actions of ziram may be via alternative pathways (33).

The molecular basis of the ability of ziram to inhibit E1 ligase activity was studied by determining the relative potencies of several of its analogs. The most potent 26 S UPS inhibitors were dimethyl- and diethyldithiocarbamates and their salts and disulfides. These compounds may act by copper or iron chelation (34) or undergo oxidative activation to the *S*-oxides of the dithiocarbamic acids (35) or of the *S*-methyl thiocarbamates (36), which are reactive with GSH and potentially with a thiol group of the UPS E1 ligase (Fig. 8).

Maneb and Ethylenebis(dithiocarbamate) Fungicides—The effect of ziram on UPS activity has not been observed by others, but the structurally related fungicide maneb is reported to inhibit 20 S protease activity (26). Although ziram and maneb have many structural features in common, our results with ziram differ significantly from those of Zhou *et al.* (26) using maneb. In our studies, ziram did not inhibit the 20 S proteasome at concentrations up to $10 \mu\text{M}$, did not cause oxidative stress as measured by 6-carboxy-2',7'-dichlorodihydrofluorescein diacetate fluorescence (11), and did not induce α -synuclein aggregates in primary cultures. These observations may be due to differences in the compounds and/or cell assays used. Maneb is an ethylenebis(dithiocarbamate) and contains manganese, which possibly could contribute to some of its effects, but manganese by itself did not alter 26 S UPS activity (data not shown).

Another difference between the effects of maneb and ziram is that maneb is reported to induce α -synuclein aggregates in a rat embryonic mesencephalon murine neuroblastoma-glioma hybrid cell line (26). The present study did not find an increase in aggregate formation in primary mesencephalic cultures but

did not evaluate aggregates in immortalized cell lines because neither HEK or SK-N-MC cells expressed significant levels. Several lines of evidence support a mechanism for ziram upstream of the 20 S: inhibition of the formation of high molecular weight ubiquitin conjugates, reduction of the E1-ubiquitin/E1 ratio, and direct inhibition of purified E1 ligase activity. Ziram effects on E2 or E3 ligase activities were not studied because they are dependent on E1 ligase, but because they transfer ubiquitin in a manner similar to that of E1, it is possible that ziram would have similar inhibitory effects on these enzymes.

Animal Studies on Dithiocarbamate Fungicides—Further support for the potential role dithiocarbamates in PD comes from animal studies. Chronic maneb exposure given with paraquat recapitulates many of the behavioral and pathological hallmarks of PD (37). Two week subcutaneous minipump treatment with NaDMDC at 50 mg/kg/day resulted in persistent motor abnormalities typically seen in mice with dysfunction of the nigrostriatal pathway (38). Abnormal motor behavior in our study was associated with a mild, delayed dopamine nerve terminal damage in the ventrolateral region of the striatum but not with nigral cell death. Motor dysfunction without dopamine cell loss may indicate functional damage to these neurons, but we cannot exclude the possibility that the behavioral tests were detecting abnormalities in other areas involved in motor control.

In summary, we show that ziram and structurally related dithiocarbamates induce dysfunction of the UPS by inhibiting E1 ligase. We demonstrate that ziram exposure increases α -synuclein levels and selectively damages dopaminergic neurons in primary cultures. Furthermore, chronic systemic exposure to NaDMDC causes persistent motor deficits and mild injury to the nigrostriatal pathway. This study, along with emerging epidemiological investigations, suggests that chronic exposure to dithiocarbamate fungicides can contribute to the pathogenesis of PD.

Acknowledgment—We thank Dr. Sheila Fleming for help with the statistical analysis.

REFERENCES

- Ascherio, A., Chen, H., Weisskopf, M. G., O'Reilly, E., McCullough, M. L., Calle, E. E., Schwarzschild, M. A., and Thun, M. J. (2006) *Ann. Neurol.* **60**, 197–203
- Kamel, F., Tanner, C., Umbach, D., Hoppin, J., Alavanja, M., Blair, A., Comyns, K., Goldman, S., Korell, M., Langston, J., Ross, G., and Sandler, D. (2007) *Am. J. Epidemiol.* **165**, 364–374
- Brown, T. P., Rumsby, P. C., Capleton, A. C., Rushton, L., and Levy, L. S. (2006) *Environ. Health Perspect.* **114**, 156–164
- McNaught, K. S., and Jenner, P. (2001) *Neurosci. Lett.* **297**, 191–194
- Manning-Bog, A. B., Reaney, S. H., Chou, V. P., Johnston, L. C., McCormack, A. L., Johnston, J., Langston, J. W., and Di Monte, D. A. (2006) *Ann. Neurol.* **60**, 256–260
- Kordower, J. H., Kanaan, N. M., Chu, Y., Suresh Babu, R., Stansell, J., 3rd, Terpstra, B. T., Sortwell, C. E., Steece-Collier, K., and Collier, T. J. (2006) *Ann. Neurol.* **60**, 264–268
- Bove, J., Zhou, C., Jackson-Lewis, V., Taylor, J., Chu, Y., Rideout, H. J., Wu, D. C., Kordower, J. H., Petrucelli, L., and Przedborski, S. (2006) *Ann. Neurol.* **60**, 260–264
- McNaught, K. S., and Olanow, C. W. (2006) *Ann. Neurol.* **60**, 243–247

9. Schapira, A. H., Cleeter, M. W., Muddle, J. R., Workman, J. M., Cooper, J. M., and King, R. H. (2006) *Ann. Neurol.* **60**, 253–255
10. McNaught, K. S., Perl, D. P., Brownell, A. L., and Olanow, C. W. (2004) *Ann. Neurol.* **56**, 149–162
11. Wang, X. F., Li, S., Chou, A. P., and Bronstein, J. M. (2006) *Neurobiol. Dis.* **23**, 198–205
12. Bence, N. F., Sampat, R. M., and Kopito, R. R. (2001) *Science* **292**, 1552–1555
13. Rayport, S., Sulzer, D., Shi, W. X., Sawasdikosol, S., Monaco, J., Batson, D., and Rajendran, G. (1992) *J. Neurosci.* **12**, 4264–4280
14. Jha, N., Kumar, M. J., Boonplueang, R., and Andersen, J. K. (2002) *J. Neurochem.* **80**, 555–561
15. Laemmli, U. K. (1970) *Nature* **227**, 680–685
16. Chow, E., Mottahedeh, J., Prins, M., Ridder, W., Nusinowitz, S., and Bronstein, J. M. (2005) *Mol. Cell Neurosci.* **29**, 405–413
17. Fleming, S. M., Salcedo, J., Fernagut, P. O., Rockenstein, E., Masliah, E., Levine, M. S., and Chesselet, M. F. (2004) *J. Neurosci.* **24**, 9434–9440
18. Bordelon, Y. M., and Chesselet, M. F. (1999) *Neuroscience* **93**, 843–853
19. McCormack, A. L., Thiruchelvam, M., Manning-Bog, A. B., Thiffault, C., Langston, J. W., Cory-Slechta, D. A., and Di Monte, D. A. (2002) *Neurobiol. Dis.* **10**, 119–127
20. West, M. J., Slomianka, L., and Gundersen, H. J. (1991) *Anat. Rec.* **231**, 482–497
21. Cohen, J., and Cohen, P. (1983) *Applied Multiple Regression/Correlation Analysis for the Behavioral Sciences*, 2nd Ed., Lawrence Erlbaum Associates, Hillsdale, NJ
22. Singleton, A. B. (2005) *Trends Neurosci.* **28**, 416–421
23. Quilty, M. C., Gai, W. P., Pountney, D. L., West, A. K., and Vickers, J. C. (2003) *Exp. Neurol.* **182**, 195–207
24. Lesuisse, C., and Martin, L. J. (2002) *J. Neurobiol.* **51**, 9–23
25. Rideout, H. J., Dietrich, P., Wang, Q., Dauer, W. T., and Stefanis, L. (2004) *J. Biol. Chem.* **279**, 46915–46920
26. Zhou, Y., Shie, F. S., Piccardo, P., Montine, T. J., and Zhang, J. (2004) *Neuroscience* **128**, 281–291
27. Burkitt, M. J., Bishop, H. S., Milne, L., Tsang, S. Y., Provan, G. J., Nobel, C. S., Orrenius, S., and Slater, A. F. (1998) *Arch. Biochem. Biophys.* **353**, 73–84
28. Rideout, H. J., Lang-Rollin, I. C., Savalle, M., and Stefanis, L. (2005) *J. Neurochem.* **93**, 1304–1313
29. Kikuchi, S., Shinpo, K., Tsuji, S., Takeuchi, M., Yamagishi, S., Makita, Z., Niino, M., Yabe, I., and Tashiro, K. (2003) *Brain Res.* **964**, 228–236
30. Hoglinger, G. U., Carrard, G., Michel, P. P., Medja, F., Lombes, A., Ruberg, M., Friguet, B., and Hirsch, E. C. (2003) *J. Neurochem.* **86**, 1297–1307
31. McNaught, K. S., Mytilineou, C., Jnobaptiste, R., Yabut, J., Shashidharan, P., Jennert, P., and Olanow, C. W. (2002) *J. Neurochem.* **81**, 301–306
32. Petrucelli, L., O'Farrell, C., Lockhart, P. J., Baptista, M., Kehoe, K., Vink, L., Choi, P., Wolozin, B., Farrer, M., Hardy, J., and Cookson, M. R. (2002) *Neuron* **36**, 1007–1019
33. Liu, Y. C. (2004) *Annu. Rev. Immunol.* **22**, 81–127
34. Montine, T. J., Underhill, T. M., Valentine, W. M., and Graham, D. G. (1995) *Neurodegeneration* **4**, 283–290
35. Schmitt, A., and Neibergall, H. (1989) *Deutsche Lebensmittel-Rundschau* **85**, 111–115
36. Staub, R. E., Sparks, S. E., Quistad, G. B., and Casida, J. E. (1995) *Chem. Res. Toxicol.* **8**, 1063–1069
37. Thiruchelvam, M., Richfield, E. K., Baggs, R. B., Tank, A. W., and Cory-Slechta, D. A. (2000) *J. Neurosci.* **20**, 9207–9214
38. Hwang, D. Y., Fleming, S. M., Ardayfio, P., Moran-Gates, T., Kim, H., Tarazi, F. I., Chesselet, M. F., and Kim, K. S. (2005) *J. Neurosci.* **25**, 2132–2137

APPENDIX B

**Geochemical and hydrologic controls on the
mobilization of arsenic derived from
herbicide application**



Contents lists available at ScienceDirect

Applied Geochemistry

journal homepage: www.elsevier.com/locate/apgeochem

Geochemical and hydrologic controls on the mobilization of arsenic derived from herbicide application

Arthur G. Fitzmaurice^a, A. Azra Bilgin^a, Peggy A. O'Day^b, Virginia Illera^b, David R. Burris^c, H. James Reisinger^c, Janet G. Hering^{a,*}

^a Department of Environmental Science and Engineering, California Institute of Technology, 1200 E. California Blvd., MC 138-78, Pasadena, CA 91125, USA

^b School of Natural Sciences, University of California, Merced, 5200 N. Lake Road, Merced, CA 95343, USA

^c Integrated Science and Technology, Inc., 1349 Old Highway 41, Suite 225, Marietta, GA 30060, USA

ARTICLE INFO

Article history:

Received 22 February 2009

Accepted 10 September 2009

Available online 17 September 2009

Editorial handling by D. Polya

ABSTRACT

The fate and transport of As was examined at an industrial site where soil- and groundwater contamination are derived from the application of As₂O₃ as a herbicide. Application of arsenical herbicides was discontinued in the 1970s and soils in the source area were partially excavated in 2003. Arsenic contamination (up to 280 mg/kg) remains in the source area soils and a plume of As-contaminated groundwater persists in the surficial aquifer downgradient of the source area with maximum observed As concentrations of 1200 µg/L near the source area. The spatial extent of As contamination as defined by the 10 µg/L contour appears to have remained relatively stable over the period 1996–2006; the boundary of the 1000 µg/L contour has retreated over the same time period indicating a decrease in total As mass in the surficial groundwater.

In column experiments conducted with source area soil, the As concentrations in the column effluent were comparable to those observed in groundwater near the source area. A substantial fraction of the As could be leached from the source area soil with ammonium sulfate and ammonium phosphate. Exhaustive extraction with background groundwater removed most of the total As. These results indicate that As in the source area soils is geochemically labile. Source area soils are low in extractable Fe, Mn and Al, and characterization by X-ray absorption spectroscopy and electron microscopy indicated that As is present primarily as arsenate sorbed to (alumino)silicate minerals. Batch sorption experiments showed much less sorption on surficial aquifer sediments than on sediments from the Jackson Bluff Formation (JBF), a presumed confining layer. This limited capacity of the surficial aquifer sediments for As sorption is consistent with the similar As contents observed for these sediments within and upgradient of the As plume. The apparent stability of the As plume cannot be explained by sequestration of As within the surficial aquifer. Sorption to JBF sediments may contribute to As sequestration, but As enrichment in JBF sediments within the plume (i.e., as compared with JBF sediments upgradient) was not observed. These results indicate that neither the persistence of As in the source area soils or the apparent stability of the plume of As-contaminated groundwater at this site can be explained by geochemical controls on As mobility. The absence of demonstrable geochemical bases for such observations suggests that possible hydrologic controls should be further investigated at this site.

© 2009 Elsevier Ltd. All rights reserved.

1. Introduction

Arsenical pesticides and herbicides were widely used in the USA throughout the 20th century until As was placed on the US Environmental Protection Agency's (USEPA) Priority List of Hazardous Substances. In 2001, concerns regarding the toxicity and carcinoge-

* Corresponding author. Present address: Eawag, Swiss Federal Institute of Aquatic Science and Technology, Ueberlandstrasse 133, CH-8600 Dübendorf, Switzerland. Tel.: +41 (0) 44 823 50 01; fax: +41 (0) 44 823 53 98.

E-mail address: Janet.Hering@eawag.ch (J.G. Hering).

nicity of As prompted the USEPA to lower the maximum contaminant level (MCL) for As in drinking water from 50 to 10 µg/L (USEPA, 2001). The leaching of As from soils previously treated with arsenical pesticides poses a potential threat to human health through contamination of drinking water supplies.

Arsenical pesticides are known to be effective for years after application (Norman et al., 1950), suggesting that they are not easily leached from soils. After the cessation of pesticide application, As has persisted at high concentrations in some soils despite decades of rainfall and irrigation (Sadler et al., 1994; McLaren et al., 1998; Folkes et al., 2001; Robinson and Ayuso, 2004; Smith et al.,

2006; Yang and Donahoe, 2007). Leaching of As applied in organic form has, however, been inferred from the accumulation of As in the sediments of lakes receiving surface runoff or groundwater discharge from treated soils (Whitmore et al., 2008).

Immobilization of As in soils under oxic conditions is often attributed to the association of As with Fe-bearing solid phases through sorption or co-precipitation (Smedley and Kinniburgh, 2002; Stoltenwerk, 2003). Evidence has also been reported for precipitation of As(V)-containing salts in soils (Bothe and Brown, 1999; Yang and Donahoe, 2007). Mobilization of As from such solids can occur when the solids or the association of As with them are destabilized due to changes in geochemical conditions. Such geochemical control of As mobility is often assumed when As is persistent in soils over long periods.

In this study, the mobilization of As from a sandy soil where it has persisted for 3 decades, after the use of As_2O_3 as a herbicide was discontinued, was examined. The controls on As mobilization have implications both for the occurrence of As in groundwater and the fate and transport of As in the subsurface environment.

2. Site description

Tyndall Air Force Base (AFB) is located in the Florida Panhandle between Panama City and Mexico Beach on a strip of barrier land that separates East Bay (the eastern portion of St. Andrew's Bay) from the Gulf of Mexico (Fig. 1). An electrical substation was constructed on the base in 1960. Arsenic trioxide was applied as a herbicide at the substation until the mid-1970s.

In 1992, As contamination in groundwater was identified at the Tyndall site with a maximum As concentration of 1700 $\mu\text{g/L}$ measured at a monitoring well (MW-1) located at the substation and screened from the water table at 1.5 m below ground surface (bgs) to 4.5 m; an even higher As concentration (2400 $\mu\text{g/L}$) was observed at MW-1 in 1993 (SCS, 1999). By 1996, 18 monitoring wells were installed at the site (two additional wells were installed later); all wells were screened over 3-m intervals at varying depths as indicated in Fig. 2. Groundwater monitoring in 1996 showed a plume of As-contaminated groundwater extending SW from the substation in the direction of groundwater flow.

In 2003, soil within the substation was partially excavated to depths ranging from 0.6 to 1.5 m. Approximately 800 t of contaminated soil was removed from the site and replaced with clean soil (SCS, 2003). Some areas of the energized substation could not be safely excavated and thus those soils remained in place. Crushed

gravel covers the entire substation ground surface where equipment is not positioned, allowing for infiltration of rainwater.

The stratigraphy of the study site is defined by three primary units: recent sands (surficial aquifer), the Jackson Bluff Formation (JBF), and the Intracoastal Formation (Schmidt and Clark, 1980; SCS, 1999). The surficial aquifer sediments are well-sorted fine- to medium-graded sands. A distinct peaty zone, 15–30 cm thick, occurs at an approximate depth of 0.9–1.5 m. Below this, the sands are tan to grayish-white, well-sorted, slightly silty, and fine-grained. At a depth of approximately 14 m, the sands grade into the JBF, which is characterized by dark greenish-gray, very fine-grained, clayey, silty sand. The thickness of the JBF varies but appears to be approximately 2.5 m thick near the substation. The JBF is underlain by the upper Intracoastal Formation, which is dark greenish-brown, fine-grained, clayey, silty sand.

Groundwater flow is generally to the SW. The water table is typically within 0.9–1.5 m of the land surface, and the aquifer is recharged by direct infiltration into the porous sands. Groundwater is lost by discharge into springs and streams or drainage ditches, subsurface flow to the ocean, evaporation, transpiration and withdrawal. In addition, some groundwater may flow downward through the intermediate leaky aquitard. The average hydraulic conductivity estimated from six slug tests (Brouwer-Rice method) is 0.02 cm/s (MW-2, 3, 5, 8, 9, and 10), and the effective porosity is estimated to be 0.2. The estimated horizontal flow rate toward the Gulf of Mexico in the surficial aquifer is 0.8 m/d based on a gradient of 0.01, but this hydraulic gradient is not uniform across the site (SCS, 1999).

3. Methods

3.1. Chemicals and analytical methods

All chemicals used were reagent grade or better, and used without further purification: OmniTrace Ultra HNO_3 , HNO_3 , HCl, H_2SO_4 , pyridine, and CertiPUR ICP standards were obtained from EMD Chemicals; $NaAsO_2$ and $CaSO_4$ from J.T. Baker; NaOH, $(NH_4)_2SO_4$, and $NH_4H_2PO_4$ from EM Science; $Na_2HAsO_4 \cdot 7H_2O$, EDTA, $MgSO_4 \cdot 7H_2O$, and NaCl from Sigma; NH_4CH_3COO , CH_3COOH , and CH_3OH from BDH; 1,10-phenanthroline and H_2O_2 from Alfa Aesar; $NH_2OH \cdot HCl$ from Fisher Scientific.

Solutions were prepared with 18.2-M Ω cm deionized water (Millipore Milli-Q 18.2-M Ω system) and stored in plastic containers that had been washed with 10% HCl. All volumetric flasks were washed with 10% HCl and rinsed several times with deionized water prior to use. All analyses were conducted in triplicate, including instrument and field blanks.

Dissolved As, Al, Mn and Si were determined by inductively-coupled plasma-mass spectrometry (ICP-MS, Hewlett-Packard 4500). Samples were diluted with Ultra HNO_3 (OmniTrace) to 1% acid.

Iron was determined as Fe(II) and total Fe using the colorimetric 1,10-phenanthroline method without boiling (adapted from Eaton et al., 2005) with a UV-Visible Spectrophotometer (Cary 480) at 510 nm.

Arsenic speciation was determined by quantifying As(III) and As(V) using coupled liquid chromatography (LC) and ICP-MS, in which As(III) and As(V) were separated by an HPLC column (Hewlett Packard 1100 series) with a 3-mM phosphate mobile phase (pH 6.0) at 0.9 mL/min flow rate and HPLC outflow was directly connected to the ICP-MS for As measurement.

Major cations and anions were quantified by ion chromatography (Dionex Model DX-500) following standard methods (Eaton et al., 2005). Colorimetric determinations of P by USEPA Method 365.1 (USEPA, 1993) and determinations of total and dissolved or-

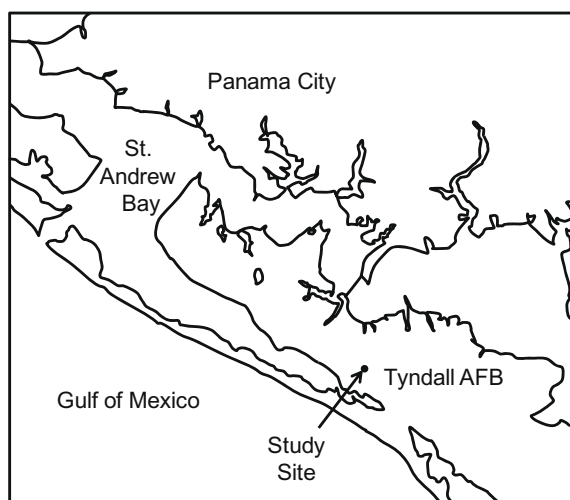


Fig. 1. Tyndall Air Force Base, FL and substation study site locations.

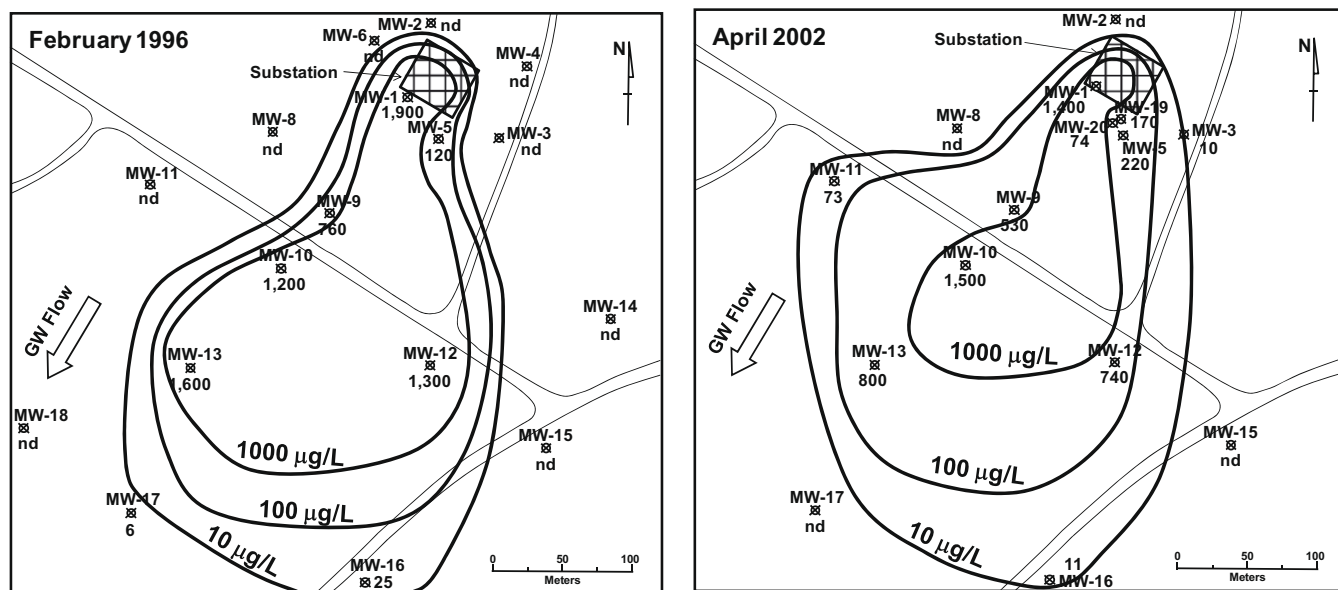


Fig. 2. Groundwater monitoring data showing extent of As contamination in surficial aquifer in February 1996 and April 2002, prior to the partial excavation of source area soils in 2003. Approximate iso-concentration contours shown based on historical monitoring data for total As concentrations ($\mu\text{g/L}$), which are shown next to the location of the monitoring wells (nd = non-detect). All screened intervals were 3 m starting at depths of 1.4 m (MW-1, 4), 1.6 m (MW-2, 3, 5, 6), 18.1 m (MW-7), 5.4 m (MW-8, -9), 10.6 m (MW-10, -11), 11.5 m (MW-12), 11.3 m (MW-13), 8.1 m (MW-14, -18), 8.4 m (MW-15–17). Source: (SCS, 1999; Gulf Power, 2004).

ganic C (TOC, DOC) by combustion/catalytic oxidation (Eaton et al., 2005) were performed by MWH Environmental Laboratories (Pasadena, CA). To avoid excessive holding times, analyses of NO_3^- and NO_2^- by ion chromatography were performed by Quality Analytical Laboratories (Panama City, FL).

Specific surface areas of selected samples were determined using the Brunauer–Emmett–Teller (BET) N_2 adsorption/desorption method (Gemini 2360 surface area analyzer, Micromeritics).

3.2. Sample collection

Three types of samples were collected at the Tyndall site: surface area soils, aquifer sediment cores and groundwater. Drilling was performed at the site in August 2005 using a direct-push drill rig to collect sediment cores and to install a new monitoring well, MW-1R, replacing well MW-1, which was removed during excavation of the source area. Well MW-1R was installed immediately downgradient of the substation boundary and screened from 1.5 to 4.5 m bgs.

3.2.1. Source area soils and aquifer sediment cores

Surficial soil samples were collected by hand trowel from 0.3 to 0.6 m bgs from two locations (denoted S3 and S27) within the substation in April 2005. An additional sample was collected at location S27 in July 2006. Soil samples were shipped on ice and stored in the dark at 4 °C until analysis or frozen for later use.

In August 2005, sediment cores were collected within the As plume (ASB-1, ASB-2, ASB-3) and in background areas cross- and upgradient of the substation (BSB-1, BSB-2, BSB-3). Upon collection, cores enclosed in acetate core sleeves were cut into intervals of 0.3–0.6 m and sealed with plastic end caps secured with duct tape; selected sections were shipped on ice and stored in the dark at 4 °C until they were sectioned into 0.15 m intervals, homogenized under N_2 in a glove box, and frozen until use.

3.2.2. Groundwater samples

In April 2005, background groundwater was collected upgradient of the substation from MW-2. Samples were shipped on ice,

stored at 4 °C until analysis (which was conducted within 10 d of sample collection), and then frozen until used in leaching experiments. Additional groundwater was collected at MW-2 in July 2006 for use in leaching experiments. In August 2005, groundwater samples were collected from 18 monitoring wells using low-flow sampling techniques. Field parameters including pH, dissolved O_2 (DO), temperature, turbidity and oxidation–reduction potential (Eh) were measured at the time of collection. Samples for analysis of NO_3^- plus NO_2^- were analyzed at a local commercial laboratory. Other samples were preserved appropriately for the intended analyte (USEPA, 1983) and shipped on ice. Note that unpreserved samples were used for determination of As speciation. Some samples were filtered through a 0.22 μm mixed cellulose ester (Millipore) filters before analysis.

3.3. Characterization of source area soils and aquifer sediment samples

3.3.1. Sample handling

Source area soil samples collected in April 2005 and July 2006 were stored frozen. Samples were thawed and homogenized without drying (April 2005) or after air-drying in the dark for 1 d (July 2006). Samples were then sieved successively through 18-mesh (1 mm), 32-mesh (500 μm), 60-mesh (250 μm), and 250-mesh (63 μm) sieves. Water content was determined gravimetrically for the April 2005 samples. Sub-samples of whole and sieved soils collected in July 2006 were freeze-dried for 2 d.

For aquifer sediments (collected August 2005), frozen samples were similarly homogenized, dried, and sieved, but under a N_2 atmosphere in the glove box. Sub-samples were transferred to 15-mL centrifuge tubes and loosely capped in the glove box before being freeze-dried for 2 d.

3.3.2. Scanning electron microscopy (SEM)

A soil representative of the source area (S3, collected April 2005) was ground to a powder and allowed to dry under N_2 in a glove box. A dried sample was mounted on C tape and imaged in a FEI Quanta 200 SEM with an EDAX Genesis 2000 energy dispersive spectrometer (EDS) for elemental analysis. The microscope

was operated at an accelerating voltage of 20 kV, with a working distance of 10 mm and magnifications of 600–5000 \times .

3.3.3. X-ray absorption spectroscopy (XAS)

Two representative source area soils (S3 and S27, collected April 2005) were analyzed by X-ray absorption spectroscopy (XAS) (performed in June 2005). Arsenic K-edge absorption spectra were collected at the Stanford Synchrotron Radiation Laboratory (SSRL) on wiggler beamline 11–2 at cryogenic temperature (~ 4 K) under dedicated conditions (3 GeV, 70–100 mA) using an unfocused beam. Powdered samples were loaded into 2-mm-thick Teflon sample holders and sealed with Kapton film. Arsenic K-edge and EXAFS fluorescence spectra (S3 only) were collected using a Si(2 2 0) monochromator crystal and a 30-element solid-state Ge array detector. Beam energy was calibrated on As foil at 11,867 eV. Multiple scans (6–8) were collected and averaged for each sample. Structural information was determined by non-linear least-squares fitting of the normalized EXAFS of sample S3 with the program EXAFSPAK (George and Pickering, 2000) using theoretical phase-shift and amplitude functions for single and multiple-scattering calculated with the program FEFF (Rehr et al., 1992).

3.3.4. Total elemental analysis

Freeze-dried samples of source area soil (S3 and S27, collected April 2005, and the 0–250 μm size fraction of S27, collected July 2006) and whole and size-fractionated aquifer sediment (collected August 2005) were sent to SGS Minerals Services (Toronto, Ontario) for total elemental analyses. Major elements were determined by X-ray fluorescence (XRF) after meta/tetraborate fusion (method XRF76Z) and reported as% oxides. Total As content was determined for source area soils by XRF on pressed pellets (method XRF75 V) and for aquifer sediments by hydride generation atomic absorption spectroscopy after sodium peroxide fusion (method HAS90A).

3.3.5. Method 3050B extractions

Sub-samples of homogenized source area and aquifer soil (whole and size-fractionated fractions) were extracted following Method 3050B, a strong acid digestion that mobilizes solid-associated “environmentally available” metals (USEPA, 1996). Elements bound in silicate structures are not extracted by this method. In brief, 1.0-g samples were reacted in 50-mL tubes in triplicate at 95–99 $^{\circ}\text{C}$ on a heating block with 35% HNO_3 for 15 min, $\sim 50\%$ HNO_3 for 4.5 h, and $\sim 5\%$ H_2O_2 for 4 h.

3.3.6. Sequential extractions

For source area soil (S27, collected July 2006), 1.0-g sub-samples of 0–250 and 63–250 μm size fractions were sequentially extracted twice with 25 mL solutions of 50 mM $(\text{NH}_4)_2\text{SO}_4$ for 4 h and twice with 50 mM $\text{NH}_4\text{H}_2\text{PO}_4$ for 16 h following a method adapted from Wenzel et al. (2001) and then subjected to 3050B extraction. Extractions were performed in triplicate. For each extraction step, samples were shaken on a shaker table at 20 $^{\circ}\text{C}$ and subsequently centrifuged for 15 min at 2000g. The supernatant was filtered and retained for measurement, while the solid was subjected to successive extraction steps.

3.4. Mobilization and sequestration experiments

3.4.1. Exhaustive extraction with groundwater

Using the 0–250 μm size fraction of source area soil (S27, collected July 2006), a 100-g sample was leached with 1 L of background groundwater (MW-2, collected July 2006). The suspension was divided into 4 opaque bottles which were shaken on a shaker table at room temperature for at least 24 h

and subsequently centrifuged at 3500g for 10 min. The supernatant was decanted, and background groundwater was replaced. This process was repeated 14 times. The soil was air-dried, and aliquots were extracted in triplicate following Method 3050B.

3.4.2. Batch leaching experiments

Batch leaching experiments were performed with 0–250 and 63–250 μm size fractions of source area soil (S27, collected July 2006) using a synthetic groundwater based on the composition of background groundwater (well MW2). The synthetic groundwater consisted of 44 μM NaCl, 75 μM CaSO_4 and 82 μM MgSO_4 , buffered to pH 5.2 with 10 mM pyridine. Soils were leached in 15-mL centrifuge tubes at solids concentrations of 5, 40, 100, 250 and 500 g/L. Suspensions were mixed by end-over-end rotation in the cold room (dark, 12.5 $^{\circ}\text{C}$) for 3 d and then centrifuged at 14,000g for 10 min. Supernatants were filtered through 0.2 μm Acrodisc nylon-membrane syringe filters (Pall) and acidified before analysis. Experiments were performed in triplicate.

3.4.3. Static column leaching experiments

Using the 63–500 μm size fraction of source area soil (S27, collected April 2005), 300 g of soil was distributed evenly into three 11-cm long Plexiglas cylindrical reactors with a 9-cm inner diameter (ID) fitted with a medium porosity (10–16 μm) fritted filter disc (Chem Glass, NJ) to retain soil. The outlet (outer diameter (OD) 90 mm) was located at the bottom of the column on the side. Approximately 100–150 mL of background groundwater (MW2, collected April 2005) was added to the reactors and allowed to saturate the soil. The reactors were left in the cold room (dark, 12.5 $^{\circ}\text{C}$) for 4 d. The leachate was then pumped out, discarding the first 50 mL, filtering and retaining the next 15 mL, and discarding the remaining leachate. The reactors were then left in the cold room for 1 d. This process of wetting for 4 d and drying for 1 d was performed six times.

3.4.4. Flow-through column leaching experiments

Using the 0–250 μm size fraction of source area soil (S-27, collected July 2006), 220 g of soil was distributed evenly into two 20-cm long Plexiglas cylindrical reactors (5-cm ID) with outlet holes (OD, 90 mm). Nylon mesh was used to retain the soil. Columns were eluted with synthetic groundwater (see Section 3.4.2) in an upflow direction under the following flow conditions: 5 mL/h for 24 h, 20 mL/h for 16 h, no flow for 48 h, 5 mL/h for 24 h. Columns were kept in the cold room (dark, 12.5 $^{\circ}\text{C}$) throughout the experiment and samples were collected with an automatic fraction collector.

3.4.5. Sorption experiments with aquifer sediments

Sediment samples (0.75 g) were added to 25 mL of background groundwater (MW-2, collected July 2006) spiked at $t = 0$ h with As(V) at initial concentrations ranging from 0.5 to 170 μM in 50-mL centrifuge tubes in a glove box. Note that, for experiments with ASB-1 sediments, 0.50 g of sediment was added to 16.67 mL solution. Suspensions were prepared in triplicate and rotated end-over-end in the cold room (dark, 12.5 $^{\circ}\text{C}$) for 36 h before centrifugation at 14,000g. Supernatants were filtered and acidified for analysis. At $t = 36$ h, the pH of the filtered supernatants was measured before acidification. Solid-associated As was calculated as the difference between the total As in the suspension (i.e., As spike plus the ambient As content of the solid) and the measured, dissolved As concentration. Sorption experiments were performed with whole and size-fractionated sediments from cores obtained within and upgradient of the As plume.

4. Results and discussion

4.1. Groundwater composition

Groundwater sampling conducted in August 2005 confirmed the extent of As contamination as observed in previous monitoring events (Figs. 2 and 3). The As concentration measured at the newly-installed well MW-1R located at the substation boundary (and replacing well MW-1) was 1160 $\mu\text{g/L}$. This value is lower than that previously measured at well MW-1 (e.g., 2400 $\mu\text{g/L}$ in 1993) before its removal in 2003, which may reflect the decrease in the source strength due to the partial excavation of contaminated soil.

Determination of As speciation demonstrated that As is present in the groundwater primarily in the +V oxidation state (Fig. 3). The highest As(III) concentration measured was 108 $\mu\text{g/L}$ at well MW-10 corresponding to 13% of the total dissolved As; As(III) was undetectable in 15 of the 18 wells sampled. In a previous study conducted at Tyndall, groundwater discharging into a ditch was collected approximately 1 m below the surface using shallow piezometers. The observed ratio of As(III):As(V) was roughly 1:1 with approximately 10% of the total dissolved As present as methylated

species (Miller, 2001). Since only As_2O_3 was applied at the site, these observations indicate that both As(III) oxidation and, to a lesser extent, methylation occurred *in situ*.

In general, the Tyndall groundwater was moderately acidic with relatively low conductivity and a major ion composition dominated by Ca, Mg and SO_4 (Tables 1 and 2). Dissolved organic C (DOC) measured at MW2 was high (10.2 mg/L) for groundwater, possibly due to the influence of the peaty organic layer in the subsurface. It is likely that DOC contributes to the observed acidity of the groundwater.

Comparison of Fe (and Mn) concentrations within the zone of As contamination (Table 2) and outside it (Table 1) does not suggest that As mobilization is associated with the reductive dissolution of Fe-containing carrier phases despite the importance of this mechanism for As mobilization in many other locations (Ravenscroft et al., 2009 and references therein).

4.2. Soil and sediment characterization

Soils collected from the source area (i.e., the substation) and sections of sediment cores collected both within and upgradient of the As plume were analyzed.

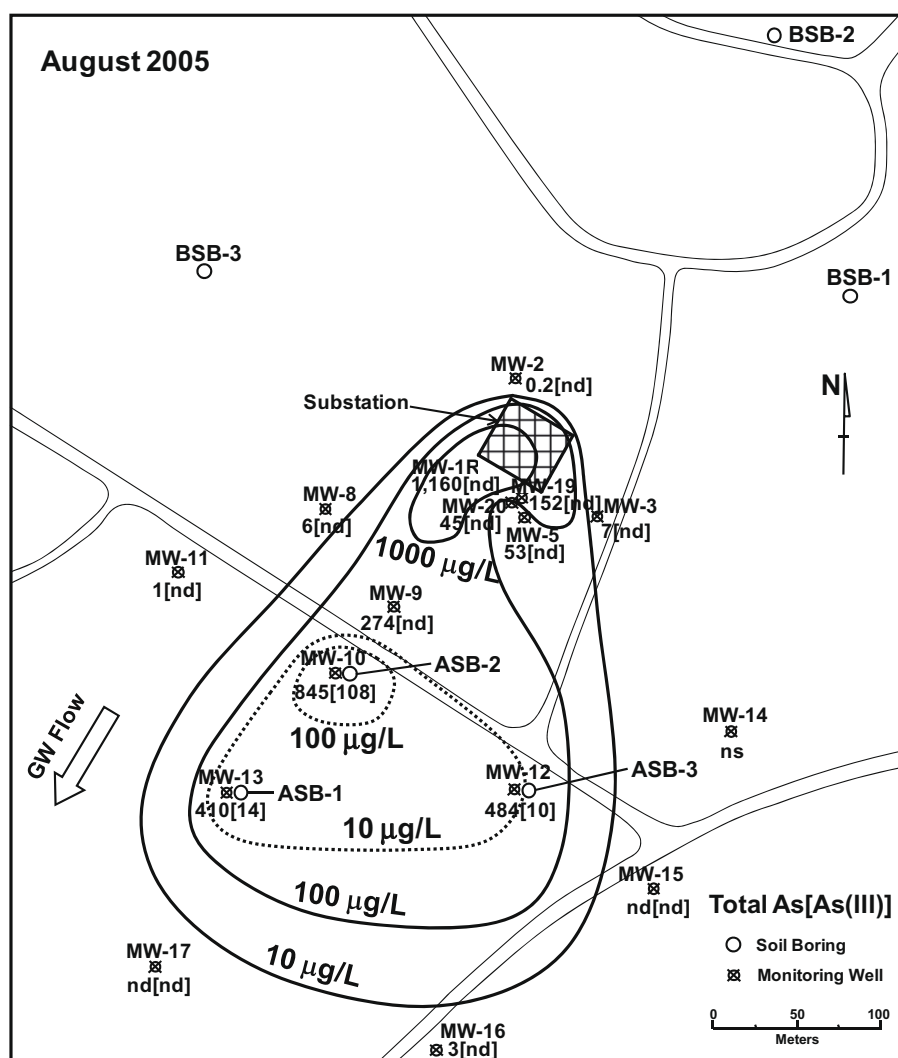


Fig. 3. Concentrations of total dissolved As and As(III) in $\mu\text{g/L}$ determined in Tyndall groundwater in August 2005; values are shown next to the monitoring wells with As(III) in brackets (nd = non-detect). Approximate iso-concentration contours are drawn for total, dissolved As (solid lines) and As(III) (dashed lines). Location of soil borings within the contaminated zone (ASB-1, -2, -3) and upgradient background area (BSB-1, -2, -3) are shown (open circles).

Table 1
Groundwater composition for wells outside zone of contamination.

Analyte ^a	Units	MW-2 (April 2005)	MW-2 (August 2005)	MW-3, 7, 8, 11, 15, 16, 17, 18 (August 2005)		
				Mean	Minimum	Maximum
As	µg/L	<1	0.15 ± 0.04	2.6	<1	7
As(III)	µg/L	NM ^b	<1	<1		
Mn	µg/L	9	8 ± 0.07	11	<1	73
Al ^c	µg/L	<1	557 ± 16	86	<1	316
Fe	µg/L	<0.25	11 ± 0.01	45	4	93
Na	mg/L	1.75	1 ± 0.05	5	2	8
Ca	mg/L	NM	3 ± 0.29	5	1	18
Mg	mg/L	NM	2 ± 0.06	1	1	2
K	mg/L	0.38	1 ± 0.02	2	<0.1	4
Cl	mg/L	9.8	2 ± 0.14	10	3	15
SO ₄	mg/L as SO ₄	14	12 ± 0.5	13	6	20
Br	mg/L	<0.1	3 ± 0.1	<1		
TOC	mg/L	NM	18	9	3	30
DOC	mg/L	10.2				
pH (unfiltered)		4.93				
pH (filtered)		4.79	NM	5	4	6

^a All samples (except for TOC, DOC and unfiltered pH samples) were filtered through 0.22 µm mixed cellulose ester (Millipore) filters after delivery to Caltech. Samples for DOC analyses were filtered through 0.2 µm nylon (PALL Life Sciences) filters. Nitrate and NO₂⁻ were measured for all samples but were not detected. For MW-2 (August 2005) samples, standard deviations are reported for triplicate analyses.

^b NM = not measured.

^c The discrepancy between the Al concentrations in samples collected in April and August may indicate loss of Al from April samples. A previous study at this site reported Al concentrations in filtered groundwater of 2.5 mg/L (Miller, 2001).

Table 2
Groundwater composition for wells within zone of contamination (samples collected August 2005).

Analyte ^a	Units	MW-1R	MW-19	MW-20	MW-5	MW-9	MW-10	MW-12	MW-13
As	µg/L	1155 ± 17	152 ± 2	45 ± 0.7	53 ± 0.5	274 ± 2	845 ± 17	484 ± 5	410 ± 3
As(III)	µg/L	<1	<1	<1	<1	<1	108	10	14
Mn	µg/L	7 ± 0.2	8 ± 0.2	<1	2 ± 0.07	<1	<1	1 ± 0.9	<1
Al	µg/L	165 ± 4	225 ± 6	36 ± 1	225 ± 4	167 ± 22	335 ± 7	109 ± 6	65 ± 2
Fe	µg/L	18 ± 0.01	11 ± 0.01	15 ± 0.01	18 ± 0.01	13 ± 0.01	7 ± 0.01	31 ± 0.01	37 ± 0.01
Na	mg/L	2 ± 0.04	3 ± 0.1	<0.1	2 ± 0.06	11 ± 0.4	15 ± 0.4	5 ± 0.1	4 ± 0.2
Ca	mg/L	21 ± 2	12 ± 1	1 ± 0.5	8 ± 0.9	5 ± 0.5	8 ± 0.8	3 ± 0.2	1 ± 0.09
Mg	mg/L	5 ± 0.14	3 ± 0.1	<0.1	2 ± 0.1	2 ± 0.07	2 ± 0.09	2 ± 0.05	1 ± 0.06
K	mg/L	2 ± 0.05	1 ± 0.06	<0.1	1 ± 0.01	1 ± 0.03	1 ± 0.05	2 ± 0.05	2 ± 0.08
Cl	mg/L	4 ± 0.2	5 ± 0.1	10 ± 1	6 ± 1	20 ± 1.4	27 ± 1.6	11 ± 2	9 ± 0.6
SO ₄	mg/L as SO ₄	20 ± 2	15 ± 0.6	19 ± 1	11 ± 2	9 ± 0.3	18 ± 1.3	17 ± 3	12 ± 0.7
Br	mg/L	2 ± 0.1	5 ± 0.2	<0.1	2 ± 0.4	<0.1	<0.1	<0.1	<0.1
TOC	mg/L	11	12	6	11	21	14	6	5
pH	–	6	6	5	5	5	5	4	NM

NM = not measured.

^a All samples (except for TOC samples) were filtered through 0.22 µm mixed cellulose ester (Millipore) filters after delivery to Caltech. Standard deviations are reported for triplicate analyses. Nitrate and NO₂⁻ were measured for all samples but NO₃⁻ was not detected and NO₂⁻ was detected only at MW-19 at 2 mg/L.

4.2.1. Source area soils

The mineralogy of the source area soils is dominated by quartz, which was observed by SEM/EDS to occur as euhedral grains (~10–50 µm) with sparse surface coatings containing mostly Al, Si and Ca (example grain shown in Fig. 4). Notably, no Fe was detected by EDS, although Fe is commonly present as a surface coating on soil minerals. Microscale observations are generally consistent with the bulk soil composition, which was determined to be 95% SiO₂ with 1.4% CaO, 0.7% Al₂O₃, 0.6% Fe₂O₃ and 0.44% MgO. The amount of 3050B-extractable Fe, Al and Mn in the source area soils were low compared with a NIST reference sandy soil, similar to a previous survey that also found Florida soils to be depleted in these elements (Chen and Ma, 1998) (Table 3).

Total As contents (determined by XRF) in two source area soil samples were 180 (S27) and 280 (S3) mg/kg, respectively, consistent with previous measurements. These values are substantially elevated relative to background As levels in Florida soils, which are characterized by a geometric mean of 0.4 mg/kg with an estimated upper limit for the background As content of 7.0 mg/kg (Chen et al., 2001).

Concentrations of 3050B-extractable As were approximately 80% of the total As concentrations determined by XRF on whole soils (Table 4). In a modified sequential extraction, a substantial fraction of the As associated with the solids was extracted by ammonium sulfate and ammonium phosphate, indicating that dissolution of the solid carrier phase is not a prerequisite for As mobilization. The distribution of As released in different sequential extraction steps was similar for the 0–250 and 63–250 µm size fractions, though this comparison is complicated by the incomplete (75%) recovery in the sequential extraction as compared with the single 3050B extraction. Exhaustive batch extractions consisting of 14 consecutive washes with background groundwater (each at a soil-solution ratio of 1:10) resulted in the leaching of 92% of the 3050B-extractable As and 79% and 92% of the 3050B-extractable Fe and Mn, respectively.

Comparable results were obtained in a previous study of soils from the southeastern USA that had been contaminated by As₂O₃; approximately 50% of the total extractable As was released from the soil by extraction with ammonium sulfate and ammonium phosphate (Yang and Donahoe, 2007). Comparison of

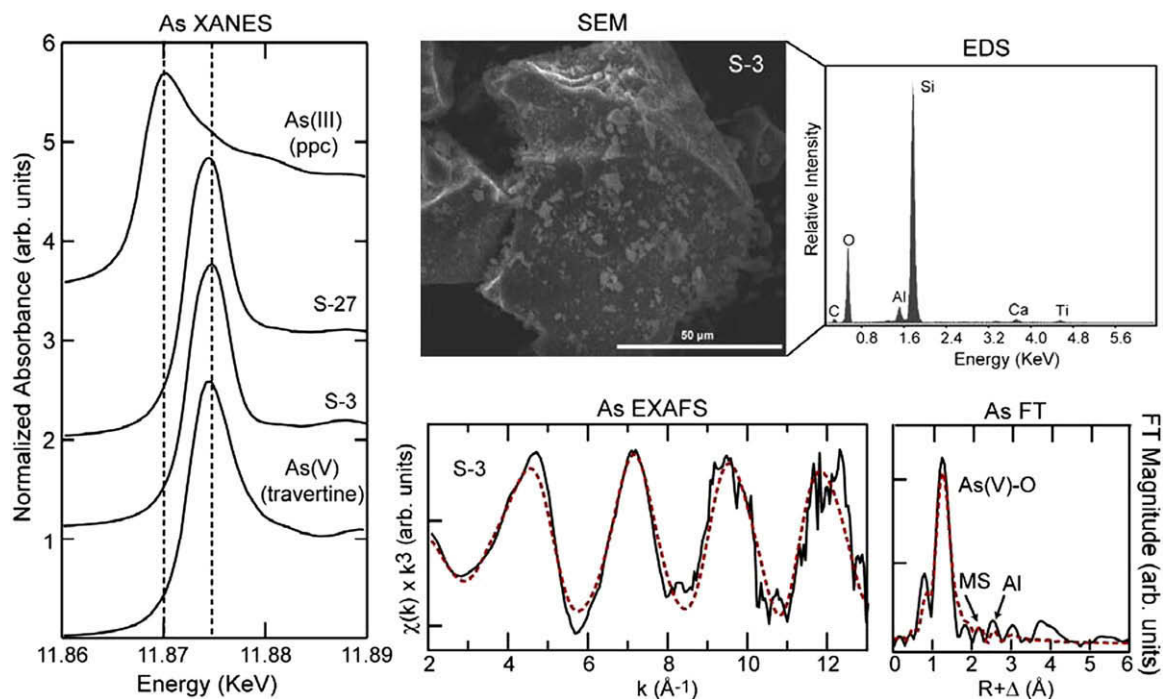


Fig. 4. Characterization of source area soils. Top: Representative SEM image and EDS analyses of sample S3. Left panel: As K-edge XANES of S3 and S27 compared with reference spectra of As(III)-oxide (precipitated with $\text{Ca}(\text{OH})_2$ and CaCO_3) and a natural sample of As(V) in travertine; dashed lines indicate characteristic absorption energies for As(III)-O and As(V)-O bonding. Bottom panel: As EXAFS of S3 (solid line) and least-squares best fit (dashed line). Fit results: 4 oxygen atoms (fixed) at 1.67 Å (varied $\sigma^2 = 0.0011 \text{ \AA}^2$) with As-O tetrahedral multiple scattering (MS) at 3.01 Å; 2 Al or Si atoms at 3.22 Å (fixed $\sigma^2 = 0.0045 \text{ \AA}^2$).

Table 3
3050B extractable contents of Al, Fe, and Mn in soils (dry weight basis).

Element	Units	Source area soils		NIST sandy soil ^a	40 FL soils ^a
		S27	S3		
Al	g/kg	2.6	14	25.4	1.8
Fe	g/kg	0.006	0.002	30.1	0.83
Mn	mg/kg	97	76	441	26.2

^a Chen and Ma (1998).

sequential extraction and (kinetic) leaching of soils with synthetic acid rain (SAR) solution indicated that, in low pH soils, the amount of As leached by SAR corresponded closely to the sequential extraction steps that did not involve any reduction (i.e., reductive dissolution) of the soil matrix (Qi and Donahoe, 2009).

The oxidation state of As in two source area soils was determined by XANES analysis of the bulk soil. The energy of maximum

absorption is indicative of As oxidation state (e.g., Foster, 2003). Soil XANES spectra show that As is present predominantly in the +V oxidation state, as indicated by the absorption maximum at 11.875 keV (Fig. 4). There is no evidence in XANES spectra for adsorption at lower energies that would indicate the presence of other As oxidation states. Quantitative EXAFS analysis of one sample (S3) indicated the arsenate geometry of tetrahedral coordination of As to 4 oxygen atoms and weak backscattering from atoms beyond the O coordination shell (Fig. 4). Second-neighbor features were fit with a combination of multiple scattering from the arsenate tetrahedra and a second shell of Si or Al atoms (which cannot be distinguished as backscatterers). The structural results are consistent with sorbed arsenate on the surface of Al-oxide surface coatings and/or aluminosilicate minerals. A previous study also found that As was generally disseminated on the surface of fine-grained soil particles; analysis of rare As-rich particles by XANES demonstrated the presence of As(V) (Yang and Donahoe, 2007). Thus the speciation of As in the solid phase further supports

Table 4
As contents (mg/kg) in source area soils (dry weight basis).

Method	Sample	As contents (mg/kg)					
		S3 (April 2005) whole soil ^a		S27 (April 2005)		S27 (July 2006) ^b	
		Whole soil ^a	63–250 µm	63–500 µm	0–250 µm	63–250 µm	
XRF		280		180		110	
3050B extraction		206		144	108	105	
Sequential extraction	Sum all steps					93	79
	Ammonium sulfate (step 1)					11 ± 0.6	11 ± 0.8
	Ammonium sulfate (step 2)					6.1 ± 0.5	5.3 ± 0.2
	Ammonium phosphate (step 3)					8.6 ± 2.4	5.1 ± 0.8
	Ammonium phosphate (step 4)					8.2 ± 1.8	4.3 ± 1.1
	3050B on residue					59 ± 5.7	54 ± 5.4

^a Samples not size-fractionated before analysis or extraction.

^b Mean value ± standard deviation for triplicate analyses.

the hypothesis of *in situ* As(III) oxidation to As(V) and lack of association with Fe-oxide phases. In many other environments, of course, Fe-oxide phases are known to be key contributors to As retention in soils (Smedley and Kinniburgh, 2002; Cances et al., 2005, 2008).

4.2.2. Vertical distribution of As content in sediment cores outside the source area

In contrast to the source area soils, As contents (as determined by both total elemental analysis and 3050B extraction) in sediments collected both within the area of the As plume (ASB cores) and upgradient of the source area (BSB cores) were generally within the range expected for uncontaminated Florida soils (Fig. 5). In the surficial sediments, 3050B-extractable As was actually slightly lower in the ASB than in the BSB cores despite the elevated As concentrations in groundwater at the locations of the ASB cores. This indicates that the surficial aquifer sediments have a limited capacity for As sorption under *in situ* conditions.

Sediments collected within the JBF were enriched in As relative to the surficial sediments both within and upgradient of the plume. Both the 3050B-extractable and total As contents appeared to be higher in the JBF sediments collected within the plume than in those collected upgradient of the plume. However, these differences were in the range of the variability observed among replicate samples from an individual core. Total As contents were higher than 3050B-extractable As contents; this difference was somewhat more pronounced for the BSB cores than for the ASB cores.

4.3. Batch and column studies of As mobilization from source area soil

Source area soil was equilibrated in batch systems with background groundwater at varying soil-solution ratios for 3 d. Dissolved As concentrations of up to 700 $\mu\text{g/L}$ were observed in the equilibrated groundwater; between 1% and 15% of the 3050B-extractable As was released from the source area soils (Fig. 6).

Also shown in Fig. 6 are the results of a static column experiment, in which soil was equilibrated with background groundwater for a period of 4 d. The equilibrated solution was then allowed to drain from the column and replaced with fresh background groundwater. In six consecutive treatments, the As concentration in the effluent was $2100 \pm 200 \mu\text{g/L}$ with no systematic variation over the course of the experiment. This As concentration corresponds to release of $0.7 \pm 0.06 \text{ mg/kg}$ of As from the soil (or 0.5% of the 3050B-extractable As). The As concentrations in the sta-

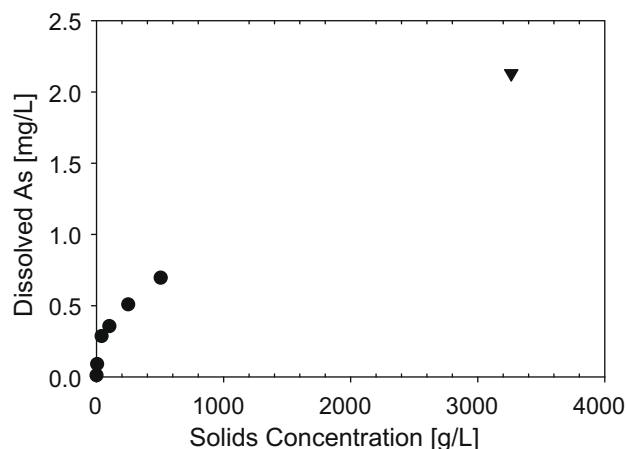


Fig. 6. Dissolved As concentrations in suspensions of source area soil (S27) equilibrated with background groundwater at varying soil-solution ratios in batch experiments (●) and static column experiments (▼). Experimental conditions: batch experiments – S27 collected July 2006, 0–250 μm size fraction, synthetic groundwater (44 μM NaCl, 75 μM CaSO_4 , and 82 μM MgSO_4 , buffered to pH 5.2 with 10 mM pyridine), rotated 28 rpm at 12.5 $^\circ\text{C}$ in the dark for 3 d, in triplicate; static column experiments – S27 collected April 2005, 63–500 μm size fraction, MW-2 groundwater collected April 2005, 300 g saturated with 100–150 mL, left 12.5 $^\circ\text{C}$ in the dark for 4 d, repeated six times and in triplicate.

tic column effluent are consistent with those observed in the plume near the source area at wells MW-1 and MW-1R.

In flow-through columns run under saturated conditions, As concentrations in the effluent varied depending on the flow conditions (Fig. 7). At a flow rate of 5 mL/h (region I), the As concentration in the effluent stabilized at 1400 $\mu\text{g/L}$, a concentration comparable to that observed in the groundwater plume near the source area.

With increasing flow rate, the As concentration in the effluent increased over time and did not reach a stable value within 16 h (region II); the maximum As concentration observed in the effluent at a flow rate of 20 mL/h was 2400 $\mu\text{g/L}$. This increase in As concentration may be attributable to the increased mobilization of colloidal particles under conditions of increased shear. In contrast, if the release of As from the solid phase were controlled by the kinetics of reaction at the solid–water interface, the As concentration in the effluent would have been expected to have decreased with increasing flow rate as a constant mass flux was increasingly diluted (Schnoor, 1990). Additionally, a constant As concentration in the effluent would have been expected if the release of As from the solid phase were transport-controlled.

After the no-flow period of 48 h (region III), no further increase in the effluent As concentration was observed. This is consistent with the observations in the static column experiments, in which effluent As concentrations were comparable. It would be expected that colloidal particles released by shear forces under the flow conditions of region II would have been recaptured by attachment to the soil under the no-flow conditions of region III. With re-initiation of the flow at 5 mL/h (region IV), the As concentration in the effluent gradually decreased to a concentration of 1500 $\mu\text{g/L}$, similar to that observed at the end of the initial flow period (region I).

4.4. Sorption of As onto sediment from the surficial aquifer and the JBF

Batch experiments were conducted to assess the capacity of surficial aquifer and JBF sediments for sorption of As(V), the principal oxidation state of As both in the groundwater and in source area soils. Sediment samples (core BSB-3, 0–125 μm size fraction) were equilibrated for 36 h in background groundwater spiked with

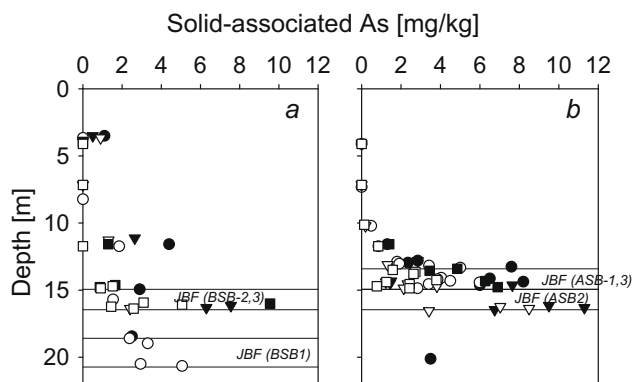


Fig. 5. Distribution of total As content (closed symbols) and 3050B-extractable As content (open symbols) with depth (a) in BSB cores collected upgradient of the source area and (b) in ASB cores collected within the As plume. The depth of the Jackson Bluff Formation (JBF) layer at each boring location is also identified. Symbols: (○, ●) ASB-1 or BSB-1, (▽, ▼) ASB-2 or BSB-2, (□, ■) ASB-3 or BSB-3.

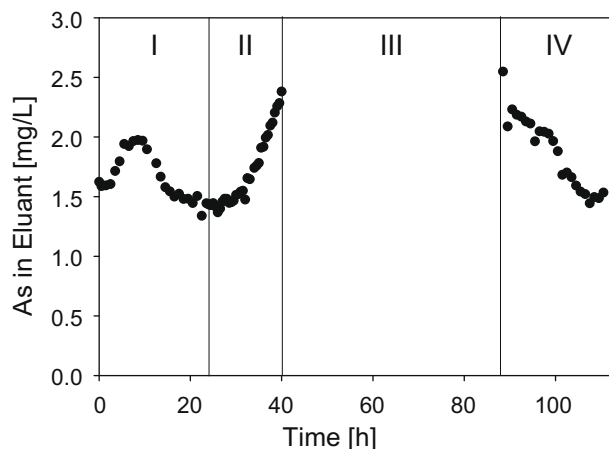


Fig. 7. Concentrations of As in the eluant of a column packed with source area soil and eluted with simulated groundwater under saturated conditions. The column was run at 5 mL/h for 24 h (region I), 20 mL/h for 16 h (region II), at no flow for 48 h (region III), and at 5 mL/h for 24 h (region IV). Experimental conditions: S27 collected July 2006, 0–250 μm size fraction, synthetic groundwater (44 μM NaCl, 75 μM CaSO_4 , and 82 μM MgSO_4 , buffered to pH 5.2 with 10 mM pyridine), pumped upward through column packed with 220 g of soil, 12.5 $^\circ\text{C}$ in the dark.

As(V). Under these conditions, substantially greater sorption was observed with the JBF sediment than with the surficial aquifer sediment (Fig. 8). Neither sediment exhibited a clear saturation, but the maximum observed value of solid-associated As (for the range of experimental conditions examined) was 114 mg/kg for the JBF sediment and only 22 mg/kg for the surficial aquifer sediment, a ratio of 5.2:1. Notably, the JBF sediment was also enriched in Fe and Al compared with the surficial aquifer sediment at ratios of 3.7:1 for Fe and 30:1 for Al based on total elemental analysis by XRF.

The effect of surface area on As(V) sorption was investigated in batch experiments with size-fractionated JBF sediments (14–15 m, core ASB-1). In sieved fractions, the 0–63 μm fraction had a BET

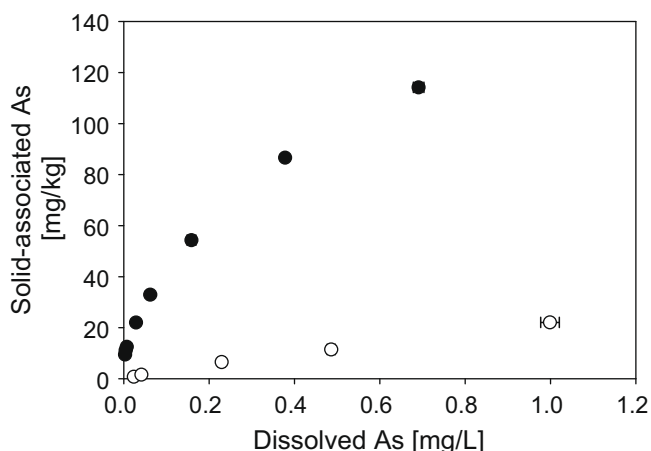


Fig. 8. Concentrations of solid-associated As as a function of dissolved As concentrations for 30 g/L suspensions of background sediments (core BSB-3, 0–125 μm size fraction) equilibrated with background groundwater (MW-2 collected July 2006) spiked with As(V). Solid-associated As was calculated as the difference between the total As concentration in the system (based on the As spike plus the ambient As content of the solid) and the measured dissolved As concentration. Symbols: (○) surficial aquifer sediment (4.0–4.3 m depth; negligible ambient As content), (●) JBF sediment (16.0–16.2 m depth; ambient As content 9.6 mg/kg). Error bars correspond to standard deviations of triplicate analyses. Experimental conditions: 0.75 g in 25 mL, rotated end-over-end at 12.5 $^\circ\text{C}$ in the dark for 36 h in triplicate.

surface area of 10.7 m^2/g and an ambient As content of 24.1 mg/kg. The 63–125 μm size fraction had both a lower BET surface area, 4.8 m^2/g , and lower ambient As content, 4.7 mg/kg. Normalizing for surface area, the 0–63 μm fraction was enriched in As compared to the 63–125 μm fraction by a ratio of 2.3:1. In the sorption experiments, the sorption capacity of the 0–63 μm fraction was substantially greater than that of the 63–250 μm fraction on a per mass basis (Fig. 9a) but very similar when normalized for surface area (Fig. 9b).

4.5. Hydrologic considerations

Although the hydrology of the Tyndall site is not fully characterized, four aspects of the site hydrology should be considered in the interpretation and integration of the field and laboratory observations. The first aspect is infiltration in the source area, the second is transport within the surficial aquifer, the third is infiltration and dilution downgradient of the source area, and the fourth is the integrity of the JBF as a confining layer.

The topography of the Tyndall site and the corresponding hydraulic gradients are variable across the site. In the source area itself, the topography is quite flat with an estimated hydraulic gradient of only 0.001. The groundwater table is also shallow

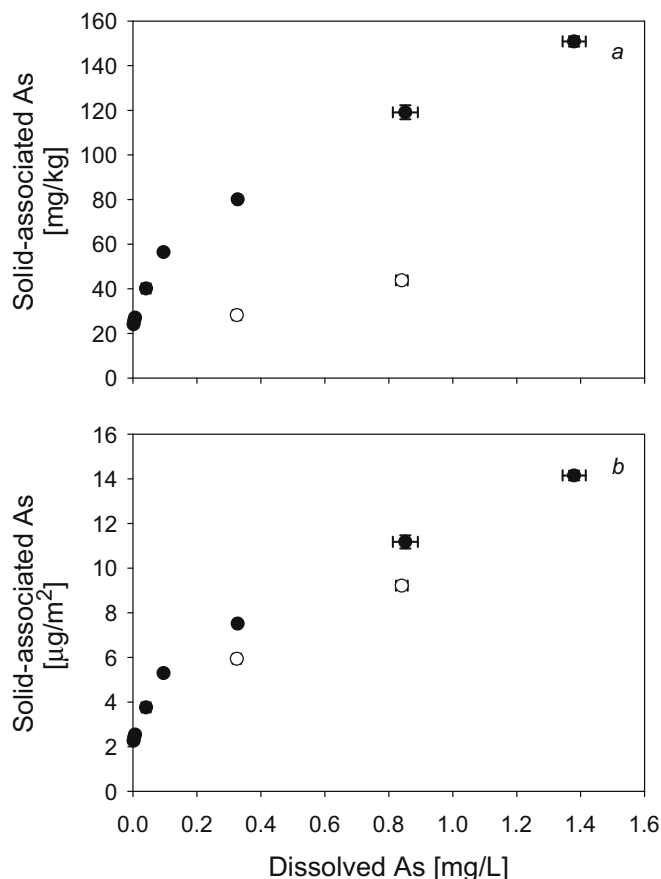


Fig. 9. Concentrations of solid-associated As as a function of dissolved As concentrations for 30 g/L suspensions of JBF sediments (core ASB-1, depth 14.0–14.9 m) equilibrated with background groundwater spiked with As(V). Solid-associated As was calculated from the difference between the total As concentration in the system (based on the As spike plus the ambient As content of the solid) and the measured dissolved As concentration. Symbols: (○) 0–63 μm fraction (ambient As content 24.1 mg/kg or 2.25 $\mu\text{g}/\text{m}^2$), (●) 63–125 μm fraction (ambient As content 4.7 mg/kg or 0.98 $\mu\text{g}/\text{m}^2$). Error bars correspond to standard deviations in triplicate analyses. Experimental conditions: 0.50 g in 16.67 mL, rotated end-over-end at 12.5 $^\circ\text{C}$ in the dark for 36 h.

(approximately 1.5 m bgs). Thus heavy precipitation would be expected to result in substantial overland flow (i.e., runoff) as well as in infiltration. After a precipitation event, high temperatures, particularly in spring and summer months, would drive evaporation and capillary rise of As-contaminated groundwater. These processes would tend to retard the transport of As from the source area and could be a basis for the observed persistence of As despite the ease of leaching of As from the source area soils observed in the static and flow-through column experiments.

One well immediately downgradient of the source area (MW-7 not shown in Fig. 2 but located between MW-1 and MW-5) was drilled through the JBF and into the underlying Intracoastal Formation. Well logs indicate that the JBF is approximately 2.5 m thick at this location. The water table elevation at MW-7 is lower than at nearby wells completed in the surficial aquifer thus indicating a potential downward hydraulic gradient. Low to non-detectable As concentrations at MW-7, however, indicate that As-contaminated groundwater is not penetrating through the JBF near the source area.

Away from the source area, specifically downgradient of well MW-10, the hydraulic gradient increases by about a factor of 10. Between MW-10 and MW-17, the evolution of the 10 and 1000 µg/L contours in As concentrations over time (Figs. 2 and 3) indicate that the extent of As contamination (as defined by the 10 µg/L contour) is stable or even retreating and that the mass of As in the surficial groundwater (corresponding to the 1000 µg/L contour) has declined. Comparison of the As contents of surficial aquifer sediments within and upgradient of the As plume indicate that As is not being sequestered in the surficial aquifer sediments; this inference is supported by the batch sorption experiments conducted in the laboratory. The apparent reduction in the mass of As in the surficial aquifer may be attributable to the partial excavation of As-contaminated soils in the source area and a consequent decrease in source strength. Infiltration of rainwater into the aquifer downgradient of the source area could lead to dilution of As concentrations in the plume. It is also possible that, in this area, the integrity of the JBF as a confining layer is compromised. Since the conclusions regarding the stability of the As plume are based only on observations from wells completed in the surficial aquifer (with the exception of MW-7), the possible penetration of the As plume into the Intracoastal Formation could provide an additional explanation for the apparent stability of the As plume in the surficial aquifer.

5. Conclusions

This study examined potential geochemical controls on As fate and transport, such as kinetic limitation of As mobilization and the sequestration of As through sorption and/or precipitation reactions, at a site with persistent As contamination in soil and groundwater. Such geochemical controls were examined in laboratory experiments to aid in the interpretation of two specific field observations: (1) the persistence of As in source area soils decades after the discontinuation of the use of As₂O₃ as a herbicide and (2) the apparent stability of the plume of As-contaminated groundwater.

Experimental results, however, suggest that the persistence of As in the source area cannot be explained by geochemical controls, as is often assumed, but may be the result of limited infiltration (i.e., hydrologic control). Column experiments with source area soil generated aqueous As concentrations comparable to those observed in groundwater near the source area. A substantial fraction of the As could be leached from the source area soil with background groundwater, or moderate leaching conditions, indicating that the As in the source area soil is geochemically labile. Because the amount of extractable Fe and Mn in source area soils was low

compared with typical soils, Fe- or Mn-reducing conditions, which are often responsible for As mobilization (Ravenscroft et al., 2009 and references therein), are not required to mobilize As from the source area.

Likewise, experimental results did not support a geochemical mechanism to explain the apparent stability of the As-contaminated groundwater plume. Batch sorption experiments showed that surficial aquifer sediments sorbed As(V) much less than sediments from the JBF, a presumed confining layer, which suggested that As sorption by surficial aquifer sediments is not a primary retention mechanism. This limited capacity of the surficial aquifer sediments for As(V) sorption is consistent with the similar As contents observed for surficial aquifer sediments within the As plume and upgradient of the plume (i.e., background conditions). Sorption to JBF sediments may contribute to As sequestration, although increased As contents in JBF sediments within the As plume area compared to upgradient background JBF sediments was not observed. The competence of the JBF as a confining unit far downgradient of source area soils has not been examined, and may be a factor in the apparent stability of the As plume.

The assessment of natural attenuation as a remedial option for As contamination in groundwater often focuses on potential geochemical mechanisms for sequestration. Studies at other sites have demonstrated the importance of sorption and precipitation processes involving Fe, Mn, Al and S for As sequestration and attenuation. This study suggests that possible hydrologic controls should also be carefully considered in assessing the apparent mobility and sequestration of As in the subsurface, particularly in settings that are depleted in the elements that can contribute to the immobilization of As.

Acknowledgements

This work was supported by the Strategic Environmental Research and Development Program (SERDP) Project #ER-1374. AGF was supported by the National Defense Science and Engineering Graduate (NDSEG) Research Fellowship. Assistance provided by Gulf Power Co. and the Southern Co. and support provided by Joe McLernan (Tyndall AFB) are gratefully appreciated. Portions of this research were carried out at the Stanford Synchrotron Radiation Laboratory, a national user facility operated by Stanford University on behalf of the US Department of Energy, Office of Basic Energy Sciences. Thanks to Rob Root (UC Merced) for assistance with XAS data analysis.

References

- Bothe, J.V., Brown, P.W., 1999. Arsenic immobilization by calcium arsenate formation. *Environ. Sci. Technol.* 33, 3806–3811.
- Cances, B., Juillot, F., Morin, G., Laperche, V., Alvarez, L., Proux, O., Hazemann, J.-L., Brown Jr., G.E., Calas, G., 2005. XAS evidence of As(V) association with iron oxyhydroxides in a contaminated soil at a former arsenical pesticide processing plant. *Environ. Sci. Technol.* 39, 9398–9405.
- Cances, B., Juillot, F., Morin, G., Laperche, V., Polya, D., Vaughan, D.J., Hazemann, J.-L., Proux, O., Brown Jr., G.E., Calas, G., 2008. Changes in arsenic speciation through a contaminated soil profile: a XAS based study. *Sci. Total Environ.* 397, 178–189.
- Chen, M., Ma, L.Q., 1998. Comparison of four USEPA digestion methods for trace metal analysis using certified and Florida soils. *J. Environ. Qual.* 27, 1294–1300.
- Chen, M., Ma, L.Q., Hoogeweg, C.G., Harris, W.G., 2001. Arsenic background concentrations in Florida, USA surface soils: determination and interpretation. *Environ. Forensics* 2, 117–126.
- Eaton, A.D., Clesceri, L.S., Rice, E.W., Greenberg, A.E., Franson, M.A.H. (Eds.), 2005. Standard Methods for the Examination of Water and Wastewater. American Public Health Association (APHA), American Water Works Association (AWWA), Water Environment Federation (WEF), Washington, DC.
- Folkes, D.J., Kuehster, T.E., Litle, R.A., 2001. Contributions of pesticide use to urban background concentrations of arsenic in Denver, Colorado, USA. *Environ. Forensics* 2, 127–139.
- Foster, A.L., 2003. Spectroscopic investigations of arsenic species in solid phases. In: Welch, A.H., Stollenwerk, K.G. (Eds.), *Arsenic in Groundwater*. Kluwer Academic Publishers, Boston, MA, pp. 27–65.

- George, G.N., Pickering, I.J., 2000. EXAFSPAK: A Suite of Computer Programs for Analysis of X-ray Absorption Spectra. Stanford Synchrotron Radiation Laboratory, Stanford CA.
- Gulf Power, 2004. Tyndall Air Force Base Project Update. Letter from Richard S. Markey. Gulf Power Company, Pensacola, FL.
- McLaren, R.G., Naidu, R., Smith, J., Tiller, K.G., 1998. Fractionation and distribution of arsenic in soils contaminated by cattle dip. *J. Environ. Qual.* 27, 348–354.
- Miller, G.P., 2001. Surface Complexation Modeling of Arsenic in Natural Water and Sediment Systems. Ph.D., New Mexico Institute of Mining and Technology. Socorro, NM.
- Norman, A.G., Minarik, C.E., Weintraub, R.L., 1950. Herbicides. *Ann. Rev. Plant Physiol. Plant Mol. Biol.* 1, 141–168.
- Qi, Y.Q., Donahoe, R.J., 2009. Modeling arsenic desorption from herbicide-contaminated soils. *Environ. Toxicol. Chem.* 28, 1338–1345.
- Ravenscroft, P., Brammer, H., Richards, K., 2009. Arsenic pollution a global synthesis. Wiley-Blackwell, Oxford.
- Rehr, J.J., Albers, R.C., Zabinsky, S.I., 1992. High-order multiple-scattering calculations of X-ray-absorption fine structure. *Phys. Rev. Lett.* 69, 3397–3400.
- Robinson, G.R., Ayuso, R.A., 2004. Use of spatial statistics and isotopic tracers to measure the influence of arsenical pesticide use on stream sediment chemistry in New England, USA. *Appl. Geochem.* 19, 1097–1110.
- Sadler, R., Olszowy, H., Shaw, G., Biltoft, R., Connell, D., 1994. Soil and water contamination by arsenic from a tannery waste. *Water Air Soil Pollut.* 78, 189–198.
- Schmidt, W., Clark, M.W., 1980. Geology of Bay County, Florida: Florida Bureau of Geology Bulletin No. 57.
- Schnoor, J.L., 1990. Kinetics of chemical weathering: a comparison of laboratory and field weathering rates. In: Stumm, W. (Ed.), *Aquatic Chemical Kinetics: Reaction Rates of Processes in Natural Waters*. Wiley-Interscience, New York, pp. 75–504.
- SCS, 1999. Tyndall Field Air Force Base Substation Remedial Action Plan for Groundwater. Report. Southern Company Services, Inc. Birmingham, AL.
- SCS, 2003. Tyndall Field Air Force Base substation, Bay County, Florida Soil Excavation Report. Report. Southern Company Services, Inc. Birmingham, AL.
- Smedley, P.L., Kinniburgh, D.G., 2002. A review of the source, behaviour and distribution of arsenic in natural waters. *Appl. Geochem.* 17, 517–568.
- Smith, E., Smith, J., Naidu, R., 2006. Distribution and nature of arsenic along former railway corridors of South Australia. *Sci. Total Environ.* 363, 175–182.
- Stollenwerk, K.G., 2003. Geochemical processes controlling transport of arsenic in groundwater: a review of adsorption. In: Welch, A.H., Stollenwerk, K.G. (Eds.), *Arsenic in Ground Water*. Kluwer Academic, Boston, pp. 7–100.
- USEPA, 1983. Sample Preservation Methods. United States Environmental Protection Agency. EPA-600/4-79-020. Cincinnati, OH.
- USEPA, 1993. Method 365.1: Determination of Phosphorus by Semi-Automated Colorimetry. <http://www.epa.gov/waterscience/methods/method/files/365_1.pdf>
- USEPA, 1996. Method 3050B: Acid Digestion of Sediments, Sludges, and Soils. SW-846 Test Methods for Evaluating Solid Wastes. <<http://www.epa.gov/SW-846/pdfs/3050b.pdf>>
- USEPA, 2001. National primary drinking water regulations; Arsenic and clarifications to compliance and new source contaminants monitoring; Final Rule. 40 CFR Parts 141 and 142. *Fed. Register.* 66, 6976–7066.
- Wenzel, W.W., Kirchbaumer, N., Prohaska, T., Stingeder, G., Lombi, E., Adriano, D.C., 2001. Arsenic fractionation in soils using an improved sequential extraction procedure. *Anal. Chim. Acta* 436, 309–323.
- Whitmore, T.J., Riedinger-Whitmore, M.A., Smoak, J.M., Kolasa, K.V., Goddard, E.A., Bindler, R., 2008. Arsenic contamination of lake sediments in Florida: evidence of herbicide mobility from watershed soils. *J. Paleolimnol.* 40, 869–884.
- Yang, L., Donahoe, R.J., 2007. The form, distribution and mobility of arsenic in soils contaminated by arsenic trioxide, at sites in southeast USA. *Appl. Geochem.* 22, 320–341.

APPENDIX C

**Geochemical processes controlling arsenic
mobility in groundwater: A case study of arsenic
mobilization and natural attenuation**

		Volume 25, Issue 1, January 2010	ISSN 0883-2927
<h1>Applied Geochemistry</h1> <p>JOURNAL OF THE INTERNATIONAL ASSOCIATION OF GEOCHEMISTRY</p>			
Executive Editor Associate Editors	RON FEAR, <i>Abeyysthik</i> L. AQUILINA, <i>Rome</i> H. ARONSSON, <i>Reykjavik</i> S. BUTTERFIELD, <i>Leeds</i> Z. CEYLAN, <i>Ankara</i> R. N. J. COMANS, <i>Petten</i> A. DARRIGAN, <i>Lindoping</i> W. M. EDMUNDS, <i>Oxford</i> G. FILIPPELLI, <i>Bellunopelle</i> D. FORTIN, <i>Ottawa</i> M. GASCONE, <i>Panama</i> J. E. GRAY, <i>Denver</i> R. S. HARBRON, <i>Research Triangle Park</i> A. HARTZIG, <i>Glen Osmond</i> M. HONSON, <i>Reading</i>	I. HUYGON, <i>Calgary</i> M. KUBISTEN, <i>Mainz</i> B. KUMAR, <i>Salt Lake City</i> A. KOKORIN, <i>Reston</i> X. D. LI, <i>Kowloon</i> W. B. LYONS, <i>Columbus</i> P. B. MCMILLON, <i>Denver</i> J. MEECEK, <i>Jacksonville</i> L. A. MUNK, <i>Anchorage</i> E. NOWATY, <i>Edinburgh</i> M. NOWAK, <i>Praha</i> J. C. POTT, <i>Gij-Sar-Yeeth</i> D. POLYA, <i>Manchester</i> R. M. PYLE, <i>Miami</i> C. REIMANN, <i>Trondheim</i>	A. N. ROYCHOKKERRY, <i>Cape Town</i> K. S. SANGAR, <i>Nashville</i> R. E. SMIL II, <i>Reston</i> O. SELASTI, <i>Uppsala</i> B. R. T. SIMONET, <i>Corvallis</i> D. B. SETHI, <i>Denver</i> L. SELLIAU, <i>Louvain</i> Y. TARDY, <i>Nailfont</i> K. G. TAYLOR, <i>Manchester</i> A. VENGISTO, <i>Durham</i> B. WANG, <i>Anchorage</i> R. B. WASTY, <i>Denver</i> R. WATKINS, <i>Perth</i> J. WEAVER-BURNS, <i>Christchurch</i>
Research papers			
	R.S. TEIXEIRA, P. CAMBIER, R.D. DIAS, J.P.P. PINESI and A. JAULIN-SOUBELET: Mobility of potentially harmful metals in latosols impacted by the municipal solid waste deposit of Londrina, Brazil	1	
	D. GASTMANS, H.K. CHANG and I. HUTCHON: Groundwater geochemical evolution in the northern portion of the Guarani Aquifer System (Brazil) and its relationship to diagenetic features	16	
	T. ITAI, Y. TAKAHASHI, A.A. SEDDIQUE, T. MARUOKA and M. MITAMURA: Variations in the redox state of As and Fe measured by X-ray absorption spectroscopy in aquifers of Bangladesh and their effect on As adsorption	34	
	P. MÖLLER and P. DULSKÉ: Transmetalation of Gd-DTPA by Cu, Y and lanthanides and its impact on the hydrosphere	48	
	Y. LIN, T. LARSEN, R.D. VOGT and X. FENG: Identification of fractions of mercury in water, soil and sediment from a typical Hg mining area in Wanshan, Guizhou province, China	60	
	Y.T. HE, A.G. FITZMAURICE, A. BILGIN, S. CHOI, P. O'DAY, J. HORST, J. HARRINGTON, H.J. REISINGER, D.R. BURRIS and J.G. HERING: Geochemical processes controlling arsenic mobility in groundwater: A case study of arsenic mobilization and natural attenuation	69	
	S. STHIANNOPKAO, K.-W. KIM, K.H. CHO, K. WANTALA, S. SOTHAM, C. SOKUNTHEARA and J.H. KIM: Arsenic levels in human hair, Kandal Province, Cambodia: The influences of groundwater arsenic, consumption period, age and gender	81	
	G. KOEHLER and L.I. WASSENAAR: The stable isotopic composition (³⁷ Cl/ ³⁵ Cl) of dissolved chloride in rainwater ...	91	
	C.F. BROWN, R.J. SERNE, J.G. CATALANO, K.M. KRUPKA and J.P. ICENHOWER: Mineralization of contaminant uranium and leach rates in sediments from Hanford, Washington	97	
	H. PAUWELS, V. AYRAUD-VERGONAUD, L. AQUILINA and J. MOLÉNAT: The fate of nitrogen and sulfur in hard-rock aquifers as shown by sulfate-isotope tracing	105	
	E. SZALINSKA, J. DOMINIK, D.A.L. VIGNATI, A. BORROWSKI and B. BAS: Seasonal transport pattern of chromium(III and VI) in a stream receiving wastewater from tanneries	116	
	V. LAVASTRE, C.L.G.L. SALLE, J.-L. MICHELOT, S. GIANNESINI, L. BENEDETTI, J. LANCELOT, B. LAVIELLE, M. MASSAULT, B. THOMAS, E. GILBERT, D. BOULLES, N. CLAUER and P. AGRINIER: Establishing constraints on groundwater ages with ¹⁴ C, ³ H, and noble gases: A case study in the eastern Paris basin, France	123	
Continued on outside back cover			

This article appeared in a journal published by Elsevier. The attached copy is furnished to the author for internal non-commercial research and education use, including for instruction at the authors institution and sharing with colleagues.

Other uses, including reproduction and distribution, or selling or licensing copies, or posting to personal, institutional or third party websites are prohibited.

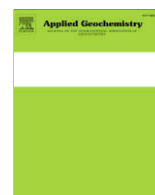
In most cases authors are permitted to post their version of the article (e.g. in Word or Tex form) to their personal website or institutional repository. Authors requiring further information regarding Elsevier's archiving and manuscript policies are encouraged to visit:

<http://www.elsevier.com/copyright>



Contents lists available at ScienceDirect

Applied Geochemistry

journal homepage: www.elsevier.com/locate/apgeochem

Geochemical processes controlling arsenic mobility in groundwater: A case study of arsenic mobilization and natural attenuation

Y. Thomas He^{a,*}, Arthur G. Fitzmaurice^a, Azra Bilgin^{a,1}, Sunkyoung Choi^b, Peggy O'Day^b, John Horst^c, James Harrington^c, H. James Reisinger^d, David R. Burris^d, Janet G. Hering^{a,2}

^a Department of Environmental Science and Engineering, California Institute of Technology, 1200 E. California Blvd., MC 138-78, Pasadena, CA 91125, USA

^b School of Natural Sciences, University of California, Merced, 5200 N. Lake Rd., Merced, CA 95343, USA

^c Arcadis G and M, Inc., 6 Terry Drive, Suite 300, Newtown, PA 18940, USA

^d Integrated Science and Technology, Inc., 1349 Old Highway 41, Marietta, GA 30060, USA

ARTICLE INFO

Article history:

Received 31 March 2009

Accepted 11 October 2009

Available online 3 November 2009

Editorial handling by D. Polya

ABSTRACT

The behavior of As in the subsurface environment was examined along a transect of groundwater monitoring wells at a Superfund site, where enhanced reductive dechlorination (ERD) is being used for the remediation of groundwater contaminated with chlorinated solvents. The transect was installed parallel to the groundwater flow direction through the treatment area. The ERD technology involves the injection of organic C (OC) to stimulate *in situ* microbial dechlorination processes. A secondary effect of the ERD treatment at this site, however, is the mobilization of As, as well as Fe and Mn. The concentrations of these elements are low in groundwater collected upgradient of the ERD treatment area, indicating that, in the absence of the injected OC, the As that occurs naturally in the sediment is relatively immobile. Batch experiments conducted using sediments from the site inoculated with an Fe(III)- and As(V)-reducing bacterium and amended with lactate resulted in mobilization of As, Fe and Mn, suggesting that As mobilization in the field is due to microbial processes.

In the areas of the transect downgradient of the ERD treatment area, however, the concentrations of OC, As, Fe and Mn in the groundwater are not elevated relative to background levels. The decrease in the dissolved concentration of OC can be attributed to mineralization by microorganisms. The losses of As, Fe and Mn from the dissolved phase must presumably be accompanied by their uptake onto aquifer solids, but chemical extractions provided evidence only for the enrichment of Fe(II). Nor could sorption of As(III) onto sediments be detected by X-ray absorption spectroscopy (XAS) against the background of native As in the sediments, which was present as As(V).

© 2009 Elsevier Ltd. All rights reserved.

1. Introduction

The mobilization of naturally-occurring (or geogenic) As poses a serious threat to human health, particularly in south and southeast Asia, where rural populations are heavily dependent on alluvial aquifers for drinking water (Nordstrom, 2002; Smith et al., 2002). Arsenic mobilization in these settings is generally attributed to reductive dissolution of Fe-bearing carrier phases, specifically Fe(III) oxyhydroxides, and the concomitant release of associated As (Amirbahman et al., 2006; Berg et al., 2001; Harvey et al.,

2002; Huang and Matzner, 2006; McArthur et al., 2001; Nickson et al., 2000; Shimada, 1996; Swartz et al., 2004; Welch et al., 2000). Various sources have been proposed for the organic C (OC) needed to support the reductive dissolution process, including terrestrial organic matter, hydrocarbons migrated from natural sources, and anthropogenic sources of fresh OC derived from agriculture and inadequate sanitation practices (Harvey et al., 2002, 2006; McArthur et al., 2004; Rowland et al., 2006).

Similar processes may occur in industrialized countries as a result of inadvertent or intentional inputs of anthropogenic OC. Inadvertent inputs include petroleum hydrocarbons released from leaking storage tanks or pipelines (Ghosh et al., 2003; Johnson and Schreiber, 2003) and organic-rich leachates generated within solid waste landfills (Delemos et al., 2006; Keimowitz et al., 2005; Pinel-Raffaitin et al., 2007; Reisinger et al., 2005; Stollenwerk and Colman, 2003). Organic C has also been intentionally introduced into the subsurface to stimulate enhanced reductive dechlorination (ERD), the *in situ* bioremediation of chlorinated

* Corresponding author. Present address: National Risk Management Research Laboratory, USEPA, Groundwater and Ecosystems Restoration Division, 919 Kerr Research Drive, Ada, OK 74820, USA. Fax: +1 580 436 8703.

E-mail address: he.yongtian@epa.gov (Y.T. He).

¹ Present address: Brown and Caldwell, 1697 Cole Blvd., Golden, CO 80401, USA.

² Present address: Eawag, Swiss Federal Institute of Aquatic Science and Technology, Ueberlandstrasse 133, CH-8600 Duebendorf, Switzerland.

organic solvents (e.g., Scheutz et al., 2008). The possibility that this process could mobilize naturally-occurring As has already been recognized and demonstrated in laboratory microcosms (McLean et al., 2006), but its occurrence in a field setting has received only passing mention (Suthersan and Horst, 2008).

The stimulation of microbial reduction of As(V) and Fe(III) by a variety of organic substrates has been demonstrated in numerous laboratory studies. The rate of microbial reductive dissolution of Fe(III)-containing solids has been shown to depend on various factors including the composition and crystallinity of the solid phase, the microbial strain, the type of organic substrate and other environmental conditions (Albrechtsen et al., 1995; Benner et al., 2002; Bonneville and Van Cappellen, 2004; Cooper et al., 2005; Cummings et al., 1999; Lovley and Phillips, 1986a,b; Lovley et al., 1989; Roden, 2006; Rowland et al., 2007). Microbial species have different inherent capacities for reducing As(V) and/or Fe(III) and different responses to stimulation by added organic substrates. Therefore, in mixed microbial communities, preferential growth of certain species in response to biostimulation may change the pattern of As(V) and/or Fe(III) reduction over time. The microbial reduction of As(V) and/or Fe(III) is not necessarily accompanied by As or Fe mobilization. Reduced As(III) and/or Fe(II) can also remain associated with the solid phase through sorption (Campbell et al., 2008; Cummings et al., 1999; Lee et al., 2005; Zobrist et al., 2000), precipitation of authigenic solids including Fe(II) arsenate or As sulfides (Bostick and Fendorf, 2003; Huang and Matzner, 2006; Keimowitz et al., 2007; Lee et al., 2005; O'Day et al., 2004), or the transformation of Fe minerals (e.g., ferrihydrite to magnetite) with subsequent As sequestration in the authigenic mineral (Tufano et al., 2008). In many cases, the microbially-mediated reductive dissolution of Fe(III) oxyhydroxides containing As as a sorbed or co-precipitated species has been found to result in the accumulation of Fe(II) and As, either as As(III) or As(V), in solution (Islam et al., 2004; Nickson et al., 2000; Swartz et al., 2004). Laboratory studies have shown, however, that the extent of As release under such conditions is influenced by the type of Fe(III) oxyhydroxide initially present and the capacity of the microorganisms for Fe(III) and/or As(V) reduction (Tufano et al., 2008).

Microorganisms capable of As(V) and Fe(III) reduction are ubiquitous in soils and sediments, and As and Fe mobilization into sediment porewater and groundwater is generally attributed to microbial activity (Albrechtsen et al., 1995; Cooper et al., 2005; Cummings et al., 1999; Zobrist et al., 2000). It is commonly, though not exclusively, observed that As-enriched groundwaters or porewaters also contain elevated concentrations of Fe and Mn, which is consistent with a reductive mechanism for As mobilization (Islam et al., 2004; McArthur et al., 2004; Nath et al., 2005; Nickson et al., 2000; Swartz et al., 2004). This mechanism for As mobilization presumes that naturally-occurring As in the subsurface is associated with Fe(III) oxyhydroxides, as is often the case in alluvial aquifers (Welch and Lico, 1988a,b; Welch et al., 2000).

The coupled biogeochemical cycling of As and Fe influences not only the mobilization of As but also its potential sequestration. Geochemical conditions that allow the oxidation of Fe(II) and precipitation of Fe(III) oxyhydroxides would also tend to promote As sequestration (Bednar et al., 2005; Espana et al., 2005; Fukushi et al., 2003; Huang and Matzner, 2006; Roberts et al., 2004; Wilkie and Hering, 1996). Such processes could allow the natural attenuation of As mobilized by anthropogenically-introduced OC. Even in the absence of oxidation, As can be sequestered by sorption onto aquifer minerals (Smedley and Kinniburgh, 2002).

Here, the processes of both As mobilization and sequestration are examined at a field site, where OC has been introduced as part of an ERD remediation strategy. Mobilization of As and Fe is observed downgradient of the OC inputs, but migration of As and Fe appears to be limited by natural attenuation processes. In this

study, field observations are combined with laboratory studies of As and Fe mobilization and characterization of sediments to explain the effects of OC inputs on the coupled biogeochemical cycling of As and Fe.

2. Site background

The field study was conducted at the former Ft. Devens, a military base that was closed in 1996 and is located 56 km west of Boston, MA, USA. The site was listed as a Superfund site in 1989 (USEPA, 2005). In one area of the Devens site, designated Area of Contamination (AOC) 50 (Fig. 1), sources of groundwater contamination include two World War II fueling systems, a drywell, and a tetrachloroethane (PCE) drum storage area. These historic sources (which were eventually removed) created an approximately 1000 m long organic contaminants plume in groundwater. Despite operation of an *in situ* soil vapor extraction system from 1994 to 1996 and intermittent operation until 1999 and excavation of the drywell and adjacent soil in 1996, the groundwater contains elevated concentrations of volatile organic compounds (VOCs) including PCE, trichloroethene (TCE), 1,1-dichloroethene (1,1-DCE), cis-1,2-dichloroethene (cis-1,2-DCE), vinyl chloride (VC), 1,2-dichloropropane, methylene chloride, 1,2-dichloroethane, and benzene; PCE has been found in groundwater in the source area at concentrations in excess of 30,000 µg/L (Horst et al., 2002).

Between December 2001 and June 2002, an ERD pilot test was conducted for remediation of chlorinated solvent contamination. Molasses was injected into the saturated zone (at a depth of 35.1–41.1 m) approximately 503 m downgradient of the source area (denoted ERD Pilot on Fig. 1A). After this initial (and largest) molasses injection, monthly injections were initiated in October 2004 at the injection wells (denoted IW) shown in Fig. 1B and continued through the sampling event in 2006. Molasses was introduced as a source of bioavailable organic C to support microbial growth but also served as a source of N and S, which are typically 0.9% and 0.7% by weight on a dry matter basis, respectively (Wythes et al., 1978).

Sediments at the site are mainly composed of fine sand with silt, and some medium to coarse sand (Horst et al., 2002). Near the ERD pilot test area, fine to coarse sand, gravel/cobble, and silt are also important at 21.3–30.5 m depth. The sediments are mainly composed of quartz, illite, kaolinite and illite-montmorillonite.

Groundwater flow from the AOC 50 source area is generally SW toward the Nashua River (USEPA, 2004). At the ERD pilot test area, the depth of the water table is 18.3 m below ground surface (bgs). The monitoring wells downgradient of the ERD pilot test area are screened over a depth interval from 38.1–41.1 m bgs. The lower bound of the screened interval corresponds to the boundary between the glacio-fluvial deposits and the glacial till, along which the PCE plume appears to migrate.

3. Experimental

3.1. Field sampling

Four sediment borings (SB-1, SB-2, SB-3 and SB-4) and 4 monitoring well sediment cores (SMW-1, SMW-2, SMW-3 and SMW-4) were collected in April 2006 using sonic drilling at locations shown in Fig. 1B. Borings were drilled from the ground surface to a depth of approximately 44.2 m; sections of core material 0.3 m in length were isolated by slicing the core and pushing a 5 cm outside diameter (OD) plastic acetate tube 0.3 m into the end of the core, slicing the other end of the section to isolate the sample, capping both ends of the tube, and securing the caps with duct tape. This procedure was intended to limit the exposure of aquifer material to

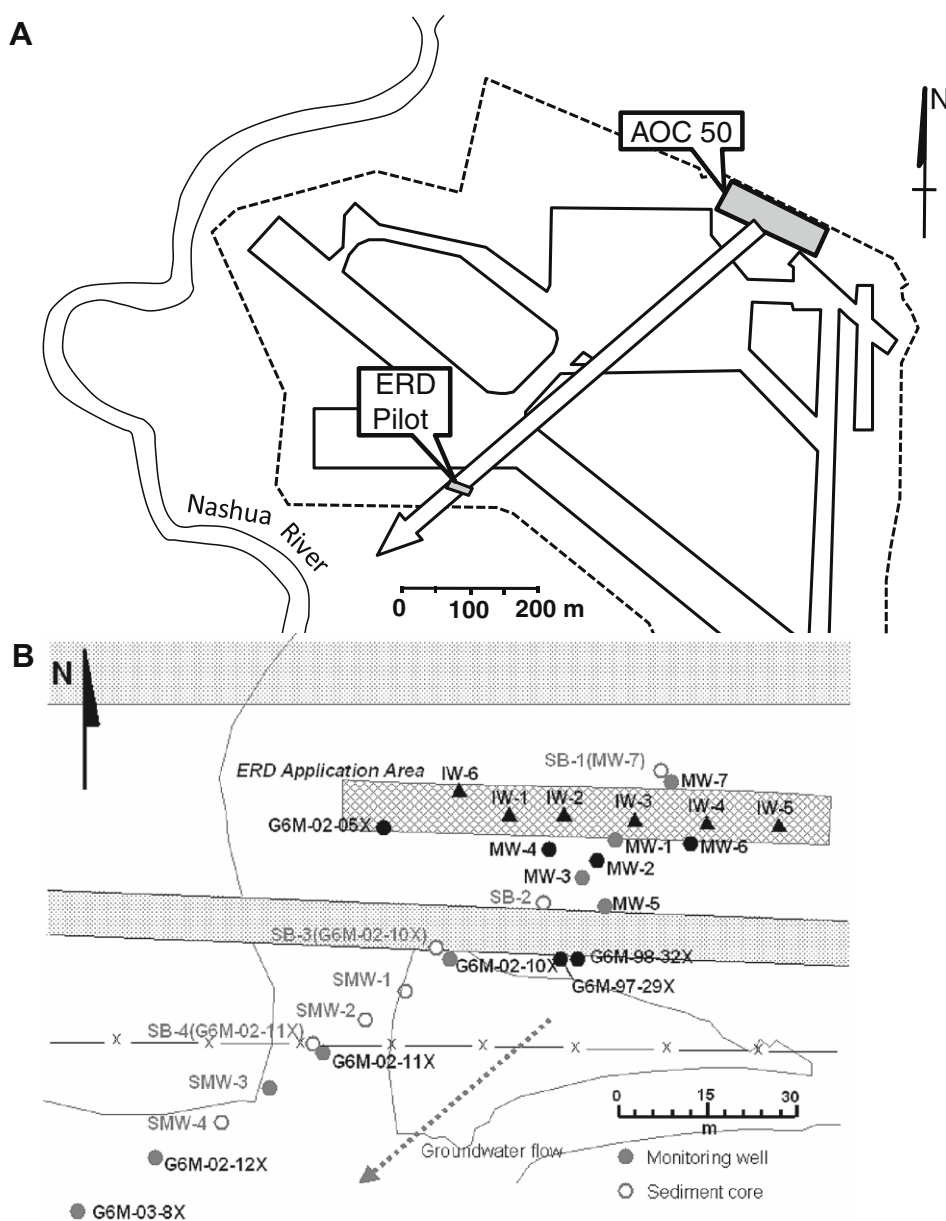


Fig. 1. Ft. Devens site. (A) map view showing source of chlorinated solvent contamination (AOC50) and ERD pilot area. (B) Blowup of ERD pilot area (from A) showing location of injection wells (filled triangles), sediment borings (gray open circles), and sampled monitoring wells (gray filled circles and gray open circles in SMW-1–4). Irregular gray lines correspond to surface topography.

atmospheric O_2 . Sample cores collected from 21.3 to 44.2 m were stored in a dark and cool ($4\text{ }^\circ\text{C}$) place, shipped to Caltech within 24 h in a cooler packed with ice, and frozen immediately upon arrival.

Groundwater was sampled on May 16–19, 2006 at monitoring wells shown in Fig. 1. Four new monitoring wells (SMW-1–4) were developed on May 15, 2006; the other wells were part of an existing monitoring network. In May 2006, groundwater sampling commenced at the well located upgradient of the molasses injection area (MW-7) and continued from wells with the least As contamination (based on previous monitoring data) to the most As-contaminated wells, closest to the molasses injection wells (IW-1–5 in Fig. 1).

Each monitoring well was purged and sampled via low stress-flow (generally $<1\text{ L/min}$) purging and sampling procedures. A submersible pump was lowered to the midpoint (39.6 m) of the screened interval of the well (38.1–41.1 m). The pump speed

was adjusted so that there was little or no water-level drawdown ($<0.1\text{ m}$) during purging. During well purging, groundwater levels and pumping rates were monitored. The indicator field parameters temperature, pH, E_h and dissolved O_2 were measured using a flow-through cell (YSI 85), turbidity with a DRT-15CE Turbidimeter and specific conductance with a Waterproof ECTestr (Eutech Instruments). Purging was considered complete and sampling begun after all the indicator field parameters had stabilized as indicated by three consecutive measurements (taken every 3–5 min) within the following limits: turbidity (10% for values $>1\text{ NTU}$), DO (10%), specific conductance (3%), temperature (3%), pH (± 0.1 unit), E_h ($\pm 10\text{ mV}$).

Sample containers were prepared at Caltech; when appropriate, preservatives were added to sample containers before the field sampling trip. Collected samples were stored on ice in a cooler and shipped daily to Caltech. Holding times, preservation and storage methods are listed in Table 1. Note that $0.45\text{-}\mu\text{m}$ in-line filters

Table 1
Information on groundwater sample collection,^a preservation and analysis.

Analyte	Method ^b	Sample volume	Preservation (4 °C)	Holding time	Test type
NO ₂ and NO ₃	SM 4500-NO3-E	125 mL HDPE	None	48 h	Colorimetric
Sulfide	SM4500D	125 mL HDPE	0.25 mL 5 mM NaOH and 0.5 ml 1 M Zn Acetate	7 days	Colorimetric (glove box)
Sulfate	EPA 300.0A	125 mL HDPE	None	28 days	IC
Org carbon– Dissolved	SM5310C	120 mL Amber Glass	Filter through 0.2 µm upon return	None	Catalytic oxidation
Org carbon– Total	SM5310C	120 mL Amber glass	0.5 ml 1.2 M H ₂ SO ₄	28 days	Catalytic oxidation
Fe	SM 3500 Fe-D	125 mL HDPE	0.5 ml 2.5 M HCl	6 months	Colorimetric
As speciation		250 mL HDPE	3.35 ml 0.1 M EDTA, 10.8 ml 2 M acetic acid	3 months	LC-ICP/MS
Metals (Si, As, Mn, Fe)	EPA 200.8	250 mL HDPE	1 ml 2.5 M HNO ₃	6 months	ICP/MS

^a Samples were filtered in the field using an in-line 0.45 µm filter (VOSS® in-line filter).

^b All methods denoted “SM” refer to Standard Methods (Clesceri et al., 1999). All methods denoted “EPA” refer to USEPA methods (USEPA, 1999).

(VOSS) were used when collecting samples for analysis of metals and determination of As speciation. Field duplicate samples were collected at wells 10×, 11× and 12× (suffixes of monitoring designations given in Fig. 1).

To confirm available information on groundwater flow velocities, this parameter was independently measured using Passive Flux Meters (PFMs) by EnviroFlux LLC under the direction of K. Hatfield (Univ. of Florida). Details of the method are available elsewhere (Annable et al., 2005; Hatfield et al., 2004). The PFMs were constructed to fit the 4 new monitoring wells (SMW-1–4). The PFMs were 1.5 m length each with partitions at 0.3-m intervals. Two PFMs were installed for each well to match the 3-m screened intervals. The PFMs were deployed in late October 2006, left in the wells for 1 week, and retrieved in early November 2006.

3.2. Chemicals and analytical methods

All chemicals were reagent grade or higher, used without further purification, and obtained from the following suppliers: HNO₃, HCl, H₃PO₄, CaSO₄ (J.T. Baker), OmniTrace Ultra HNO₃, CaCl₂, FeCl₂ (EMD Chemicals), NaOH (EM Science), NaAsO₂, Na₂HAsO₄, EDTA, NaCl (Sigma), ammonium acetate, acetic acid, methanol (BDH), 1,10-phenanthroline, Na₂SiO₃·9H₂O, H₂O₂ (Alfa Aesar), MgCl₂ (Aldrich), MES (MP Biomedicals), formaldehyde (VWR). Solutions were prepared with 18.2 MΩ deionized water (Millipore Milli-Q system) and stored in plastic containers that had been washed with 3% HNO₃. All volumetric flasks had been washed with 3% HNO₃ and rinsed several times with deionized water prior to use. Disposable 50-mL Falcon® tubes were used for batch reactors.

Total concentrations of As, Fe and Mn were determined by ICP-MS (Hewlett–Packard 4500). Total Fe and Fe(II) were determined using the colorimetric 1,10-phenanthroline method (Standard methods 3500-Fe B, Clesceri et al., 1999) with a UV–Visible spectrophotometer (Cary 480) at 510 nm. Arsenic speciation was determined by quantifying As(III) and As(V) using coupled liquid chromatography (LC) and ICP-MS; As(III) and As(V) were separated using an HPLC column (Hewlett Packard 1100 series) with a 3-mM phosphate mobile phase (pH 6.0) at 0.9 mL/min flow rate and the HPLC outflow was directly connected to ICP-MS for As measurement. Major cations and anions were quantified by ion chromatography (Dionex DX-500), sulfide and NO₃⁻/NO₂⁻ by colorimetry, and alkalinity by titration. Total and dissolved organic C (TOC/DOC) concentrations were determined by the persulfate oxidation method (Clesceri et al., 1999) with an Aurora TOC analyzer (Model 1030).

3.3. Sediment extraction experiments

Sediment core samples were defrosted, sectioned, and homogenized inside a N₂ glove box. Sediment adjacent to the capped ends of the core samples (i.e., within a few cm of the cap) was discarded.

Sub-samples were then refrozen for later use in extraction and mobilization experiments. Water content was determined gravimetrically for each sediment sample (Table 2).

3.3.1. EPA 3050B extractions

Sediment sub-samples were extracted following the EPA 3050B extraction method (USEPA, 1996), which is not a total digestion but is designed to estimate “environmentally available” metal contents of sediments. The extractions were conducted on 1–2 g (wet weight) sediment and can be briefly described as follows: digestion at 95 ± 5 °C with 10 mL of 1:1 HNO₃ for 10–15 min and with 5 mL of concentrated HNO₃ for 2 h; digestion with 30% H₂O₂ (added in approximately 1-mL increments until the reaction was complete) and heating to reduce the volume to approximately 5 mL; dilution to 50 mL volume with H₂O and centrifugation at 3000 rpm for at least 10 min to separate any remaining particulate matter; dilution of supernatant with 2% (v/v) HNO₃ for ICP-MS analysis. Throughout the digestion procedure, the vessel was loosely covered and the bottom of the vessel was always covered with solution.

3.3.2. Sequential extraction of As and extraction of Fe(II)

For these extractions, all sample handling was performed in the N₂ glove box. Sequential extractions were performed by adding the extractants listed in Table 3 to 1 g of wet sediment in a modification of a published method (Wenzel et al., 2001). After each specified time interval, suspensions were centrifuged at 3000 rpm for 10 min and the supernatant was carefully removed with a pipette for solution analysis. Each extraction step was followed by a wash step. The extractants and corresponding washes were pooled for each step, and samples were diluted 10-fold with 2% HNO₃ prior to ICP-MS analysis.

Table 2
Water content of sediment samples.

Sediment core	Depth (m)	H ₂ O (%)	Sediment core	Depth (m)	H ₂ O (%)
SB-1	41.1	21.5	SMW-4	41.1	22.4
SB-1	42.7	20.5	SMW-4	42.7	23.1
SB-2	41.1	22.9	SMW-2	35.1	16.8
SB-2	42.7	19.3	SMW-2	36.6	11.7
SB-4	35.1	12.6	SMW-2	38.1	13.5
SB-4	36.6	16	SMW-2	39.6	14
SB-4	38.1	14.6	SMW-2	41.1	23.7
SB-4	39.6	17.8	SMW-2	42.7	18.4
SB-4	41.1	11.8	SMW-3	41.1	24.6
SB-4	42.7	17.3	SMW-3	42.7	23.4
SMW-1	41.1	22.2	SMW-3 composite ^a		21.5
SMW-1	42.7	19.3			

^a SMW-3 composite is a mixture of homogenized sediment samples from depths of 39.6, 41.1 and 42.7 m collected at SMW-3.

Table 3
Sequential extraction procedure for As in sediments.^a

Step	Target phases for As speciation	Extractant	SSR ^b	Wash step
1	Non-specifically sorbed	0.05 M (NH ₄) ₂ SO ₄ ; 4 h, 20 °C	1:25	15 mL H ₂ O
2	Specifically sorbed	0.05 M (NH ₄)H ₂ PO ₄ ; 16 h; 20 °C	1:25	15 mL H ₂ O
3	Amorphous and poorly crystalline hydrous oxides of Fe and Al	0.2 M NH ₄ -oxalate buffer, pH 3.25; 4 h (dark), 20 °C	1:25	0.2 M NH ₄ -oxalate buffer, pH 3.25; 10 min (dark), SSR 1:15
4	Well crystallized hydrous oxides of Fe and Al	0.2 M ammonium oxalate buffer + 0.1 M ascorbic acid, pH 3.25; 30 min, 96 ± 3 °C	1:25	0.2 M NH ₄ -oxalate buffer, pH 3.25; 10 min (dark), SSR 1:15
5	Residual phases (excluding silicates)	HNO ₃ /H ₂ O ₂ ^c		

^a All sample handling up to step 5 was performed under N₂-atmosphere.

^b SSR: solid–solution ratio.

^c Same as 3050B extraction.

For extraction of Fe(II), 1 g of wet sediment was extracted with 0.5 M HCl for 10 h in the dark as previously described (Dixit and Hering, 2006). Supernatants were separated from residual sediments by centrifugation (3000 rpm, 10 min) and analyzed for dissolved Fe(II) and Fe(III) colorimetrically using the 1,10-phenanthroline method.

3.4. Mobilization experiments

Sediment collected at the far-field well SMW-3 at depths of 39.6, 41.2 and 42.7 m was homogenized in the glove box and 1 g of wet sediment was added to 20 mL of synthetic groundwater (Table 4). Suspensions were amended with either or both 10 mM Na lactate or 2% (v/v) formaldehyde (as final concentrations). All suspensions were inoculated with 0.2 mL of a culture of *Shewanella* sp. strain ANA-3 (obtained from D.K. Newman) that had been incubated anaerobically in LB medium at 30 °C in the dark for 24 h. Cells were at stationary phase at the time of inoculation, and the estimated initial cell density in the inoculated suspensions was 10⁷ cells/mL. Inoculated suspensions were incubated at 15 °C in a cold room with shaking at low speed (Labline Environ Shaker, model 3527). Triplicate samples were prepared for each treatment and time point. At each time point, individual batch reactors were sacrificed and supernatants were separated from residual sediments for analysis by centrifugation at 3000 rpm for 10 min.

3.5. X-ray absorption spectroscopy (XAS)

Sediment samples from borings were selected for X-ray Absorption Spectroscopy (XAS) characterization and kept frozen until analysis. Cores were defrosted in a N₂-atmosphere, and a sample from the center of the core was taken and homogenized. In a N₂-atmosphere glovebox, ~0.5 mg of sample was ground to a fine powder, loaded into Teflon sample holders, sealed with Kapton tape, and quenched in liquid N₂. Data were collected at Stanford Synchrotron Radiation Laboratory (SSRL) on BL11-2 (3 GeV, 80–100 mA). During data collection, samples were held at liquid He

Table 4
Synthetic groundwater composition.

Constituent	Concentration (M)
NaCl	3.53 × 10 ⁻³
CaSO ₄	1.71 × 10 ⁻⁴
CaCl ₂	1.77 × 10 ⁻⁴
MgCl ₂	1.19 × 10 ⁻⁴
Na ₂ SiO ₃ ·9H ₂ O ^a	3.20 × 10 ⁻⁴
MES ^b	1.00 × 10 ⁻²
pH	6.1 ^c

^a Silicon AA standard (sodium metasilicate nonahydrate, lot #3602128, product #AS11KW, Ricca Chemical Co.,) in deionized water.

^b MES = 4-morpholineethanesulfonic acid.

^c pH units.

temperature (4–8 K). Fluorescence spectra were collected using a 30-element Ge solid-state array detector. For XANES, 3–5 successive scans were collected and averaged to obtain sufficient signal/noise. No change in oxidation state of As was detected during XAS data collection. Spectral background was subtracted using the pre-edge absorption and normalized to the average post-edge absorption (fluorescence/incident energy).

4. Results and discussion

To assess the effects of molasses injection on the occurrence and mobility of As, Fe and Mn, groundwater composition was examined along a transect of wells installed along the direction of groundwater flow up- and down-gradient of the molasses injection area (Fig. 1B). Sediments from borings were characterized by chemical extraction and spectroscopic analysis to assess the amount, speciation, and potential for release and sequestration of As, Fe and Mn. Batch experiments were conducted to assess the potential for microbially-mediated mobilization of As, Fe and Mn.

4.1. Groundwater composition

Analysis of samples collected in May 2006 at MW-7, upgradient of the molasses injection area for the pilot ERD test, demonstrated that the ambient groundwater is low in total, dissolved As (<1 µg/L), Mn (0.1 mg/L), and Fe (<0.1 mg/L) with a SO₄²⁻ concentration of 16.4 mg/L. Parameters measured at MW-7 in the field included temperature (12.5 °C), pH (5.9) and E_h (+105 mV). As a comparison, uncontaminated groundwater in the Cape Cod (MA) aquifer is also mildly acidic (pH 5.7) with undetectable As and Fe concentrations and SO₄²⁻ concentrations of approximately 8 mg/L (Savoie et al., 2004).

Immediately downgradient of the molasses injection area, a distinct change in groundwater composition was observed. This was particularly apparent in the decrease in field-measured E_h (which dropped below –100 mV) as well as a decrease in SO₄²⁻ concentration and increase in the concentrations of total dissolved As, Fe and Mn (Fig. 2). Maximum concentrations of As and Fe were observed at well 10×, while the maximum Mn concentration was observed farther downgradient at well SMW-2. Below SMW-2, As and Fe concentrations declined sharply, though still exceeding the background values at MW-7; Mn concentrations declined more gradually. The pattern in Fe(II) concentrations (not shown) corresponded to that observed for total dissolved Fe. The maximum Fe(II) concentration was observed at well 10×, where it constituted 58% of the total dissolved Fe concentration. At all other wells, the contribution of Fe(II) to total, dissolved Fe was higher (ranging from 71 to 100%).

Along the transect, pH values ranged from 5.7 to 6.7. Sulfide was not detected except at well MW-1 (0.62 mg/L), the closest well downgradient of the molasses injection area, which is reasonable

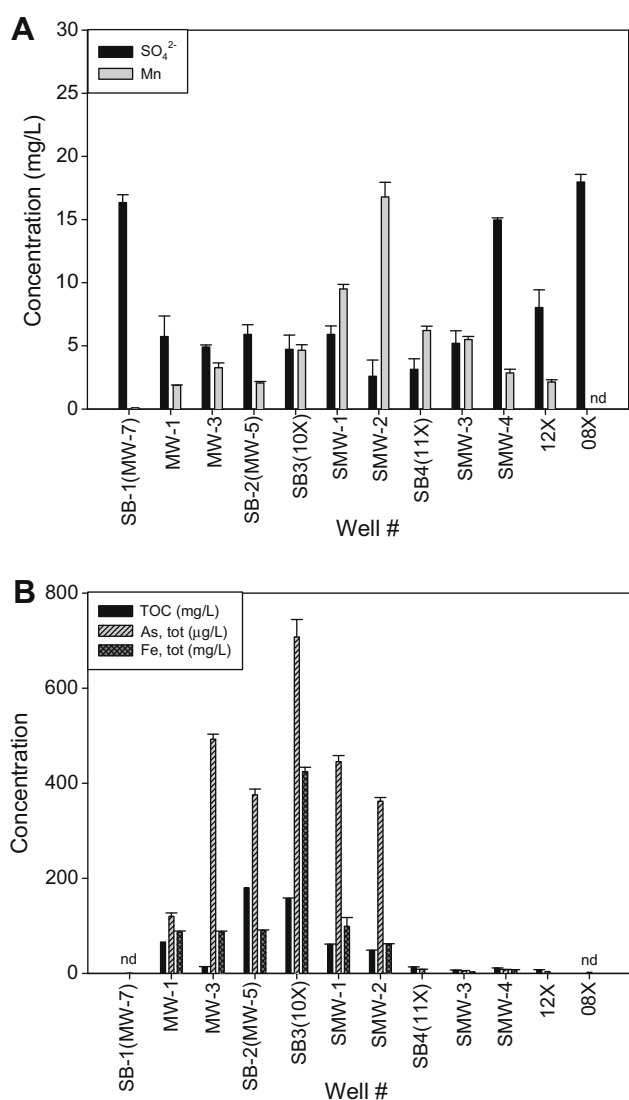


Fig. 2. May 2006 groundwater composition (A) sulfate and total, dissolved Mn, (B) TOC and total, dissolved As and Fe determined by ICP-MS. Wells are ordered in the direction of groundwater flow. TOC was not measured for MW-1 and MW-5 on the samples collected in May 2006; the TOC values shown for these wells are from a monitoring survey conducted in September 2005 by Arcadis G&M Inc. nd = not detected. Error bars indicate standard deviation of triplicate samples. Field duplicate samples show good agreement for analytes shown here.

given that elevated Fe(II) concentrations would be expected to lead to sulfide precipitation. In contrast, NO₃⁻ and/or NO₂⁻ were detected only in the farthest downgradient well 8× (1.2 mg/L as NO₃⁻).

The concentrations of TOC (Fig. 2) and DOC (not shown) also exhibited maximum values in the intermediate wells along the transect. In all samples measured, DOC concentrations were 90 ± 6% of TOC concentrations. The increase in TOC immediately downgradient of the molasses injection site likely reflects the intermittent injection schedule. Like Fe, As and Mn, TOC decreased from its maximum value farther along the transect. However, TOC remained somewhat elevated even in wells SMW-3, SMW-4 and 12×, returning to non-detectable levels only in the farthest downgradient well (8×).

At well 8×, background conditions appeared to be re-established, as indicated by non-detectable Fe and Mn, SO₄²⁻ concentration (17.9 mg/L) comparable to that at the upgradient well MW-7, and E_h > 150 mV. The total, dissolved As concentration was 2.2 µg/L, well below the drinking water standard of 10 µg/L.

4.1.1. Arsenic speciation in groundwater

Both As(III) and As(V) were detected in most groundwater samples. Arsenic(III) could be detected in samples collected from all wells except the upgradient well MW-7 and the farthest downgradient well 8×, where total As concentrations were also quite low. Arsenic (V) was undetectable in well MW-7 and in well 11× and all wells farther downgradient. In the wells MW-1 through SMW-2, the concentrations of As(III) and As(V) were approximately equal except for well 10×, where As(III) was predominant (~78%).

In the wells closest to the molasses injection area (MW-1, MW-3 and MW-5), methylated As species were also detected. Although these species were not quantified, an LC-ICP-MS chromatogram of groundwater collected from well MW-1 (Fig. 3) indicates that a significant fraction of As was present as dimethylarsinic acid (DMA) and suggests that monomethylarsonic acid may also have been present. The occurrence of DMA in the groundwater at Ft. Devens was unexpected because there is no known source of organic arsenical compounds at the site. The microbial conversion of inorganic As to MMA and DMA has, however, been observed in freshwater sediments (Nicholas et al., 2003) and may have been stimulated by the molasses injections.

4.2. Sediment characterization

The changes in the dissolved concentrations of inorganic constituents observed in groundwater collected along the well transect imply some corresponding changes in the composition of the aquifer material along the flow path. Increases in dissolved concentrations of an inorganic constituent imply its mobilization from, and hence depletion in, the solid phase. Conversely, decreases in dissolved concentrations imply sequestration into, and hence enrichment in, the solid phase. To examine these processes, selected sediments collected along the transect were subjected to various extraction procedures and examined by XAS.

4.2.1. Sediment extractions

Sediment samples were collected at various depths during the construction of new monitoring wells (SMW-1–4) or at sediment boring locations near existing wells (SB-1 near the upgradient well MW-7, SB-2 near MW-5, SB-3 near 10× and SB-4 near 11×) (Fig. 1B). Extractions following EPA method 3050B were performed on sediments collected along the transect at and just below the depth of the screened interval of the wells (38.1–41.1 m) and at

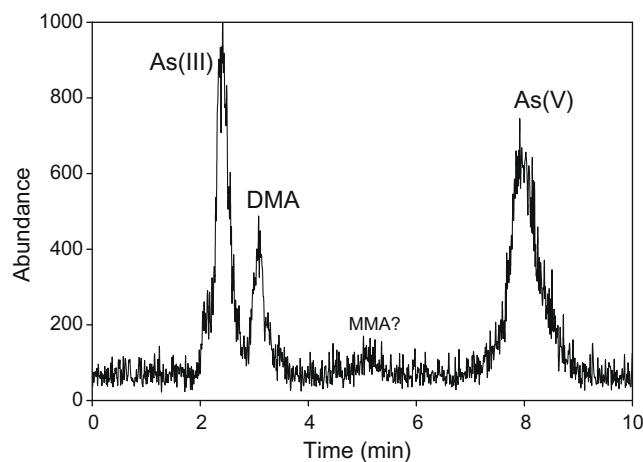


Fig. 3. LC-ICP-MS chromatogram showing the presence of DMA and possibly MMA in addition to inorganic As(III) and As(V) in wells close to the molasses injection area. Sample from well MW-1 collected May 19, 2006.

depths ranging from 34.2–42.7 m for selected locations (SB-4 near well 11× and SMW-2). 3050B-extractable As, Fe, and Mn showed

no meaningful trends along the transect (Fig. 4). It is likely that the reservoir of 3050B-extractable As, Fe and Mn in the sediments is sufficient to obscure any small changes that might occur as a result of mobilization or sequestration. Some trends in 3050B-extractable As, Fe, and Mn were observed as a function of depth (Fig. 5). For all three elements, higher 3050B-extractable concentrations were found in the deeper sediments. This pattern is consistent with the change in the appearance of the sediment from sand

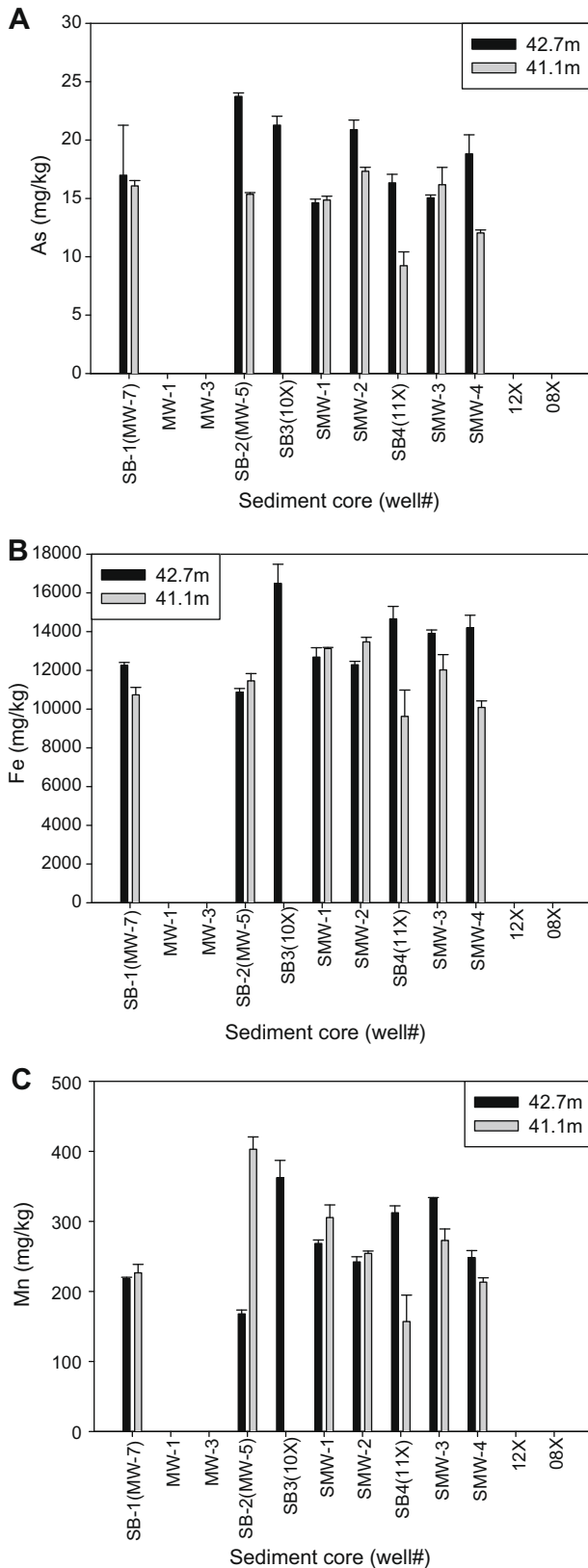


Fig. 4. 3050B-extractable (A) As, (B) Fe, and (C) Mn in core samples from 41.2 m (135 ft) and 42.7 m (140 ft) along the well transect. No samples were collected near wells MW-1, MW-3, 12× and 08×. All values reported on a dry weight basis. Extractions performed on wet sediment with water contents listed in Table 2. Error bars correspond to standard deviation of triplicate samples.

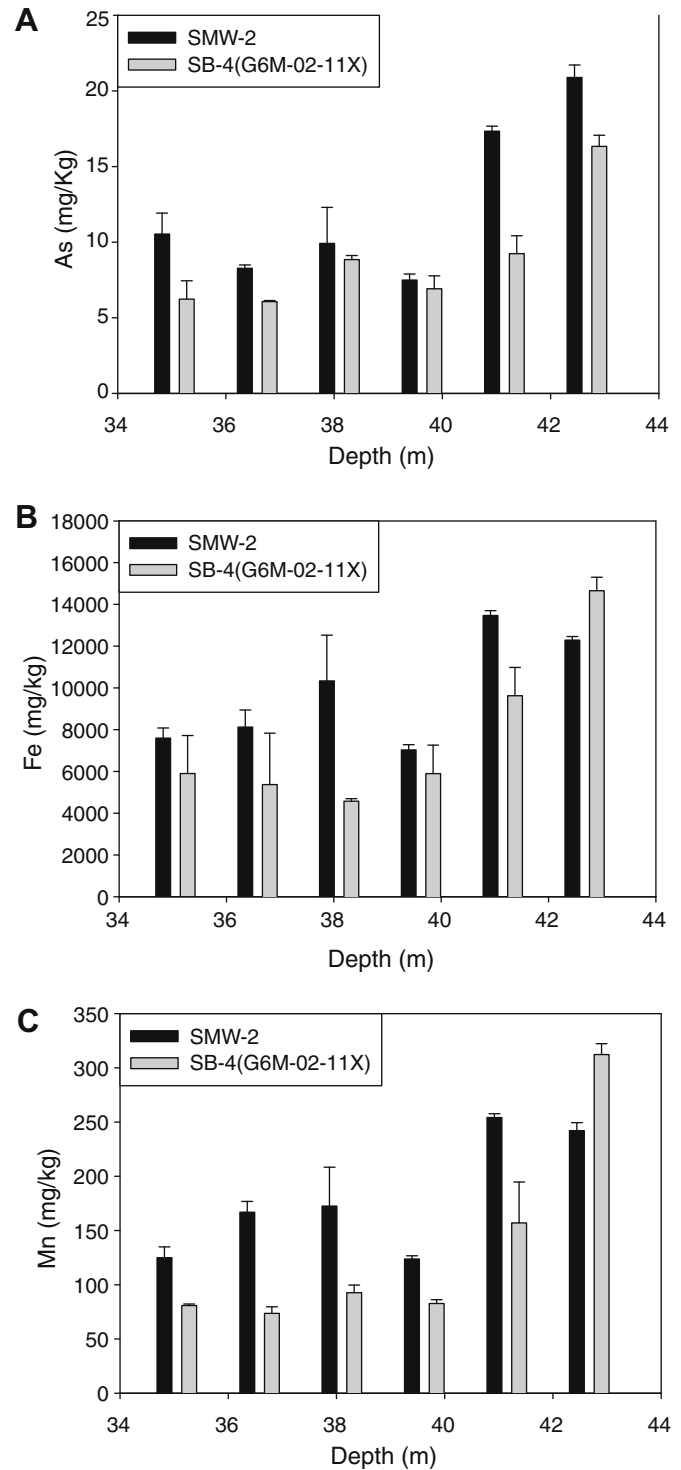


Fig. 5. Depth profile of 3050B-extractable (A) As, (B) Fe and (C) Mn in sediments from soil borings at SB-4 (near well 11×) and SMW-2. All values reported on a dry weight basis. Extractions performed on wet sediment with water content listed in Table 2. Error bars correspond to standard deviation of triplicate samples.

to silt and silty clay in the deepest sediments and is thus likely to be related to the mineralogical characteristics of the sediment.

In contrast, the HCl-extractable Fe(II) did show a pattern along the transect with the highest value at the intermediate location of well SMW-2 (Fig. 6). The HCl-extractable Fe(II) contents are much lower than the 3050B-extractable Fe contents and thus may more readily exhibit a signature of sequestration.

The speciation of As in the solid phase was also examined along the transect and as a function of depth at one location using a sequential extraction procedure (Fig. 7). Although such methods provide only an operational definition of speciation, it appears that As is primarily extracted by non-reductive dissolution with ammonium oxalate (step 3, which targets As associated with amorphous and poorly crystalline hydrous oxides of Fe and Al) and reductive dissolution with ammonium oxalate and ascorbic acid (step 4, which targets As associated with well crystallized hydrous oxides

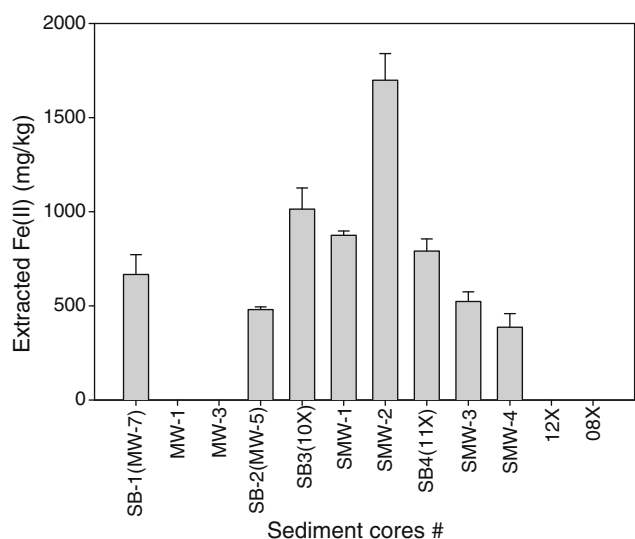


Fig. 6. 0.5 M HCl-extractable Fe(II) in sediments collected at a depth of 42.7 m along the well transect. Wells are ordered in the direction of groundwater flow. No samples were collected near wells MW-1, MW-3, 12× and 08×. All values reported on a dry weight basis. Extractions performed on wet sediment with water content listed in Table 2. Error bars correspond to standard deviation of triplicate samples.

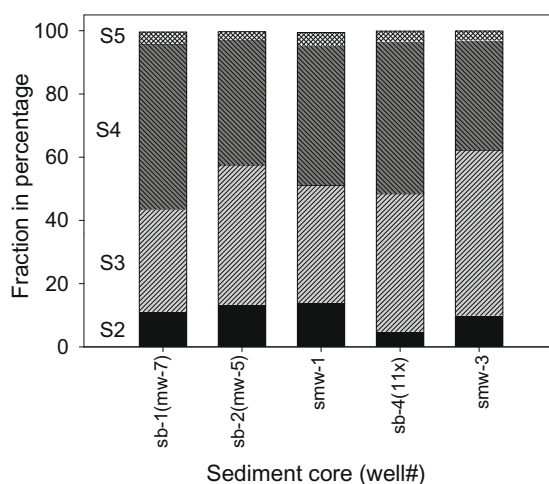
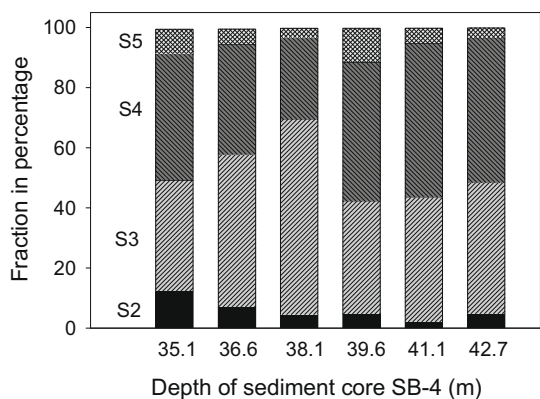


Fig. 7. Speciation of As in the solid phase as defined (operationally) by the sequential extraction procedure described in Table 3. Target phases are: for S1, non-specifically sorbed As; for S2, specifically sorbed As; for S3, As associated with amorphous and poorly crystalline hydrous oxides of Fe and Al; for S4, As associated with well crystallized hydrous oxides of Fe and Al; for S5, As associated with residual phases (excluding silicates). Fraction S1 (not shown) is negligible (<1%). (left) SB-4 sediment as a function of depth, and (right) sediments at 41.2 m (135 ft) along the well transect.

of Fe and Al). Lesser amounts of As were extracted by ammonium phosphate (step 2, which targets specifically sorbed As) or by the HNO₃/H₂O₂ (step 5, which targets As associated with residual phases though excluding silicate minerals) corresponding to the 3050B extraction method. Negligible amounts of As (<1%) were extracted by ammonium sulfate (step 1, which targets non-specifically sorbed As). Recoveries in sequential extractions (sum of steps 1–5) corresponded to 92 ± 11% of the 3050B-extractable As. Similar results were observed in sequential extractions of samples collected along the well transect at 41.1 m or at different depths at SB-4 (near well 11×).

4.2.2. Spectroscopic characterization

Sediment samples collected along the well transect were examined by XAS to assess directly the oxidation state of As in the solid phase. XANES spectra obtained for sediment samples were compared with spectra for a number of reference As(III) and As(V) compounds and sorption samples and with several As-sulfide minerals. Except for one sample from core SMW-4 (42.7 m depth), the XANES spectra from all core samples were very similar and indicated that As was present as As(V) in the sediments (Fig. 8). The appearance of most of the samples was also quite similar (brown, silt and silty clay, trace fine sand, stiff) and distinct from the appearance of the 42.7-m sample from SMW-4 (gray, silt and silty clay, trace fine sand, stiff). Comparison of the XANES spectrum of this sample with reference compounds indicated a mixture of As(V) and As sulfide. The energy of maximum absorption of the As-sulfide component is similar to that of reference arsenopyrite and As-bearing hydrothermal pyrite (Foster et al., 1998; Savage et al., 2000), suggesting a detrital origin for this component in the sediment.

4.3. Mobilization of As, Fe, and Mn in batch experiments

The possible influence of microbial activity on the mobilization of As, Fe and Mn from Devens sediments (collected from the soil boring at well SMW-3 at depths of 39.6, 41.1 and 42.7 m and homogenized before use) was investigated in batch systems inoculated with *Shewanella* sp. strain ANA-3, a known Fe(III)- and As(V)-reducing bacterium (Malasarn et al., 2008). Experiments were conducted with and without addition of lactate as an exogenous organic C source and with and without formaldehyde to

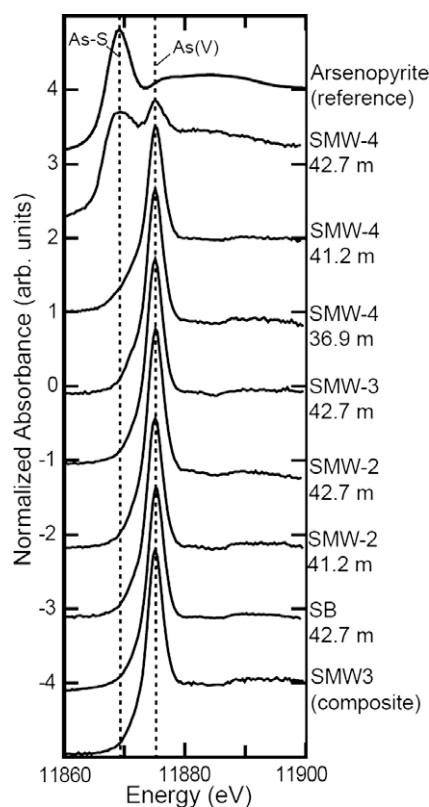


Fig. 8. Arsenic XANES spectra of Fort Devens core sediments compared with a reference spectrum of arsenopyrite. Dashed lines show the characteristic absorption energy for As in arsenopyrite and pyrite (11,869 eV), and As(V) bonded to O (11,875 eV). SMW-3 (composite) is sediment homogenized from three depths (39.6, 41.2 and 42.7 m).

inhibit microbial activity. Substantial release of As, Fe and Mn was observed over time in the experiments stimulated with lactate, though the patterns of release differed somewhat for As, Fe and Mn (Fig. 9). Iron concentrations increased linearly over time, while the Mn concentration showed a distinct plateau after about 20 h. The rate of As release appeared to decrease slightly over the course of the experiment (120 h). The Mn concentration at the plateau corresponded to 25% of the 3050B-extractable Mn; over the course of the experiment, the As concentration reached 33% of the 3050B-extractable As, but the Fe concentration reached only 4% of the 3050B-extractable Fe. It is, of course, quite reasonable that only a fraction of the 3050B-extractable metal content would be released in the microbial incubations. Very little release was observed when formaldehyde was added; the addition of lactate had little or no effect in the presence of formaldehyde. In the absence of lactate, some initial release of As and Fe was observed but concentrations did not increase over time. In contrast, a steady increase in Mn concentration was observed over time. These observations suggest that native organic C present in the sediments and/or residual organic C transferred with the inoculum supported this level of microbial activity.

Determination of the speciation of As and Fe released into solution indicated that all dissolved Fe was present as Fe(II), consistent with field observations. All dissolved As was present as As(III), which contrasts with field observations of the co-occurrence of As(III), As(V) and DMA in some samples. However, the activity of the microorganism used for the inoculation is not necessarily the same as that of the ambient microbial community. The nature and loading of the organic substrate (i.e., lactate vs. molasses) may also influence microbial activity.

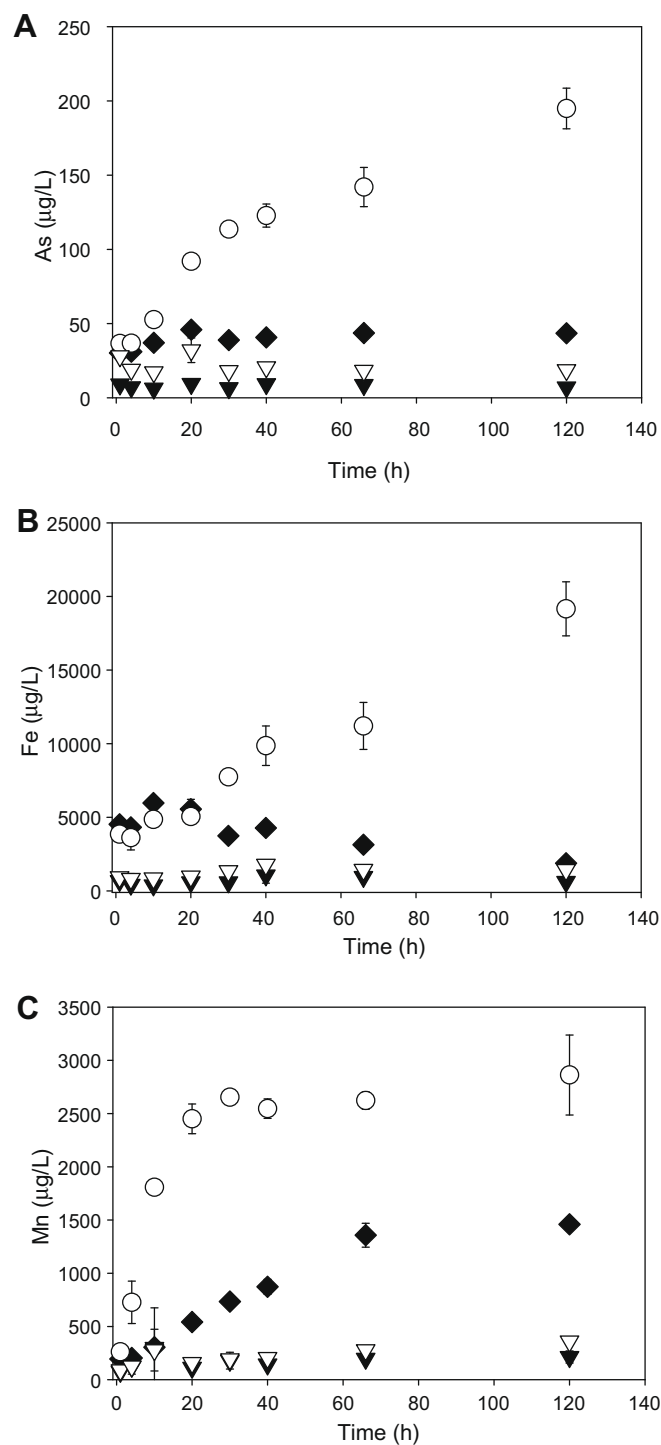


Fig. 9. Release of (A) As, (B) Fe and (C) Mn over time in simulated mobilization experiments. Conditions: 1 g wet sediment of SMW-3 mixture (21.5% water content) incubated with *Shewanella* sp. strain ANA-3 in 20 mL synthetic groundwater (Table 2). Symbols: (○) 10 mM lactate, (◆) no lactate, (▽) 2% formaldehyde, (◐) 10 mM lactate, (◑) 2% formaldehyde, no lactate. Error bars correspond to standard deviation of triplicate samples.

The stimulation of release of As, Fe and Mn by lactate in the presence of the model organism ANA-3 indicates that As, Fe and Mn are present in the sediments in forms that are susceptible to dissolution by microbial activity. It also suggests that exogenous organic C can strongly stimulate microbial activity. Although the activity of the native microbial community was not assessed in

these experiments, the freezing and thawing of the sediments is likely to have depressed this activity.

4.4. Evidence for natural attenuation of As and possible mechanisms for As sequestration

The initial (and largest) molasses injection at Devens was performed as a pilot test in December 2001 through June 2002; subsequent injections were performed on a monthly basis starting in October 2004. The estimated groundwater flow velocity based on tracer experiments is ~ 89 m/a. This is consistent with an estimated groundwater flow rate of 101 m/a calculated using the average Darcy velocity of 0.083 m/d determined from the passive flux meters (data not shown) and assuming a porosity of 0.3. The travel time from the injection area to well 11 \times (located just downgradient of the toe of the dissolved As plume in May 2006 (SMW-2) and 61 m from injection area) is approximately 0.6 a (assuming a groundwater flow velocity of 101 m/a). Since 4.5 a has elapsed between the initial molasses injection and the May 2006 groundwater sampling, some effect of the pilot molasses injection (e.g., a signature of a conservative species co-injected with the OC) could, in principle, be observed approximately 450 m downgradient of the injection wells by May 2006 (i.e., seven times farther downgradient than well 11 \times).

It is clear from the field observations, however, that the TOC signature of the molasses injection does not persist across the entire transect; rather the signal is strongly attenuated downgradient of well SMW-2. Concentrations of TOC, As and Fe are low (though above background levels) at wells 11 \times , SMW-3 and SMW-4 and essentially at background levels at the farthest downgradient well, 8 \times . Notably, Mn concentrations are observed to be elevated farther downgradient than those of either As or Fe. Loss of OC as a result of mineralization is expected in this setting and is likely to be the primary reason that OC is not detected at the end of the transect (though some retardation due to sorption cannot be excluded).

Field observations and laboratory mobilization experiments indicate that As, Fe and Mn are mobilized in response to the molasses injections and that mobilization is associated with reduction of these elements, presumably coupled to microbial oxidation of OC. As the groundwater moves downgradient, however, these species are apparently sequestered, presumably by processes of sorption and/or precipitation.

The contents of HCl-extractable Fe(II) in the sediments along the transect show an enrichment at well SMW-2 suggesting that Fe(II) is sequestered into the solid phase in this vicinity. XANES analyses indicate that As in the solid phase in sediments from both background and sequestration zones is present as As(V) (with the exception of one sample with detrital sulfides), even though As(V) and As(III) are nearly evenly distributed in the groundwater. This may be indicative of preferential sorption of As(V), precipitation of an As(V)-containing solid phase, or oxidation of As(III) to As(V) at the surface of aquifer minerals. The amount of As removal from groundwater required to lower the dissolved concentrations in the plume to background levels is less than the average As concentration present naturally in the sediments. Thus, As(III) sorbed from the contaminated groundwater may be below detection by XAS relative to native As(V). In addition, laboratory experiments with field sediments indicate some capacity for abiotic oxidation of sorbed As(III) to As(V) after sorption from solution, coupled to Mn reduction (Choi et al., 2009). This capacity is limited, however, and less than 30% of the As(III) sorbed in laboratory experiments was oxidized to As(V).

Sorption of both As(III) and As(V) with Devens sediments was examined in batch and column experiments (Choi et al., 2009). In batch studies, the extent of sorption at pH 6 was similar for As(III) and As(V). In column studies, somewhat greater retardation was

observed for As(V) than for As(III). Reversibility of sorption was observed in column studies; addition of Fe(II) to As(III)-containing column influent solutions increased As sorption but also desorption during wash-out resulting in minimal net effect on As sequestration.

If Fe(II) in the groundwater plume were to undergo oxidation to Fe(III), the precipitation of Fe(III)-containing solids, principally Fe(III) oxyhydroxides, would be expected to result in effective sequestration of As (España et al., 2005; Roberts et al., 2004). Iron(II) could also be oxidized by reaction with native Mn(III,IV) oxide minerals present in the sediments, which would compete with As(III) oxidation, but the oxidative capacity of the Devens sediments appears to be quite limited (Choi et al., 2009; He and Hering, 2009). Introduction of oxidants, however, could be an effective means to augment the natural attenuation of As.

5. Conclusions

The Ft. Devens case study shows that As is mobilized under ERD conditions designed to remediate contamination by chlorinated solvents. Under ambient conditions (i.e., at well MW-7 upgradient of the molasses injection area), As, Fe and Mn concentrations in groundwater are low. The As that occurs naturally in the aquifer sediments as As(V) is relatively immobile. Reducing conditions are generated by the introduction of OC (here molasses) leading to elevated concentrations of As, Fe and Mn in a mobilization zone (roughly corresponding to wells MW-1, MW-3, MW-5, 10 \times , SMW-1 and SMW-2). Consistent with these field observations, naturally-occurring As was also observed to be released from aquifer sediments in laboratory batch experiments inoculated with a known As(V)- and Fe(III)-reducing microbe and stimulated by addition of lactate.

The distance between SMW-2 (downgradient edge of mobilization zone) and 11 \times is approximately 9 m, and over the short distance, both Fe and As concentrations dropped about two orders of magnitude. The sudden decline of the concentrations of As, Fe and Mn indicates a transition to an apparent sequestration zone (roughly corresponding to wells 11 \times , SMW-3 and SMW-4). Low TOC concentrations observed within this zone can be attributed to mineralization of OC by microorganisms. Although the losses of As, Fe and Mn from the groundwater must presumably be accompanied by their uptake onto aquifer solids, no enrichment could be detected in the 3050B-extractable contents of these elements in the sediments, nor could sorbed As(III) be detected with bulk XAS. However, the content of HCl-extractable Fe(II) was enriched in sediments collected at SMW-2. The most likely mechanism for As, Fe, and Mn sequestration is sorption onto aquifer sediments. Although the most effective sequestration mechanism for As would involve oxidative precipitation of Fe(III) oxyhydroxides and concurrent As sorption or co-precipitation, this process could not be demonstrated on the basis of the field observations and/or sediment characterization.

Natural attenuation processes appear to be effective in limiting the migration of As at this site. However, continuing OC inputs would be expected to mobilize additional As, Fe and Mn in the subsurface and could eventually overwhelm the natural attenuation capacity of the system. This makes the loading of OC over the ERD remediation period a critical factor determining whether natural attenuation will be sufficiently protective or whether contingency measures will need to be implemented. The ERD operation at this site was conducted over 4.5 a. This time frame would have allowed approximately 50 pore volume flushes between SMW-2 (downgradient edge of the ERD treatment/mobilization zone) and 11 \times (upgradient edge of the sequestration zone) based on the seepage velocities measured by the PFMs. That background condi-

tions (with low concentrations of As, Fe and Mn) continue to prevail in the farthest downgradient well along the study transect is an indication of the robustness of natural attenuation at this site.

Acknowledgements

Funding for this work was provided by the Strategic Environmental Research and Development Program (SERDP, #ER1374). The authors would like to acknowledge Bob Simeone (BRAC Coordinator for Ft. Devens) for his assistance, D. Newman and D. Malasarn (Caltech) for providing the bacterial culture, and Nathan Dalleska (Caltech) for assistance with instrumental analysis. Part of this research was carried out at the Stanford Synchrotron Radiation Laboratory, a national user facility operated by Stanford University on behalf of the US Department of Energy, Office of Basic Energy Sciences.

References

- Albrechtsen, H.J., Heron, G., Christensen, T.H., 1995. Limiting factors for microbial Fe(III)-reduction in a landfill leachate polluted aquifer (Vejen, Denmark). *FEMS Microbiol. Ecol.* 16, 233–247.
- Amirbahman, A., Kent, D.B., Curtis, G.P., Davis, J.A., 2006. Kinetics of sorption and abiotic oxidation of arsenic(III) by aquifer materials. *Geochim. Cosmochim. Acta* 70, 533–547.
- Annable, M.D., Hatfield, K., Cho, J., Klammler, H., Parker, B.L., Cherry, J.A., Suresh, P., Rao, C., 2005. Field scale evaluation of the passive flux meter for simultaneous measurement of groundwater and contaminant fluxes. *Environ. Sci. Technol.* 39, 7194–7201.
- Bednar, A.J., Garbarino, J.R., Ranville, J.F., Wildeman, T.R., 2005. Effects of iron on arsenic speciation and redox chemistry in acid mine water. *J. Geochem. Explor.* 85, 55–62.
- Benner, S.G., Hansel, C.M., Wielinga, B.W., Barber, T.M., Fendorf, S., 2002. Reductive dissolution and biomineralization of iron hydroxide under dynamic flow conditions. *Environ. Sci. Technol.* 36, 1705–1711.
- Berg, M., Tran, H.C., Nguyen, T.C., Pham, H.V., 2001. Arsenic contamination of groundwater and drinking water in Vietnam: a human health threat. *Environ. Sci. Technol.* 35, 2621–2626.
- Bonneville, S., Van Cappellen, P., 2004. Microbial reduction of iron(III) oxyhydroxides: effects of mineral solubility and availability. *Chem. Geol.* 212, 255–268.
- Bostick, B.C., Fendorf, S., 2003. Arsenite sorption on troilite (FeS) and pyrite (FeS₂). *Geochim. Cosmochim. Acta* 67, 909–921.
- Campbell, K.M., Root, R., O'Day, P., Hering, J.G., 2008. A gel probe equilibrium sampler for measuring arsenic porewater profiles and sorption gradients in sediments: II. Field application to Haiwee Reservoir sediment. *Environ. Sci. Technol.* 42, 504–510.
- Choi, S., O'Day, P.A., Hering, J.G., 2009. Natural attenuation of arsenic by sediment sorption and oxidation. *Environ. Sci. Technol.* 43, 4253–4259.
- Clesceri, L.S., Greenberg, A.E., Eaton, A.D. (Eds.), 1999. American Public Health Association, American Water Works Association, Water Environment Federation, Washington DC, USA.
- Cooper, D.C., Neal, A.L., Kukkadapu, R.K., Brew, D., Coby, A., Picardal, F.W., 2005. Effects of sediment iron mineral composition on microbially mediated changes in divalent metal speciation: importance of ferrihydrite. *Geochim. Cosmochim. Acta* 69, 1739–1754.
- Cummings, D.E., Caccavo, F., Fendorf, S., Rosenzweig, R.F., 1999. Arsenic mobilization by the dissimilatory Fe(III)-reducing bacterium *Shewanella* alga BrY. *Environ. Sci. Technol.* 33, 723–729.
- Delemos, J.L., Bostick, B.C., Renshaw, C.E., St. Uerup, S., Feng, X., 2006. Landfill-stimulated iron reduction and arsenic release at the Coakley superfund site (NH). *Environ. Sci. Technol.* 40, 67–73.
- Dixit, S., Hering, J.G., 2006. Sorption of Fe(II) and As(III) on goethite in single- and dual-sorbate systems. *Chem. Geol.* 228, 6–15.
- Espana, J.S., Pamo, E.L., Pastor, E.S., Andres, J.R., Rubi, J.A.M., 2005. The natural attenuation of two acidic effluents in Tharsis and La Zarza-Perrunal mines (Iberian Pyrite Belt, Huelva, Spain). *Environ. Geol.* 49, 253–266.
- Foster, A.L., Brown Jr., G.E., Tingle, T.N., Parks, G.A., 1998. Quantitative arsenic speciation in mine tailings using X-ray absorption spectroscopy. *Am. Mineral.* 83, 553–568.
- Fukushi, K., Sasaki, M., Sato, T., Yanase, N., Amano, H., Ikeda, H., 2003. A natural attenuation of arsenic in drainage from an abandoned arsenic mine dump. *Appl. Geochem.* 18, 1267–1278.
- Ghosh, R., Deutsch, W., Geiger, S., McCarthy, K.B.D., 2003. Petroleum hydrocarbons and organic chemicals in groundwaters. American Petroleum Institute, National Ground Water Association, Costa Mesa, CA. pp. 266–280.
- Harvey, C.F., Swartz, C.H., Badruzzaman, A.B.M., Keon-Blute, N., Yu, W., 2002. Arsenic mobility and groundwater extraction in Bangladesh. *Science* 298, 1602–1606.
- Harvey, C.F., Ashfaq, K.N., Yu, W., Badruzzaman, A.B.M., Ashraf Ali, M., Oates, P.M., Michael, H.A., Neumann, R.B., Beckie, R., Islam, S., Ahmed, M.F., 2006. Groundwater dynamics and arsenic contamination in Bangladesh. *Chem. Geol.* 228, 112–136.
- Hatfield, K., Annable, M.D., Cho, J., Rao, P.S.C., Klammler, H., 2004. A direct passive method for measuring water and contaminant fluxes in porous media. *J. Contamin. Hydrol.* 75, 155–181.
- He, Y.T., Hering, J.G., 2009. Enhancement of arsenic(III) sequestration by manganese oxides in the presence of iron(II). *Water, Air, Soil Poll.* 203, 359–368.
- Horst, J., Mowder, C., Hansen, M., Matters, S., 2002. Final feasibility study, AOC 50, Devens Reserve Forces Training Area, Devens, MA, Arcadis G&M Inc., MA00664.0004.MD001.
- Huang, J.H., Matzner, E., 2006. Dynamics of organic and inorganic arsenic in the solution phase of an acidic fen in Germany. *Geochim. Cosmochim. Acta* 70, 2023–2033.
- Islam, F.S., Gault, A.G., Boothman, C., Polya, D.A., Charnock, J.M., Chatterjee, D., Lloyd, J.R., 2004. Role of metal reducing bacteria in arsenic release from Bengal delta sediments. *Nature* 430, 68–71.
- Johnson, J.A., Schreiber, M., 2003. Petroleum hydrocarbons and organic chemicals in groundwater. American Petroleum Institute, National Ground Water Association, Costa Mesa, CA. pp. 257–265.
- Keimowitz, A.R., Simpson, H.J., Stute, M., Datta, S., Chillrud, S.N., Ross, J., Tsang, M., 2005. Naturally occurring arsenic: mobilization at a landfill in maine and implications for remediation. *Appl. Geochem.* 20, 1985–2002.
- Keimowitz, A.R., Mailloux, B.J., Cole, P., Stute, M., Simpson, H.J., Chillrud, S.N., 2007. Laboratory investigations of enhanced sulfate reduction as a groundwater arsenic remediation strategy. *Environ. Sci. Technol.* 41, 6718–6724.
- Lee, M.K., Saunders, J.A., Wilkin, R.T., Shahnewaz, M., 2005. Geochemical modeling of arsenic speciation and mobilization: implications for bioremediation. In: O'Day, P., Vlassopoulos, D., Meng, X., Benning, L.G. (Eds.), *Advances in Arsenic Research: Integration of Experimental and Observational Studies and Implications for Mitigation*. Am. Chem. Soc. Symp. Ser. 915, 398–423.
- Lovley, D.R., Phillips, E.J.P., 1986a. Availability of ferric iron for microbial reduction in bottom sediments of the fresh-water tidal Potomac River. *Appl. Environ. Microbiol.* 52, 751–757.
- Lovley, D.R., Phillips, E.J.P., 1986b. Organic-matter mineralization with reduction of ferric iron in anaerobic sediments. *Appl. Environ. Microbiol.* 51, 683–689.
- Lovley, D.R., Phillips, E.J.P., Lonergan, D.J., 1989. Hydrogen and formate oxidation coupled to dissimilatory reduction of iron or manganese by *alteromonas-putrefaciens*. *Appl. Environ. Microbiol.* 55, 700–706.
- Malasarn, D., Keefe, J.R., Newman, D.K., 2008. Characterization of the arsenate respiratory reductase from *Shewanella* sp. strain ANA-3. *J. Bacteriol.* 190, 135–142.
- McArthur, J.M., Ravenscroft, P., Safiulla, S., Thirlwall, M.F., 2001. Arsenic in groundwater: testing pollution mechanisms for sedimentary aquifers in Bangladesh. *Water Resour. Res.* 37, 109–117.
- McArthur, J.M., Lowry, D., Houghton, S., Chadha, D.K., 2004. Natural organic matter in sedimentary basins and its relation to arsenic in anoxic groundwater: the example of west Bengal and worldwide implications. *Appl. Geochem.* 19, 1255–1293.
- Mclean, J.E., Dupont, R.R., Sorensen, D.L., 2006. Iron and arsenic release from aquifer solids in response to biostimulation. *J. Environ. Qual.* 35, 1193–1203.
- Nath, B., Berner, Z., Mallik, S.B., Chatterjee, D., Charlet, L., Stubben, D., 2005. Characterization of aquifers conducting groundwaters with low and high arsenic concentrations: a comparative case study from West Bengal, India. *Mineral. Mag.* 69, 841–854.
- Nicholas, D.R., Ramamoorthy, S., Palace, V., Spring, S., Moore, J.N., Rosenzweig, R.F., 2003. Biogeochemical transformations of arsenic in circumneutral freshwater sediments. *Biodegradation* 14, 123–137.
- Nickson, N.T., McArthur, J.M., Ravenscroft, P., Burgess, W.G., Ahmed, K.M., 2000. Mechanism of arsenic release to groundwater, Bangladesh and West Bengal. *Appl. Geochem.* 15, 403–413.
- Nordstrom, D.K., 2002. Worldwide occurrences of arsenic in ground water. *Science* 296, 2143–2145.
- O'Day, P.A., Vlassopoulos, D., Root, R., Rivera, N., 2004. The influence of sulfur and iron on dissolved arsenic concentrations in the shallow subsurface under changing redox conditions. *Proc. Nat. Acad. Sci.* 101, 13703–13708.
- Pinel-Raffaitin, P., Le Hecho, I., Amouroux, D., Potin-Gautier, M., 2007. Distribution and fate of inorganic and organic arsenic species in landfill leachates and biogases. *Environ. Sci. Technol.* 41, 4536–4541.
- Reisinger, H.J., Burris, D.R., Hering, J.G., 2005. Remediating subsurface arsenic contamination with monitored natural attenuation. *Environ. Sci. Technol.* 39, 458A–464A.
- Roberts, L.C., Hug, S.J., Ruettimann, T., Billah, M.M., Khan, A.W., Rahman, M.T., 2004. Arsenic removal with Iron(II) and Iron(III) in waters with high silicate and phosphate concentrations. *Environ. Sci. Technol.* 38, 307–315.
- Roden, E.E., 2006. Geochemical and microbiological controls on dissimilatory iron reduction. *Compt. Rend. Geosci.* 338, 456–467.
- Rowland, H.A.L., Polya, D.A., Lloyd, J.R., Pancost, R.D., 2006. Characterization of organic matter in a shallow, reducing, arsenic-rich aquifer, West Bengal. *Org. Geochem.* 37, 1101–1114.
- Rowland, H.A.L., Pederick, R.L., Polya, D.A., Pancost, R.D., Van Dongen, B.E., Gault, A.G., Vaughan, D.J., Bryant, C., Anderson, B., Lloyd, J.R., 2007. The control of organic matter on microbially mediated iron reduction and arsenic release in shallow alluvial aquifers, Cambodia. *Geobiology* 5, 281–292.

- Savage, K.E., Tingle, T.N., O'Day, P.A., Waychunas, G.A., Bird, D.K., 2000. Arsenic speciation in pyrite and secondary weathering phases, Mother Lode Gold District, Tuolumne County, California. *Appl. Geochem.* 15, 1219–1244.
- Savoie, J.G., Kent, D.B., Smith, R.L., LeBlanc, D.R., Hubble, D.W., 2004. Changes in groundwater quality near two granular iron permeable reactive barriers in a sand and gravel aquifer, Cape Cod, Massachusetts, 1997–2000, US Geol Surv. Water Resour. Invest. Rep. 03–4409.
- Scheutz, C., Durant, N.D., Dennis, P., Hansen, M.H., Jorgensen, T., Jakobsen, R., Cox, E.E., Bjerg, P.L., 2008. Concurrent ethene generation and growth of *dehalococcoides* containing vinyl chloride reductive dehalogenase genes during an enhanced reductive dechlorination field demonstration. *Environ. Sci. Technol.* 42, 9302–9309.
- Shimada, N., 1996. Geochemical conditions enhancing the solubilization of arsenic into groundwater in Japan. *Appl. Organometal. Chem.* 10, 667–674.
- Smedley, P.L., Kinniburgh, D.G., 2002. A review of the source, behavior, and distribution of arsenic in natural waters. *Appl. Geochem.* 17, 517–568.
- Smith, A.H., Lopipero, P.A., Bates, M.N., Steinmaus, C.M., 2002. Arsenic epidemiology and drinking water standards. *Science* 296, 2145–2146.
- Stollenwerk, K.G., Colman, J.A., 2003. Natural remediation potential of arsenic contaminated groundwater. In: Welch, A.H., Stollenwerk, K.G. (Eds.), *Arsenic in Ground Water: Geochemistry and Occurrence*. Kluwer Academic Publishers, Boston, MA, pp. 351–379.
- Suthersan, S., Horst, J., 2008. Aquifer minerals and in situ remediation: the importance of geochemistry. *Ground Water Monitor. Remed.* 28, 153–160.
- Swartz, C.H., Blute, N.K., Badruzzman, B., Ali, A., Brabander, D., Jay, J.B.J., Islam, S., Hemond, H.F., Harvey, C.F., 2004. Mobility of arsenic in a Bangladesh aquifer: inferences from geochemical profiles, leaching data, and mineralogical characterization. *Geochim. Cosmochim. Acta* 68, 4539–4557.
- Tufano, J.J., Reyes, C., Saltikov, C.W., Fendorf, S., 2008. Reductive processes controlling arsenic retention: revealing the relative importance of iron and arsenic reduction. *Environ. Sci. Technol.* 42, 8263–8289.
- USEPA, 1996. Methods 3050B: Acid digestion of sediment, sludges, and soils, pp. 1–12.
- USEPA, 1999. USEPA Methods and guidance for analysis of water, EPA 821-C-99-004, Washington D.C., USA.
- USEPA, 2004. Final record of decision, AOC 50, Devens, Massachusetts. <<http://www.epa.gov/region01/superfund/sites/devens/201577.pdf>>.
- USEPA, 2005. Five year review report: former Fort Devens. <<http://www.epa.gov/region1/superfund/sites/devens/237422.pdf>>.
- Welch, A.H., Lico, M.S., 1988a. Aqueous geochemistry of groundwater with high concentrations of arsenic and uranium. *Carson River Basin, Nevada Chem. Geol.* 70, 19.
- Welch, A.H., Lico, M.S., 1988b. Arsenic in groundwater of the western United States. *Ground Water* 26, 333–347.
- Welch, A.H., Westjohn, D.B., Helsel, D.R., Wanty, R.B., 2000. Arsenic in groundwater of United States: occurrence and geochemistry. *Ground Water* 38, 589–604.
- Wenzel, W.W., Kirchbaumer, N., Prohaska, T., Stinger, G., Lombi, E., Adriano, D.C., 2001. Arsenic fractionation in soils using an improved sequential extraction procedure. *Anal. Chim. Acta* 436, 309–323.
- Wilkie, J.A., Hering, J.G., 1996. Adsorption of arsenic onto hydrous ferric oxide: effects of adsorbate/adsorbent ratios and co-occurring solutes. *Colloid Surf. A* 107, 97–110.
- Wythes, J.R., Wainwright, D.H., Blight, G.W., 1978. Nutrient composition of Queensland molasses. *Austr. J. Experim. Agric. Animal Husbandry* 18, 629–634.
- Zobrist, J., Dowdle, P.R., Davis, J.A., Oremland, R.S., 2000. Mobilization of arsenite by dissimilatory reduction of adsorbed arsenate. *Environ. Sci. Technol.* 34, 4747–4752.

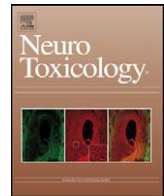
APPENDIX D

**Mechanisms of rotenone-induced
proteasome inhibition**



Contents lists available at ScienceDirect

NeuroToxicology



Mechanisms of rotenone-induced proteasome inhibition

Arthur P. Chou^a, Sharon Li^a, Arthur G. Fitzmaurice^a, Jeff M. Bronstein^{a,b,*}^a Department of Neurology, University of California at Los Angeles David Geffen School of Medicine, United States^b The Greater Los Angeles Veterans Administration Medical Center, Los Angeles, CA, United States

ARTICLE INFO

Article history:

Received 20 February 2010

Accepted 15 April 2010

Available online 22 April 2010

Keywords:

Parkinson's disease

Mitochondria

Nitric oxide

Microtubules

ABSTRACT

The etiology of Parkinson's disease is unclear but appears to involve mitochondrial dysfunction, proteasome inhibition, and environmental toxins. It has been shown that pesticides, including the complex I inhibitor rotenone, cause proteasome inhibition but the mechanism of rotenone-induced proteasome dysfunction remains largely unknown. In this study, we examined the role of mitochondrial inhibition, oxidative stress, and microtubule dysfunction as potential mediators of rotenone-induced proteasome inhibition. Proteasome activity (26S) was measured in HEK and SK-N-MC cells expressing an EGFP-U degron fusion protein that is selectively degraded by the proteasome. We found that complexes I and III inhibition led to the production of peroxides and decreased proteasome activity. We also found that rotenone increased nitric oxide production and nitric oxide and peroxynitrites led to proteasome inhibition. The effects of rotenone were attenuated by anti-oxidants and nitric oxide synthase inhibition. Since rotenone can also inhibit microtubule assembly, we tested a specific MT inhibitor and found it led to proteasome dysfunction. Rotenone also led to a decrease in 20S proteasome activity and 20S proteasome subunit immunoreactivity without a change in subunit mRNA. Together, these data suggest that rotenone-induced decreases in proteasome activity are due to increased degradation of proteasome components secondary to oxidative damage and possibly microtubule dysfunction.

Published by Elsevier Inc.

1. Introduction

The etiology of Parkinson's disease (PD) remains unclear although it may involve mitochondria dysfunction and environmental toxins such as pesticides (Beal, 2003; Brown et al., 2006). The pesticide rotenone has been extensively studied because it is a mitochondria complex I inhibitor. Chronic rotenone infusion in rats results in nigrostriatal dopaminergic degeneration, signs of oxidative stress in the brain, and motor dysfunction (Betarbet et al., 2000; Fleming et al., 2004; Sherer et al., 2003). These animals also developed alpha-synuclein positive intraneuronal inclusions that resembled Lewy Bodies, the pathological hallmark of PD (Betarbet et al., 2000).

The reason for the relatively selective toxicity to nigral neurons following systemic administration of rotenone is not clear. Complex I impairment can lead to compromised cell respiration, loss of mitochondrial membrane potential, and generation of free radicals such as superoxide anion ($O_2^{\cdot-}$) and hydrogen peroxide (H_2O_2) (Barrientos and Moraes, 1999; Kudin et al., 2008). At low

rotenone concentrations (5 nM), ATP production is not significantly altered (Betarbet et al., 2006). It is possible that rotenone generates oxidative stress, which is compounded by the increased production of reactive oxygen species (ROS) from dopamine metabolism making dopaminergic neurons particularly vulnerable. The exact pathophysiology of how oxidative stress leads to cell death is controversial. One potential downstream effector is the cellular ubiquitin proteasome system (UPS).

The UPS is responsible for degrading damaged proteins and has been implicated in the etiology of PD (Kitada et al., 1998; Leroy et al., 1998; McNaught et al., 2002). Studies by our group and others have demonstrated that treatment of cells with rotenone leads to proteasomal dysfunction (Betarbet et al., 2006; Shamoto-Nagai et al., 2003; Wang et al., 2006). However, although several mechanisms have been proposed, including decreased ATP levels, acrolein-modification of proteasome subunits, and induction of oxidative stress (Hoglinger et al., 2003; Shamoto-Nagai et al., 2003), the exact mechanism by which rotenone causes inhibition of the proteasome remains unclear.

Since rotenone, a complex I inhibitor, can cause many of the pathological features of PD in rats and complex I dysfunction has been associated with PD in humans, it is important to determine the mechanisms by which rotenone acts. One known effect of rotenone-induced toxicity is reduced UPS activity. The aim of this study was to evaluate the mechanisms by which rotenone inhibits

* Corresponding author at: Department of Neurology, UCLA David Geffen School of Medicine, Reed Neurological Research Center, 710 Westwood Plaza, A-153, Los Angeles, CA 90095, United States. Tel.: +1 310 206 9799; fax: +1 310 206 9819.

E-mail address: jbronste@ucla.edu (J.M. Bronstein).

the proteasome. A better understanding of these mechanisms could provide important insights into the pathological processes underlying PD. We found that rotenone likely acts through multiple mechanisms including oxidative stress, nitric oxide (NO) production and possibly microtubule dysfunction. These processes, and possibly others, led to increased degradation of UPS 20S subunits.

2. Methods

2.1. Chemicals

All compounds were purchased from Sigma–Aldrich (St. Louis, MO), ChemService (West Chester, PA), EMD Chemicals (Gibbstown, NJ), or Dojindo Molecular Technologies (Kumamoto, Japan).

2.2. Proteasome activity measurement

UPS activity was measured as previously described (Wang et al., 2006). Briefly, human embryonic kidney (HEK) and neuroblastoma SK-N-MC cells were grown in DMEM/F12 supplemented with 10% FBS and 1% Pen/Strep and passaged every 2–3 days. HEK and SK-N-MC cells transfected with the EGFP-degron fusion protein (GFP-U) were grown in the same media supplemented with 400 µg/mL of geneticin for selection. UPS activity was measured in HEK and SK-N-MC cells by quantitating the level of EGFP-degron fusion protein that is selectively degraded by the proteasome, using flow cytometry (Bence et al., 2001). We chose to use these cell lines since SK-N-MC cells are neuronal-like and HEK cells are non-neuronal. In some experiments, cells were also stained with 10 µg/mL of propidium iodide for 30 min at room temperature to detect dead cells. After PI staining, cells were trypsinized and triturated before analysis using a Beckman XL-MCL flow cytometer. Cells were gated for GFP-U measurement by forward and side scatter, and fluorescence was expressed relative to vehicle control. In experiments examining the effects of anti-oxidants on the toxicity of rotenone, fluorescence was expressed as a percent of the increase in fluorescence caused by rotenone (anti-oxidant GFP-U – control GFP-U)/(rotenone GFP-U – control GFP-U).

Proteasome chymotryptic activity (20S) was also measured in cell homogenates by the conversion of N-Suc-LLVY-AMC (100 µM, Sigma) into the fluorescent compound AMC by active protease cleavage. Epoxomicin (5 µM, Sigma) or lactacystin (5 µM) was used to estimate total proteasome activity and fluorescence was measured using a Wallac multi-plate reader.

2.3. Oxidative stress measurement

Oxidative stress was measured by quantitating the oxidation of carboxy-DCF (Invitrogen) in untransfected HEK cells. Cells were loaded with 10 µM of carboxy-DCF for 1 h. The media containing the fluorescent probe was then removed and new media containing the treatment compound was added and incubated for 2 h before being analyzed by flow cytometry as previously described (Wang et al., 2006). Nitric oxide was quantitated using the NO-specific dye DAF-FM acetate (20 µM, Invitrogen) and assayed in a similar manner as carboxy-DCF.

2.4. Western blot analysis

Cells were harvested and lysed in PBS containing 0.1% (vol/vol) Triton, 5 mM EDTA and protease inhibitor cocktail (Complete-mini; Roche Applied Science, Indianapolis, IN, USA). Cells were then sonicated for 3–5 s while kept cold on ice, followed by centrifugation for 20 min at 10,000 rpm at 4 °C. Protein concentration was determined by Bradford dye binding assay (Bio-rad, Hercules, CA). Equal volume of 2× SDS loading buffer (125 mM Tris, pH 6.8, 5% (wt/vol) SDS, 2.5 mg/mL Bromophenol Blue, 25% (vol/vol) glycerol) was added to samples and boiled for 5 min prior to loading. Proteins were separated by SDS-polyacrylamide gel using a 6% stacking phase and 12% separating phase. Proteins were then transferred to a Protran nylon membrane (Schleicher and Schuell, Dassel, Germany) using a wet transfer method. Membranes were blocked in PBS with 0.1% (vol/vol) Tween 20 (Sigma, St. Louis, MO, USA) and 5% non-fat dry milk for at least 1 h. Membranes were washed and then probed with a mouse antibody to proteasome α-subunit 1, 2, 3, 5, 6 and 7 (Affiniti, UK) overnight at 4 °C. Membranes were washed and then probed with anti-mouse secondary antibody (Amersham Biosciences, UK) for 1 h at room temperature. Membranes were washed a final time before detection by ECL plus (Amersham Biosciences, UK). Each wash consisted of 5–10-min washes in PBS plus 0.1% (vol/vol) Tween 20.

2.5. Quantitative real-time RT-PCR (qRT-PCR)

To measure proteasome mRNA levels, SK-N-MC cells were treated with 0, 10, or 100 nM of rotenone in fresh media for 48 h. Total RNA was isolated using RNAwiz (Ambion) according to the manufacturer's instructions and was reverse-transcribed to cDNA with SuperScript First Strand Synthesis System for RT-PCR (Invitrogen) using oligo-dT primers. Relative cDNA levels were quantitated by real-time PCR using SYBR-Green (SYBR-green master mix, Applied Biosystems) as reporter dye on an ABI PRISM 7700 at the UCLA Sequencing and Genotyping Core. Proteasome cDNA levels were standardized to the levels of GAPDH and quantitated by the relative Ct method ($2^{-\Delta\Delta C_t}$). Vehicle treated cells were used as the calibrator. Primers were designed with Primer3 software (Table 1).

2.6. Statistical analysis

Statistical analysis was performed with GraphPad Prism software. Unless otherwise specified, values are expressed as mean ± SEM. The level of significance is shown as * $p < 0.05$ or ** $p < 0.01$. Statistical significance was determined using one-way ANOVA with Dunnett's or Bonferroni's multiple comparison post-test.

3. Results

3.1. Proteasome inhibition by mitochondria inhibitors

HEK and SK-N-MC cells expressing GFP-U were exposed to various concentrations of rotenone to determine its dose–response relationship with UPS inhibition (Fig. 1A). Rotenone significantly lowered UPS activity at doses as low as 10 nM and lowered it

Table 1
Oligonucleotide PCR primers used to measure proteasome subunit mRNA.

Gene	Sense 5'–3'	Anti-sense 5'–3'
PSMA1.C2.BC022372	CCATGTTTCGAAATCAGTATGAC	TTCAATGCAACAAAACCTGC
PSMB1.C5.BC000508	CAATTCATACGGCGGATAGC	CATCAAGTCCACCGATGATG
PAMB7.Z.BC000509	TCTGCGTCATCAGCAAGAAC	GCCATTCAGGAAGTGTCAT
GAPDH.BC013852	ACCACAGTCCATGCCATCAC	ACAGCAACAGGGTGGTGGGA

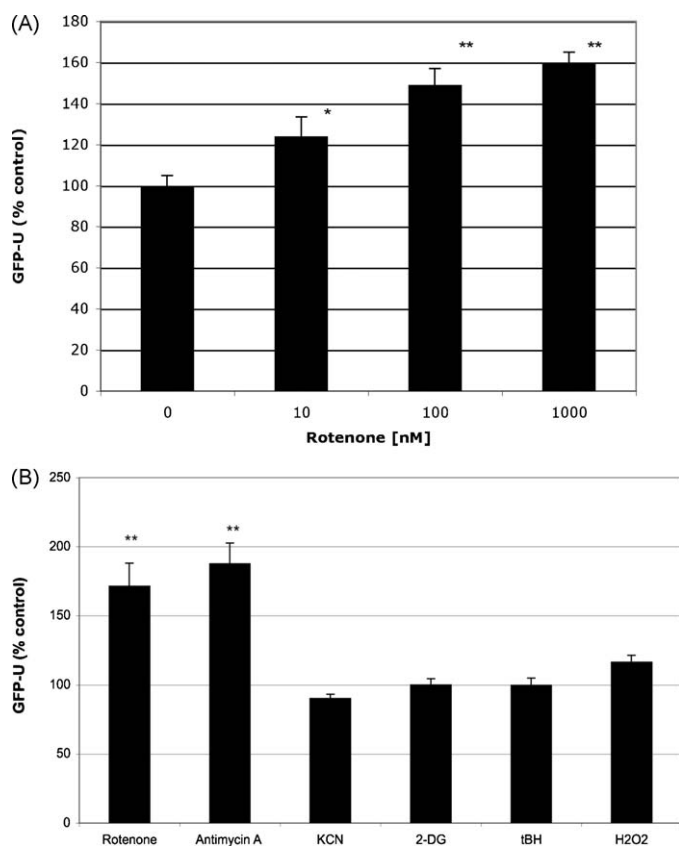


Fig. 1. Inhibition of mitochondrial respiration, oxidative stress and 26S UPS activity. HEK cells were exposed to rotenone (complex I), antimycin A (2 μ g/mL, complex III), KCN (2 mM, complex IV), 2-DG (10 mM, ATP depletion), and the oxidants tBH and H₂O₂ (100 μ M) for 24 h and GFP-U fluorescence (26S UPS activity) was measured. Increased GFP-U indicates decreased UPS activity. In (B) 100 nM rotenone was used. $N = 8$ per data point. Statistics by one-way ANOVA with Dunnett's multiple comparison post-test (* $p < 0.05$, ** $p < 0.01$).

further at higher concentrations. Similar results were obtained using other pesticides that inhibit complex I including pyridaben and fenazaquin (data not shown).

Oxidative stress generated by complex I inhibition has been postulated to be the main determinant of the ability of rotenone to lower UPS activity. In order to further dissect the mechanisms of rotenone, we tested other inhibitors of the mitochondrial electron transport chain (ETC). Complex III inhibition (antimycin A, 2 μ g/mL) resulted in a 232% increase in GFP-U (Fig. 1B). Rotenone at 100 nM and antimycin A at 2 μ g/mL would be expected to inhibit 100% their respective mitochondrial respiratory complexes. On the other hand, complete inhibition of complex IV by 2 mM potassium cyanide (KCN), or ATP depletion by 10 mM 2-deoxyglucose (2-DG), did not result in proteasome inhibition (Fig. 1B). Interestingly, complex IV inhibitors and 2-DG have been shown not to increase ROS in contrast to complex I and III inhibitors (McLennan and Degli Esposti, 2000). These data support the hypothesis that rotenone induces oxidative stress which leads to UPS inhibition. We further tested the contribution of ROS to proteasome inhibition by exposing cells directly to oxidants that do not directly alter mitochondrial function and to anti-oxidants. Cells were exposed to H₂O₂, oxidant *tert*-butyl hydroperoxide (tBH), and iron chloride (FeCl₂, not shown) for 24 h but all failed to inhibit UPS activity (Fig. 1B). Some but not all anti-oxidants attenuated rotenone-induced (100 nM) UPS inhibition (Fig. 2A) but this did not correlate with their ability to reduce ROS (measured by DCF fluorescence, Fig. 2B) adding further doubt that oxidative stress is the primary mechanism for rotenone's UPS inhibitory activity.

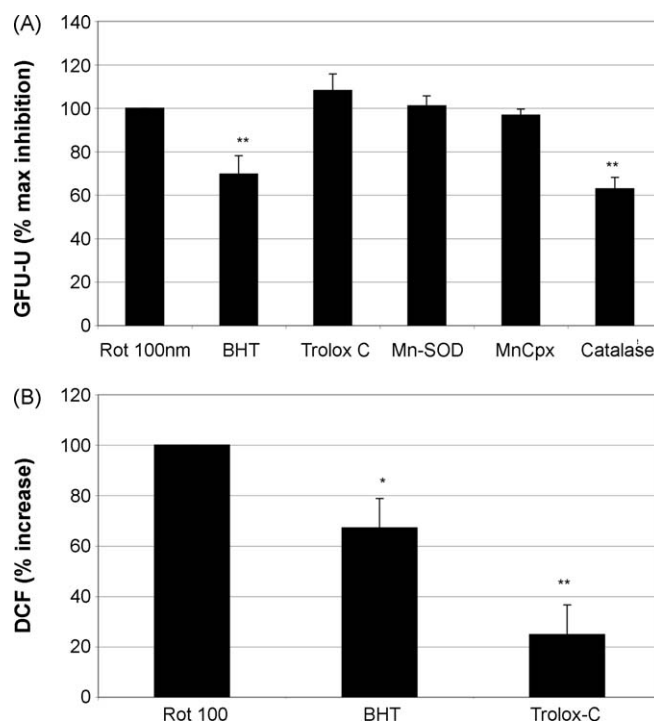


Fig. 2. (A) Beta-hydroxy toulene (BHT) and catalase, but not other anti-oxidants, attenuated rotenone's UPS inhibitory effects. HEK cells were treated with 100 nM rotenone in combination with the various anti-oxidants for 24 h before being analyzed by flow cytometry. GFP-U is expressed as a percent of the increase in GFP-U caused by rotenone alone. A value of 100% would indicate no effect on rotenone, and 0% would indicate a complete reversal of rotenone's effects ($N = 5-9$). (B) BHT and Trolox-C attenuated the formation of peroxides caused by 100 nM rotenone as measured by DCF fluorescence ($N = 4-11$ per data point). Note that although both reduced ROS produced by rotenone, only BHT attenuated UPS inhibition.

3.2. Reactive nitrogen species (RNS) and proteasome activity

Given that ROS did not appear to account for the ability of rotenone to inhibit the proteasome, we examined the possibility that rotenone induces the generation of RNS and these lead to UPS inhibition. We first tested the effect of the NO donor SNAP and the peroxynitrite donor SIN-1 on UPS activity and found that both lead to 26S proteasome inhibition (Fig. 3A). Furthermore, the NO synthase inhibitor L-NMMA attenuated the ability of rotenone to inhibit UPS activity by 20% (Fig. 3A). We confirmed that rotenone induces NO formation by measuring DAF fluorescence and found that rotenone (100 nM) induced an increase in RNS in a similar manner as the NO donor SNAP (Fig. 3B). Proteasome inhibition by SNAP was very potent, causing a 334% increase in GFP-U fluorescence at 1 mM. We also found that RNS can directly affect protease activity by using a 20S proteasome assay. NO and peroxynitrite donors added directly to cell homogenates led to a decrease in 20S activity (Fig. 3C). Taken together, these observations suggest that NO and peroxynitrite can contribute to rotenone-induced UPS inhibition possibly by nitration of proteasome subunits.

3.3. Microtubule dysfunction and proteasome activity

In addition to the direct effects of rotenone on mitochondrial respiration, it has also been shown to interfere with microtubule assembly at concentrations as low as 20 nM (Ren et al., 2005). We hypothesized that rotenone may inhibit UPS activity via its ability to alter microtubule assembly. To test this, we exposed GFP-U expressing SK-N-MC cells to the specific microtubule assembly

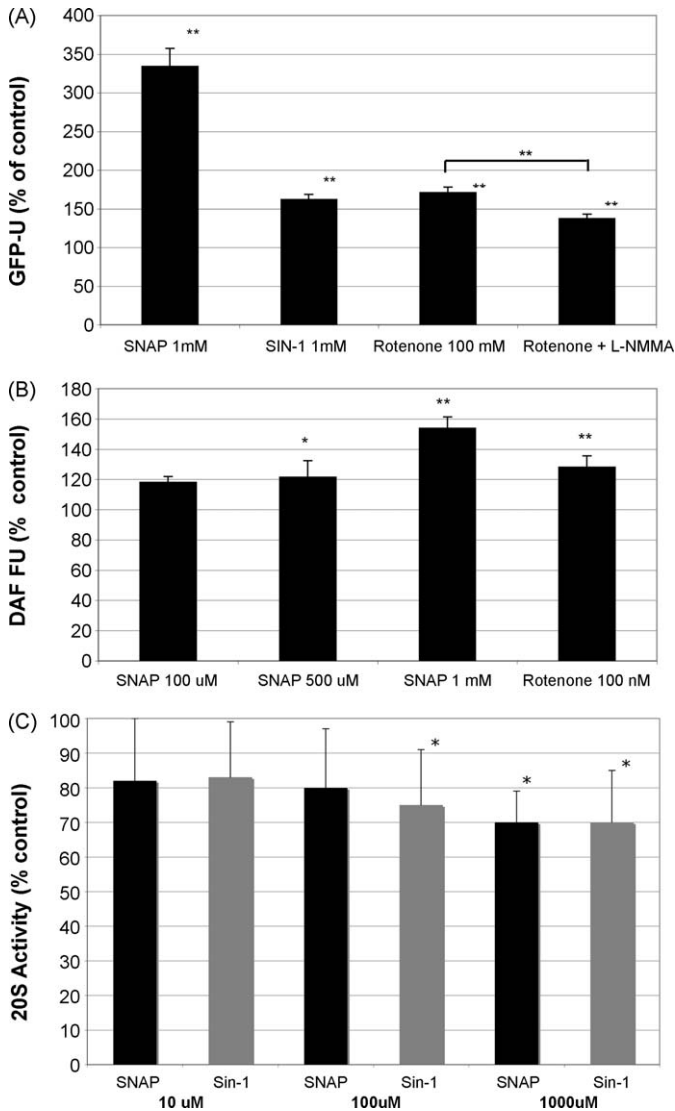


Fig. 3. (A) NO donor SNAP and peroxynitrite donor SIN-1 cause 26S proteasome inhibition in SK-N-MC cells. Inhibiting NO synthase with L-NMMA attenuated rotenone's ability to inhibit the UPS ($N = 6$). (B) Rotenone-induced NO formation as measured by DAF staining ($N = 6$). (C) The NO donor SNAP and peroxynitrite donor SIN-1 inhibited 20S proteasome activity in cell homogenates ($N = 8$).

inhibitor nocodazole for 48 h and found that it caused proteasome inhibition at 10 μ M, the concentration needed to cause complete depolymerization of tubulin (Liao et al., 1995) (Fig. 4). We have also found a similar effect of carbendazem (another microtubule inhibitor) on proteasome activity providing evidence that altering microtubules may be a mechanism by which rotenone alters proteasome function.

3.4. Rotenone lowers proteasome subunit levels

Our data suggest that ROS, RNS and MT dysfunction contribute to the UPS inhibition induced by rotenone but the mechanism through which these processes lower protease activity is unclear. One possibility is that the proteasome components are damaged by oxidation and/or nitration leading to their degradation. To test this possibility, we measured 20S proteasome activity and immunoreactivity in rotenone-treated lysates. We found that rotenone caused a reduction in the 20S proteasome activity and a dose-dependent decrease in proteasome α -subunit immunoreactivity (Fig. 5A and B). To assess whether the observed decrease in

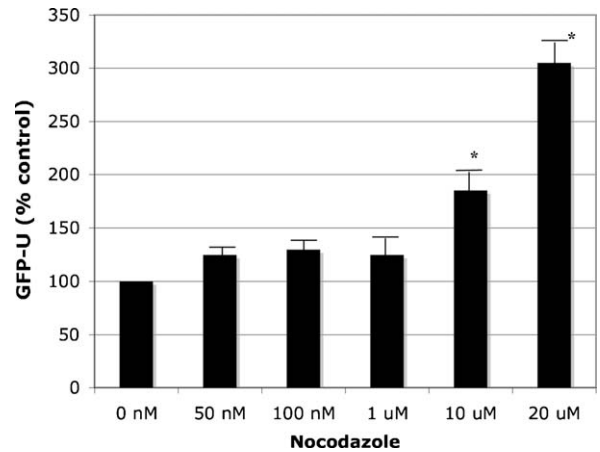


Fig. 4. Inhibition of microtubule assembly by nocodazole resulted in 26S UPS activity as measured by GFP-U fluorescence ($N = 4$, $*p < 0.05$).

proteasome levels were due to decreased synthesis, we performed qRT-PCR to measure proteasome mRNA levels. RT-PCR of α - and β -subunits all showed the same level of expression regardless of rotenone treatment (data not shown). These data suggest that rotenone increases proteasome subunit degradation but does not alter synthesis.

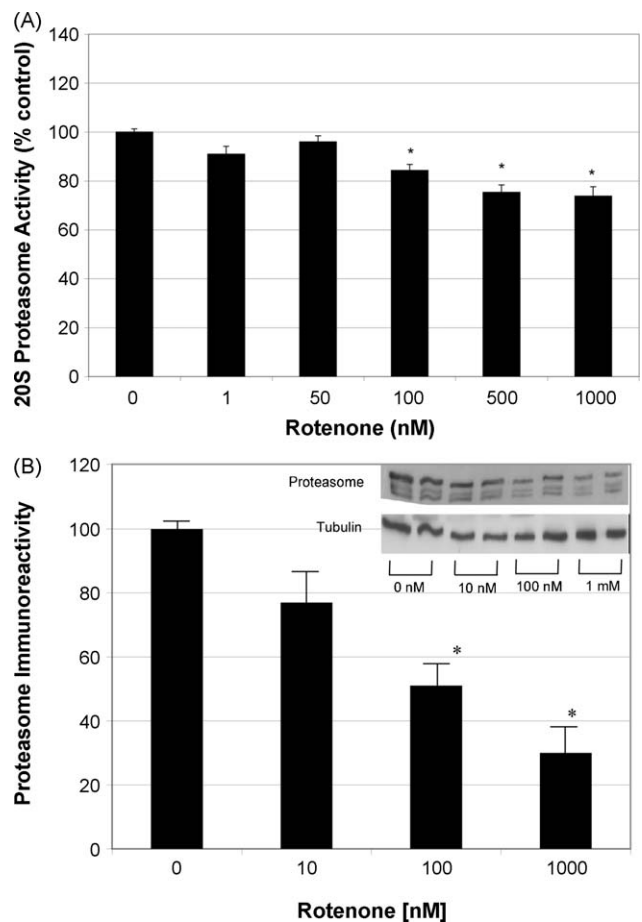


Fig. 5. Rotenone decreased the 20S proteasome activity and immunoreactivity. SK-N-MC cells were treated with rotenone for 48 h and the cell homogenate collected and assayed for the 20S proteasome activity (A, $N = 9-11$) and immunoreactivity (B, $N = 4$). Both 20S proteasome activity and immunoreactivity measured by Western blot (α -subunits) were significantly lower at 100 nM or more rotenone.

4. Discussion

In this study, we examined the mechanisms by which rotenone inhibits proteasome activity and found that it likely involves multiple processes that appear to include mitochondrial inhibition, oxidative stress, RNS, microtubule assembly, and increased degradation of proteasome subunits. We propose that the unique toxicity of rotenone is due to a combination of these pathways, most of which have been implicated in the pathogenesis of PD.

Oxidative stress in part appears to contribute to the actions of rotenone. Compounds that inhibited mitochondrial respiration and also induced the generation of ROS (complex I and III inhibitors) led to proteasome inhibition. Blocking mitochondrial complex IV did not cause the generation of ROS nor did it inhibit the proteasome (Liu et al., 2002; Turrens and Boveris, 1980). Furthermore, the involvement of ROS in the actions of rotenone is supported by the fact that some anti-oxidants attenuated rotenone-induced proteasome inhibition. This is consistent with a previous report that demonstrated that α -tocopherol attenuated rotenone-induced (5 nM rotenone) proteasome inhibition (Betarbet et al., 2006). In our study, some anti-oxidants could only protect rotenone-induced inhibition (100 nM) by approximately a third suggesting that other mechanisms are at play at this concentration. Furthermore, we did not find a good correlation with the ability of anti-oxidants to lower ROS and protect against rotenone-induced UPS inhibition (Fig. 2). In contrast to the study of Berarbet et al., we did not see any protective qualities of α -tocopherol but these differences may be due to the differences in the concentration of and the length of exposure to rotenone.

Induction of RNS is also likely to contribute to the toxicity of rotenone. RNS inhibited the proteasome both in cells and directly in cellular homogenates using NO and perinitrate donors. Based on DAF staining, rotenone stimulated NO production and the NOS inhibitor L-NMMA attenuated the effects of rotenone on proteasome activity. Although DAF staining may not be specific for NO, taken together with experiments using an NO and perinitrate donor and a NOS inhibitor, it is possible that RNS induced by rotenone play at least a partial role in inhibiting proteasome activity. Osna et al. reported that nitrate stress in the form of NO or peroxynitrite can inhibit the proteasome *in vitro* (Osna et al., 2004) but nitrated proteasome subunits following rotenone treatment could not be detected (Shamoto-Nagai et al., 2003) although others have found that oxidation or nitration of UPS subunits can alter protease activity (Szweda et al., 2002) for review.

A potential third mechanism for the ability of rotenone to cause proteasome inhibition is via the disruption of microtubules as demonstrated by the ability of nocodazole to also inhibit the UPS. We have also found that carbendazim, another MT inhibitor, also leads to UPS dysfunction (data not shown). Nocodazole significantly inhibited the UPS at concentrations that causes almost complete MT depolymerization. The ability of rotenone to inhibit microtubule assembly is well established even at 10 nM (Ren et al., 2005), but it is likely that rotenone concentrations need to be closer to 0.2–1 μ M to cause MT depolymerization similar to that of 10 μ M nocodazole, Srivastava and Panda, 2007, #1516). Interestingly, MT dysfunction has been shown to induce selective dopaminergic cell death in primary cultures (Ren et al., 2005). The association of MT and the UPS has not been well studied but it has been shown that Parkin, an E3 ligase linked to PD, binds to tubulin and alters its degradation (Ren et al., 2003). It is possible that UPS components are associated with MT and disassembly of MTs leads to impaired proteasome activity but more work is needed to establish causality between the ability of rotenone to alter MT assembly and decrease UPS activity.

We found that ROS, RNS and MT assembly are involved in rotenone's proteasome inhibitory activity but the molecular events that lead to reduced protease activity remains unclear. We do know that the decrease in UPS activity is not simply reflecting a decrease in cell viability since some toxins kill cells but do not lead to decreased UPS activity (Wang et al., 2006). Importantly, we did find that proteasome subunit immunoreactivity was decreased following rotenone treatment. Changes in proteasome immunoreactive protein were not caused by decreased transcription of the subunits and therefore it is likely that the decreased protein level was caused by increased degradation of proteasome subunits. Considering the likely involvement of ROS and RNS in rotenone's actions, it is possible that rotenone causes increased degradation of proteasome subunits by oxidation or nitration of the proteasome. This observation is in contrast to that by Shamoto-Nagai and coworkers who found no changes in the amount of proteasome protein (Shamoto-Nagai et al., 2003) and instead suggests that acrolein-modification of the proteasome subunits is the cause for lowered proteasome activity. Additional studies need to be performed to directly test the effects of UPS subunit oxidation and nitration on its degradation.

In summary, we have found several pathological processes that can account for rotenone's effects on the UPS. Synergistic action of these processes is an attractive hypothesis for the toxicity of rotenone and the pathogenesis of PD.

Conflict of interest

None declared.

Acknowledgments

This study was supported by grants from the NIEHS (5 U54 ESO12078 and 1P01ES016732-01) and the Veterans Administration SW PADDRREC. We would also like to thank Drs. Erik Schweitzer and Xue-Feng Wang, for their technical assistance.

References

- Barrientos A, Moraes CT. Titrating the effects of mitochondrial complex I impairment in the cell physiology. *J Biol Chem* 1999;274:16188–97.
- Beal MF. Mitochondria, oxidative damage, and inflammation in Parkinson's disease. *Ann N Y Acad Sci* 2003;991:120–31.
- Bence NF, Sampat RM, Kopito RR. Impairment of the ubiquitin–proteasome system by protein aggregation. *Science* 2001;292:1552–5.
- Betarbet R, Canet-Aviles RM, Sherer TB, Mastrobardino PG, McLendon C, Kim JH, et al. Intersecting pathways to neurodegeneration in Parkinson's disease: effects of the pesticide rotenone on DJ-1, alpha-synuclein, and the ubiquitin–proteasome system. *Neurobiol Dis* 2006;22:404–20.
- Betarbet R, Sherer TB, MacKenzie G, Garcia-Osuna M, Panov AV, Greenamyre JT. Chronic systemic pesticide exposure reproduces features of Parkinson's disease. *Nat Neurosci* 2000;3:1301–6.
- Brown TP, Rumsby PC, Capleton AC, Rushton L, Levy LS. Pesticides and Parkinson's disease—is there a link? *Environ Health Perspect* 2006;114:156–64.
- Fleming SM, Salcedo J, Fernagut PO, Rockenstein E, Masliah E, Levine MS, et al. Early and progressive sensorimotor anomalies in mice overexpressing wild-type human alpha-synuclein. *J Neurosci* 2004;24:9434–40.
- Hoglinger GU, Carrard G, Michel PP, Medja F, Lombes A, Ruberg M, et al. Dysfunction of mitochondrial complex I and the proteasome: interactions between two biochemical deficits in a cellular model of Parkinson's disease. *J Neurochem* 2003;86:1297–307.
- Kitada T, Asakawa S, Hattori N, Matsumine H, Yamamura Y, Minoshima S, et al. Mutations in the parkin gene cause autosomal recessive juvenile parkinsonism. *Nature* 1998;392:605–8.
- Kudin AP, Malinska D, Kunz WS. Sites of generation of reactive oxygen species in homogenates of brain tissue determined with the use of respiratory substrates and inhibitors. *Biochim Biophys Acta* 2008;1777:689–95.
- Leroy E, Boyer R, Auburger G, Leube B, Ulm G, Mezey E, et al. The ubiquitin pathway in Parkinson's disease. *Nature* 1998;395:451–2.
- Liao G, Nagasaki T, Gundersen GG. Low concentrations of nocodazole interfere with fibroblast locomotion without significantly affecting microtubule level: implications for the role of dynamic microtubules in cell locomotion. *J Cell Sci* 1995;108(Pt 11):3473–83.

- Liu Y, Fiskum G, Schubert D. Generation of reactive oxygen species by the mitochondrial electron transport chain. *J Neurochem* 2002;80:780–7.
- McLennan HR, Degli Esposti M. The contribution of mitochondrial respiratory complexes to the production of reactive oxygen species. *J Bioenerg Biomembr* 2000;32:153–62.
- McNaught KS, Mytilineou C, Jnobaptiste R, Yabut J, Shashidharan P, Jennert P, et al. Impairment of the ubiquitin–proteasome system causes dopaminergic cell death and inclusion body formation in ventral mesencephalic cultures. *J Neurochem* 2002;81:301–6.
- Osna NA, Haorah J, Krutik VM, Donohue TM Jr. Peroxynitrite alters the catalytic activity of rodent liver proteasome in vitro and in vivo. *Hepatology* 2004;40:574–82.
- Ren Y, Liu W, Jiang H, Jiang Q, Feng J. Selective vulnerability of dopaminergic neurons to microtubule depolymerization. *J Biol Chem* 2005;280:34105–12.
- Ren Y, Zhao J, Feng J. Parkin binds to alpha/beta tubulin and increases their ubiquitination and degradation. *J Neurosci* 2003;23:3316–24.
- Shamoto-Nagai M, Maruyama W, Kato Y, Isobe K, Tanaka M, Naoi M, et al. An inhibitor of mitochondrial complex I, rotenone, inactivates proteasome by oxidative modification and induces aggregation of oxidized proteins in SH-SY5Y cells. *J Neurosci Res* 2003;74:589–97.
- Sherer TB, Betarbet R, Testa CM, Seo BB, Richardson JR, Kim JH, et al. Mechanism of toxicity in rotenone models of Parkinson's disease. *J Neurosci* 2003;23:10756–64.
- Srivastava P, Panda D. Rotenone inhibits mammalian cell proliferation by inhibiting microtubule assembly through tubulin binding. *FEBS J* 2007;274(18):4788–801.
- Szweda PA, Friguet B, Szweda LI. Proteolysis, free radicals, and aging. *Free Radic Biol Med* 2002;33:29–36.
- Turrens JF, Boveris A. Generation of superoxide anion by the NADH dehydrogenase of bovine heart mitochondria. *Biochem J* 1980;191:421–7.
- Wang XF, Li S, Chou AP, Bronstein JM. Inhibitory effects of pesticides on proteasome activity: implication in Parkinson's disease. *Neurobiol Dis* 2006;23:198–205.

APPENDIX E

Pesticides and Parkinson's disease

In Pesticides in the Modern World – Effects of Pesticides Exposure.

Margarita Stoytcheva (Ed.), ISBN: 978-953-307-454-2, InTech, Available from
<http://www.intechopen.com/articles/show/title/pesticides-and-parkinsons-disease>

Pesticides and Parkinson's Disease

Arthur G. Fitzmaurice and Jeff M. Bronstein
*David Geffen School of Medicine at UCLA
United States of America*

1. Introduction

1.1 Clinical and pathological aspects of Parkinson's disease

Parkinson's disease (PD) is the second most prevalent neurodegenerative disorder, affecting millions of people worldwide (Dorsey, Constantinescu et al. 2007). While some cases of familial PD have been reported, the etiology of most cases is still unknown. Significant progress in understanding the pathophysiology of PD has been made from genetic and epidemiologic studies that have implicated defects in a few key biological processes as potential final common pathological pathways.

PD is a progressive motor disorder characterized by death of dopaminergic neurons in the region of the brain called the substantia nigra pars compacta although other areas of the central and peripheral nervous system are involved (Braak, Del Tredici et al. 2003). The loss of dopaminergic neurons in PD leads to motor symptoms that include akinesia (inability to initiate movement), bradykinesia (slowness of movement), resting tremor, and balance problems. Non-motor symptoms can include cognitive impairments, mood disturbances, sleep dysfunction, gastrointestinal problems, and dysautonomia. PD is a progressive disorder and despite several effective therapies that treat many of the symptoms, there are no treatments that alter disease progression. Uncovering the causes of PD is likely necessary to find effective disease modifying therapies.

The pathological hallmark of PD is the presence of Lewy bodies, which are cytosolic inclusions with several molecular components although α -synuclein (α -syn) is the predominant protein (Spillantini, Schmidt et al. 1997). Lewy bodies also contain ubiquitin, a polypeptide that targets proteins to the ubiquitin proteasome system (UPS) for degradation.

1.2 Genes versus environment

Despite the elucidation of approximately 18 genes in familial PD and the identification of multiple risk factor genes using genome wide association studies on thousands of patients, only a small fraction of PD risk has been accounted for (Hardy 2010). Thus, environmental factors almost certainly play a major role in the pathogenesis of PD.

One of the first important clues that the environment may contribute to the pathogenesis of PD came in 1982 from the observation that a street drug contained a contaminant called 1-methyl-4-phenyl-1,2,3,6-tetrahydropyridine (MPTP) which caused almost overnight a clinical syndrome resembling PD. It was subsequently found that MPTP killed dopaminergic neurons by being converted enzymatically to MPP⁺, specifically entering dopamine neurons via the dopamine transporter, and inhibiting complex I in the

mitochondrial respiratory chain. Notably, the chemical structure of the MPTP metabolite MPP⁺ is similar to paraquat, a commonly used pesticide. These and other observations led to a series of epidemiologic studies probing pesticides as potential contributors to the etiology of PD.

Although genetics hasn't found the cause of 95% of PD cases, the identification of specific genes and their functions have provided important clues into pathological processes that appear to be involved in non-genetic forms of PD. For example, mutations in the α -syn gene led to the finding that α -syn is the major component of Lewy bodies. Mutations in other genes have identified dysfunction of protein degradation (the UPS and autophagy) as possibly being involved in the pathogenesis of PD. Since other PD genes are involved in mitochondrial function and MPTP inhibits oxidative respiration, mitochondrial dysfunction also has been implicated in the pathogenesis of PD. We believe that environmental toxins may increase the risk of PD by causing dysfunction in these cellular processes. Here, we will review the evidence that pesticides are associated with the development of PD and the mechanisms by which they might act.

2. Pathophysiology of Parkinson's disease

2.1 Lewy bodies and α -synuclein homeostasis

Lewy bodies are the pathological hallmark of PD and the major component of these intracytosolic inclusions is α -syn (Spillantini, Schmidt et al. 1997). α -Syn exists in multiple forms including soluble monomers, oligomers and fibrils. The multimeric forms appear to be the toxic species and their formation is dependent on several factors including amino acid substitutions due to mutations in its gene, α -syn concentration, and the presence of dopamine and dopamine adducts (Li, Lin et al. 2005; Mazzulli, Arakola et al. 2007; Burke, Kumar et al. 2008). Exogenous factors such as pesticides have also been reported to increase α -syn aggregation. Given that α -syn aggregation appears central to the pathogenesis of PD and pesticides appear to promote this process via a variety of mechanisms, we will briefly discuss α -syn homeostasis.

2.1.1 α -Synuclein

α -Syn is a predominantly neuronal protein that was first implicated in the development of Alzheimer's disease. The identification of three mutations—A53T, A30P, and G188A—in its gene in a few families with dominantly-inherited PD led to the finding that fibrillar α -syn is the major component of Lewy bodies not only in these patients but also in sporadic PD (Nussbaum and Polymeropoulos 1997; Spillantini, Schmidt et al. 1997; Kruger, Kuhn et al. 1998; Trojanowski, Goedert et al. 1998; Giasson, Jakes et al. 2000). Overexpression of normal α -syn by gene multiplication causes fairly typical PD (Farrer, Kachergus et al. 2004), and people who have an α -syn promoter that confers a higher level of expression are at higher risk of developing PD (Pals, Lincoln et al. 2004; Mueller, Fuchs et al. 2005). Thus, increased levels of normal α -syn increases one's risk of getting PD and if it is high enough, it causes it. Importantly with respect to this review, certain pesticides can cause α -syn levels to increase providing a theoretical mechanism to contribute to PD (see below for individual pesticides). Furthermore, pesticides can directly increase the rate of α -syn fibril formation adding another method they can contribute to the pathogenesis of PD (Uversky, Li et al. 2001).

2.1.2 Ubiquitin-proteasome system dysfunction in Parkinson's disease

α -Syn concentrations are determined by the relative amount of its expression and degradation, and the higher the concentration, the more likely it is to form aggregates. Both the ubiquitin-proteasome system (UPS) and autophagy have been shown to degrade α -syn. The soluble form appears to be degraded by the UPS while the lysosomal pathway appears to degrade aggregated forms of the protein (Liu, Corboy et al. 2003; Cuervo, Stefanis et al. 2004; Zhang, Tang et al. 2008; Mak, McCormack et al. 2010). The UPS is a highly regulated ATP-dependent degradative multi-subunit pathway that helps clear the cell of damaged, misfolded or otherwise unneeded proteins. Proteins are targeted to the UPS by ubiquitin-activating enzymes (E1), ubiquitin-conjugating enzymes (E2), and ubiquitin-protein ligases (E3). Once polyubiquitinated, proteins are recognized by the 19S regulatory complex of the 26S proteasome and translocated to the 20S complex for degradation. Finally, ubiquitin is recycled via thiol proteases called deubiquitinating enzymes, which fall into the ubiquitin carboxyl-terminal hydrolase (UCH) or ubiquitin-specific processing protease (UBP) families (Goldberg 2003).

Three known genetic causes of PD involve aspects of UPS function. Parkin gene mutations cause autosomal recessive PD and is an E3 ubiquitin ligase necessary for targeting proteins for degradation. UCH-L1 gene mutations cause autosomal dominant (AD) PD and UCH-L1 is necessary for the recycling of ubiquitin. Finally, α -syn is a substrate for the UPS and mutations and duplication of its gene cause AD PD. There is also evidence that UPS dysfunction is involved in sporadic PD. Reduced UPS activity has been found in brains of PD patients (McNaught and Jenner 2001) and some investigators have found that administration of UPS inhibitors to rodents can recreate some of the features of PD although these models remain controversial (Bove, Zhou et al. 2006; Kordower, Kanaan et al. 2006; Manning-Bog, Reaney et al. 2006; McNaught and Olanow 2006; Schapira, Cleeter et al. 2006; Zeng, Bukhatwa et al. 2006). Finally, we have found that several commonly used pesticides inhibit the UPS and are associated with an increased risk of developing PD (Wang, Li et al. 2006; Chou, Maidment et al. 2008).

2.1.3 Autophagy and Parkinson's disease

Autophagy is a cellular process that involves protein and organelle degradation. Dysfunction of autophagy has long been known to be involved in disease but only recently has been implicated in the pathogenesis of PD. Gaucher's disease is an autosomal recessive lysosomal storage disease caused by mutations in its gene that lead to dysfunction of autophagy and are associated with a marked increased risk of developing typical PD with Lewy bodies (Aharon-Peretz, Rosenbaum et al. 2004; Neumann, Bras et al. 2009; Sun, Liou et al. 2010). Another autosomal recessive Parkinsonian disorder (PARK9) is caused by a mutation in another lysosomal gene, ATP13A2 (Ramirez, Heimbach et al. 2006). PINK1 has also been shown to be a modifier of autophagy and mutations in its gene cause PD with Lewy bodies (PARK6) (Narendra, Jin et al. 2010; Samaranch, Lorenzo-Betancor et al. 2010). Additional evidence for a role of autophagy in PD comes from studies of sporadic PD brains where increased numbers of autophasomes have been described (Anglade, Vyas et al. 1997).

α -Syn clearance is likely carried out by both the UPS and autophagy. Large aggregates of α -syn proteins are likely degraded by macroautophagy but soluble α -syn can undergo degradation via an alternate lysosomal pathway, chaperone-mediated autophagy (CMA)

(Massey, Zhang et al. 2006). α -Syn has also been found to inhibit lysosomal macroautophagy and oligomers are resistant to CMA adding further support for a possible role of protein degradation dysfunction in the pathogenesis of PD (Martinez-Vicente, Talloczy et al. 2008).

2.2 Mitochondrial dysfunction and oxidative stress

The role of mitochondrial dysfunction in the pathophysiology of PD was first suggested by the discovery that 1-methyl-4-phenyl-1,2,3,6-tetrahydropyridine (MPTP), a neurotoxin selective for nigral dopaminergic neurons, acts through inhibition of complex I of the electron transport chain. MPTP is converted by monoamine oxidase (MAO-B) to its toxic metabolite 1-methyl-4-phenylpyridinium (MPP⁺), which is rapidly concentrated by dopaminergic neurons into the mitochondria and produces cell death (Langston, Ballard et al. 1983; Chiba, Trevor et al. 1985; Javitch, D'Amato et al. 1985; Gainetdinov, Fumagalli et al. 1998). This discovery led to the findings that complex I activity is reduced not only in brains of PD patients but also in peripheral mitochondria (Schapira, Cooper et al. 1990; Haas, Nasirian et al. 1995). Furthermore, mutations in some genes that code for mitochondrial associated proteins can cause PD (e.g. DJ1 and PINK1) and chronic systemic administration of complex I inhibitor (rotenone) in rodents reproduces many of the clinical and pathological aspects of PD (Betarbet, Sherer et al. 2000).

It is still unclear what are the downstream targets of mitochondrial dysfunction. ATP depletion is not necessary in the rotenone rodent model for its toxicity but the generation of reactive oxygen species (ROS) appears to be essential. ROS are known to oxidize DNA, lipids and proteins to cause cellular damage. Interestingly, ROS from complex I inhibition leads to UPS inhibition (Chou, Li et al. 2010). Furthermore, the formation of ROS from complex I inhibition likely contributes to the Lewy-like bodies observed in the rotenone model (Betarbet, Canet-Aviles et al. 2006).

2.2.1 Aldehyde dehydrogenase (ALDH) inhibition

Another form of mitochondrial dysfunction implicated in PD involves the inhibition of aldehyde dehydrogenase 2 (ALDH2), a mitochondrial ALDH. This enzyme is responsible for the detoxification of aldehydes that could otherwise modify proteins. For example, the lipid peroxidation product 4-hydroxy-2-nonenal (HNE) is detoxified by ALDH2 and increased HNE has been reported in post mortem PD brains as adducts (Yoritaka, Hattori et al. 1996) and as a component of Lewy bodies (Castellani, Perry et al. 2002). Furthermore, HNE has been shown to prevent α -syn fibrillation and form α -syn oligomers, which are toxic to primary mesencephalic cultures (Qin, Hu et al. 2007). Another ALDH2 substrate, the dopamine metabolite 3,4-dihydroxyphenylacetaldehyde (DOPAL), has also been reported to induce α -syn aggregation and be toxic to dopaminergic neurons (Burke, Kumar et al. 2008). ALDH involvement in the pathogenesis of PD is not yet well established but preliminary *in vitro* and epidemiology studies have implicated this enzyme as a possible mediator of some pesticides' toxicity (see benomyl below).

2.3 Altered dopamine homeostasis

Conventional wisdom in the pathophysiology of PD is that dopaminergic neurons are selectively vulnerable, although more recent evidence suggests that neuronal loss is more widespread. One hypothesis for this possible vulnerability is via the metabolism of dopamine itself (Hastings 2009).

Dopamine and its metabolites are toxic and dopamine adducts have been shown to stabilize α -syn oligomers. DOPAL, a substrate for ALDH2, is particularly toxic. Interestingly, DOPAL is formed by the enzyme MAO-B and blocking this enzyme with specific drugs appears to alter the progression of PD (Olanow, Rascol et al. 2009). Thus, alterations in levels of dopamine or its metabolites might contribute to neuronal loss. Increased levels of VMAT2, a vesicular transporter that lowers cytosolic dopamine levels, lowers the risk of developing PD (Glatt, Wahner et al. 2006). Further support for altered dopamine homeostasis in PD comes from a recent report that polymorphisms in the dopamine transporter (DAT) gene in combination with pesticide exposure also increases the risk of PD (Ritz, Manthripragada et al. 2009).

Taken together, dysfunction of several cellular processes appears to contribute to the pathogenesis of PD. Aggregation of α -syn (oligomerization and possibly fibril formation) is the leading candidate for the final common pathway for neurons to die in PD. There is evidence that pesticides cause dysfunction in many of these processes providing potential mechanisms for their toxicity (Figure 1).

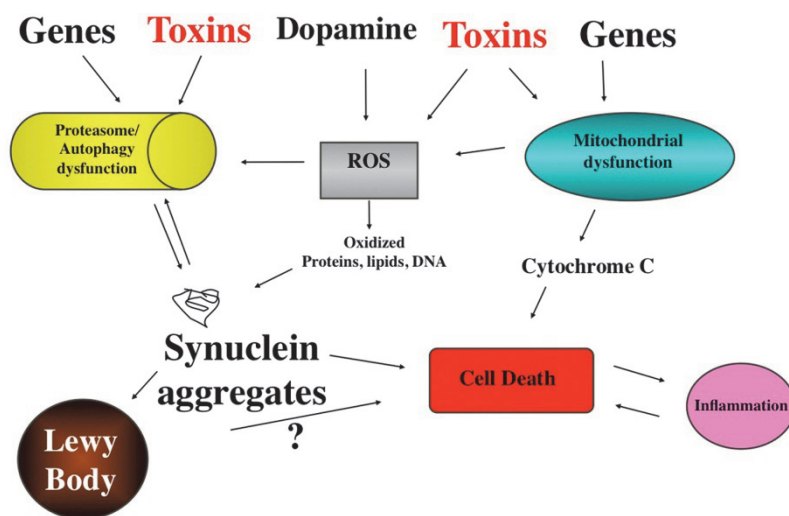


Fig. 1. Proposed pathophysiology of Parkinson's disease.

3. Epidemiology of Parkinson's disease

3.1 Environment and Parkinson's disease

Over the past two decades, several epidemiologic studies have identified a number of environmental factors that are associated with an altered risk of developing PD. Smoking tobacco is almost universally found to be associated with a lower risk of developing the disease (Ritz, Ascherio et al. 2007). Caffeine and alcohol consumption have also been associated with a reduced risk of PD (Hellenbrand, Seidler et al. 1996). Since all of these addictive behaviors are associated with reduced incidence, it has been proposed that they may be surrogate markers for a common behavioral phenotype of pre-clinical PD patients rather than these exposures all being protective. The use of nonsteroidal anti-inflammatory

drugs has also been found to reduce the risk of PD suggesting inflammation may be somehow involved in its pathogenesis (Wahner, Bronstein et al. 2007).

A number of studies have found strong associations between an increased risk of PD and rural living, well-water consumption, farm occupations, and pesticide exposure. These reports have been reviewed extensively by others so we will not review all the studies here (Le Couteur, McLean et al. 1999; Di Monte 2003; Alavanja, Hoppin et al. 2004; Kamel and Hoppin 2004; Li, Mink et al. 2005; Brown, Rumsby et al. 2006). The association with pesticide exposure has been the most provocative association with developing PD to date although almost all of these reports were based on self-reporting pesticide exposure (i.e. potential recall bias) and the diagnosis of PD was not confirmed (Gartner, Battistutta et al. 2005). Despite these weaknesses, a meta-analysis of case-control studies obtained a combined odds ratio (OR) for PD risk of 1.94 (95% CI, 1.49–2.53) (Priyadarshi, Khuder et al. 2000). Subsequent studies reported OR of up to 7.0 (Brown, Rumsby et al. 2006).

Recently, the issue of potential recall bias was mitigated by determining pesticide exposure in a prospective manner. Petrovitch et al reported an increased risk of developing PD in Japanese-American men who worked on a plantation and were exposed to pesticides (Petrovitch, Ross et al. 2002). Similarly, Ascherio et al found a 70% increased risk of developing PD in those who reported significant pesticide exposure (Ascherio, Chen et al. 2006). These reports add support for a true association between pesticides and PD but still are limited in that they did not identify individual toxins and dose response relationships could not be determined.

3.2 Specific pesticides as risk factors

There are a few ongoing studies that address both the issue of recall bias and are identifying specific pesticides that confer an altered risk of developing PD. The Agricultural Health Study (AHS) is a prospective study, including 84,740 private pesticide applicators (mostly farmers) and their spouses recruited in 1993-97 in Iowa and North Carolina. Pesticide exposure was self-reported but felt to be reliable. The diagnosis of PD was also self-reported but later confirmed by direct examination. The first report from this study found an association between PD with increasing lifetime days of use of any pesticide but no specific pesticide could be definitely implicated due to lack of statistical power (Kamel, Tanner et al. 2007). Recently, the investigators reported that PD was associated with rotenone (OR 2.5, 95% CI 1.3, 4.7) and paraquat use (OR 2.5, 95% CI 1.4, 4.7) (Tanner, Kamel et al. 2011). The strength of this study is that it is prospective, the diagnosis was confirmed by examination, and specific toxins were identified. The primary weakness of this study is that they have only 110 cases limiting their power to test a number of pesticides individually and in combinations. The small number of cases also limits their ability to test gene-environment interactions. One additional limitation was that quantitation of pesticide exposure, types of exposure and length of exposures were self-reported. Despite these shortcomings, this study adds strong epidemiological evidence that pesticides are associated with an increased risk of developing PD, especially for rotenone and paraquat.

Ritz and colleagues at UCLA have taken another approach to identifying specific pesticides that are associated with an altered risk of PD. We took advantage of the California Pesticide Use Reporting database and Geographic Information System land-use maps to estimate historical exposure. All commercial pesticide applications have been recorded by compound, quantity, and specific location since 1974. Thus, individual subject exposures

can be approximated by using their residential and occupational addresses for the past 37 years. In this Parkinson's Environment Gene (PEG) study, neurologists specializing in movement disorders went into the field to confirm the diagnosis in over 350 incident PD cases in the central California valley where pesticides are applied liberally and the risk of PD appears to be increased (Ritz and Yu 2000; Kang, Bronstein et al. 2005). A similar number of age and sex matched control subjects were also recruited from the same communities. In addition to several lifestyle and medical assessments, DNA and serum samples were also obtained.

Individual pesticides were investigated in the PEG study based on previous reports implicating the agents as possibly involved in the pathogenesis of PD based on previous epidemiologic and/or laboratory studies. Maneb and paraquat were investigated because administration of pesticides to rodents produces a nice model of PD (see below). Estimates for maneb and paraquat exposures incurred between 1974 and 1999 were generated based on their residence. Exposure to both pesticides within 500m of their homes increased PD risk by 75% (95% CI 1.13, 2.73). Subjects aged ≤ 60 yo were at much higher risk of developing PD when exposed to either maneb or paraquat alone (odds ratio (OR) = 2.27, 95% CI: 0.91, 5.70) or to both pesticides in combination (OR = 4.17, 95% CI: 1.15, 15.16) (Costello, Cockburn et al. 2009). PEG investigators have found similar associations with organophosphate pesticides—diazinon (OR 1.73, CI 1.23, 2.45) and chlorpyrifos (OR 1.50, CI 1.04, 2.18) (Manthripragada, Costello et al. 2010)—and ziram (OR 3.01, CI 1.69, 5.38). In subjects ≤ 60 yo, exposure to both ziram and paraquat had a 6-fold increase in risk of PD (CI 1.94, 18.33) (Wang, Costello et al. 2011). It is important to note that all estimates of exposures were not dependent on subject recall for total exposure or duration of exposure. Recent exposure to pesticides (1990 to 1999) was not generally associated with an increased risk of PD consistent with the theory that PD pathology likely starts several years before it manifests itself clinically.

The population is exposed to pesticides in a variety of ways, not just inhalation from spraying and crop dusters. Gatto et al. looked at five pesticides that were likely to be detected in well water (Gatto, Cockburn et al. 2009). Although local well water was not analyzed, these pesticides were identified based on their solubility, half-lives, and adsorptive properties. These included organophosphates (diazinon, dimethoate, chlorpyrifos), a carbamate (methomyl), and a sulfite ester (propargite). Excluding those who did not consume well water, potential inhalation and ingestion of each pesticide was associated with 23-57% increased risk of PD. Consuming well water potentiated this effect to a 41-75% increased risk. Up to a two-fold increase was observed for those who consumed water with the highest potential contamination of at least one of these pesticides. Finally, those with PD were found to have consumed well water an average of 4.3 years longer than controls. Because PEG has enrolled over 350 cases, we have statistical power to test gene-environment interactions. Not surprisingly, the risk of developing PD in pesticide-exposed subjects is clearly altered based on the subject's genetic background (see below).

3.3 Gene-environment interactions

Gene-environment interaction analyses for pesticides and PD have been rare due to small sample size and difficulty obtaining exposure data (Deng, Newman et al. 2004; Elbaz, Leveque et al. 2004; Kelada, Checkoway et al. 2006; Hancock, Martin et al. 2008). Elbaz et al found that pesticides had a modest effect in subjects who were not CYP2D6 poor

metabolizers, had an increased effect in poor metabolizers (approximately twofold), but poor metabolizers were not at increased PD risk in the absence of pesticide exposure (Elbaz, Levecque et al. 2004). Hancock et al found a gene-environment association in PD for pesticides and nitric oxide synthase 1 polymorphisms (Hancock, Martin et al. 2008). Kelada et al described a very modest risk of developing PD with specific dopamine transporter (DAT) alleles but a 5.7 fold increase (CI 1.73-18.53) in developing PD in subjects with occupational exposure to pesticides. These studies added proof of concept that the effect of environmental exposures on the risk of developing PD is at least partially dependent on one's genetic background (Kelada, Checkoway et al. 2006). Unfortunately, exposure assessments were very limited in all of these studies and individual toxins could not be determined.

Gene-environment analysis in Ritz's PEG study has only recently begun but has already revealed intriguing results. We replicated the DAT polymorphism's interaction with pesticide exposure described by Kelada et al for at least maneb and paraquat (Ritz, Manthripragada et al. 2009). Unexposed subjects with more susceptibility alleles had a 30% increased risk of developing PD whereas exposed subjects had an almost five-fold increased risk (OR = 4.53; 95% CI, 1.70-12.1). Importantly, there was a gene dose effect as well. In a similar manner, variations in PON1, the gene that encodes Paraoxonase 1 that metabolizes chlorpyrifos and diazinon, potentiated the increased PD risks associated with these organophosphates (Manthripragada, Costello et al. 2010).

For example, diazinon was associated with a 73% increased risk of PD (CI 1.23, 2.45) but the risk increases to 267% (CI 1.09, 6.55) in individuals who carry PON1 risk alleles. Variations in the dinucleotide repeat sequence (REP1) within the α -syn promoter appear to alter the risk to paraquat exposure (Gatto et al., 2010). Finally, we have preliminary evidence that variations in ALDH2 gene potentiate the increased risks associated with dithiocarbamates and other pesticides that inhibit ALDH activity (Fitzmaurice, Rhodes et al. 2010).

Clearly, the number of potential gene-environment interactions is enormous but we have clear proof of concept that these interactions need to be considered to truly understand environmental risks in PD. It will take very large sample sizes and good exposure analysis to obtain a better understanding of the many potential interactions that confer the bulk of PD risk factors. Alternatively, a candidate gene approach coupled with a better understanding of the pharmacokinetics and toxicity of specific pesticides may allow us to test gene-environment interactions using smaller sample sizes.

4. From association to causality - do pesticides cause PD and if so, how?

Epidemiological studies have clearly established the association between pesticide exposure and the development of PD. The possibility that this association represents causality has been strengthened by recent studies that addressed the problem of recall bias and have demonstrated a dose-effect relationship. Now that some individual pesticides have been implicated, mechanistic studies could be pursued. These studies are reviewed within the context of our current understanding of the pathophysiology of PD.

4.1 Rotenone

Rotenone is produced naturally in roots of certain plant species such as the jicama vine. It is a widely used domestic garden pesticide and because it is degraded by the sun in a matter of days, users tend to spray rotenone frequently. Rotenone is also a well-

characterized, high-affinity, specific inhibitor of complex I of the mitochondrial respiratory electron transport chain. Low complex I activity had been reported to be associated with PD both in brain and peripheral mitochondria but it wasn't known whether this is causal or a surrogate marker for something else. To further investigate this, Greenamyre and colleagues chronically administered the complex I inhibitor, rotenone, systemically into rodents. Some of these rats developed selective dopaminergic neuronal death as well as many of the motor features of PD. Importantly, neurons developed intracytoplasmic inclusions that were found to contain α -syn (Betarbet, Sherer et al. 2000). α -Syn pathology in the gastro-intestinal tract has also been described in the rotenone model similar to that seen in PD (Drolet, Cannon et al. 2009). Even small amounts of rotenone delivered intragastrically reproduces many of the same features described in rats given rotenone subcutaneously but in this model, the various stages of PD are reproduced in a progressive manner (Pan-Montojo, Anichtchik et al. 2010).

The mechanisms of rotenone toxicity are not completely clear but likely are more dependent on oxidative stress than energy failure (Sherer, Betarbet et al. 2002). The downstream targets of rotenone-induced oxidative damage are likely vast but the UPS appears to be one of them (Betarbet, Canet-Aviles et al. 2006; Wang, Li et al. 2006; Chou, Li et al. 2010).

Until recently, there have not been convincing epidemiologic reports linking rotenone exposure to PD. Dhillon et al reported an over 10 fold increase in risk although this study was limited because exposures were self-reported (Dhillon, Tarbutton et al. 2008). The Agricultural Health Study did find a 2.5 fold increased risk with prospective questionnaires adding further support for rotenone as a PD risk factor (Tanner, Kamel et al. 2011). Furthermore, many organic farmers in the 1970s used rotenone as a natural pesticide and a number of them have developed PD at a young age although scientific confirmation of these anecdotal reports is lacking. Other pesticides that are complex I inhibitors are used even less frequently than rotenone so little is known about associations with PD although one would predict a similar effect.

4.2 Paraquat

One of the first pesticides investigated for its potential link to PD was paraquat due to its structural similarity to MPTP, the drug that caused acute Parkinsonism in drug addicts. MPTP kills dopaminergic neurons by being metabolized to MPP⁺ by MAO-B, entering dopamine cells via the dopamine transporter and then inhibiting complex I in the mitochondrial respiratory chain. Paraquat is ubiquitously used as an herbicide to control weed growth and exposure to paraquat is associated with an increased risk of PD (Hertzman, Wiens et al. 1990; Semchuk, Love et al. 1992; Liou, Tsai et al. 1997).

Additional support for paraquat increasing the risk of PD comes from animal studies. Mice infused with paraquat for three consecutive weeks exhibit dopamine cell loss and cytosolic α -syn aggregates (Brooks, Chadwick et al. 1999; Manning-Bog, McCormack et al. 2002; McCormack, Thiruchelvam et al. 2002). The mechanism by which paraquat causes dopamine cell death is not clear. Since it is structurally very similar to MPTP, it was presumed that paraquat acted in a similar manner. Surprisingly, unlike MPP⁺, paraquat is not a substrate for the dopamine transporter and does not inhibit complex I except at very high concentrations (Richardson et al 2005). Paraquat toxicity does appear to be dependent on increasing oxidative stress and its action as a redox-cycler appears likely involved in its toxicity (McCormack, Atienza et al. 2005).

4.3 Dithiocarbamates (maneb and ziram)

Dithiocarbamates (DTCs) are a class of some of the most commonly used organic fungicides. They are classified into 2 groups based on whether there is a carbonyl (group 1) or hydrogen on the nitrogen carbamate. Most DTCs are complexed with metals including zinc (e.g. ziram and zineb), iron (e.g. ferbam) and manganese (e.g. maneb). DTCs first became relevant to PD researchers in 1985 when Corsini et al found that diethyldithiocarbamate pretreatment enhanced MPTP toxicity in mice (Corsini, Pintus et al. 1985). They proposed that diethyldithiocarbamate would potentiate MPTP toxicity by inhibiting superoxide dismutase since they believed at that time that MPTP acted primarily as a redox cyclizer. Thiruchelvam et al. later reported that maneb potentiated the toxicity of paraquat preferentially in the nigrostriatal dopaminergic system (Thiruchelvam, Brockel et al. 2000; Thiruchelvam, McCormack et al. 2003). Furthermore, maneb and paraquat exposure was found to exacerbate α -synucleinopathy in A53T transgenic mice (Norris, Uryu et al. 2007).

The animal models using maneb and paraquat were intriguing but it was only recently that an association between maneb and paraquat exposures and PD were reported (Costello, Cockburn et al. 2009). Similar to the animals studies, residential exposure to maneb and paraquat exposure together is associated with a 114% increased risk of newly diagnosed PD. Furthermore, the risk of PD was increased to 317% for cases \leq 60 yo. Neither pesticide alone was associated with PD but there were few subjects with maneb only exposure so that the true effect for maneb alone could not be assessed. When both occupational and residential exposures are taken into account, subjects exposed to maneb and paraquat alone had a 126% and 50% increase in risk of developing PD respectively but for exposure to maneb and paraquat together, the risk increased to 8.75x (CI 2.3-33.2) in the younger group (Wang, Costello et al. 2011). These epidemiologic data taken together with the animal data are quite compelling that these pesticides truly increase the risk of PD.

As mentioned above, DTCs are a large group of fungicides with similar structures. We identified another DTC, ziram, in an unbiased screen to identify pesticides that inhibit the proteasome (Wang, Li et al. 2006). Maneb and some other DTCs were also found to inhibit the UPS but at higher concentrations (Chou, Maidment et al. 2008). Ziram selectively killed dopaminergic neurons in primary cultures and increased α -syn levels in the remaining neurons. Systemic administration of ziram alone into mice caused progressive motor dysfunction and dopaminergic neuronal damage (Chou et al 2008). Furthermore, subjects exposed to ziram alone had a 201% (CI 1.69, 5.38) increase of risk of developing PD and a 598% (CI 1.95, 18.3) increased risk when exposed with paraquat in subjects \leq 60 yo (Wang, Costello et al. 2011). These data add further support for the role of DTCs as a causal risk factor for PD.

It is still not completely clear how DTCs act biologically. We have found that they do not increase oxidative stress and therefore are unlikely acting through the mitochondrial respiratory chain (Wang, Li et al. 2006). DTCs clearly inhibit the UPS and their potency depends on whether they contain a tertiary or a secondary amino group. Ziram was studied extensively given its high potency to inhibit the UPS and we found that it acts by interfering with the ubiquitin E1 ligase with an IC_{50} of 161 nM (Chou, Maidment et al. 2008). Zhou et al reported that maneb also inhibited the UPS but at higher concentrations (IC_{50} of approx. 6 μ M) and increased protein carbonyls suggesting increased oxidative stress (Zhou, Shie et al. 2004). We also found that maneb inhibits the UPS at much higher concentrations than ziram but we did not find evidence of oxidative stress. Differences may very well be due to differences in the techniques used since we used an *in vitro* 26S UPS assay and DCF

fluorescence to detect ROS and Zhou et al used an *in vitro* 20S UPS assay and protein carbonyl immunohistochemistry for detection of oxidative stress. Recently, we have found that both maneb and ziram inhibit ALDH2 at environmentally-relevant concentrations, adding another potential mechanism of toxicity, especially to dopaminergic neurons (Fitzmaurice, Rhodes et al. 2010). Since ziram does not contain manganese, it is very unlikely that it is the manganese in maneb that confers its toxicity as some have suggested.

4.4 Benomyl

Another important fungicide implicated in PD pathogenesis is the benzimidazole compound benomyl. It was developed as a microtubule inhibitor and is sprayed on fruits, nuts, and leaves to prevent fungal growth. Preliminary findings from the PEG study revealed benomyl exposure increased PD risk by 138% (CI 1.33, 4.27) (Fitzmaurice, Rhodes et al. 2010).

Benomyl metabolizes spontaneously into another fungicide (carbendazim) and enzymatically into several thiocarbamate compounds. We have shown that benomyl and carbendazim are UPS inhibitors, although they are not as potent as ziram (Wang, Li et al. 2006; Fitzmaurice, Ackerman et al. 2010). Furthermore, benomyl has also been reported to inhibit mitochondrial ALDH (Staub, Quistad et al. 1998). Although these studies focused on hepatic ALDH, we recently reported that benomyl exposure reduced ALDH2 activity *ex vivo* in rat neuronal suspensions (Fitzmaurice, Ackerman et al. 2010). We have also found that exposure to benomyl or one of its ALDH2-inhibiting metabolites (S-methyl-N-butylthiocarbamate, or MBT) causes dopaminergic neuronal death *in vitro*, while the UPS-inhibiting metabolite (carbendazim) does not. These findings, combined with the observation that DTCs also inhibit ALDH2, suggest that ALDH2 inhibition may be an important mechanism in pesticide toxicity with respect to PD.

The toxicity of ALDH2 inhibition is likely due to the accumulation of toxic aldehydes. We would predict that ALDH2 inhibition would lead to increased levels of DOPAL and HNE adducts and preliminary studies in primary cultures support this hypothesis. Furthermore, the loss of dopaminergic neurons due to benomyl was attenuated by co-treatment with the MAO-B inhibitor pargyline which decreases DOPAL formation (Fitzmaurice, Ackerman et al. 2010). Since DOPAL and HNE accumulation have been reported to induce α -syn aggregation (Burke, Kumar et al. 2008), these findings support ALDH2 inhibition as an important mediator of pesticide toxicity in PD.

5. Summary

The causes of PD are not completely understood but both genetic and epidemiologic studies suggest that dysfunction of one or more biological processes lead to α -syn aggregation and neuronal death. Epidemiologic studies have clearly shown PD to be associated with pesticide exposure and specific pesticides conferring at least some of this increased risk have recently been identified. The fact that administration of pesticides to animals recapitulates many of the behavioral and pathological features of PD provides evidence that the associations found in epidemiologic studies are causal. Elucidating the mechanisms of pesticide toxicity in mammals not only strengthens the hypothesis that exposure to these toxins can increase the risk of developing PD, but also furthers our understanding of the pathophysiology of the disease in general. It is clear that the list of pesticides discussed in this chapter is not complete and that pesticides are not the only environmental toxins that

alter the risk of PD, but the preponderance of evidence taken together supports an important role of pesticides in the pathogenesis of PD. A better understanding of these issues will take us one step closer to a cure.

6. References

- Aharon-Peretz, J., H. Rosenbaum, et al. (2004). "Mutations in the glucocerebrosidase gene and Parkinson's disease in Ashkenazi Jews." *N Engl J Med* 351(19): 1972-1977.
- Alavanja, M. C., J. A. Hoppin, et al. (2004). "Health effects of chronic pesticide exposure: cancer and neurotoxicity." *Annu Rev Public Health* 25: 155-197.
- Anglade, P., S. Vyas, et al. (1997). "Apoptosis and autophagy in nigral neurons of patients with Parkinson's disease." *Histol Histopathol* 12(1): 25-31.
- Ascherio, A., H. Chen, et al. (2006). "Pesticide exposure and risk for Parkinson's disease." *Annals of Neurology* 60(2): 197-203.
- Betarbet, R., R. M. Canet-Aviles, et al. (2006). "Intersecting pathways to neurodegeneration in Parkinson's disease: Effects of the pesticide rotenone on DJ-1, [alpha]-synuclein, and the ubiquitin-proteasome system." *Neurobiology of Disease* 22(2): 404-420.
- Betarbet, R., R. M. Canet-Aviles, et al. (2006). "Intersecting pathways to neurodegeneration in Parkinson's disease: effects of the pesticide rotenone on DJ-1, alpha-synuclein, and the ubiquitin-proteasome system." *Neurobiol Dis* 22(2): 404-420.
- Betarbet, R., T. B. Sherer, et al. (2000). "Chronic systemic pesticide exposure reproduces features of Parkinson's disease." *Nat Neurosci* 3(12): 1301-1306.
- Bove, J., C. Zhou, et al. (2006). "Proteasome inhibition and Parkinson's disease modeling." *Annals of neurology* 60(2): 260-264.
- Braak, H., K. Del Tredici, et al. (2003). "Staging of brain pathology related to sporadic Parkinson's disease." *Neurobiol Aging* 24(2): 197-211.
- Brooks, A. I., C. A. Chadwick, et al. (1999). "Paraquat elicited neurobehavioral syndrome caused by dopaminergic neuron loss." *Brain Res* 823(1-2): 1-10.
- Brown, T. P., P. C. Rumsby, et al. (2006). "Pesticides and Parkinson's disease--is there a link?" *Environ Health Perspect* 114(2): 156-164.
- Burke, W. J., V. B. Kumar, et al. (2008). "Aggregation of alpha-synuclein by DOPAL, the monoamine oxidase metabolite of dopamine." *Acta Neuropathol* 115(2): 193-203.
- Castellani, R. J., G. Perry, et al. (2002). "Hydroxynonenal adducts indicate a role for lipid peroxidation in neocortical and brainstem Lewy bodies in humans." *Neurosci Lett* 319(1): 25-28.
- Chiba, K., A. J. Trevor, et al. (1985). "Active uptake of MPP+, a metabolite of MPTP, by brain synaptosomes." *Biochemical and biophysical research communications* 128(3): 1228-1232.
- Chou, A. P., S. Li, et al. (2010). "Mechanisms of rotenone-induced proteasome inhibition." *NeuroToxicology* 31(4): 367-372.
- Chou, A. P., N. Maidment, et al. (2008). "Ziram causes dopaminergic cell damage by inhibiting E1 ligase of the proteasome." *J Biol Chem* 283(50): 34696-34703.
- Corsini, G. U., S. Pintus, et al. (1985). "1-Methyl-4-phenyl-1,2,3,6-tetrahydropyridine (MPTP) neurotoxicity in mice is enhanced by pretreatment with diethyldithiocarbamate." *Eur J Pharmacol* 119(1-2): 127-128.
- Costello, S., M. Cockburn, et al. (2009). "Parkinson's disease and residential exposure to maneb and paraquat from agricultural applications in the central valley of California." *Am J Epidemiol* 169(8): 919-926.

- Cuervo, A. M., L. Stefanis, et al. (2004). "Impaired degradation of mutant alpha-synuclein by chaperone-mediated autophagy." *Science* 305(5688): 1292-1295.
- Deng, Y., B. Newman, et al. (2004). "Further evidence that interactions between CYP2D6 and pesticide exposure increase risk for Parkinson's disease." *Ann Neurol* 55(6): 897.
- Dhillon, A. S., G. L. Tarbutton, et al. (2008). "Pesticide/environmental exposures and Parkinson's disease in East Texas." *J Agromedicine* 13(1): 37-48.
- Di Monte, D. A. (2003). "The environment and Parkinson's disease: is the nigrostriatal system preferentially targeted by neurotoxins?" *Lancet Neurol* 2(9): 531-538.
- Dorsey, E. R., R. Constantinescu, et al. (2007). "Projected number of people with Parkinson disease in the most populous nations, 2005 through 2030." *Neurology* 68(5): 384-386.
- Drolet, R. E., J. R. Cannon, et al. (2009). "Chronic rotenone exposure reproduces Parkinson's disease gastrointestinal neuropathology." *Neurobiol Dis* 36(1): 96-102.
- Elbaz, A., C. Leveque, et al. (2004). "CYP2D6 polymorphism, pesticide exposure, and Parkinson's disease." *Ann Neurol* 55(3): 430-434.
- Farrer, M., J. Kachergus, et al. (2004). "Comparison of kindreds with parkinsonism and alpha-synuclein genomic multiplications." *Ann Neurol* 55(2): 174-179.
- Fitzmaurice, A. G., L. C. Ackerman, et al. (2010). "Aldehyde dehydrogenase inhibition by the fungicide benomyl leads to dopaminergic cell death: Relevance of dopamine metabolism to Parkinson's disease." *Soc Neurosci (abstract)*: 655.24.
- Fitzmaurice, A. G., S. L. Rhodes, et al. (2010). "Biochemical and epidemiologic screens link pesticide exposure, aldehyde dehydrogenase inhibition, and Parkinson's disease." *Soc Neurosci (abstract)*: 752.3.
- Gainetdinov, R. R., F. Fumagalli, et al. (1998). "Increased MPTP neurotoxicity in vesicular monoamine transporter 2 heterozygote knockout mice." *Journal of neurochemistry* 70(5): 1973-1978.
- Gartner, C. E., D. Battistutta, et al. (2005). "Test-retest repeatability of self-reported environmental exposures in Parkinson's disease cases and healthy controls." *Parkinsonism & Related Disorders* 11(5): 287-295.
- Gatto, N. M., M. Cockburn, et al. (2009). "Well-water consumption and Parkinson's disease in rural California." *Environ Health Perspect* 117(12): 1912-1918.
- Giasson, B. I., R. Jakes, et al. (2000). "A panel of epitope-specific antibodies detects protein domains distributed throughout human alpha-synuclein in Lewy bodies of Parkinson's disease." *J Neurosci Res* 59(4): 528-533.
- Glatt, C. E., A. D. Wahner, et al. (2006). "Gain-of-function haplotypes in the vesicular monoamine transporter promoter are protective for Parkinson disease in women." *Hum Mol Genet* 15(2): 299-305.
- Goldberg, A. L. (2003). "Protein degradation and protection against misfolded or damaged proteins." *Nature* 426(6968): 895-899.
- Haas, R. H., F. Nasirian, et al. (1995). "Low platelet mitochondrial complex I and complex II/III activity in early untreated Parkinson's disease." *Ann Neurol* 37(6): 714-722.
- Hancock, D. B., E. R. Martin, et al. (2008). "Nitric oxide synthase genes and their interactions with environmental factors in Parkinson's disease." *Neurogenetics* 9(4): 249-262.
- Hardy, J. (2010). "Genetic analysis of pathways to Parkinson disease." *Neuron* 68(2): 201-206.
- Hastings, T. G. (2009). "The role of dopamine oxidation in mitochondrial dysfunction: implications for Parkinson's disease." *J Bioenerg Biomembr* 41(6): 469-472.
- Hellenbrand, W., A. Seidler, et al. (1996). "Diet and Parkinson's disease. I: A possible role for the past intake of specific foods and food groups. Results from a self-administered food-frequency questionnaire in a case-control study." *Neurology* 47(3): 636-643.

- Hertzman, C., M. Wiens, et al. (1990). "Parkinson's disease: a case-control study of occupational and environmental risk factors." *Am J Ind Med* 17(3): 349-355.
- Javitch, J. A., R. J. D'Amato, et al. (1985). "Parkinsonism-inducing neurotoxin, N-methyl-4-phenyl-1,2,3,6-tetrahydropyridine: uptake of the metabolite N-methyl-4-phenylpyridine by dopamine neurons explains selective toxicity." *Proceedings of the National Academy of Sciences of the United States of America* 82(7): 2173-2177.
- Kamel, F. and J. A. Hoppin (2004). "Association of pesticide exposure with neurologic dysfunction and disease." *Environ Health Perspect* 112(9): 950-958.
- Kamel, F., C. Tanner, et al. (2007). "Pesticide exposure and self-reported Parkinson's disease in the agricultural health study." *Am J Epidemiol* 165(4): 364-374.
- Kang, G. A., J. M. Bronstein, et al. (2005). "Clinical characteristics in early Parkinson's disease in a central California population-based study." *Mov Disord* 20(9): 1133-1142.
- Kelada, S. N., H. Checkoway, et al. (2006). "5' and 3' region variability in the dopamine transporter gene (SLC6A3), pesticide exposure and Parkinson's disease risk: a hypothesis-generating study." *Hum Mol Genet* 15(20): 3055-3062.
- Kordower, J. H., N. M. Kanaan, et al. (2006). "Failure of proteasome inhibitor administration to provide a model of Parkinson's disease in rats and monkeys." *Annals of neurology* 60(2): 264-268.
- Kruger, R., W. Kuhn, et al. (1998). "Ala30Pro mutation in the gene encoding alpha-synuclein in Parkinson's disease." *Nat Genet* 18(2): 106-108.
- Langston, J. W., P. Ballard, et al. (1983). "Chronic Parkinsonism in humans due to a product of meperidine-analog synthesis." *Science* 219(4587): 979-980.
- Le Couteur, D. G., A. J. McLean, et al. (1999). "Pesticides and Parkinson's disease." *Biomedicine & Pharmacotherapy* 53(3): 122-130.
- Li, A. A., P. J. Mink, et al. (2005). "Evaluation of epidemiologic and animal data associating pesticides with Parkinson's disease." *J Occup Environ Med* 47(10): 1059-1087.
- Li, H. T., D. H. Lin, et al. (2005). "Inhibition of alpha-synuclein fibrillization by dopamine analogs via reaction with the amino groups of alpha-synuclein. Implication for dopaminergic neurodegeneration." *The FEBS journal* 272(14): 3661-3672.
- Liou, H. H., M. C. Tsai, et al. (1997). "Environmental risk factors and Parkinson's disease: a case-control study in Taiwan." *Neurology* 48(6): 1583-1588.
- Liu, C. W., M. J. Corboy, et al. (2003). "Endoproteolytic activity of the proteasome." *Science* 299(5605): 408-411.
- Mak, S. K., A. L. McCormack, et al. (2010). "Lysosomal degradation of alpha-synuclein in vivo." *Journal of Biological Chemistry* 285(18): 13621-13629.
- Manning-Bog, A. B., A. L. McCormack, et al. (2002). "The herbicide paraquat causes up-regulation and aggregation of alpha-synuclein in mice: paraquat and alpha-synuclein." *J Biol Chem* 277(3): 1641-1644.
- Manning-Bog, A. B., S. H. Reaney, et al. (2006). "Lack of nigrostriatal pathology in a rat model of proteasome inhibition." *Annals of neurology* 60(2): 256-260.
- Manthripragada, A. D., S. Costello, et al. (2010). "Paraoxonase 1, agricultural organophosphate exposure, and Parkinson disease." *Epidemiology* 21(1): 87-94.
- Martinez-Vicente, M., Z. Talloczy, et al. (2008). "Dopamine-modified alpha-synuclein blocks chaperone-mediated autophagy." *J Clin Invest* 118(2): 777-788.
- Massey, A. C., C. Zhang, et al. (2006). "Chaperone-mediated autophagy in aging and disease." *Curr Top Dev Biol* 73: 205-235.
- Mazzulli, J. R., M. Armarkola, et al. (2007). "Cellular oligomerization of alpha-synuclein is determined by the interaction of oxidized catechols with a C-terminal sequence." *The Journal of biological chemistry* 282(43): 31621-31630.

- McCormack, A. L., J. G. Atienza, et al. (2005). "Role of oxidative stress in paraquat-induced dopaminergic cell degeneration." *J Neurochem* 93(4): 1030-1037.
- McCormack, A. L., M. Thiruchelvam, et al. (2002). "Environmental risk factors and Parkinson's disease: selective degeneration of nigral dopaminergic neurons caused by the herbicide paraquat." *Neurobiol Dis* 10(2): 119-127.
- McNaught, K. S. and P. Jenner (2001). "Proteasomal function is impaired in substantia nigra in Parkinson's disease." *Neurosci Lett* 297(3): 191-194.
- McNaught, K. S. and C. W. Olanow (2006). "Proteasome inhibitor-induced model of Parkinson's disease." *Annals of neurology* 60(2): 243-247.
- Mueller, J. C., J. Fuchs, et al. (2005). "Multiple regions of α -synuclein are associated with Parkinson's disease." *Annals of Neurology* 57(4): 535-541.
- Narendra, D. P., S. M. Jin, et al. (2010). "PINK1 is selectively stabilized on impaired mitochondria to activate Parkin." *PLoS Biol* 8(1): e1000298.
- Neumann, J., J. Bras, et al. (2009). "Glucocerebrosidase mutations in clinical and pathologically proven Parkinson's disease." *Brain : a journal of neurology* 132(Pt 7): 1783-1794.
- Norris, E. H., K. Uryu, et al. (2007). "Pesticide exposure exacerbates alpha-synucleinopathy in an A53T transgenic mouse model." *Am J Pathol* 170(2): 658-666.
- Nussbaum, R. L. and M. H. Polymeropoulos (1997). "Genetics of Parkinson's disease." *Hum Mol Genet* 6(10): 1687-1691.
- Olanow, C. W., O. Rascol, et al. (2009). "A double-blind, delayed-start trial of rasagiline in Parkinson's disease." *The New England journal of medicine* 361(13): 1268-1278.
- Pals, P., S. Lincoln, et al. (2004). " α -Synuclein promoter confers susceptibility to Parkinson's disease." *Annals of Neurology* 56(4): 591-595.
- Pan-Montojo, F., O. A. Nischtchik, et al. (2010). "Progression of Parkinson's disease pathology is reproduced by intragastric administration of rotenone in mice." *PloS one* 5(1): e8762.
- Petrovitch, H., G. W. Ross, et al. (2002). "Plantation work and risk of Parkinson disease in a population-based longitudinal study." *Arch Neurol* 59(11): 1787-1792.
- Priyadarshi, A., S. A. Khuder, et al. (2000). "A meta-analysis of Parkinson's disease and exposure to pesticides." *Neurotoxicology* 21(4): 435-440.
- Qin, Z., D. Hu, et al. (2007). "Effect of 4-hydroxy-2-nonenal modification on alpha-synuclein aggregation." *J Biol Chem* 282(8): 5862-5870.
- Ramirez, A., A. Heimbach, et al. (2006). "Hereditary parkinsonism with dementia is caused by mutations in ATP13A2, encoding a lysosomal type 5 P-type ATPase." *Nat Genet* 38(10): 1184-1191.
- Ritz, B., A. Ascherio, et al. (2007). "Pooled analysis of tobacco use and risk of Parkinson disease." *Archives of neurology* 64(7): 990-997.
- Ritz, B. and F. Yu (2000). "Parkinson's disease mortality and pesticide exposure in California 1984-1994." *Int J Epidemiol* 29(2): 323-329.
- Ritz, B. R., A. D. Manthripragada, et al. (2009). "Dopamine transporter genetic variants and pesticides in Parkinson's disease." *Environ Health Perspect* 117(6): 964-969.
- Samaranch, L., O. Lorenzo-Betancor, et al. (2010). "PINK1-linked parkinsonism is associated with Lewy body pathology." *Brain* 133(Pt 4): 1128-1142.
- Schapira, A. H., M. W. Cleeter, et al. (2006). "Proteasomal inhibition causes loss of nigral tyrosine hydroxylase neurons." *Annals of neurology* 60(2): 253-255.
- Schapira, A. H., J. M. Cooper, et al. (1990). "Mitochondrial complex I deficiency in Parkinson's disease." *J Neurochem* 54(3): 823-827.

- Semchuk, K. M., E. J. Love, et al. (1992). "Parkinson's disease and exposure to agricultural work and pesticide chemicals." *Neurology* 42(7): 1328-1335.
- Sherer, T. B., R. Betarbet, et al. (2002). "An in vitro model of Parkinson's disease: linking mitochondrial impairment to altered alpha-synuclein metabolism and oxidative damage." *J Neurosci* 22(16): 7006-7015.
- Spillantini, M. G., M. L. Schmidt, et al. (1997). "Alpha-synuclein in Lewy bodies." *Nature* 388(6645): 839-840.
- Staub, R. E., G. B. Quistad, et al. (1998). "Mechanism for Benomyl Action as a Mitochondrial Aldehyde Dehydrogenase Inhibitor in Mice." *Chemical Research in Toxicology* 11(5): 535-543.
- Sun, Y., B. Liou, et al. (2010). "Neuronopathic Gaucher disease in the mouse: viable combined selective saposin C deficiency and mutant glucocerebrosidase (V394L) mice with glucosylsphingosine and glucosylceramide accumulation and progressive neurological deficits." *Human molecular genetics* 19(6): 1088-1097.
- Tanner, C. M., F. Kamel, et al. (2011). "Rotenone, Paraquat and Parkinson's Disease." *Environ Health Perspect*.
- Thiruchelvam, M., B. J. Brockel, et al. (2000). "Potentiated and preferential effects of combined paraquat and maneb on nigrostriatal dopamine systems: environmental risk factors for Parkinson's disease?" *Brain Res* 873(2): 225-234.
- Thiruchelvam, M., A. McCormack, et al. (2003). "Age-related irreversible progressive nigrostriatal dopaminergic neurotoxicity in the paraquat and maneb model of the Parkinson's disease phenotype." *Eur J Neurosci* 18(3): 589-600.
- Trojanowski, J. Q., M. Goedert, et al. (1998). "Fatal attractions: abnormal protein aggregation and neuron death in Parkinson's disease and Lewy body dementia." *Cell Death Differ* 5(10): 832-837.
- Uversky, V. N., J. Li, et al. (2001). "Pesticides directly accelerate the rate of [alpha]-synuclein fibril formation: a possible factor in Parkinson's disease." *FEBS Letters* 500(3): 105-108.
- Wahner, A. D., J. M. Bronstein, et al. (2007). "Nonsteroidal anti-inflammatory drugs may protect against Parkinson disease." *Neurology* 69(19): 1836-1842.
- Wang, A., S. Costello, et al. (2011). "Parkinson's Disease Risk from Ambient Exposure to Maneb, Ziram, And Paraquat at Work and Home." *European Journal of Epidemiology* in press.
- Wang, X.-F., S. Li, et al. (2006). "Inhibitory effects of pesticides on proteasome activity: Implication in Parkinson's disease." *Neurobiology of Disease* 23(1): 198-205.
- Yoritaka, A., N. Hattori, et al. (1996). "Immunohistochemical detection of 4-hydroxynonenal protein adducts in Parkinson disease." *Proceedings of the National Academy of Sciences of the United States of America* 93(7): 2696-2701.
- Zeng, B. Y., S. Bukhatwa, et al. (2006). "Reproducible nigral cell loss after systemic proteasomal inhibitor administration to rats." *Annals of neurology* 60(2): 248-252.
- Zhang, N. Y., Z. Tang, et al. (2008). "alpha-Synuclein protofibrils inhibit 26 S proteasome-mediated protein degradation: understanding the cytotoxicity of protein protofibrils in neurodegenerative disease pathogenesis." *J Biol Chem* 283(29): 20288-20298.
- Zhou, Y., F. S. Shie, et al. (2004). "Proteasomal inhibition induced by manganese ethylene-bis-dithiocarbamate: relevance to Parkinson's disease." *Neuroscience* 128(2): 281-291.